

**NOVEL APPROACHES TO THE ASSESSMENT  
AND STRATEGIC MODIFICATION OF FLEXOR  
TENDON ADHESION FORMATION**

**Olivier Alexandre Branford**

**2011**



A thesis submitted as part of a Degree of Doctor of  
Philosophy, at University College London,  
University of London

## **DECLARATION OF ORIGINALITY**

I, Olivier Alexandre Branford confirm that the work presented in this thesis is my own. Where information has been derived from other sources, I confirm that this has been indicated in the thesis. The research forming this thesis is entirely original and my ideas were developed with the guidance of my supervisors. All experiments were performed by myself with the technical assistance of the laboratory and scientific staff at: the RAFT Institute of Plastic and Reconstructive Surgery, Mount Vernon Hospital; University College London, Division of Surgical and Interventional Sciences, Tissue Repair and Engineering Centre, Institute of Orthopaedics, Stanmore Campus; and School of Engineering and Materials Science, Queen Mary, University of London, Mile End Road, London. Statistical advice was provided by the University of Hertfordshire and University College London.

# ABSTRACT

Mobilisation of injured tendons results in improved tendon healing and reduced adhesions. The precise mechanism for the effect on adhesions is unknown. This thesis presents the development of a series of techniques to examine the hypotheses: that mobilisation exerts its favourable effects by modifying local strain responses to applied stress by altering cell attachment to the extracellular matrix; that selectively blocking cell-matrix attachment can mimic these effects.

Attachment of tendon-synovial complex cells and mobilised and immobilised adhesion cells to collagen and fibronectin was examined *in vitro*. Attachment of intrinsic cells and mobilised adhesion cells was higher than that of extrinsic cells and immobilised adhesion cells. These data suggest that mobilisation favours intrinsic cell attachment to the matrix and their contribution to healing.

An *in vivo* model system was developed in the injured flexor tendon-synovial complex, enabling quantitative hierarchical mechanical assessment of mobilised and immobilised adhesions. Three-fold higher local strain values and increased heterogeneity of local strain values were seen in mobilised adhesions. Mobilisation may result in localised mechanical failure due to altered local strain patterns.

A novel biomaterial was investigated *in vitro* and *in vivo*. Reduction in restrictive adhesion parameters was observed, with an associated decrease in adhesion cellularity without compromising tendon cellularity. Inhibition of fibroblast attachment resulted in a mimicking of the effects of mobilisation.

# ACKNOWLEDGEMENTS

I would like to express my immense gratitude to a number of people, without whom none of this research would have been possible. They include my supervisors: Mr Addie Grobbelaar for his continuous support and advice throughout and Dr Kerstin Rolfe for her tireless involvement and gentle guidance. Their time has been invaluable in the preparation of material for submission for publication and proof reading of this thesis. In addition, I would like to extend my sincerest thanks to Professor Angus McGrouther (University of Manchester), Dr Vivek Mudera (University College London), Professor David Lee (Queen Mary), and Professor Dan Bader (Queen Mary), who have helped to shape my scientific thoughts and helped me to plan my experiments.

Mrs Liz Clayton within the histology department at RAFT deserves a huge thank you for her efforts. I would also like to thank Dr Julian Dye for his guidance in the laboratory. Several parts of this thesis involved working at the animal house of Northwick Park, and I would particularly like to thank Cathy who was a pleasure to work with and provided advice on request. I would also like to thank all the administration at RAFT, Hilary, Stephanie, Christine and Amanda who guided me through the challenges of three years of research.

Thanks are also due to my friend and fellow research colleague Robert Pearl who has been a companion throughout my time at RAFT. He has provided much help in times of need as well as many laughs along the way.



It must also be remembered that none of this work would have been possible without the financial support from The Restoration of Appearance and Function Trust, The Royal College of Surgeons of England, The Big Lottery UK, and The Rosetrees Trust, and to them I am truly grateful.

Last but not least, to my family who have supported me through everything I have ever done and achieved, I owe an enormous debt, especially to my wife Clare, my daughter Amélie, our twins, Estelle and Xavier, and my parents Danièle and Joe. This work is dedicated to them.

# **CONTENTS**

<b>DECLARATION OF ORIGINALITY</b>	<b>2</b>
<b>ABSTRACT</b>	<b>3</b>
<b>ACKNOWLEDGEMENTS</b>	<b>4</b>
<b>CONTENTS</b>	<b>6</b>
<b>LIST OF FIGURES</b>	<b>16</b>
<b>LIST OF TABLES</b>	<b>22</b>
<b>LIST OF ADDITIONAL ILLUSTRATIVE DIGITAL MATERIAL</b>	<b>24</b>
<b>LIST OF ABBREVIATIONS</b>	<b>25</b>
<b>AIMS AND HYPOTHESES</b>	<b>28</b>
<b>NOMENCLATURE AND TENDON HISTOLOGY</b>	<b>29</b>

## **CHAPTER 1**

### **GENERAL INTRODUCTION**

<b>1.1</b>	<b>INTRODUCTION: THE CLINICAL PROBLEM</b>	<b>32</b>
<b>1.2</b>	<b>HISTORY OF TENDON HEALING AND ADHESION FORMATION</b>	<b>36</b>
<b>1.2.1</b>	<b>Extrinsic Model of Tendon Healing</b>	<b>36</b>
<b>1.2.2</b>	<b>Intrinsic Model of Tendon Healing</b>	<b>37</b>
<b>1.2.3</b>	<b>Modern Concepts in Tendon Healing</b>	<b>38</b>
<b>1.2.4</b>	<b>The Effects of Mobilisation on Tendon Healing and Adhesion Formation</b>	<b>42</b>
<b>1.3</b>	<b>FLEXOR TENDON ANATOMY AND FUNCTION</b>	<b>45</b>

1.3.1	<b>Flexor Digitorum Superficialis</b>	<b>45</b>
1.3.2	<b>Flexor Digitorum Profundus</b>	<b>45</b>
1.3.3	<b>Flexor Tendon Synovial Sheath</b>	<b>46</b>
1.4	<b>ANIMAL MODELS IN THE STUDY OF TENDON HEALING</b>	<b>47</b>
1.4.1	<i>In Vitro</i> Tendon Healing Models	47
1.4.2	<i>In Vivo</i> Tendon Healing Models	48
1.4.3	Rabbit Tendon Healing Model	49
1.4.4	Types of Tendon Injury	49
1.5	<b>THE EXTRACELLULAR MATRIX IN TENDON HEALING</b>	<b>51</b>
1.5.1	Phases of Tendon Healing	51
1.5.2	Cell Interaction with the Extracellular Matrix	52
1.5.3	Fibronectin	53
1.5.4	Collagen	60
1.5.5	An Extracellular Matrix Gradient	62
1.5.6	Integrins	65
1.5.7	Mechanotransduction	75
1.6	<b>ASSESSMENT OF TENDON HEALING AND ADHESIONS</b>	<b>80</b>
1.6.1	Clinical Assessments	80
1.6.2	Histological Assessments	81
1.6.3	Biomechanical Assessments	81
1.7	<b>METHODS OF ADHESION REDUCTION</b>	<b>83</b>
1.7.1	Mechanical Barriers	83
1.7.2	Biochemical Agents	84
1.8	<b>BIOMATERIALS AND TISSUE ENGINEERING</b>	<b>87</b>

## **CHAPTER 2** **88**

### **MATERIALS AND METHODS**

<b>2.1</b>	<b>MATERIALS AND METHODS</b>	<b>90</b>
<b>2.2</b>	<b><i>IN VITRO</i> METHODS</b>	<b>90</b>
<b>2.2.1</b>	<b>Primary Rabbit Tissue Culture</b>	<b>90</b>
<b>2.2.2</b>	<b>Preparation of Derivative Fibronectin Biomaterial and Fibronectin Control</b>	<b>93</b>
<b>2.2.3</b>	<b>Protein Analysis of Derivative Fibronectin Biomaterial and Fibronectin Control</b>	<b>102</b>
<b>2.2.4</b>	<b>Measurement of Cell Attachment to Derivative Fibronectin Biomaterial and Fibronectin Control</b>	<b>107</b>
<b>2.2.5</b>	<b>Assessment of Synovial Sheath Fibroblast Migration into Derivative Fibronectin Biomaterial and Fibronectin Control</b>	<b>109</b>
<b>2.2.6</b>	<b>Determination of Synovial Sheath Fibroblast Viability on Derivative Fibronectin Biomaterial</b>	<b>110</b>
<b>2.2.7</b>	<b>Time Lapse Observation of Cells on Derivative Fibronectin Biomaterial</b>	<b>112</b>
<b>2.2.8</b>	<b>Determination of Cell Attachment and Examination of Morphology of Cells on Collagen Type-I and Fibronectin</b>	<b>112</b>
<b>2.3</b>	<b><i>IN VIVO</i> METHODS</b>	<b>118</b>
<b>2.3.1</b>	<b>Tendon Injury Model</b>	<b>118</b>
<b>2.3.2</b>	<b>Investigation of the Effects of Derivative Fibronectin Biomaterial Treatment on Adhesions</b>	<b>123</b>

<b>2.3.3</b>	<b>Investigation of the Effects of Mobilisation on the Hierarchical Biomechanical Properties of Adhesions</b>	<b>129</b>
<b>2.3.4</b>	<b>Histology and Immunohistochemical Scoring in Derivative Fibronectin Biomaterial Treated and Untreated Injured Tendons and Adhesions</b>	<b>140</b>
<b>2.4</b>	<b>STATISTICAL ANALYSIS</b>	<b>145</b>

## **CHAPTER 3** **146**

### **RESULTS**

#### **SHEAR-AGGREGATED FIBRONECTIN WITH ANTI-ADHESIVE PROPERTIES**

<b>3.1</b>	<b>INTRODUCTION</b>	<b>148</b>
<b>3.1.1</b>	<b>Aim</b>	<b>149</b>
<b>3.2</b>	<b>MATERIALS AND METHODS</b>	<b>149</b>
<b>3.2.1</b>	<b>Protein analysis of Derivative Fibronectin Biomaterial and Fibronectin Control</b>	<b>149</b>
<b>3.2.2</b>	<b>Biodegradability of Derivative Fibronectin Biomaterial and Fibronectin Control</b>	<b>149</b>
<b>3.2.3</b>	<b>Synovial Sheath Fibroblast Culture</b>	<b>149</b>
<b>3.2.4</b>	<b>Assessment of Fibroblast Attachment</b>	<b>150</b>
<b>3.2.5</b>	<b>Assessment of Migration</b>	<b>150</b>
<b>3.2.6</b>	<b>Fibroblast Viability Assessment</b>	<b>150</b>
<b>3.2.7</b>	<b>Time Lapse Assessment</b>	<b>150</b>
<b>3.2.8</b>	<b>Statistical Analysis</b>	<b>151</b>

<b>3.3</b>	<b>RESULTS</b>	<b>151</b>
<b>3.3.1</b>	<b>Protein Analysis of Derivative Fibronectin Biomaterial and Fibronectin Control</b>	<b>151</b>
<b>3.3.2</b>	<b>Biodegradability of Derivative Fibronectin Biomaterial and Fibronectin Control</b>	<b>155</b>
<b>3.3.3</b>	<b>Assessment of Fibroblast Attachment</b>	<b>158</b>
<b>3.3.4</b>	<b>Assessment of Migration</b>	<b>161</b>
<b>3.3.5</b>	<b>Fibroblast Viability Assessment</b>	<b>161</b>
<b>3.3.6</b>	<b>Time Lapse Assessment</b>	<b>164</b>
<b>3.4</b>	<b>DISCUSSION</b>	
<b>3.4.1</b>	<b>Preventing Cell Attachment to Fibronectin: A Therapeutic Strategy</b>	<b>167</b>
<b>3.4.2</b>	<b>Cell Binding and Fibronectin</b>	<b>167</b>
<b>3.4.3</b>	<b>An Anti-Adhesive Biomaterial</b>	<b>168</b>
<b>3.4.4</b>	<b>Inhibitory Fragments Within the Fibronectin Molecule</b>	<b>169</b>
<b>3.4.5</b>	<b>Cryptic Anti-Adhesive Site and Exposure to Urea</b>	<b>170</b>
<b>3.4.6</b>	<b>The Anti-Adhesive Nature of the Derivative Fibronectin Biomaterial</b>	<b>171</b>
<b>3.4.7</b>	<b>Cryoprecipitate Contains Fibronectin Fragments</b>	<b>172</b>
<b>3.4.8</b>	<b>Inhibition of Myofibroblastic Conversion by the Derivative Fibronectin Biomaterial</b>	<b>173</b>
<b>3.4.9</b>	<b>Biomaterial Degradation</b>	<b>174</b>
<b>3.4.10</b>	<b>Barrier Effects of the Derivative Fibronectin Biomaterial</b>	<b>174</b>
<b>3.4.11</b>	<b>Summary</b>	<b>174</b>

## **CHAPTER 4** **176**

### **RESULTS**

#### **A NOVEL BIOMIMETIC MATERIAL FOR ENGINEERING POSTSURGICAL ADHESION IN THE INJURED DIGITAL FLEXOR TENDON COMPLEX**

<b>4.1</b>	<b>INTRODUCTION</b>	<b>178</b>
<b>4.1.1</b>	<b>Aim</b>	<b>179</b>
<b>4.2</b>	<b>MATERIALS AND METHODS</b>	<b>179</b>
<b>4.2.1</b>	<b>Tendon Injury Model</b>	<b>179</b>
<b>4.2.2</b>	<b>Mechanical Evaluation</b>	<b>179</b>
<b>4.2.3</b>	<b>Histology and Immunohistochemical Scoring</b>	<b>179</b>
<b>4.2.4</b>	<b>Statistical Analysis</b>	<b>180</b>
<b>4.3</b>	<b>RESULTS</b>	<b>180</b>
<b>4.3.1</b>	<b>Mechanical Evaluation</b>	<b>180</b>
<b>4.3.2</b>	<b>Histology and Immunohistochemical Scoring</b>	<b>183</b>
<b>4.4</b>	<b>DISCUSSION</b>	<b>196</b>
<b>4.4.1</b>	<b>A Combined Mechanical and Histological Approach</b>	<b>196</b>
<b>4.4.2</b>	<b>Cellular Effects of the Biomaterial</b>	<b>196</b>
<b>4.4.3</b>	<b>A Mechanism for Differential Cellular Effects on Injured Tendon and the Synovial Surface</b>	<b>197</b>
<b>4.4.4</b>	<b>Suitability for Surgical Use</b>	<b>199</b>
<b>4.4.5</b>	<b>Summary</b>	<b>199</b>

## **CHAPTER 5**

**201**

### **RESULTS**

#### **RELATING STRUCTURE TO HIERARCHICAL MECHANICS OF IMMOBILISED AND MOBILISED FLEXOR TENDON ADHESIONS**

<b>5.1</b>	<b>INTRODUCTION</b>	<b>203</b>
<b>5.1.1</b>	<b>Aims</b>	<b>204</b>
<b>5.2</b>	<b>MATERIALS AND METHODS</b>	<b>204</b>
<b>5.2.1</b>	<b>Gross Adhesion Mechanics</b>	<b>204</b>
<b>5.2.2</b>	<b>Micromechanical Assessment</b>	<b>204</b>
<b>5.2.3</b>	<b>Image Analysis</b>	<b>205</b>
<b>5.2.4</b>	<b>Data Analysis</b>	<b>205</b>
<b>5.2.5</b>	<b>Statistical Analysis</b>	<b>205</b>
<b>5.3</b>	<b>RESULTS</b>	<b>206</b>
<b>5.3.1</b>	<b>Gross Adhesion Mechanics</b>	<b>206</b>
<b>5.3.2</b>	<b>Micromechanical Assessment</b>	<b>210</b>
<b>5.4</b>	<b>DISCUSSION</b>	<b>218</b>
<b>5.4.1</b>	<b>A Hierarchical Approach to Adhesion Assessment</b>	<b>218</b>
<b>5.4.2</b>	<b>Local Strains in Adhesions Cannot be Inferred from Applied Strain</b>	<b>218</b>
<b>5.4.3</b>	<b>Mobilisation Favours Dynamic Patterns with Higher Local Strain</b>	<b>219</b>
<b>5.4.4</b>	<b>Mobilisation Favours Tissue Heterogeneity</b>	<b>220</b>



5.4.5	Summary	221
<b>CHAPTER 6</b>		<b>222</b>
<b>RESULTS</b>		
<b>ATTACHMENT OF INTRINSIC AND EXTRINSIC TENDON CELLS AND ADHESION CELLS TO COLLAGEN AND FIBRONECTIN</b>		
6.1	INTRODUCTION	224
6.1.1	Aims	225
6.2	MATERIALS AND METHODS	225
6.2.1	Preparation of Explant Cultures	225
6.2.2	Cell Adhesion Assay	225
6.2.3	Cell Adhesion Assessment	226
6.2.4	Morphological Assessment	226
6.2.5	Statistical Analysis	226
6.3	RESULTS	227
6.3.1	Cell Adhesion Assessment	227
6.3.2	Morphological Assessment	237
6.4	DISCUSSION	255
6.4.1	Selectivity in Tendon Healing	255
6.4.2	Intrinsic Cells Show Greater Attachment to Collagen and Fibronectin	256
6.4.3	Mobilisation Increases Cell Attachment and Favours Elongated Cellular Morphology	258

6.4.4	A New Therapeutic Strategy: Selectively Preventing Extrinsic Cell Attachment to Fibronectin	260
6.4.5	Summary	260
<b>CHAPTER 7</b>		<b>262</b>
<b>DISCUSSION</b>		
7.1	INTRODUCTION	263
7.2	MAJOR FINDINGS AND CRITIQUE OF METHODOLOGIES	264
7.2.1	Shear-Aggregated Fibronectin with Anti-Adhesive Properties	265
7.2.2	A Novel Biomimetic Material for Engineering Postsurgical Adhesion in the Injured Digital Flexor Tendon	266
7.2.3	Relating Structure to Hierarchical Mechanics of Immobilised and Mobilised Flexor Tendon Adhesions	267
7.2.4	The Attachment of Intrinsic and Extrinsic Tendon Cells and Adhesion Cells to Collagen and Fibronectin	268
7.3	NOVEL APPROACHES TO THE ASSESSMENT AND STRATEGIC MODIFICATION OF FLEXOR TENDON ADHESION FORMATION	269
7.3.1	Assessment of Adhesions	269
7.3.2	Modification of Adhesions	271
7.4	FUTURE WORK	276
7.5	GENERAL SUMMARY	279

<b>REFERENCES</b>	<b>282</b>
-------------------	------------

<b>APPENDIX</b>	<b>327</b>
-----------------	------------

<b>Appendix I Solutions and Protocols</b>	<b>327</b>
-------------------------------------------	------------

<b>Appendix II Publications and Conference Proceedings from this Thesis</b>	<b>330</b>
-----------------------------------------------------------------------------	------------

# LIST OF FIGURES

## CHAPTER 1

- Figure 1.1** The hypothetical spatial distribution of fibronectin in the healing tendon-synovial complex during the early stages of healing. 34
- Figure 1.2** A diagrammatic representation of the structure of a single strand of cellular fibronectin 55
- Figure 1.3** A diagrammatic representation of the common pathway linking growth factor signalling and local mechanical forces through the integrin receptor via the cytoskeleton and intracellular signal transduction to the cell nucleus. 66
- Figure 1.4** A diagrammatic representation of a transmembrane integrin receptor. 68

## CHAPTER 2

- Figure 2.1** The cryoprecipitate raw material. 96
- Figure 2.2** The process of heat depletion resulting in the precipitation of fibrinogen, removing it from the biomaterial preparation. 97
- Figure 2.3** Fibronectin pellets produced following polyethylene glycol precipitation and centrifugation of the preparation. 98
- Figure 2.4** Shear aggregation of biomaterial onto a rotating rod. 99
- Figure 2.5** Air dried biomaterial tube prior to being cut into mats. 100
- Figure 2.6** Air dried biomaterial tube end-on showing thin wall. 101
- Figure 2.7** Metal ring used to hold the derivative fibronectin biomaterial apposed to plated cells. 111

<b>Figure 2.8</b>	Crystal violet cell adhesion assay.	115
<b>Figure 2.9</b>	Morphological assessment.	117
<b>Figure 2.10</b>	The dew claw seen just proximal to the apex of the incision.	120
<b>Figure 2.11</b>	The ‘V’ shaped incision.	121
<b>Figure 2.12</b>	Partial tenotomy injury in the intrasynovial portion of the flexor digitorum profundus tendon in the rabbit prior to removal of the segment.	122
<b>Figure 2.13</b>	Biomaterial tube insertion around the injured tendon using a temporary suture.	124
<b>Figure 2.14</b>	Diagram of biomaterial <i>in situ</i> around tendon injury.	125
<b>Figure 2.15</b>	Study design showing randomisation of animals and digits to biomaterial treated or untreated injury groups.	126
<b>Figure 2.16</b>	Mechanical pullout assessment with the digital claw being held at one end and the FDP tendon of the same digit being held using a transfixion suture at the other.	128
<b>Figure 2.17</b>	Study design showing randomisation of digits to either gross tensile testing or to micromechanical assessment.	131
<b>Figure 2.18</b>	Macromechanical testing of adhesions.	132
<b>Figure 2.19</b>	Micromechanical testing of adhesions.	134
<b>Figure 2.20</b>	Processed confocal images of adhesion cell nuclei.	138
<b>Figure 2.21</b>	Schematic of the measurements relevant to calculating local strain.	139
<b>Figure 2.22</b>	Micrograph of an adhesion bridging interface between tendon and surrounding soft tissues.	141

<b>Figure 2.23</b>	Quantification of the cellularity of tendon and adhesion tissue using cell counts over a grid.	142
--------------------	------------------------------------------------------------------------------------------------	-----

## CHAPTER 3

<b>Figure 3.1</b>	Immunoelectrophoresis plate showing precipitin arcs for fibronectin and fibrinogen.	153
<b>Figure 3.2</b>	Calculation of fibronectin concentration in solution from protein standards.	154
<b>Figure 3.3</b>	Protein dissolution curves for derivative fibronectin biomaterial and fibronectin control biomaterials.	157
<b>Figure 3.4</b>	Immunofluorescent micrographs of biomaterials cultured with fibroblasts after washing and $\alpha$ -Smooth Muscle Actin and Propidium Iodide staining.	159
<b>Figure 3.5</b>	Average attached fibroblast and myofibroblast cell counts per microscopy field to the derivative fibronectin biomaterial, fibronectin control and plain glass.	160
<b>Figure 3.6</b>	Micrographs of biomaterials 24 hours after seeding with fibroblasts after washing and Haematoxylin and Eosin staining.	162
<b>Figure 3.7</b>	Micrograph demonstrating fibroblasts that have been exposed to a derivative fibronectin biomaterial mat for 24 hours and stained with Trypan Blue.	163
<b>Figure 3.8</b>	Micrograph from the time lapse assessment of the interaction between cells and the derivative fibronectin biomaterial at 6 hours.	165
<b>Figure 3.9</b>	Detail micrographs from the time lapse assessment of the interaction between cells and the derivative fibronectin biomaterial.	166

## CHAPTER 4

- Figure 4.1** Force displacement graph showing a reduced mean pullout force in the biomaterial treated group relative to the untreated injured control group. 181
- Figure 4.2** A comparison of mean peak force required to overcome adhesions in untreated injured digits, treated injured digits and uninjured digits. 182
- Figure 4.3** A comparison of cell counts measured from the tendon surface in microns at 2 weeks post injury in treated injured digits, untreated injured digits and negative control digits. 184
- Figure 4.4** Haematoxylin and Eosin stain of tendon injury groups. 186
- Figure 4.5** A comparison of cell counts measured from the adhesion surface in microns in treated injured digits and untreated injured digits. 187
- Figure 4.6** Haematoxylin and Eosin stain of adhesion groups. 188
- Figure 4.7** A comparison of Ki67 positive cell counts measured from the adhesion surface in microns in treated injured digits and untreated injured digits. 190
- Figure 4.8** Ki67 stained sections through adhesion surface in untreated and treated adhesions. 191
- Figure 4.9** A comparison of Ki67 positive cell counts measured from the tendon surface in microns in uninjured tendons and untreated injured tendons. 192
- Figure 4.10** Ki67 positive cell counts measured from the tendon surface in microns in uninjured tendons and treated injured tendons. 193

**Figure 4.11** Ki67 positive cell counts measured from the tendon surface in microns in untreated injured tendons and treated injured tendons.194

**Figure 4.12** Ki67 stained sections through tendon surface in untreated injured tendon, treated injured tendon and uninjured control. 195

## CHAPTER 5

**Figure 5.1** Dissection of tendon-adhesion-synovial complexes at 14 days. 207

**Figure 5.2** Load displacement graph for mobilised and immobilised adhesions. 208

**Figure 5.3** Confocal images showing characteristic appearance of component tissues in specimens. 212

**Figure 5.4** Example graphs of the local strain for adhesion samples at 10% applied strain. 213

**Figure 5.5** Graphical comparison of mean local strain values at 10% applied strain for mobilised and immobilised adhesion samples. 214

## CHAPTER 6

**Figure 6.1** Representative micrographs of tendon-synovial cell groups attached to collagen type-I. 229

**Figure 6.2** Representative micrographs of tendon-synovial cell groups attached to fibronectin. 230

**Figure 6.3** Representative micrographs of adhesion cell groups attached to collagen type-I. 231



<b>Figure 6.4</b>	Representative micrographs of adhesion cell groups attached to fibronectin.	232
<b>Figure 6.5</b>	Graph of attachment of tendon-synovial complex cell groups to collagen type-I.	233
<b>Figure 6.6</b>	Graph of attachment of tendon-synovial complex cell groups to fibronectin.	235
<b>Figure 6.7</b>	Graph of attachment of mobilised and immobilised adhesion cell groups to collagen type-I.	239
<b>Figure 6.8</b>	Graph of attachment of mobilised and immobilised adhesion cell groups to fibronectin.	241
<b>Figure 6.9</b>	Graphs of morphology of cells attached to collagen type-I. Results are shown for tendon core, tendon surface, and synovial sheath cell groups.	247
<b>Figure 6.10</b>	Graphs of morphology of cells attached to fibronectin. Results are shown for tendon core, tendon surface, and synovial sheath cell groups.	248
<b>Figure 6.11</b>	Graphs of morphology of cells attached to collagen type-I. Results are shown for mobilised and immobilised adhesion cell groups.	253
<b>Figure 6.12</b>	Graphs of morphology of cells attached to fibronectin. Results are shown for mobilised and immobilised adhesion cell groups.	254

# LIST OF TABLES

## CHAPTER 5

<b>Table 5.1</b>	Mobilised versus immobilised adhesions: Comparison of structural stiffness and load at failure.	209
<b>Table 5.2</b>	Comparison of mean local strain values at 10% applied strain for mobilised and immobilised adhesion samples.	216
<b>Table 5.3</b>	Frequency and mean local strain of regional patterns seen in mobilised and immobilised adhesions.	217

## CHAPTER 6

<b>Table 6.1</b>	Cell attachment for tendon-synovial complex cell groups to collagen type-I.	234
<b>Table 6.2</b>	Cell attachment for tendon-synovial complex cell groups to fibronectin.	236
<b>Table 6.3</b>	Cell attachment for mobilised and immobilised adhesion cell groups to collagen type-I.	240
<b>Table 6.4</b>	Cell attachment for mobilised and immobilised adhesion cell groups to fibronectin.	242
<b>Table 6.5</b>	Cell area for tendon-synovial complex cell groups attached to collagen type-I and fibronectin.	243
<b>Table 6.6</b>	Cell perimeter for tendon-synovial complex cell groups attached to collagen type-I and fibronectin.	244
<b>Table 6.7</b>	Cell circularity for tendon-synovial complex cell groups attached to collagen type-I and fibronectin.	245

<b>Table 6.8</b>	Percentage elongated morphology for tendon-synovial complex cell groups attached to collagen type-I and fibronectin.	246
<b>Table 6.9</b>	Cell area for mobilised and immobilised adhesion cell groups attached to collagen type-I and fibronectin.	249
<b>Table 6.10</b>	Cell perimeter for mobilised and immobilised adhesion cell groups attached to collagen type-I and fibronectin.	250
<b>Table 6.11</b>	Cell circularity for mobilised and immobilised adhesion cell groups attached to collagen type-I and fibronectin.	251
<b>Table 6.12</b>	Percentage elongated morphology for mobilised and immobilised adhesion cell groups attached to collagen type-I and fibronectin.	252

## **LIST OF ADDITIONAL ILLUSTRATIVE DIGITAL MATERIAL**

- Video 5.1** Video demonstrating the stretching dynamic pattern for a mobilised adhesion tissue sample.
- Video 5.2** Video demonstrating the stretching dynamic pattern for an immobilised adhesion tissue sample.
- Video 5.3** Video demonstrating the compressing dynamic adhesion pattern.
- Video 5.4** Video demonstrating the shearing dynamic adhesion pattern.
- Video 5.5** Video demonstrating the random dynamic adhesion pattern.
- Video 5.6** Video demonstrating the tearing dynamic adhesion pattern.

## LIST OF ABBREVIATIONS

$\alpha$ -SMA	$\alpha$ -Smooth Muscle Actin
A	Annular
ANOVA	Analysis of Variance
BCA	Bicinchoninic Acid
BHK	Baby Hamster Kidney
BM	Biomaterial
BSA	Bovine Serum Albumin
C	Cruciate
Cryo	Cryoprecipitate
CTGF	Connective Tissue Growth Factor
DFn	Derivative Fibronectin Biomaterial
DAB	Diaminobenzidine
dH <sub>2</sub> O	Distilled Water
DMEM	Dulbecco's Modified Eagle's Medium
DMSO	Dimethyl Sulphoxide
ECM	Extracellular Matrix
EDTA	Ethylenediamine Tetraacetic Acid
EGCG	Epigallocatechin-3-Gallate
ELISA	Enzyme-linked immunosorbent assay
FAK	Focal Adhesion Kinase
FDP	Flexor Digitorum Profundus
FDS	Flexor Digitorum Superficialis
FCS	Fetal Calf Serum
FDS	Flexor Digitorum Superficialis

FITC	Fluorescein Isothiocyanate
Fn	Fibronectin
Fn Control	Fibronectin Control Biomaterial
5FU	5-Fluorouracil
GFP	Green Fluorescent Protein
GTP	Guanine Triphosphate
H and E	Haematoxylin and Eosin
Hep	Heparin
IEP	Immunoelectrophoresis
IMS	Industrial Methylated Spirit
Int	Integrin
IQR	Interquartile Range
mRNA	messenger RNA
MTS	Mechanical Testing System
MMP	Matrix Metalloproteinase
N	Newtons
NZW	New Zealand White
NSAID	Non-Steroidal Anti-Inflammatory Drug
PBS	Phosphate Buffered Saline
PBS-BSA	Phosphate buffered saline-bovine serum albumin
PI	Propidium Iodide
PTK	Protein Tyrosine Kinase
RT-PCR	Reverse Transcription-Polymerase Chain Reaction
SD	Standard Deviation
SEM	Standard Error of the Mean

Sup	Supernatant
TBS	Tris Buffered Saline
TGF	Transforming Growth Factor
TIMP	Tissue Inhibitors of Metalloproteinase
WHS	Whole Human Serum

## AIMS AND HYPOTHESES

Mobilisation of injured tendons results in improved tendon healing and reduced adhesion formation. The precise mechanism for this is unknown. The work presented in this thesis tests the hypotheses in the healing flexor-tendon synovial complex: that mobilisation results in increased intrinsic cell attachment and reduced extrinsic cell attachment in adhesions; that mobilisation has a favourable effect on the local strain responses of adhesions to applied stress, which reduces the restrictive nature of adhesions; and that selectively blocking cell-matrix attachment mimics the effects of mobilisation by reducing adhesion formation without compromising tendon cellularity.

These hypotheses were tested through the following aims:

- To investigate the properties of a novel biomaterial *in vitro* (Chapter 3).
- To test the biomaterial to determine its efficacy in reducing restrictive adhesion and its effects of tendon and adhesion cellularity, using a flexor tendon-synovial complex injury model *in vivo* (Chapter 4).
- To develop a suitable model for analysing the effect of mobilisation on tendon adhesion tissue organisation, to quantify local strain responses produced in adhesions to applied strain and to relate these micromechanical findings to gross restrictive parameters (Chapter 5).
- To determine if there is a difference in cell attachment between the cells of different origins from within the digital tendon-synovial complex to collagen and fibronectin *in vitro*. To determine if mobilisation has an effect on attachment of cells contributing to tendon adhesion formation (Chapter 6).



# NOMENCLATURE AND TENDON HISTOLOGY

Tendons are connective tissue structures, which are made up of a large number of collagen fibres, predominantly type I, but also types III and IV. Within the tendon core, collagen fibrils are orientated in a longitudinal fashion to form fibres, which are encased by a loose connective tissue to form fascicles.

The various cells within the tendon-synovial complex have been termed fibroblasts, tenocytes (tendon embedded fibroblasts) or fibrocytes (Manske, Gelberman et al. 1985). In this thesis, the term fibroblast will be used throughout. Fibroblasts are, in fact, found in all parts of the tendon, at different levels and may represent different sub-populations (Banes, Donlon et al. 1988). Each group may have a modified role in cell attachment, migration and ECM production in response to wounding (Riederer-Henderson, Gauger et al. 1983; Khan, Occleston et al. 1998; Ragoowansi, Khan et al. 2003; Klass, Rolfe et al. 2009; Wong, Lui et al. 2009).

Tendons may be either intrasynovial or extrasynovial. The former, in whole or part, have a synovial sheath, whilst the latter do not. The synovial sheath is a synovial lined fibro-osseous tunnel through which the tendon passes freely. The functional unit of the intrasynovial long flexor tendons in zone 2 is composite, having the main tendon core, an outer tendon surface and a tendon synovial sheath. The whole composite unit is referred to in this thesis as the tendon-synovial complex. In order to simplify and reduce confusion, in this thesis the fibroblasts of different origins within the healing tendon are termed tendon core, tendon surface, and synovial sheath fibroblasts.

# **CHAPTER 1**

## **GENERAL INTRODUCTION**

### **1.1 INTRODUCTION: THE CLINICAL PROBLEM**

#### **1.1.1 Nomenclature and Tendon Histology**

### **1.2 HISTORY OF TENDON HEALING AND ADHESION FORMATION**

#### **1.2.1 Extrinsic Model of Tendon Healing**

#### **1.2.2 Intrinsic Model of Tendon Healing**

#### **1.2.3 Modern Concepts in Tendon Healing**

#### **1.2.4 The Effects of Mobilisation on Tendon Healing and Adhesion Formation**

### **1.3 FLEXOR TENDON ANATOMY AND FUNCTION**

#### **1.3.1 Flexor Digitorum Superficialis**

#### **1.3.2 Flexor Digitorum Profundus**

#### **1.3.3 Flexor Tendon Synovial Sheath**

### **1.4 ANIMAL MODELS IN THE STUDY OF TENDON HEALING**

#### **1.4.1 *In Vitro* Tendon Healing Models**

#### **1.4.2 *In Vivo* Tendon Healing Models**

#### **1.4.3 Rabbit Tendon Healing Model**

#### **1.4.4 Types of Tendon Injury**

- 1.5 THE EXTRACELLULAR MATRIX IN TENDON HEALING**
  - 1.5.1 Phases of Tendon Healing**
  - 1.5.2 Cell Interaction with the Extracellular Matrix**
  - 1.5.3 Fibronectin**
  - 1.5.4 Collagen**
  - 1.5.5 An Extracellular Matrix Gradient**
  - 1.5.6 Integrins**
  - 1.5.7 Mechanotransduction**
- 1.6 ASSESSMENT OF TENDON HEALING AND ADHESIONS**
  - 1.6.1 Clinical Assessments**
  - 1.6.2 Histological Assessments**
  - 1.6.3 Biomechanical Assessments**
- 1.7 METHODS OF ADHESION REDUCTION**
  - 1.7.1 Mechanical Barriers**
  - 1.7.2 Biochemical Agents**
- 1.8 BIOMATERIALS AND TISSUE ENGINEERING**

## **1.1 INTRODUCTION: THE CLINICAL PROBLEM**

After injury or surgery default mechanism are to repair wounds. In the adult the resultant repair is identified by the formation of scar tissue characterised by extracellular matrix (ECM) being deposited in an excessive and disorganised way (Whitby and Ferguson 1991). However, scarring is unnecessary for tissue repair as identified in fetal wound healing (Rowlatt 1979; Larson, Longaker et al. 2010), and following hepatic or gingival injury (Schor, Ellis et al. 1996; Michalopoulos 2007).

The initial fibrinous connection of two or more injured tissue surfaces ultimately leads to collagen deposition and fibrotic adhesion formation (Thompson and Whawell 1995). Post surgical adhesions occur in up to 93% of patients undergoing abdominal operations and 97% of gynaecological pelvic procedures (Liakakos, Thomakos et al. 2001). Adhesions can be associated with debilitating pain, infertility and bowel obstruction, which has a mortality of up to 15% (Jeekel 1997; Menzies, Parker et al. 2001). In tendons, adhesions are most frequent in the digital flexor tendon synovial sheath (Potenza 1962; Potenza 1963; Matthews and Richards 1976; Phillips, McGrouther et al. 1985). Peritendinous adhesions impede the functionality of the normally separate tissue interfaces, restricting tendon movement.

Interventions aim to improve outcomes by restoring tendon glide whilst minimising the risk of tendon rupture by not impeding tendon healing. These include the use of suture techniques (Savage and Risitano 1989; Lee 1990; Messina 1992) and controlled motion regimes such as the Belfast regimen (Small, Brennen et al. 1989). Small and colleagues described early active mobilisation following flexor tendon repair in zone 2. In this regime the two passive movements of flexion and extension

were followed by two corresponding active movements of the digit. The range of motion was increased over 6 weeks, at which time the splint was removed. In the prospective study in 114 patients with 138 zone 2 flexor tendon injuries the results of early active mobilisation commenced within 48 hours of surgery was assessed using the grading system recommended by the American Society for Surgery of the Hand. The authors found that the active range of motion recovered was graded excellent or good in 77% of digits, fair in 14% and poor in 9%. Dehiscence of the repair occurred in 11 digits (9.4%) and in these an immediate re-repair followed by a similar programme of early active mobilisation resulted in an excellent or good outcome in seven digits. The authors proposed that, in contrast to immobilisation or passive mobilisation, early active mobilisation could safely achieve a greater range of gliding with reduced adhesions.

During healing there is a loss in tensile strength of repaired tissue. However, the application of early postoperative motion stress in tendons mitigates this loss (Aoki, Kubota et al. 1997). When injured flexor tendons are immobilised, adhesions are formed within the synovial sheath between the tendon and synovial sheath surfaces (Wong, Lui et al. 2009) (Figure 1.1). A tendon repair is required that can withstand early active motion. The resistance to active digital flexion has been shown to increase rapidly over the first 5 days after surgery (Xie, Cao et al. 2008), supporting the need for early mobilisation. However, early active mobilisation protocols produce optimal results in only 69% (Peck, Bucher et al. 1998) to 89% of cases (Kitsis, Wade et al. 1998). In addition, lack of patient compliance continues to impede success (Silfverskiold, May et al. 1993). Persistent reduced excursion due to adherent repairs may require flexor tenolysis. This is effective in only 67% of

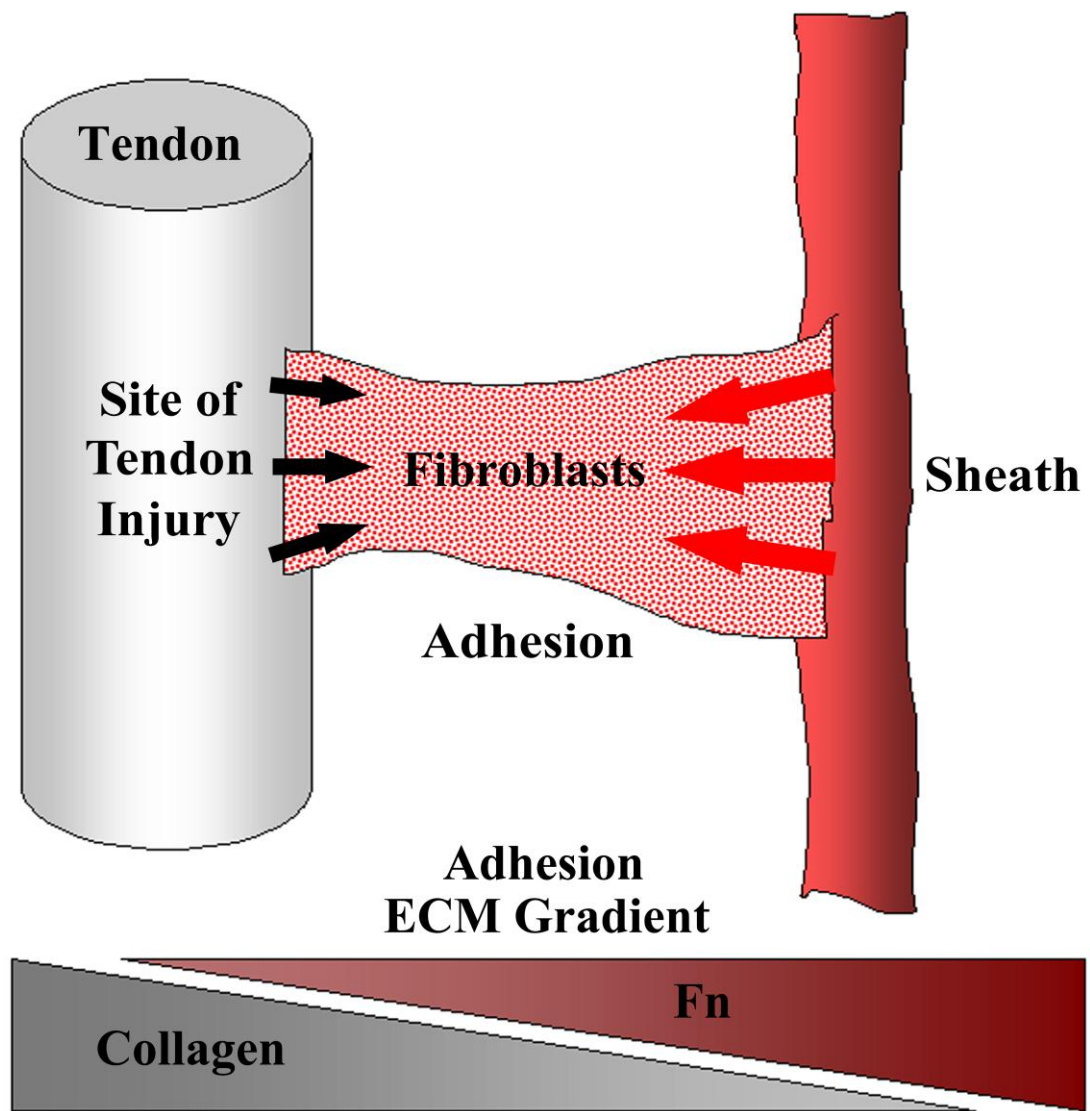


**Figure 1.1** The hypothetical spatial distribution of Fn in the healing tendon-synovial complex during the early stages of healing. The influx of synovial sheath fibroblasts (red arrows) and tendon surface fibroblasts (black arrows) to the early adhesion matrix is shown. There is minimal contribution from tendon core cells during early healing. The synovial sheath cells produce greater quantities of Fn than tendon surface cells. Tendon surface cells produce greater quantities of collagen than synovial sheath cells. There is therefore an extracellular matrix gradient within the adhesion from a Fn matrix closer to the synovial sheath to a collagen matrix closer to the tendon.

cases (Lister, Kleinert et al. 1977; Strickland 2000). Tenolysis acts as a further stimulus to adhesion formation (Strickland 1985; Menzies and Ellis 1990; Holmdahl 1999). One study has suggested waiting 6 months to a year before considering tenolysis (May and Silfverskiold 1993). In summary, the entire process of tendon repair, rehabilitation and subsequent intervention can require over a year to complete. Consequently, adhesions are a common, debilitating and costly surgical problem. There is, therefore, a significant and unmet need for a safe, successful and cost effective anti-adhesion therapy.

Adhesion formation and tendon healing have been described as a “double-edged sword” (Lin, Cardenas et al. 2004). That is, while adhesions may contribute to tendon healing, excessive scarring can restrict tendon gliding: Deficient or impaired repair may lead to premature rupture at the injury site. With regard to the cellular and ECM response, a combination of many factors must be simultaneously balanced in order to achieve a functionally healed tendon (Lin, Cardenas et al. 2004). Current research into tendon healing aims to manipulate the interplay between the biological and mechanical factors affecting healing, which may further improve outcomes (James, Kesturu et al. 2008).

Mobilisation augments tendon strength by favouring intrinsic tendon healing (Gelberman, Amiel et al. 1981; Gelberman, Nunley et al. 1991; Gelberman, Steinberg et al. 1991; Kubota, Manske et al. 1996), and decreasing adhesion formation (Takai, Woo et al. 1991; Khanna, Gougoulis et al. 2009). The exact mechanism for how mobilisation affects adhesion formation is not known. This thesis investigates the effect of mobilisation on adhesion formation in terms of how

it influences cell behaviour and consequently modifies the biomechanical properties of adhesions. The study explores strategies that reduce formation of adhesions without impairing healing at the tendon surface.

## **1.2 HISTORY OF TENDON HEALING AND ADHESION FORMATION**

Two mechanisms of tendon healing have been proposed: the extrinsic model and the intrinsic model.

### **1.2.1 Extrinsic Model of Tendon Healing**

In the extrinsic model of tendon healing, it was thought that the tendon had no internal ability to heal on its own (Skoog and Persson 1954; Potenza 1962; Potenza 1963; Peacock 1965). Potenza showed that cells of granulation tissue proliferated from synovial sheath cells and invaded the laceration site (Potenza 1962; Potenza 1963; Potenza 1964). He demonstrated *in vivo* that mechanically separating the laceration site from the surrounding synovial sheath only delayed the invasion of peripheral fibroblasts into the wound site, as they circumvented the barrier. Potenza regarded the fibrous adhesions between the tendon and the surrounding tissues as an integral part of the healing process and essential for vascular and nutritional support of the healing tendon. As a result of this, adhesions were thought to be inevitable. Potenza deduced from his observations that granulation tissue formed in proportion to the amount of tissue injury with resultant new collagen formation. Granulation tissue is made of inflammatory cells, fibroblasts, neo capillaries, cytokines and chemokines. Potenza recognised that tendon collagen fibres must mature and increase in size and those collagen fibres in adhesions must become loosely arranged



and selectively absorbed to restore tendon glide. The mechanisms of how this would be achieved are not understood.

### **1.2.2 Intrinsic Model of Tendon Healing**

The extrinsic concept was later refuted by authors who put forward an alternative intrinsic theory of tendon healing (Matthews and Richards 1974; Furlow 1976; Lundborg 1976; Matthews and Richards 1976; Lundborg and Rank 1978; Manske, Gelberman et al. 1984; Manske and Lesker 1984; Lundborg, Rank et al. 1985; Manske, Lesker et al. 1985; Mass and Tuel 1991). In this theory tendon healing was the result of fibroblasts intrinsic to the tendon itself, namely those from the tendon core and tendon surface, invading the healing site. Intrinsic tendon healing was thought to be associated with lack of adhesion formation.

Matthews and Richards produced lacerations in isolated rabbit flexor tendon segments while maintaining integrity of the flexor synovial sheath environment (Matthews and Richards 1974; Matthews and Richards 1975; Matthews and Richards 1976). They observed healing of lacerations in the absence of peripheral adhesions. Lundborg studied rabbit flexor tendon segments kept isolated in the knee joint cavity as a "tissue culture in situ" model (Lundborg and Rank 1978). Healing was observed, and no adhesions were formed. These studies supported the concept that tendon healing is an intrinsic process and thus that adhesions are a non-essential response at the site of injury.

Potenza and Herte demonstrated that acellular canine profundus tendons placed in knee joints also healed, proposing that extrinsic synovial cells must have seeded onto

the nonviable tendon (Potenza and Herte 1982). Lundborg later refuted this explanation after modifying the experiments in a way that prevented cell seeding. (Lundborg, Rank et al. 1985). This was achieved by isolating rabbit tendons in silicone tubes sealed with GORE-TEX and placing these subcutaneously in the back of the rabbits. Tendons healed by 6 weeks.

Becker and colleagues prepared explants from chicken tendons, and found that these produced collagen synthesising fibroblasts (Becker, Graham et al. 1981). Manske and Lesker maintained rabbit, dog, chicken and monkey flexor tendon explants in culture for 6 weeks (Manske and Lesker 1984). These workers found that the cells proliferated and migrated from both the tendon surface and tendon core, and could synthesise collagen. They provided both biochemical and histological evidence of the capacity for intrinsic tendon healing. Gelberman and colleagues demonstrated evidence of healing in the same species (Gelberman, Manske et al. 1984). They used lacerated tendon segments maintained in culture, showing that the tendon surface layer of cells initiated the repair process by proliferating and migrating into the laceration site.

### **1.2.3 Modern Concepts in Tendon Healing**

The biology of tendon healing has been dominated by the extrinsic and intrinsic models. There has been much debate in the literature, and much experimental evidence to prove or disprove each healing mechanism. Previous studies have shown, using vital tracker dye techniques, that cells from both tendon surface (Jones, Mudera et al. 2003) and the surrounding synovial sheath (Harrison, Mudera et al. 2003) have been observed directly to migrate into the zone of flexor tendon injury.

These studies have provided direct evidence of both extrinsic and intrinsic cellular contributions to tendon healing. Strickland has proposed that the relative contributions of each will depend on factors that relate to both the nature of the injury and the repair (Strickland 2005).

The differences between extrinsic and intrinsic mechanisms extend beyond the site of origin of the healing cells. The extrinsic mechanism appears to be active earlier in the healing sequence, whereas the intrinsic mechanism is often delayed (Khan, Occleston et al. 1998; Khan, Kakar et al. 2000). Khan and colleagues have shown *in vivo*, using monoclonal antibody location of different inflammatory markers, that the synovial sheath reacts with a greater proliferative and inflammatory response compared to the tendon core and tendon surface (Khan, Edwards et al. 1996). Kakar and colleagues demonstrated, using a rabbit model, that the tendon surface and synovial sheath became hypercellular at one week post injury, with decrease in the cellularity and apoptosis of cells of the tendon core (Kakar, Khan et al. 1998). This occurred even though the investigators avoided any direct injury to the synovial sheath. They found that by twelve weeks after injury, however, the tendon core itself also started to show hypercellularity.

Other studies suggest that extrinsic synovial sheath fibroblasts may contribute more actively to adhesion formation than intrinsic cells in a number of ways. Synovial sheath fibroblasts have a higher proliferative level relative to tendon core fibroblasts (Khan, Occleston et al. 1998). Synovial sheath fibroblasts are significantly larger in terms of their area and perimeter, and have numerous extensions and lamellopodia, indicating a migratory phenotype (Ragoowansi, Khan et al. 2003). They have an

increased capacity to degrade the ECM as reflected by matrix metalloproteinase (MMP)-2 and MMP-9 production, facilitating the process of migration (Ragoowansi, Khan et al. 2003). Khan and colleagues also showed greater MMP production by synovial sheath fibroblasts than tendon core cells (Khan, Occleston et al. 1998), although neither of these studies specifically assessed MMP activity. Ragoowansi and colleagues found that synovial sheath fibroblasts were more aggressive contractors of a collagen lattice when compared to tendon core cells. This indicates that synovial sheath fibroblasts have the cytoskeletal infrastructure to actively participate in fibrous tissue contraction (Ragoowansi, Khan et al. 2003).

Other studies have shown that predominance of the extrinsic mechanism of healing is associated with increased collagen content at the injury site as well as reduction in the level of collagen organisation and material properties of the reparative tendon tissue (Matthews and Richards 1976; Nyska, Porat et al. 1987). Wong and colleagues have also shown that greatest activity following tendon injury occurs in tissues surrounding the tendons such as the subcutaneous tissues (Wong, Lui et al. 2009). For these reasons, it is believed that the extrinsic mechanism of healing leads to increased peritendinous adhesions.

Modulating the healing process to enhance the intrinsic pathway (and augment end-to-end tendon healing) while suppressing the extrinsic pathway (and diminishing adhesions from forming between the tendon and the surrounding tissues) could lead to improvement in treatment of tendon injuries. While investigations into the biology of tendon healing have shed light on the mechanisms by which tendon tissue heals, there has been relatively little progress toward biological enhancement of the healing

process after injury and repair. Novel strategic approaches are required to reduce adhesion formation by selectively favouring intrinsic healing over extrinsic healing in the tendon-synovial complex.

The difference in cell attachment between extrinsic and intrinsic fibroblasts to the ECM has not been previously studied. Fibroblasts must attach to the ECM to gain traction for migration, but they also have to detach from the ECM to translocate (Lauffenburger and Horwitz 1996; Palecek, Loftus et al. 1997). Optimum migration rates occur at intermediate attachment conditions as cells need to form stable attachments for traction by the leading cell edge whilst allowing attachments at the trailing end to be broken during locomotion (Ahmed, Underwood et al. 2000; Munevar, Wang et al. 2001). Cell migration speed is the result of cell integrin expression levels, substratum ligand levels and integrin-ligand binding affinity (Palecek, Loftus et al. 1997). It would follow that cells that express maximal migration speed have modified integrin-ligand interactions, and a lower binding affinity. Tendon surface and tendon core cells have a less migratory phenotype than synovial sheath cells (Ragoowansi, Khan et al. 2003). This would suggest that they have a higher affinity for attachment than the synovial sheath cells. This has been confirmed *in vitro* (Riederer-Henderson, Gauger et al. 1983). However, these authors did not assess attachment of cells to ECM components.

As fibroblast attachment is a prerequisite for migration, the attachment of intrinsic and extrinsic tendon cells to collagen type-I and fibronectin (Fn) was tested in this thesis. This was investigated to determine if there was a difference, which could be used as a selective strategy in modifying adhesion formation during tendon healing.

As a well recognised modulator of adhesion formation, the effect of mobilisation on attachment of cells present within healing adhesions was also tested. This thesis also investigated the effects of preventing cell attachment on adhesion formation using a novel anti-adhesive biomaterial. Due to greater adhesion forming characteristics of synovial sheath cells, these were used when testing the anti-adhesive properties of a novel biomaterial *in vitro*.

#### **1.2.4 The Effects of Mobilisation on Tendon Healing and Adhesion Formation**

Interrelated biochemical, structural and mechanical changes are seen in tendons as a result of increased or decreased applied loads (Lin, Cardenas et al. 2004). Tendons that are immobilised exhibit decreased mechanical properties, and increased adhesion formation (Gelberman, Vande Berg et al. 1983; Murrell, Lilly et al. 1994; Palmes, Spiegel et al. 2002). Mobilisation after tendon repair results in improved tensile properties at the repair site, enhanced gliding function, decreased adhesions and therefore improved clinical outcome (Woo, Gelberman et al. 1981; Gelberman, Vande Berg et al. 1983; Gelberman, Manske et al. 1986; Hitchcock, Light et al. 1987; Feehan and Beauchene 1990).

Gelberman and colleagues demonstrated that application of early passive motion stress to repaired canine tendons led to a more rapid recovery of tensile strength, fewer adhesions, improved excursion and better tendon nutrition compared with immobilised tendons (Gelberman, Manske et al. 1986). These authors concluded that healing is enhanced by stimulating maturation of the tendon wound simultaneously with remodelling of the tendon adhesion. Aoki and colleagues found that active (in

contrast to passive) mobilisation applied stress to sutured tendons, enhanced strength of repair and the biological response (Aoki et al, 1997). Kitis and colleagues have demonstrated that controlled active mobilisation results in improved outcomes relative to controlled passive movement (Kitis, Buker et al. 2009). It has been shown that combined effects of both motion and tension on the healing response in injured chicken flexor tendons resulted in significantly greater tendon repair strength and cellular activity when compared to either motion or tension applied alone (Kubota, Manske et al. 1996). Previous authors have proposed that controlled motion may augment tendon strength by favouring intrinsic repair (Gelberman, Amiel et al. 1981; Gelberman, Nunley et al. 1991; Gelberman, Steinberg et al. 1991; Kubota, Manske et al. 1996). Mobilisation may result in increased cellular activity, DNA content, weight, vascularisation, collagen and glycosaminoglycan content in tendons, whereas immobilisation may cause increased collagen degradation and reduction in collagen crosslinking (Birdsell, Tustanoff et al. 1966; Munro, Lindsay et al. 1970; Gelberman, Amiel et al. 1981; Amiel, Woo et al. 1982; Gelberman, Woo et al. 1982; Woo, Gomez et al. 1982; Vailas, Pedrini et al. 1985; Gelberman, Manske et al. 1986; Hannafin, Arnoczky et al. 1995; Kubota, Manske et al. 1996; Yasuda and Hayashi 1999; Sharma and Maffulli 2006).

However, the precise mechanism by which postoperative mobilisation enhances tendon excursion compared to immobilisation remains unclear (Strickland and Glogovac 1980; Woo, Gelberman et al. 1981; Hitchcock, Light et al. 1987; Halikis, Manske et al. 1997). What is established is that cells within tissues react to mechanical stimuli with molecular responses that aim to maintain the overall integrity of the tissue (Huang, Kamm et al. 2004). Indeed, fibroblasts are known to

increase collagen synthesis and structural stiffness of collagen gels under cyclic strain *in vitro* (Berry, Shelton et al. 2003). Juncosa-Melvin and colleagues have shown that applying a tensile stimulus to stem cell seeded constructs in a rabbit tendon healing model resulted in increased collagen type-I and collagen type-III gene expression, as well as an increase in linear stiffness and elastic modulus, relative to nonstimulated constructs (Juncosa-Melvin, Matlin et al. 2007). Slack and colleagues have also demonstrated that when a mechanical load is applied to cells *in vitro*, protein production and cell division increases (Slack, Flint et al. 1984). This is in accord with *in vivo* observations by Aoki and colleagues who found that active mobilisation applied stress to the sutured tendon and enhanced strength of the repair (Aoki, Kubota et al. 1997). The question remains, however, why fibroblasts subjected to tensile forces, and the associated collagen formation, do not produce stronger adhesions when the tendons themselves demonstrate improved tensile strength? Spalazzi and colleagues have shown that compression of tendon grafts upregulates transforming growth factor- $\beta$ 3 (TGF-  $\beta$ 3), which may be associated with anti-scarring effects in some tissues (Spalazzi, Vyner et al. 2008). Fong and colleagues have demonstrated using microarray analysis in rat flexor tendon cultures that shear stress induced an anti-fibrotic expression pattern with decreased transcription of collagen type-I, collagen type-III and TGF-  $\beta$ 2, with increased expression of MMPs and decreased expression of tissue inhibitors of metalloproteinase (TIMP) (Fong, Trindade et al. 2005). However, these studies did not assess the micromechanical effects of these changes on local adhesion tissue strain. Clearly, a more sophisticated model is required to predict the behaviour of adhesions in relation to mobilisation.



The effect of tendon mobilisation on cell attachment in the healing tendon-synovial complex has not been extensively investigated. The effect of mobilisation on determining local adhesion tissue strains and their relation to gross adhesion mechanics has not previously been determined. These lines of investigation form the basis for this thesis.

### **1.3 FLEXOR TENDON ANATOMY AND FUNCTION**

#### **1.3.1 Flexor Digitorum Superficialis**

In humans, the flexor digitorum superficialis (FDS) tendons diverge in the palm and bifurcate. This allows transmission of the deeper profundus tendon, which becomes more superficial at a site corresponding to the level of the A2 pulley. At the point of bifurcation the central fibres continue into 2 equal slips, which insert into the anterior surface of the middle phalanx (Grays 1989).

#### **1.3.2 Flexor Digitorum Profundus**

The flexor digitorum profundus (FDP) is a deep flexor muscle in the forearm. It divides into 4 tendons, which gain entry into the palm via the carpal tunnel deep to the flexor retinaculum. The tendon to each finger remains deep to the flexor digitorum superficialis as it enters the mouth of the first annular (A1) pulley. As the FDS tendon bifurcates at the distal end of this pulley, the profundus tendon becomes superficial to it. It then courses distally within the synovial sheath and inserts into the base of the distal phalanx in each finger (Grays 1989).

### **1.3.3 Flexor Tendon Synovial Sheath**

The flexor tendon synovial sheath is a fibro-osseous tunnel which encases the long flexors to the fingers and thumb. The synovial sheath produces an almost frictionless surface for tendon gliding and hence digital movement. The synovial lining also produces synovial type fluid, which is important in tendon nutrition, and thus healing (Lundborg, Holm et al. 1980). The synovial sheath has a number of specialised thickenings, or pulleys, the number of which varies between the fingers and the thumb. These have an important functional role preventing flexor tendons from bowstringing away from the normal close proximity of the phalanges during digital flexion (Strauch and de Moura 1985). This arrangement adds to the biomechanical efficiency of the tendons, ensuring maximal digital movement relative to tendon excursion.

The fingers have 5 annular pulleys which arch transversely over the tendons. The narrow A1, A3, and A5 pulleys all lie over joints, the metacarpophalangeal, proximal interphalangeal, and distal interphalangeal joints respectively. The functionally more important and broader A2 and A4 pulleys lie over the base of the proximal and middle phalanx respectively. There are 3 cruciate pulleys whose fibres run diagonally across the tendon and perpendicular to each other.

For the purpose of description, tendon injuries of the hand are divided up into zones. With respect to the deep and superficial flexors of the fingers, the anatomical location of the tendon insult can be ascribed to one of 5 zones. The most commonly affected zone with the poorest outcome of repair is zone 2.

## **1.4 ANIMAL MODELS IN THE STUDY OF TENDON HEALING**

A number of different animal models have been employed in the study of tendons, including, mouse (Wong, Lui et al. 2009; Katzel, Wolenski et al. 2010), rat (Iwuagwu and McGrouther 1998; Ishiyama, Moro et al. 2010), chicken (Chen, Zhou et al. 2009; Bhavsar, Shettko et al. 2010; Ishiyama, Moro et al. 2010; Yilmaz, Avci et al. 2010), rabbit (Khan, Edwards et al. 1996; Abrahamsson 1997; Chang, Most et al. 1998; Kakar, Khan et al. 1998; Berglund, Reno et al. 2006; Healy, Mulhall et al. 2007; Branford, Mudera et al. 2008; Liu, Skardal et al. 2008; de Wit, de Putter et al. 2009; Klass, Rolfe et al. 2009; Branford, Brown et al. 2010; Dogramaci, Kalac et al. 2010; Henn, Kuo et al. 2010; Ozboluk, Ozkan et al. 2010; Tan, Nourbakhsh et al. 2010), dog (Gelberman, Boyer et al. 1999; Zhao, Zobitz et al. 2009; Thomopoulos, Kim et al. 2010; Zhao, Sun et al. 2010), pig (Hausmann, Vekszler et al. 2009), sheep (Haddad, Peltz et al. 2010), cow (Samiric, Ilic et al. 2004; Hausmann, Vekszler et al. 2009), horse (Lin, Moolenaar et al. 2006; Schnabel, Lynch et al. 2009), and monkey (Manske, Lesker et al. 1985; Russell and Manske 1990). Comparisons between species have also been conducted (Gelberman, Manske et al. 1984; Hausmann, Vekszler et al. 2009).

### **1.4.1 *In Vitro* Tendon Healing Models**

*In vitro* tendon cell culture has been widely adopted in order to examine a range of different processes thought to be involved in tendon healing. Techniques for acquisition of tendon cells for culture include explanting, enzymatic digestion and tissue dicing. By far the most popular method of obtaining cells in culture is the explant method (Klass, Rolfe et al. 2009; Branford, Brown et al. 2010). A segment

of tendon is dissected and then incubated in sterile culture media. Cell monolayers can be obtained within 2 to 5 weeks.

When using *in vivo* animal models of tendon healing, a multitude of biological processes directly or indirectly affects the repair, some of which the researcher has no control over. Investigators must try to standardise these variables. In contrast, *in vitro* models enable assessment of only isolated changes in the culture environment.

Whilst tendons from different species undergo similar steps to effect repair in culture, they do so at different rates. Gelberman and colleagues compared rabbit, chicken, dog and monkey tendons sustained in culture for 3 months (Gelberman, Manske et al. 1984). A characteristic sequence of repair, including tendon surface thickening, cell differentiation, cell migration, and phagocytosis was demonstrated. Rabbit tendons showed nearly complete closure of the repair site by 12 weeks. A lesser response was seen in chicken, followed by dog and monkey. This repair in culture in absence of extrinsic cell input has also been demonstrated in human tendon culture (Mass and Tuel 1989; Mass and Tuel 1990). Whilst repair seen in culture has many parallels with its *in vivo* counterpart, it appears to progress in a slower and less regulated fashion (Abrahamsson, Lundborg et al. 1991).

#### **1.4.2     *In Vivo* Tendon Healing Models**

In order for improvements in the outcome of tendon repair to be made in humans, research relies on essential animal work. These models allow hypotheses of disease pathogenesis and its treatment to be rigorously tested. Important criteria should be adhered to when choosing a model, so that comparisons can be drawn with the

human condition under investigation. The size of animal should be large enough to allow adequate and reproducible tissue manipulation. The animal must be available and affordable, giving sufficient numbers to allow statistical comparison. Finally, the tissue must be amenable to measurement in a controlled reproducible fashion (Carpenter, Thomopoulos et al. 1999).

### **1.4.3 Rabbit Tendon Healing Model**

The rabbit has been used extensively *in vitro* and *in vivo* to examine flexor tendon healing and peritendinous adhesion formation (Khan, Edwards et al. 1996; Abrahamsson 1997; Chang, Most et al. 1998; Kakar, Khan et al. 1998; Berglund, Reno et al. 2006; Healy, Mulhall et al. 2007; Branford, Mudera et al. 2008; Liu, Skardal et al. 2008; de Wit, de Putter et al. 2009; Klass, Rolfe et al. 2009; Branford, Brown et al. 2010; Dogramaci, Kalac et al. 2010; Henn, Kuo et al. 2010; Ozboluk, Ozkan et al. 2010; Tan, Nourbakhsh et al. 2010). The rabbit was used in this thesis to investigate both *in vitro* and *in vivo* tendon healing. Rabbit is relevant to man in terms of cellular behaviour during healing and structural anatomy. Deep flexor tendons of the forepaw have gained popularity due to their accessibility and ease of use (Ngo, Pham et al. 2001; Henn, Kuo et al. 2010; Tan, Nourbakhsh et al. 2010). The hind deep flexors have also been used (Malaviya, Butler et al. 1998; Churei, Yoshizu et al. 1999). In this thesis the grooming forepaw was chosen over the hind paw as it is functionally more akin to human hand tendons.

### **1.4.4 Types of Tendon Injury**

In previous experiments the nature of the tendon injury has varied greatly for studying tendon healing and repair. It has ranged from complete transection and

repair (Chang, Thunder et al. 2000; Ngo, Pham et al. 2001; Chen, Cao et al. 2008; Tan, Nourbakhsh et al. 2010), partial transection (Zhao, Moran et al. 2007; Dogramaci, Kalac et al. 2010), crush injury, avulsion injury or partial tenotomy window (Matthew, Moore et al. 1987; Iwuagwu and McGrouther 1998; Kakar, Khan et al. 1998; Akali, Khan et al. 1999; Khan, Kakar et al. 2000; Jones, Burnett et al. 2002; Harrison, Mudera et al. 2003). In this thesis partial tenotomy window was used. This has been used in several rabbit models (Kakar, Khan et al. 1998; Akali, Khan et al. 1999; Khan, Kakar et al. 2000; Jones, Burnett et al. 2002). This injury avoids the need for suture repair, thereby minimising the number of injury variables and allows for immediate postoperative mobilisation (Kubota, Manske et al. 1996; Chan, Fu et al. 1998).

Previous tendon immobilisation methods have used internal and external fixators, splints, casts and frames (Carlstedt, Madsen et al. 1986; Enwemeka, Spielholz et al. 1988; Murrell, Lilly et al. 1994; Palmes, Spiegel et al. 2002; Tan, Nourbakhsh et al. 2010). In this thesis, where immobilisation was required, a proximal division of the FDP tendon was used as in a previous flexor tendon adhesion model (Jones, Burnett et al. 2002). This avoided the need for a splint, for the purpose of animal welfare.

In this thesis a rabbit model was developed using the digital tendon-synovial complex in which the mechanical restriction was in one axis only. This facilitates assessment, enabling the restrictive nature of an adhesion to be defined in biomechanical terms.

## **1.5 THE EXTRACELLULAR MATRIX IN TENDON HEALING**

### **1.5.1 Phases of Tendon Healing**

Following tendon injury the process of tendon healing and adhesion formation can be divided into phases, distinguishable by specific peaks in a cascade of cellular and biochemical events. These phases overlap and their duration can vary greatly (Gomez 1995).

Almost immediately after tendon injury there is a phase of haemostasis and inflammation (Wong, Lui et al. 2009). During this phase there is an increase in Fn, which along with glycosaminoglycan, water and collagen type-III stabilise the newly formed ECM (Grinnell 1984).

A causative relation has been reported between Fn secretion and fibroblast chemotaxis and attachment to the ECM in the days after injury and repair (Gelberman, Steinberg et al. 1991). Well-hydrated provisional ECM supports cellular migration from tissue margins (Lorenz 2003).

The proliferative/fibroblastic phase occurs approximately from 3 days until 2 weeks. During this time, there is disorganised ECM of granulation tissue at the injury site. This is the precursor of adhesion tissue. This phase is characterised by fibroplasia, fibroblast migration and proliferation and ECM formation. Histologically, the predominant cell type here is the fibroblast (Stadelmann, Digenis et al. 1998). Fibroblasts proliferate and migrate (Yamada 1996; Greiling and Clark 1997). This is a phase of active ECM synthesis by the cells (Jozsa 1997). During this time there is

a sequential appearance of Fn and collagen (Kurkinen, Vaheri et al. 1980), with collagen type-I, collagen type-III and Fn being widespread throughout the ECM (Abrahamsson 1991).

The process of maturation, organisation and remodelling can last many months, fibroblasts depositing an increasingly mature, mechanically functional collagen matrix (Stadelmann, Digenis et al. 1998). There is optimisation of collagen synthesis and gradual conversion of collagen type-III to collagen type-I (Gomez 1995). During this time there is reduced ECM synthesis by the fibroblasts, collagen fibre reorientation and crosslinking.

### **1.5.2 Cell Interaction with the Extracellular Matrix**

Fibrous proteins of the tendon ECM constitute two subclasses: the structural collagens and elastin and the adhesive Fn and laminin that support the attachment and migration of cells (Abrahamsson 1991). The interaction of cells, ECM and growth factors affects adhesion, morphology, viability, gene expression and growth of cells (Hynes 2009; Schultz and Wysocki 2009). Subcomponents of ECM molecules can bind to cell surface receptors and affect cellular activities (Schultz and Wysocki 2009).

Human fibroblasts have differential properties when attaching to ECM proteins. In a study by Shimo-Oka and colleagues production of a Fn fragment following trypsinisation inhibited fibroblasts from attaching to and spreading on Fn (Shimo-Oka, Hasegawa et al. 1988). However, the Fn fragment did not cause inhibition of



attachment to collagen, vitronectin or laminin. This is the result of fibroblasts having different binding sites for different proteins.

The binding site for collagen in Fn is distinct from that interacting with cell surfaces, as cell attachment promoting activity is found with collagen-nonbinding fragments of Fn (Ruoslahti, Hayman et al. 1980). Therefore, strategies that prevent cell attachment to Fn based on non-collagen binding fragments of the Fn molecule may preserve cell to collagen binding. This may be a potential therapeutic mechanism to achieve a differential effect in cell binding. In this way, tendon healing may be preserved while adhesion formation is prevented. Attachment of cells to the ECM is investigated in this thesis. Intrinsic and extrinsic tendon fibroblasts and the cells found in healing tendon adhesions from immobilised and mobilised digits were investigated for differences in their attachment to collagen and Fn.

The relationship between changes in cell morphology and tissue strain is thought to occur through binding of cells to ECM proteins (Ingber 1991; Banes, Tsuzaki et al. 1995; Rosales, O'Brien et al. 1995). Therefore, in this thesis the effect of mobilisation on adhesion derived cell attachment, cell morphology and local tissue strain were examined.

### **1.5.3 Fibronectin**

Fn (from *fibra*, fibre and *nectere*, connect) is an important component of the early healing process (Grinnell 1984; Gelberman, Steinberg et al. 1991). Fn is, in its main functional form, a high molecular weight glycoprotein multimer which interacts with numerous ECM components and cell surfaces (Ruoslahti, Hayman et al. 1982)

(Figure 1.2). Fn has been found to bind to collagen, sulphated proteoglycans, hyaluronic acid, fibrin, fibrinogen, heparin, thrombin, plasmin and factor XIIIa (Hynes and Yamada 1982; Castellani, Siri et al. 1986). *In vitro* Fn is found associated with fibroblast membranes, cell culture surface and the culture medium (Sekiguchi, Siri et al. 1985).

Fn plays a major role in cell adhesion, promoting attachment and migration of fibroblasts on the ECM (Schwarzbauer 1991). Fn also acts as an intermediary scaffold for deposition of collagen by fibroblasts (Grinnell 1984). It is central to most aspects of cell phenotype behaviour during early tendon healing. In summary, Fn binding affects cell morphology, division and spreading, cytoskeletal organisation, migration, differentiation and haemostasis (Hynes and Yamada 1982).

Consequently, fibroblast to Fn adhesion is central to migration, collagen deposition and therefore fibrotic adhesion formation. Strategies that prevent fibroblast to Fn attachment without compromising fibroblast to collagen binding may prevent adhesion formation without compromising tendon cellularity. This concept is explored in this thesis through the *in vitro* and *in vivo* testing of a novel derivative Fn-fragment based biomaterial (DFn).

#### **1.5.3.1 Structure of Fibronectin**

Fn exists in two main forms, as an insoluble fibrillar dimer in the ECM, and as a soluble dimer in plasma, amniotic and synovial fluids (Akiyama, Hasegawa et al. 1985). These are known as cellular Fn and plasma Fn, respectively (Hayashi and Yamada 1981). Plasma Fn is secreted by hepatocytes. Cellular Fn is secreted by

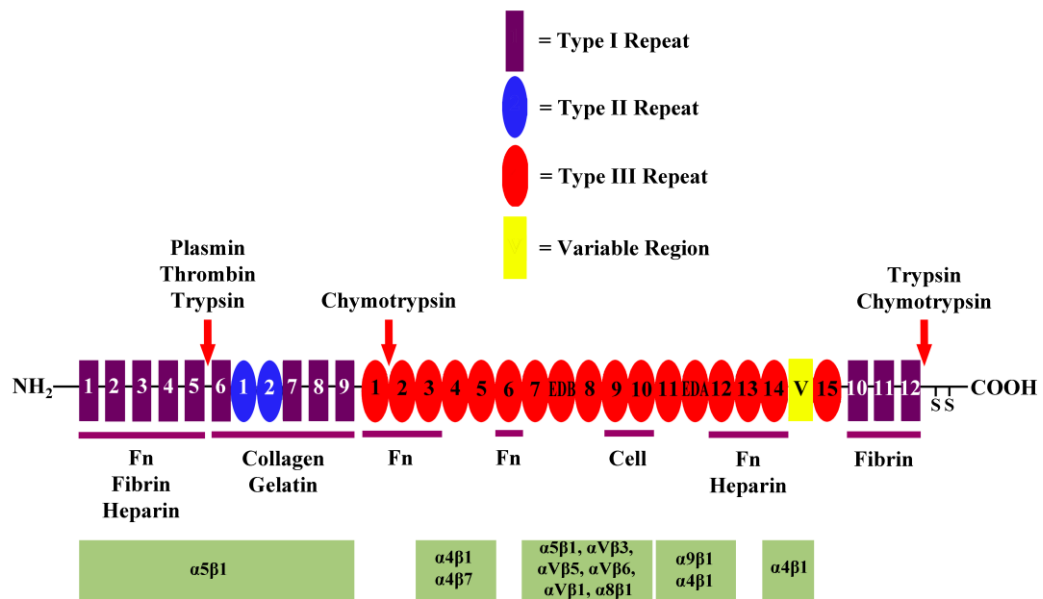


**Figure 1.2** A diagrammatic representation of the structure of a single strand of cellular fibronectin (Fn). Sites of major proteolytic digestion are shown (red arrows, above Fn molecule). Interaction sites for Fn with other molecules are shown (purple lines, below molecule). Sites for integrin binding are also shown (in green, below molecule). S = Disulphide bond.

fibroblasts and many other cell types and is incorporated into a fibrillar matrix on the cell surface (Hynes 1990).

The Fn molecule consists of 2 nearly identical subunits, each of between 220 and 250 kDa molecular weight, joined at the C-terminus (Johansson, Svineng et al. 1997). The 2 subunits are covalently linked by a pair of disulphide bonds, and may exist as a homodimer of 2 identical subunits or a heterodimer of 2 similar but non-identical subunits (Hynes 1990). The subunits of Fn are flexible, and can exist in a compact globular form or extend into an elongated, fibrous form (Ejim, Blunn et al. 1993; Phillips, King et al. 2004).

Each Fn monomer is made up of homologous modules of 40-90 amino acids, classified as type I, II, or III repeats or modules (Miyamoto, Katz et al. 1998). Each Fn subunit contains 12 type I repeats, located near the N and C termini, 2 type II repeats at the N terminus, and 15-17 type III repeats encoded in the Fn gene (Hohenester and Engel 2002). Types I and II repeats contain 2 intrachain disulphide bonds while type III repeats do not have disulphide bridges. Each type I repeat is made of  $\beta$ -sheets surrounding a hydrophobic core. Type II repeats consists of 2 anti-parallel  $\beta$ -sheets, linked by disulphide bonds and perpendicular in relation to each other (Constantine, Brew et al. 1992). The type III repeats are composed of 7  $\beta$ -strands arranged in 2 anti-parallel  $\beta$ -sheets, enclosing a hydrophobic core (Copie, Tomita et al. 1998).

### **1.5.3.2 Fibronectin Binding Domains**

Some of the early work with plasma Fn molecule identified the Fn binding domains using affinity chromatography and molecular mass on Fn proteolytic digests, as Fn is sensitive to proteases. Collagen, heparin, fibrin, gelatin and cell binding domains were identified this way (Hayashi and Yamada 1983; Zardi, Carnemolla et al. 1985). Relative positions of the corresponding domains in intact Fn are now well characterised (Hynes 1990).

Fn mediates attachment of different cell types to the rest of the ECM via several cell-binding sites distributed in the type III repeating modules. The major cell-binding site located in the central region of the tenth type III repeat, bearing the amino acid sequence arg-gly-asp-ser (RGDS), and its synergistic sequence in the III9 module pro-his-ser-arg-asn (PHSRN), are recognised by cell adhesion receptor integrin  $\alpha 5\beta 1$  (Aota, Nomizu et al. 1994). Blocking of either site with monoclonal antibodies leads to a greater than 90% reduction in cell spreading of baby hamster kidney (BHK) cells (Nagai, Yamakawa et al. 1991).

The heparin binding domain (Hep 2), consisting of 12-14 type III repeats has 6 major cell adhesive sites that mediate RGDS-independent, heparin dependent cell adhesion. Heparin is abundant on cell surfaces and in the ECM. The IIICS region is recognised by the integrin receptor  $\alpha 4\beta 1$  (Mould, Komoriya et al. 1991). Recently, it has been suggested that alternative splicing of the IIICS domain may influence signalling between cell surface heparan proteoglycans and Hep 2 binding domain of Fn (Santas, Peterson et al. 2002). In this way, Fn can mediate with cell surface adhesive

sites and hence has the ability to regulate cellular processes like growth, spreading, migration, and differentiation.

#### **1.5.3.3 Fibronectin Fragments Inhibit Cell Attachment**

Attachment of cells to Fn is inhibited by some fragments of Fn. These include a soluble GRGDSC fragment (Streeter and Rees 1987), 2 synthetic RGD containing peptides (Yamada and Kennedy, 1984), and a 10-residue peptide including the RGD sequence (Sethi et al., 2002). This inhibition is competitive, non-cytotoxic and reversible (Yamada and Kennedy 1984). Although there is negligible binding of Fn to cells in suspension (Carter, Rauvala et al. 1981), high concentrations of plasma Fn almost completely inhibit fibroblastic cell adhesion to a Fn substrate (Yamada and Kennedy 1984; Yamada, Akiyama et al. 1985). RGD peptides have been shown to prevent focal adhesion formation (Wang, Collighan et al. 2010), which is required for cell attachment. Fn-derived fragments, possessing anti-adhesive properties, may provide a therapeutic strategy to reduce cell attachment. This may modify subsequent deposition of adhesion tissue *in vivo*. A novel biomaterial with potential anti-adhesive properties is tested in this thesis *in vitro* and *in vivo*.

#### **1.5.3.4 Fibronectin Matrix Assembly**

Fn matrix assembly is a cell-mediated step-wise process that converts soluble Fn into an organised matrix of Fn fibrils presenting binding sites to orchestrate assembly of several other extracellular proteins (Hynes 2009). Subjecting the Fn molecule to tensile forces through mechanical shearing and at a moving plastic-liquid interface results in Fn self-assembly (Ejim, Blunn et al. 1993; Brown, Blunn et al. 1994). Fn fibril formation is the result of Fn interacting with cell surface integrins, which

initiate a process involving conformational activation of Fn outside and organisation of the actin cytoskeleton inside. Apart from supporting the cell adhesion process, cell surface receptors, and notably the  $\alpha 5\beta 1$  receptor, are also involved in assembly of inactive soluble Fn dimers into insoluble Fn fibrils to further support the cell adhesion process (Huveneers, Truong et al. 2008).

Firstly, Fn accumulates at focal adhesions where integrins bind to the RGD site. This induces conformational change of Fn, exposing a site near its N-terminus that binds to  $\alpha 5\beta 1$  integrins on the cell surface (Johansson, Svineng et al. 1997). This process is saturable and reversible (Magnusson and Mosher 1998), and is required for Fn fibrillogenesis (Wierzbicka-Patynowski and Schwarzbauer 2003). Over-expression of  $\alpha 5\beta 1$  results in a large increase in Fn assembly, whereas  $\beta 1$  knockout cells are unable to assemble a Fn matrix (Zhang, Sakai et al. 1999). Fn molecules lacking the 70 kDa N-terminal fragment containing the  $\alpha 5\beta 1$  binding site do not assemble into fibrils (Magnusson and Mosher 1998; Wierzbicka-Patynowski and Schwarzbauer 2003).

Initial  $\alpha 5\beta 1$ -Fn binding occurs at focal adhesions. As a dimeric ligand, Fn induces  $\alpha 5\beta 1$  integrin aggregation which results in increase in the local external concentration of Fn and internal co-localisation and phosphorylation of focal adhesion kinase (FAK) (Wierzbicka-Patynowski and Schwarzbauer 2003). Activated FAK recruits Src and these kinases mediate early assembly (Wierzbicka-Patynowski and Schwarzbauer 2003). The  $\alpha 5\beta 1$  integrin, still bound to Fn, then translocates from the focal adhesion to fibrillar adhesions. Acto-myosin generated tension is translocated to Fn, via the  $\alpha 5\beta 1$  integrin, stretching the globular protein into a linear

conformation that promotes fibrillogenesis by exposing 4 cryptic self-association sites (Pankov, Cukierman et al. 2000).

Initially Fn fibrils are short and only extend from cell to neighbouring cell or nearby substrate. As more Fn accumulates the fibrils become more stable and are thought to be gradually converted into high molecular weight, disulphide-stabilised multimers (Wierzbicka-Patynowski and Schwarzbauer 2003).

Fn in solution exists as a compact folded dimer, incapable of undergoing fibril assembly. Extension of the Fn molecule occurs in solution by changes in pH, ionic strength, or mechanical shear (Phillips, King et al. 2004). It is clear that forces generated by mobile cells may be important in Fn fibril shear aggregation and assembly, in a manner analogous to Fn shear aggregation used at the gross level to prepare scaffolds (Ejim, Blunn et al. 1993; Phillips, King et al. 2004).

#### **1.5.4 Collagen**

The word ‘collagen’ is derived from the Greek word for ‘glue’. This super family of ECM proteins comprises 15-35% of all proteins in the human body.

##### **1.5.4.1 Collagen Synthesis**

Collagen is constitutively synthesised by fibroblasts and other connective tissue cells (Parsons, Kessler et al. 1999). Individual polypeptide chains are generated at free ribosomes as precursor prepropeptides called pro- $\alpha$  chains. These pro- $\alpha$  chains undergo processing in the endoplasmic reticulum and Golgi apparatus (Canty and Kadler 2005). Proline and lysine residues are hydroxylated to hydroxyproline and



hydroxylysine and a proportion of the hydroxylysine residues are glycosylated. This is followed by the assembly of 3 pro- $\alpha$  chains to form a procollagen triple helix. This is initiated by folding and disulphide bond formation within the C-terminal extensions (Canty and Kadler 2005). The protein is then shuttled directly and continuously from the trans-Golgi network to the cell membrane in coated vesicles and secreted into the ECM (Ross 1975). Cleavage of the amino and carboxy-terminal extensions by peptidases reduces solubility of the molecule and leads to the spontaneous formation of collagen fibres (Mayne and Brewton 1993).

Despite the ability of collagens to spontaneously form fibrils *in vitro* collagen fibrillogenesis is tightly controlled by cells *in vivo* (Stopak, Wessells et al. 1985). Fibrillogenesis may also be affected by the small leucine-rich proteoglycan decorin, which is prevalent in collagenous tissues, interacts with Fn and affects TGF- $\beta$ 1 activity (Douglas, Heinemann et al. 2006). The final diameter of fibrils varies between tissues depending on their function. Large fibrils, around 500 nm, can be found in mature tendon, which are subjected to tensile strain (Jokinen, Dadu et al. 2004). Collagen fibrillogenesis has been shown to require a Fn matrix, collagen-Fn binding and be influenced by the collagen binding integrins  $\alpha$ 2 $\beta$ 1 and  $\alpha$ 11 $\beta$ 1 (Velling, Risteli et al. 2002; Canty and Kadler 2005).

#### **1.5.4.2 Fibronectin and Collagen Binding**

The effect of Fn on collagen type-I has been widely studied (Yamada and Okigaki 1983; Gildner, Lerner et al. 2004). Fn only contains one binding site for all collagens. Denatured collagen I binds this site more effectively than native collagen type-I; and collagen type-III binds more effectively than collagens I and II (Hynes

1990). Presence of Fn has been reported to increase the attachment of epithelial cells to collagen type-I coated tissue culture plastic (Johansson, Svineng et al. 1997), and to decrease the rate of migration of neonatal and foetal fibroblasts on collagen I coated glass (Park, Park et al. 2001); presumably by increased adhesion. However, Burrill and colleagues found that whilst pre-adsorbed Fn increased attachment of rabbit intestinal epithelial cells to collagen I, soluble Fn in the medium did not (Burrill, Bernardini et al. 1981).

### **1.5.3 An Extracellular Matrix Gradient**

#### **1.5.5.1 A Spatial Extracellular Matrix Gradient**

##### ***1.5.5.1.1 Tendon Surface Cells Produce More Collagen Than Synovial Sheath Cells***

Tendon cells have been shown to produce three times as much collagen *in vitro* than synovial sheath cells (Riederer-Henderson, Gauger et al. 1983). During the first 2 weeks in *in vitro* tendon culture, tendon surface cells have been shown to proliferate, migrate and encapsulate the tendon (Mass and Tuel 1989). In contrast, tendon core cells have been shown to produce collagen after 2 weeks in culture (Gelberman, Manske et al. 1984; Manske, Gelberman et al. 1984). Russell and Manske confirmed that tendon surface cells have a role in collagen production in culture at an earlier time-point than tendon core fibroblasts (Russell and Manske 1990). Gelberman and colleagues later confirmed that tendon surface cells contribute the greatest quantity of native tendon collagen to the repair site during early intervals after tendon suture (Gelberman, Amiel et al. 1992). These authors used an *in situ* hybridisation technique to analyse production of pro-alpha (I) collagen messenger RNA in repaired intrasynovial flexor tendons. This was to determine the precise mechanism

by which tendon healing occurs at the cellular level treated with early controlled passive mobilisation. They showed that increasing levels of collagen activity were detected through 10 days, decreasing at 17 days. Genetic expression of procollagen mRNA was localised specifically to the tendon surface cells overlying the repair site and to cells in the gap between the tendon stumps. No detectable expression was noted in the tendon core fibroblasts.

#### ***1.5.5.1.2 Synovial Sheath Cells Produce More Fibronectin than Tendon Cells***

Banes and colleagues have shown qualitatively with immunological staining that synovial sheath cells, rather than tendon derived cells preferentially secrete Fn both *in vitro* and *in vivo* (Banes, Link et al. 1988). Brigman and colleagues later confirmed using an enzyme-linked immunosorbent assay that synovial sheath fibroblasts in culture produce higher levels of Fn than cells derived from the tendon core (Brigman, Hu et al. 1994). Primary cell cultures from these tissues and their secretions were also assayed for Fn levels using the polymerase chain reaction and northern blot analysis. Levels of Fn in tendon surface were almost 4-fold higher than in the tendon core, and levels in the outer sheath were 21-fold greater than in the inner portion of sheath. These *in vitro* experiments suggested that this preponderance of Fn associated with the synovial sheath was not the product of plasma deposition but of local cell synthesis. In addition, the synovial cells secreted significantly greater amounts of Fn than remained cell associated, whereas there was no difference in secreted and cell-associated Fn levels from the tendon core fibroblasts. The steady-state levels of Fn mRNA were almost 2-fold greater with the synovial cells than with the tendon cells by RT-PCR. This was supported by a proportionately greater level of Fn mRNA quantitated by northern blot. This study showed that the

majority of Fn found in the tendon complex is produced and exists within the synovial sheath layer. It could be argued that there is an anatomical or spatial distribution of Fn within the healing tendon-synovial complex with higher Fn levels closer to the synovial layer (Figure 1.1). Recently, it has been found that TGF- $\beta$ 1 upregulates Fn production in tendon core, tendon surface and synovial sheath fibroblasts and may explain why the growth factor it is associated with tendon adhesion formation (Klass, Rolfe et al. 2009).

#### **1.5.5.2 A Temporal Extracellular Matrix Gradient**

Following tendon injury granulation tissue is initially largely Fn based and becomes more collagenous over time. During the fibroblastic phase of tendon healing there is a sequential appearance of Fn and collagen (Kurkinen, Vaheri et al. 1980). There is also sequential utilisation of Fn then collagen receptors for cell to ECM attachment during healing (Sethi, Yannas et al. 2002). Mature tendon is a highly collagenous structure, akin to an ‘end-product’ of the healing process. It follows from these observations that there is both a temporal gradient (as healing progresses) and spatial gradient (from the synovial sheath to the tendon) from a Fn-based matrix to a collagen-based matrix. Previous authors have identified spatial and temporal-specific aspects to the healing process in a rabbit flexor tendon injury model (Berglund, Reno et al. 2006). They demonstrated a shift in collagen expression over time in the tendon and the sheath. Wong and colleagues demonstrated that the peak in collagen type-I production was later for tendon than in peritendinous tissues (Wong, Lui et al. 2009). These concepts suggest that a differential effect on tendon healing may be possible using an approach based on the selective prevention of cell attachment. A reduction in adhesion formation may be achieved by preventing peritendinous cell attachment

to Fn, while maintaining cellularity at the collagenous tendon surface. This forms the basis of the *in vitro* and *in vivo* testing of the novel biomaterial in this thesis.

### **1.5.6 Integrins**

Integrins are a super family of heterodimeric transmembrane protein cell surface receptors. Integrins are important in cell-cell adhesion and cell-ECM adhesion, migration, division, differentiation, wound healing, morphogenesis, orientation, immune recognition, development and programmed cell death in vertebrate organisms (Katz and Yamada 1997; Damsky and Ilic 2002; Rosso, Giordano et al. 2004).

Integrins provide a physical and biochemical bridge that links the ECM to the intracellular environment both physically to the actin cytoskeleton and biochemically to signaling pathways controlling metabolism and gene expression (Schwartz 2001) (Figure 1.3). In this way integrins mediate signal transduction and mechanical force through the plasma membrane in both directions (Liu, Calderwood et al. 2000). Integrin-mediated responses include the aggregation of receptors, activation of signal transduction, cytoskeletal rearrangements and co-regulation of growth factor activities (Rosso, Giordano et al. 2004).

#### **1.5.6.1 Structure of Integrins**

Different combinations of  $\alpha$  and  $\beta$  subunits give rise to receptors with different ligand specificities, including receptors for Fn, vitronectin, collagen and laminin. Both  $\alpha$  and  $\beta$  subunits are subject to alternative splicing and post-translational modifications (Arnaout, Goodman et al. 2002). Both subunits are type I

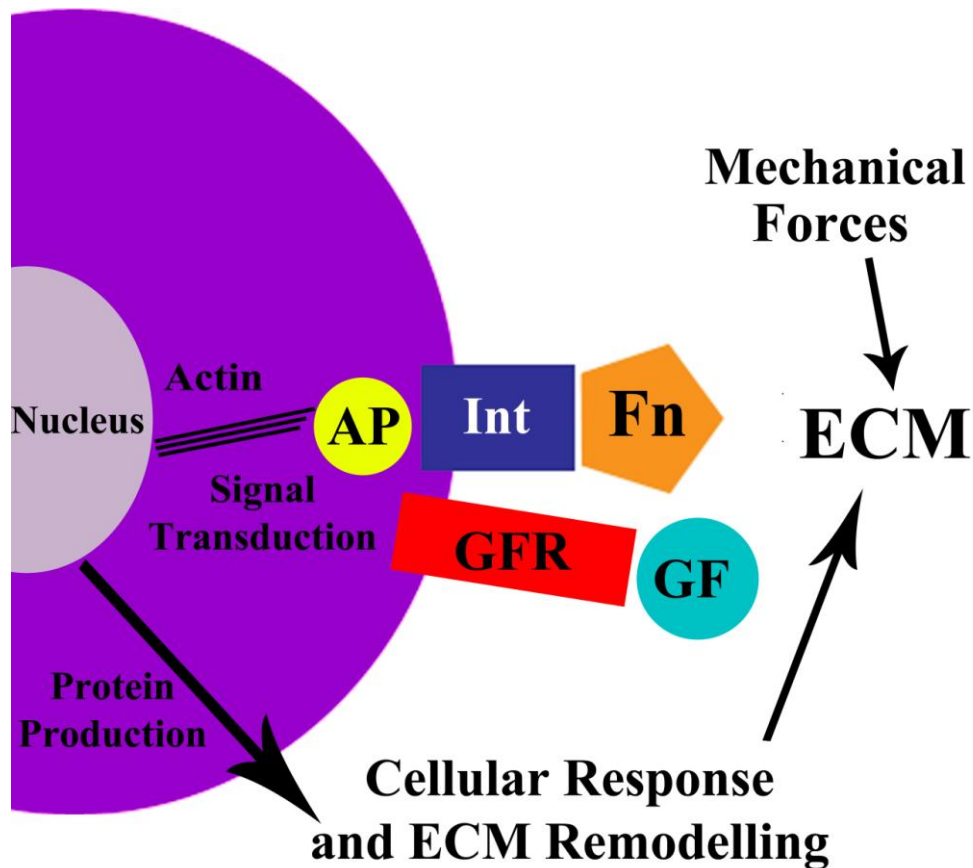


**Figure 1.3** A diagrammatic representation of the common pathway linking growth factor signalling and local mechanical forces through the integrin receptor via the cytoskeleton and intracellular signal transduction to the cell nucleus. Growth factors released by fibroblasts in response to local mechanical stimuli modulate signaling events that lead to gene expression and protein synthesis. Integrin-growth factor cross-talk may be due to proximity of growth factor receptors and ligand-integrin interactions in focal adhesion complexes, or modulation of growth factor receptor activity by adaptor protein recruitment or receptor internalisation. The binding, or prevention of binding, of fibronectin (Fn) to integrins may be a target that has wide ranging effects on modifying the nature of adhesions. Int = integrin. GF = Growth Factor. GFR = Growth Factor Receptor, AP = Adaptor Proteins.

transmembrane proteins expressed on the cell surface membrane (Calderwood, Shattil et al. 2000) (Figure 1.4). There are several  $\alpha$  subunits ( $\alpha 1$  to  $\alpha 11$ ,  $\alpha \text{Ib}$ ,  $\alpha \text{D}$ ,  $\alpha \text{E}$ ,  $\alpha \text{L}$ ,  $\alpha \text{M}$ ,  $\alpha \text{V}$  and  $\alpha \text{X}$ ) and  $\beta$  subunits ( $\beta 1$  to  $\beta 8$ ) identified forming a number of different integrins (Humphries, Byron et al. 2006). The  $\alpha$  and  $\beta$  subunits each contain a large, N-terminal extracellular domain, a single C-terminal transmembrane domain and a cytoplasmic domain that in most cases consists of 20-70 amino acid residues (Calderwood, Shattil et al. 2000).

Integrins are able to bind multiple ligands (Katz and Yamada 1997). For instance,  $\alpha \text{V}\beta 3$  integrin binds to vitronectin, Fn, fibrinogen, von Willenbrand factor, thrombospondin and osteopontin. Further, several integrins may bind to one ligand. Fn is an example of this, as it currently binds to 10 integrins. This does not necessarily result in redundancy as the intracellular signals generated depend on the specific combination of ligand and integrin.

#### **1.5.6.2 Integrins for Collagen Binding**

Collagen is recognised by 5 members of the integrin family:  $\alpha 1\beta 1$ ,  $\alpha 2\beta 1$ ,  $\alpha 3\beta 1$ ,  $\alpha 10\beta 1$  and  $\alpha 11\beta 1$  (Xu, Gurusiddappa et al. 2000; Tulla, Pentikainen et al. 2001). Expression of these integrins is cell type dependent (Nykqvist, Tu et al. 2000).

#### **1.5.6.3 Integrins for Fibronectin Binding**

Fn is recognised by 10 members of the integrin family:  $\alpha 3\beta 1$ ,  $\alpha 4\beta 1$ ,  $\alpha \text{Ib}\beta 3$ ,  $\alpha \text{V}\beta 3$ ,  $\alpha \text{V}\beta 1$ ,  $\alpha \text{V}\beta 5$ ,  $\alpha \text{V}\beta 6$ ,  $\alpha 5\beta 1$ ,  $\alpha 8\beta 1$  and  $\alpha 4\beta 7$  (Pankov and Yamada 2002).  $\alpha 5\beta 1$  was the first integrin found to bind to Fn, it is also the only integrin to bind solely to Fn and as such, it is often referred to as 'the Fn integrin'. Integrin  $\alpha 5\beta 1$  is involved in

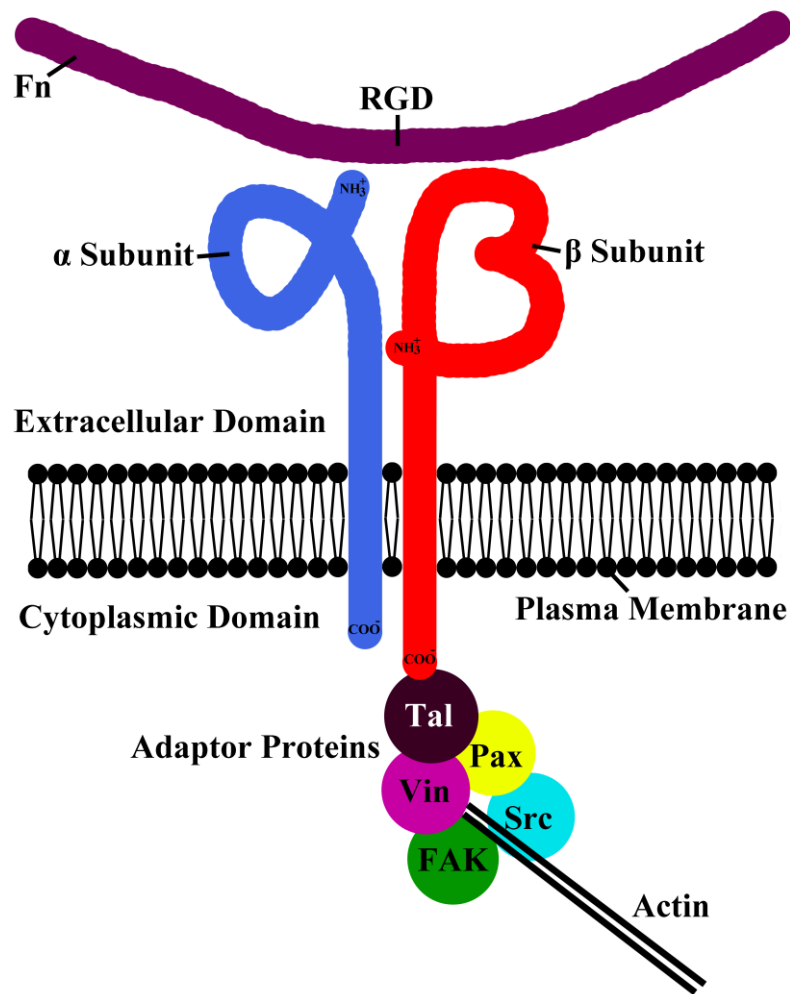


**Figure 1.4** A diagrammatic representation of a transmembrane integrin receptor. A representative  $\alpha 5 \beta 1$  receptor is shown attached to the RGD central cell binding site of fibronectin. The cytoplasmic adaptor proteins and associated protein tyrosine kinases are also shown. With this arrangement forces may be transmitted across the plasma membrane in both directions. Integrin-ligand binding results in the activation of intracellular proteins via the action of the protein kinases. Tal = Talin; Pax = Paxillin; Vin = Vinculin; FAK = Focal Adhesion Kinase.



adhesion, binding to Fn fibrils, slowing of cell migration and is crucial for assembly of a Fn matrix (Zamir, Katz et al. 2000; Wierzbicka-Patynowski and Schwarzbauer 2003). Most Fn integrins recognise the RGD sequence on the 10<sup>th</sup> type III repeat, however, there are several other binding sites for integrins.

#### **1.5.6.4 Integrin Activation**

Integrin activation is a complex process involving several factors that affect the avidity of integrin-ligand binding. Integrin avidity is under tight spatial and temporal control (Calderwood, Shattil et al. 2000). Occupancy by a ligand is one of the main events in integrin activation (LaFlamme, Akiyama et al. 1992). Ligand occupancy alone results in integrin localisation to pre-existing contacts but not FAK phosphorylation (Yamada, Pankov et al. 2003). Formation of cell-cell contacts reduces migration, cell-surface protrusion and actin cytoskeletal dynamics (Braga 2000). Integrin clustering, or aggregation, is another event important in integrin function (LaFlamme, Akiyama et al. 1992). Integrins are dispersed at the cell surface but become aggregated at cell-ECM adhesion sites during binding (Singer, Scott et al. 1988).

#### **1.5.6.5 Cell-Extracellular Matrix Attachments**

Binding of integrins with their ECM ligands results in the formation of large, stable, cytoplasmic, multi-protein assemblies composed of both cytoskeletal and signalling molecules (Katz and Yamada 1997; Danen and Yamada 2001). Formation of these cell-substrate adhesions requires integrin-ligand binding, integrin clustering, tyrosine phosphorylation events and actin cytoskeleton integrity (Danen and Yamada 2001). Composition and activity of these assemblies is regulated by the nature of the

integrin-ligand interaction, and intracellular regulators including protein tyrosine kinases (PTKs) and phosphatases and guanine triphosphate (GTP)ases (Katz and Yamada 1997).

Four types of cell-ECM attachment have currently been described; these are known as focal complexes, focal adhesions, fibrillar adhesions and mosaic adhesions.

#### ***1.5.6.5.1 Focal Complexes***

The term 'point contact' refers to the short-lived adhesions formed at the leading edges of lamellopodia (Riveline, Zamir et al. 2001; Zaidel-Bar, Ballestrem et al. 2003). These can mature into focal complexes (Galbraith, Yamada et al. 2002). Time-dependent analysis of these adhesions revealed that they are formed by  $\alpha V\beta 3$  integrins which become tyrosine phosphorylated. Focal complexes are precursors of focal adhesions (Galbraith, Yamada et al. 2002). Maturation from focal complex to focal adhesion requires both tensile force and intracellular signalling (Zamir, Katz et al. 2000; Riveline, Zamir et al. 2001; Galbraith, Yamada et al. 2002). This force can be generated from either inside or outside the cell (Galbraith, Yamada et al. 2002).

#### ***1.5.6.5.2 Focal Adhesions***

One common pathway for force transmission is via focal adhesions. Focal adhesions, also known as focal contacts, are mature, elongated, attachments (Riveline, Zamir et al. 2001). The number, size and distribution of these vary between cell types (Braga 2000). Focal adhesions are promoted by the stiffness of the underlying ECM. They are the major link connecting the ECM to the actin cytoskeleton through integrin receptors (Geiger, Spatz et al. 2009). Focal adhesions are generally associated with

the end of actin stress fibres (Zamir, Katz et al. 1999; Rivelino, Zamir et al. 2001), where they act as anchoring sites and are therefore under isometric tension (Pankov, Cukierman et al. 2000). Time dependent analysis of focal adhesions with GFP-paxillin revealed that they are highly dynamic (Zamir, Katz et al. 2000).

#### ***1.5.6.5.3 Fibrillar Adhesions***

Fibrillar adhesions are also known as ECM contacts or adhesion plaques (Zamir, Katz et al. 1999). They are elongated or beaded in structure and are located more centrally than focal adhesions (Katz, Zamir et al. 2000). Tensin,  $\alpha 5$  and  $\beta 1$  also co-localise with the thin actin fibrils that associate with fibrillar adhesions (Katz, Zamir et al. 2000). Fibrillar adhesions are observed on the exterior surface of the plasma membrane (Katz, Zamir et al. 2000).

Fibrillar adhesions emerge from the ends of focal adhesions and are transported towards the cell centre in an actomyosin dependent manner (Zamir, Katz et al. 2000). Formation of fibrillar adhesions involves mobilisation and reorganisation of extracellular Fn and this ECM mobilisation is responsible for the segregation of focal adhesions and fibrillar adhesions (Katz, Zamir et al. 2000). If Fn is prevented from moving, for example by covalent attachment to a surface, fibrillar adhesions do not form. Instead, large focal adhesions containing integrins  $\alpha V\beta 3$  and  $\alpha 5\beta 1$ , and tensin, vinculin, paxillin and phosphorylated tyrosine residues form. Cells plated on covalently attached Fn show little Fn fibrillogenesis (Katz, Zamir et al. 2000; Zamir, Katz et al. 2000).

Analysis of fibrillar adhesions with GFP-tensin revealed that they are highly dynamic (Zamir, Katz et al. 2000) and are motile under tensile stress (Pankov, Cukierman et al. 2000).

#### **1.5.6.5.4 Mosaic Adhesions**

Between mature focal adhesions and newly formed fibrillar adhesions Zamir and colleagues observed ‘mosaic’ adhesions (Zamir, Katz et al. 1999). These contain a combination of classical focal adhesion proteins and fibrillar adhesion proteins organised in a polarised manner (Zamir, Katz et al. 2000).

#### **1.5.6.6 Focal Adhesion Kinase**

FAK was first identified in 1991 as a non-receptor tyrosine kinase activated by integrin mediated adhesion (Guan, Trevithick et al. 1991). Integrin aggregation results in localisation of FAK at sites of adhesion, but FAK phosphorylation relies on an intact actin cytoskeleton (Gemba, Valbracht et al. 2002). The response is modulated by growth factors via the actin cytoskeleton (Guan 1997).

FAK phosphorylation precedes cell spreading and stable adhesions, and FAK null cells spread more slowly on ECM proteins, have enhanced focal adhesions and impaired migration. As such, FAK is thought to play a role in focal adhesion assembly (Guan 1997; Parsons 2003; Wozniak, Modzelewska et al. 2004). Interestingly, studies of focal adhesions of cells in 3-dimensional matrices show differences from those on 2-dimensional matrices including poor phosphorylation of FAK. FAK may, therefore, not be as important *in vivo* as *in vitro* (Yamada, Pankov et al. 2003; Wozniak, Modzelewska et al. 2004). The major downstream effect

controlled by FAK is cell migration, but it is also important in the control of cell adhesion, survival, and growth, actin polymerisation and protein degradation.

#### **1.5.6.7 Signalling Via the Actin Cytoskeleton**

Integrin mediated attachment to ECM proteins initiates reorganisation of the actin cytoskeleton, which results in changes in cell shape and increased tension, influencing cellular behaviour and gene expression. Cell spreading has been found to be important in many responses to cell adhesion. Rapid cell spreading on ECM proteins occurs within the first 4 to 6 hours. However, F-actin is required for cell spreading over the next 48 hours (Mooney, Langer et al. 1995). Cell attachment to laminin, Fn, collagen I or collagen IV results in a 20-fold increase in F-actin mass within 30 minutes, before any significant changes in cell shape, and does not require protein synthesis (Mooney, Langer et al. 1995). Disruption of the actin cytoskeleton results in loss of attachment and spreading and inactivation of several signalling pathways (Assoian 1997).

Integrins action via the cytoskeleton is mediated by actin binding proteins. These bind primarily with  $\beta$  subunit cytoplasmic tails and modulate actin cytoskeletal dynamics. Actin binding proteins include  $\alpha$ -actinin, talin, filamin, tensin, vinculin and paxillin (Parsons 2003). Talin,  $\alpha$ -actinin and filamin localise to focal adhesions and are associated with focal complex formation and force-dependent adhesion strengthening (Wozniak, Modzelewska et al. 2004). Talin is a key player in integrin activation, acting as an intracellular ligand: interaction of talin with integrin cytoplasmic tails causes conformational changes within the extracellular domains, which increase binding affinities for ECM ligands at the cell surface (Calderwood

2004; Shattil, Kim et al. 2010).  $\alpha$ -actinin and filamin are also localised along stress fibres, and in the case of filamin, along cortical actin fibres. Their recruitment to  $\beta 1$ -integrin containing focal adhesions is stimulated by mechanical stress and leads to F-actin recruitment (Liu, Calderwood et al. 2000).

There are three types of cytoskeleton within cells: microtubules, intermediate filaments and microfilaments (Qin, Buehler et al. 2010). Microfilaments, chiefly actin filaments, have several essential roles in the normal function of eukaryotic organisms. These include cell locomotion, cell spreading and cell division as well as membrane dynamics (Chen, Bernstein et al. 2000). Actin filaments act in a number of different subcellular structures including focal adhesions, dorsal arcs, stress fibres and dendritic structures (Tseng, An et al. 2002). *In vivo*, actin is generally located in a complex and highly dynamic network just below the plasma membrane known as the membrane cortex, and there is an intracellular web and a perinuclear web. This allows the network to control cell surface movements and respond to cell-surface receptor-binding and mechanical deformation.

The actin cytoskeleton-integrin linkage is dynamic and responds to tensile forces. This was demonstrated by 'trap-retrap-retrap' experiments using ligand coated beads and a laser trap (Felsenfeld, Schwartzberg et al. 1999). A ligand-coated bead was placed on the upper surface of a cell and allowed to attach. The bead was then moved by the cell in an actin cytoskeleton dependent manner. If the bead was then held by the laser trap, the force exerted by the cell increased to pull the bead from the trap. Retrapping the bead the following time required a proportional increase in laser power.

### **1.5.7 Mechanotransduction**

There has been much focus on the process of mechanotransduction in tendons (Screen, Shelton et al. 2005; Yamamoto, Kogawa et al. 2005; Wang 2006; Maeda, Shelton et al. 2009). Mechanotransduction is the process of converting physical forces into biochemical signals and integrating these signals into cellular responses (Arnoczky, Lavagnino et al. 2002; Huang, Kamm et al. 2004). Cells dynamically adapt to force by modifying their behaviour and modifying their microenvironment (Regent, Planus et al. 2010). Mechanotransduction provides a framework for understanding how tissues “perceive” and are modified by mechanical forces. It has a central position in understanding the manipulation of healing tissues.

#### **1.5.7.1 Integrins and Mechanotransduction**

Integrins have been shown to be involved in the process of mechanotransduction (Salter, Robb et al. 1997). This has been investigated in diseased cartilage, where the signalling pathway via the  $\alpha 5 \beta 1$  integrin in response to mechanical stimulation may be of importance in the production of phenotypic changes (Millward-Sadler, Wright et al. 2000; Millward-Sadler, Wright et al. 2000). These authors showed tyrosine phosphorylation of 3 major proteins (including FAK) within 1 minute of onset of mechanical stimulation. This was inhibited by RGD containing oligopeptides (and gadolinium, which is known to block the stretch-activated ion channels) in human articular chondrocytes. As Fn has only a moderate affinity for its integrins, changes in Fn (or integrin concentration) could shift the binding equilibria and therefore the number or organisation of Fn-integrin complexes, within minutes. This may be important in regulation of Fn activity (Brigman, Hu et al. 1994), making Fn binding a potential anti-adhesion therapeutic target (Branford, Mudera et al. 2008; Branford,

Brown et al. 2010). The  $\alpha 5 \beta 1$  integrin is considered to be of major importance in the formation of Fn fibrils and for ECM deposition and remodelling in mechanotransduction (Regent, Planus et al. 2010).

#### **1.5.7.2 Tissue Load is Transmitted Intracellularly**

Mechanotransduction in response to tissue load is likely to be mediated through the deformation of the ECM, which in turn results in *in situ* cell deformation (Banes, Tsuzaki et al. 1995; Sung, Whittemore et al. 1996). Integrins provide the connection for the transmission of load between the ECM and the actin cytoskeleton via the focal adhesions (Geiger, Spatz et al. 2009). As such, integrins are a primary pathway for intracellular force transmission and, therefore, are initiating sensors for local ECM mechanical forces as mechanoreceptors (Regent, Planus et al. 2010). Fn binding integrins have mechanotransduction related properties and can be involved in “perception” of force by cells (Wang, Butler et al. 1993). Lutz and colleagues have demonstrated that pericellular Fn, secreted by normal fibroblasts, is a necessary component of the strain-sensing machinery and is integral to mechanotransduction (Lutz, Sakai et al. 2010). The relationship between cell morphology and tissue strain is thought to be mediated through cell interactions with ECM proteins such as Fn (Banes, Tsuzaki et al. 1995; Sung, Whittemore et al. 1996). Thus the common connection or nexus between tissue load following mobilisation and the physical nature of the resultant adhesions may be Fn-fibroblast integrin attachment (Figure 1.3). In this thesis a novel DFn with potential anti-adhesive effects was therefore investigated *in vitro* and *in vivo* for its effects on modifying cell attachment and consequently adhesion formation.



### **1.5.7.3                   Mechanotransduction and Tendon Adhesion Formation**

Local tissue strains are the result of cellular processes resulting from applied forces. However, it is not clear from the literature how local tissue strains in adhesions are related to gross tissue strain and how local tissue strains are affected by mobilisation and, therefore, tissue load. Mechanotransduction principles are consequently very relevant to investigating tendon adhesion formation.

The importance of load (stress) in the homeostasis of connective tissues has been well documented (Woo, Gomez et al. 1982; Hannafin, Arnoczky et al. 1995; Yasuda and Hayashi 1999). Several studies have shown that stress deprivation in ligaments and tendons results in significant alterations in their structural and functional properties (Woo, Gomez et al. 1982; Hannafin, Arnoczky et al. 1995; Yasuda and Hayashi 1999). Application of dynamic strains influences the structural integrity of both healthy and healing soft tissues (Tipton, Vailas et al. 1986). Tendons are known to be highly responsive to mechanical loading (Asundi and Rempel 2008). These effects are believed to be mediated by changes in metabolism of cells in response to the changing mechanical environment (Amiel, Akeson et al. 1983). Cells are, therefore, both the detectors and effectors of adaptation of tissues to their mechanical environment, as occurs during physiological change or disease. Tendon fibroblasts detect mechanical stimuli *in vivo* and it is through mechanotransduction pathways that they initiate ECM remodelling (McNeilly, Banes et al. 1996; Lee and Bader 1997; Akhouayri, Lafage-Proust et al. 1999; Bouten, Knight et al. 2001; Screen, Lee et al. 2003; Chiquet, Gelman et al. 2009). This is also likely to be the case for tendon adhesions. Cells within tissues react to mechanical stimuli with molecular responses and ECM production that aim to protect the overall integrity of the tissue (Lee and

Bader 1997; Akhouayri, Lafage-Proust et al. 1999; Bouten, Knight et al. 2001; Huang, Kamm et al. 2004). Cyclical strain applied to cultured tendon cells can enhance cell proliferation and ECM production (Riboh, Chong et al. 2008). It would follow that applying load to fibroblasts may result in greater collagen deposition and the strengthening of adhesions. However, from a review of the literature this does not appear to be the case (Woo, Gelberman et al. 1981; Gelberman, Vande Berg et al. 1983; Gelberman, Manske et al. 1986; Hitchcock, Light et al. 1987; Feehan and Beauchene 1990). It is therefore not clear why the tensile strength of tendons is improved by mobilisation yet mobilised adhesions are more likely to fail.

ECM turnover in tendons is influenced by mechanical activity. Collagen synthesis and MMP production increase with mechanical loading, and growth factor release is enhanced following exercise (Kjaer 2004; Asundi and Rempel 2008). Cells involved in the tendon repair process and adhesion formation are responsible for maintaining the balance between synthesis and breakdown of ECM components in response to injury and mechanical stress (Abrahamsson 1991). It is possible that mobilisation has a differential effect on this balance either at the tendon surface or in the surrounding synovial sheath. This may account for the strengthening of tendon repair and reduced adhesions that are seen following mobilisation. Fong and colleagues have shown, using rat tendon cultures using microarray analysis, that mechanical shear stress induced an anti-fibrotic expression pattern (Fong, Trindade et al. 2005). There was decreased transcription of collagen type-I and collagen type-III. Shear stress induced an overall decrease in TGF- $\beta$  signalling pathway molecules with down-regulation of TGF- $\beta$ 2, TGF- $\beta$ 3, T $\beta$ RI, and T $\beta$ RII expression, although TGF- $\beta$ 1 was differentially up-regulated by shear stress. Sheared tendon cells increased

expression of MMPs and decreased expression of tissue inhibitors of metalloproteinase (TIMP), an expression pattern consistent with an anti-fibrotic increase in ECM degradation. However, these authors also found up-regulation of genes implicated in tendon healing, specifically, vascular endothelial growth factor-A. However, they did not examine local strain responses to mechanical shear stress.

Central to probing mechanotransduction, is the development of techniques used to apply controlled mechanical stresses to non-fixed cells and tissues. Local strains have been shown to be significantly less in tendons relative to applied strains (Screen, Lee et al. 2003). While the stress strain behaviour of tendons has been well documented (Woo, Gomez et al. 1982; Banes, Horesovsky et al. 1999; Arnoczky, Lavagnino et al. 2002), little information exists regarding *in situ* strains which may take place on a cellular level in response to tensile load in tendon adhesions. It is clear from a review of the literature that much of the work on tendon adhesions has been secondary to that of the investigation of tendons themselves. While the underlying mechanotransduction mechanisms are also likely to operate for adhesions, the literature does not inform us directly how an adhesion responds to applied strain. Any biomechanical assessment of injured tendon function that does not also specifically assess adhesions is incomplete as these are so critical to tendon glide. Few studies have focussed on changes in the properties of adhesions themselves following mobilisation. Masuda and colleagues have previously demonstrated that changes in two digital flexor tendon adhesion tissue models may be due to alterations in ECM collagen crosslinking (Masuda, Ishii et al. 2002). However, that study did not assess effects of mobilisation and did not assess adhesions biomechanically. Akeson and colleagues found that collagen in

periarticular connective tissue surrounding immobilised rabbit knee joints was increasingly crosslinked as a result of lack of physical stress and immobilisation (Akeson, Amiel et al. 1977). However, they did not specifically assess tendon adhesions.

It is the local strains experienced by cells that are important in the process of mechanotransduction, as those are strains exerted at the level of the ECM. It is therefore important to describe what the local mechanical environment is like for cells. In this thesis an *in vivo* model system was developed in the injured flexor tendon-synovial complex. The techniques employed have investigated how adhesion tissues are organised at a local level, and how they respond to forces experienced during mobilisation, by modifying the ECM. In this way local strain responses produced in adhesions to applied strain were quantified. These micromechanical findings were also related to gross restrictive parameters.

## **1.6 ASSESSMENT OF TENDON HEALING AND ADHESIONS**

### **1.6.1 Clinical Assessments**

Although a number of clinical outcome measurements for flexor tendon surgery exist, there is no universal agreement as to what constitutes an ideal evaluation system. The widely accepted and simple Boyes' method measures the distance from the fingertip pulp to the distal palmar crease during maximal active finger flexion (Boyes 1950; Boyes 1955). Several other evaluation methods exist including the Louisville system (Lister, Kleinert et al. 1977), the American Society for Surgery of the Hand method (Hand 1976), and the Buck-Gramcko system (Buck-Gramcko,

Dietrich et al. 1976). However, although useful clinically, these methods do not allow for specific assessment of severity and quality of adhesions.

## **1.6.2 Histological Assessments**

Much of the data in the literature investigating adhesion formation is based on histological assessment, some using quantifiable methods (Akali, Khan et al. 1999). Cell proliferation in response to injury as measured by cell counts has been shown to be greater within the synovial sheath and tendon surface than within the tendon core in a rabbit model (Kakar, Khan et al. 1998). This reaction has variously been described as “thickening” (Gelberman, Manske et al. 1984; Manske, Gelberman et al. 1984) or “capping” (Manske and Lesker 1984).

## **1.6.3 Biomechanical Assessments**

### **1.6.3.1 Gross Mechanical Testing**

Gross mechanical testing of tendon has been performed, under a variety of testing conditions (Woo, Gomez et al. 1982; Butler, Grood et al. 1984). These studies are required to define functional parameters of restriction following adhesion formation so that anti-adhesive treatments may be compared.

However, few studies have incorporated both biomechanical and histopathological assessments of adhesions in a quantitative way (Isik, Ozturk et al. 1999; Strick, Filan et al. 2004; Thomopoulos, Kim et al. 2010). Tang and colleagues described a biomechanical and histological method of assessing tendons (Tang, Shi et al. 1996). However, mechanical evaluation used in that study assessed whole tendon-adhesion-synovial complex and not adhesions specifically. The authors’ adhesion assessment,

although measuring extent, was not dynamic and did not assess quality of the adhesions. Furthermore, these descriptions tell us little about adaptations and mechanical response of adhesions to applied load.

#### **1.6.3.2 Micromechanical Testing**

Screen and colleagues have quantified local strain fields in tendons by monitoring relative movement and deformation of fibroblast nuclei, where local strains were found to be significantly less than gross applied strain, and to be non-homogenous (Screen, Lee et al. 2003). Structural heterogeneity within tissues may alter their response to load and lead to mechanical failure (Zioupos, Gresle et al. 2008). It is also likely that adhesions are non-uniform and therefore to predict their behaviour it is necessary to assess their organisation and response to mechanical strain. The nature of a strain field associated with a tensile system is important in determining ultimate cell response *in vivo* (Shelton, Bader et al. 2003). In order to be able to examine tissue cellular responses and to apply representative physiological strains to cells in *in vitro* experiments it is therefore necessary to first determine local strains experienced by those cells (Screen, Lee et al. 2003). In this thesis a method for determining the stress strain behaviour of adhesions was developed. This has permitted examination of both local strains in response to tensile load and dynamic local changes in adhesion tissue morphology as a result of mobilisation. A dynamic local mechanical assessment of changes in the adhesion following application of strain may provide greater understanding of local tissue arrangement, forces and strains involved over the ‘snapshot’ assessment afforded by histology. This is necessary to begin to understand how externally applied forces to an adhesion may

be linked to the process of mechanotransduction and the modulation of the nature of the ECM.

## **1.7 METHODS OF ADHESION REDUCTION**

In addition to using different suture techniques and rehabilitation regimes, various strategies to modify adhesion formation in flexor tendon healing have previously been investigated experimentally, which may be categorised as either physical barriers or biochemical agents.

### **1.7.1 Mechanical Barriers**

Barriers are interposed between tendon and the surrounding synovial sheath in order to physically block adhesion formation. Examples of physical barriers are cellophane sheeting (Potenza 1963), silicone film (Eskeland, Eskeland et al. 1977; Stark, Boyes et al. 1977), hydroxyapatite and alumina sheaths (Siddiqi, Hamada et al. 1995), polytetrafluoroethylene membranes (Hanff and Hagberg 1998), ADCON-T/N (a carbohydrate polymer) (Mentzel, Hoss et al. 2000; Golash, Kay et al. 2003), lubricin (Zhao, Sun et al. 2010), Seprafilm (carboxymethylcellulose) (Yilmaz, Avci et al. 2010) and a phospholipid polymer hydrogel (Ishiyama, Moro et al. 2010), alginate (Namba, Shimada et al. 2007) and FocalSeal-L (hydrogel sealant) (Ferguson and Rinker 2006).

Potenza observed that mechanically excluding the site of injury from the surrounding synovial sheath did not prevent invasion by the peripheral fibroblasts as they bypassed the barrier (Potenza 1963). Golash and colleagues conducted a prospective randomized clinical trial to study the effects of ADCON-T/N after flexor tendon

repair. ADCON-T/N had no significant effect on total active finger motion, and a higher rupture rate was noted in the treatment group. Zhao and colleagues demonstrated decreased adhesions in dogs following treatment with lubricin, but at the expense of a significant increase in tendon rupture rates (Zhao, Sun et al. 2010). In addition, barrier materials have variably caused infection, material fragmentation, impaired healing (and tendon rupture), or have had little effect. Many of these materials are not biodegradable and may therefore stimulate fibrosis. As a result none are used routinely following tendon repair (Strickland 2000).

### **1.7.2 Biochemical Agents**

Biochemical agents are used to modify or suppress the cellular or inflammatory response. Examples of these are cis-hydroxyproline (Lane, Bora et al. 1975), antihistamines (Lindsay and Walker 1961), steroid preparations (Carstam, 1953), beta-aminopropionitrile (Peacock and Madden 1969; Speer, Feldman et al. 1985), ibuprofen (Kulick, Brazlow et al. 1984; Tan, Nourbakhsh et al. 2010), hyaluronate (sodium hyaluronate or hyaluronic acid) (Amiel, Ishizue et al. 1989; Hagberg and Gerdin 1992; Salti, Tuel et al. 1993), fibrin sealant (Frykman, Jacobsson et al. 1993; Jones, Burnett et al. 2002), neutralising antibody to TGF- $\beta$ 1 (Chang, Thunder et al. 2000; Xia, Yang et al. 2009), mannose-6-phosphate (Bates, Morrow et al. 2006), and 5-fluorouracil (Khan, Occleston et al. 1997; Akali, Khan et al. 1999; Khan, Kakar et al. 2000; Zhao, Zobitz et al. 2009).

Carstam examined the role of parenteral cortisone in reduction of post-surgical adhesions in the extensor hallucis longus tendon of 341 rabbits (Carstam, 1953). He suggested that if started several days prior to surgery and continued postoperatively,



cortisone therapy resulted in suppression of adhesion formation, as measured by tensiometer pulls. This was in contrast to those rabbits that commenced parenteral steroid therapy 3 weeks after repair. Groups who did not receive treatment or received local application of cortisone at the time of repair did not result in appreciable effect on subsequent adhesion formation. In spite of these findings pre-and postoperative parenteral steroid courses have not become standard procedure due to associated increased rupture and infection rates (Douglas *et al.*, 1967).

Peacock and Madden later examined the role of beta-aminopropionitrile, a lathyrogenic compound and showed it to be successful in treating peritendinous adhesions (Peacock and Madden 1969). However, the compound produced significant side effects such as hepatotoxicity, fever and dermatitis after 20 days of administration.

Kulick and colleagues injected ibuprofen at the time of tendon repair with over 50% reduction in adhesion formation (Kulick, Brazlow et al. 1984). A further study by the same group showed significant benefits of oral ibuprofen in reduction of tendon adhesion formation in a primate model (Kulick, Smith et al. 1986). Tan and colleagues also demonstrated reduction in adhesion formation following ibuprofen administration in an *in vivo* rabbit model (Tan, Nourbakhsh et al. 2010).

Hagberg and Gerdin showed that efficacy of sodium-hyaluronate is affected by both concentration and molecular weight of the sodium-hyaluronate preparation used (Hagberg and Gerdin 1992).

Khan and colleagues, using a rabbit flexor tendon model, assessed the effect of a single intraoperative application of 5-fluorouracil (5FU) to the tendon synovial sheath in repair of a partial tendon laceration was assessed. At one week there was a significant reduction in synovial sheath reaction/thickening, cell counts and proportional length of adhesions in treated tendons (Khan, Occleston et al. 1997). However, Zhao and colleagues found that 5FU had only a transient effect in an *in vivo* canine model where injured FDP tendons were mobilised (Zhao, Zobitz et al. 2009).

Bates and colleagues investigated the effect of mannose-6-phosphate, a natural inhibitor of TGF- $\beta$  (as it prevents activation of latent TGF- $\beta$ ) *in vitro* and *in vivo* in a rabbit model and found that it reduced TGF- $\beta$  upregulated collagen production, and significantly improved range of motion of the operatively treated digits. The effect on breaking strength of the tendon repair was inconclusive (Bates, Morrow et al. 2006).

Other agents have been investigated including neutralising antibody to TGF- $\beta$ 1 (Chang, Thunder et al. 2000; Xia, Yang et al. 2009), and fibrin sealant (Frykman, Jacobsson et al. 1993), with varying results. Other techniques, such as thermal preconditioning, have also been tested (Healy, Mulhall et al. 2007) in a rabbit model. Some of these compounds and methods have demonstrated favourable effects *in vivo*, but none have found their way into widespread clinical usage (Strickland 2000).

## **1.8 BIOMATERIALS AND TISSUE ENGINEERING**

A biomaterial is “a material intended to interface with biological systems to evaluate, treat, augment or replace any tissue, organ or function of the body” (Williams, Black et al. 1992). Biomaterials play crucial roles in reconstructive surgery, tissue engineering and regenerative medicine (Maskarinec and Tirrell 2005). These materials include a wide range of polymers. They may be natural (derived from natural sources such as the modified polysaccharides cellulose, chitin, and dextran, or modified proteins such as fibrin, Fn, gelatin and collagen) or synthetic (for example polylactide, polyglycolide, and polydioxanone). Although protein based polymer biomaterials may have weaker mechanical properties than their synthetic counterparts, they offer other significant advantages. They have an ability to guide cell and tissue behaviour during healing as a function of complex interplay that exists between their mechanical and bioactive properties (Maskarinec and Tirrell 2005; Brown and Phillips 2007). They may also have the capacity to be remodelled and degraded by cells and integrated into tissues. The key is what is happening at the cell-material interface. Advances in biomimetic polymeric biomaterials, which send receptor mediated signals to cells, have resulted in cell type specific influences.

Tissue engineering has been defined as "the application of engineering principles to create devices for the study, restoration, modification, and assembly of functional tissues from native or synthetic sources" (Williams, Black et al. 1992). The challenge of tissue engineering is to control cell behaviour through rational design of biomaterials, incorporating the biomechanical principles and methods of engineering design. An ideal polymer biomaterial would have adequate mechanical properties to match the application. It would be biodegradable reducing its likelihood to stimulate

further inflammation and adhesion formation. It would also be fully metabolised once it degrades. It would be sterilisable and easily processed into a final end product with an acceptable shelf-life. A good example of a protein based biomaterial is Fn. During healing, Fn is required for attachment of fibroblasts to fibrin and is important in migration of fibroblasts. There is subsequent formation of a Fn scaffold by these fibroblasts, upon which collagen is deposited (Ruoslahti, Hayman et al. 1982; Grinnell 1984; Gelberman, Steinberg et al. 1991; Stadelmann, Digenis et al. 1998). Preventing fibroblast attachment to Fn is therefore a potential strategy to reduce adhesion formation.

Production of Fn mats and cables for tissue engineering has been described (Ejim, Blunn et al. 1993; Brown, Blunn et al. 1994; Underwood, Afoke et al. 2001; Phillips, King et al. 2004). These constructs guide attachment and migration of cells *in vitro*. These have also been tested *in vivo* in nerve and tendon healing (Whitworth, Brown et al. 1995; Wojciak-Stothard, Denyer et al. 1997; Ahmed and Brown 1999; Zavahir, McGrouther et al. 2001; Harding, Afoke et al. 2002; Priestley, Ramer et al. 2002; King, Henseler et al. 2003). However, certain fragments of the Fn molecule are anti-adhesive, inhibiting attachment of fibroblasts to Fn (Yamada and Kennedy 1984; Fukai, Takahashi et al. 1996; Ruoslahti 1996; Fukai, Hasebe et al. 1997; Watanabe, Takahashi et al. 2000). During production of shear aggregated Fn based biomaterials with adhesive properties in this laboratory, withdrawal of a washing step resulted in a derivative of Fn (DFn) with inhibitory properties (Djerkovic, Phillips et al. 2005). This thesis explores the anti-adhesion properties of this novel material (DFn) investigating its *in vitro* effects on cell attachment (Branford, Brown et al. 2010) and its adhesion modifying effects *in vivo* (Branford, Mudera et al. 2008).

## **CHAPTER 2**

### **MATERIALS AND METHODS**

#### **2.1 MATERIALS AND METHODS**

#### **2.2 *IN VITRO* METHODS**

##### **2.2.1 Primary Rabbit Tissue Culture**

##### **2.2.2 Preparation of Derivative Fibronectin Biomaterial and Fibronectin Control**

##### **2.2.3 Protein Analysis of Derivative Fibronectin Biomaterial and Fibronectin Control**

##### **2.2.4 Measurement of Cell Attachment to Derivative Fibronectin Biomaterial and Fibronectin Control**

##### **2.2.5 Assessment of Synovial Sheath Fibroblast Migration into Derivative Fibronectin Biomaterial and Fibronectin Control**

##### **2.2.6 Determination of Synovial Sheath Fibroblast Viability on Derivative Fibronectin Biomaterial**

##### **2.2.7 Time Lapse Observation of Cells on Derivative Fibronectin Biomaterial**

##### **2.2.8 Determination of Cell Attachment and Examination of Morphology of Cells on Collagen Type-I and Fibronectin**

#### **2.3 *IN VIVO* METHODS**

- 2.3.1 Tendon Injury Model**
- 2.3.2 Investigation of the Effects of Derivative Fibronectin Biomaterial Treatment on Adhesions**
- 2.3.3 Investigation of the Effects of Mobilisation on the Hierarchical Biomechanical Properties of Adhesions**
- 2.3.4 Histology and Immunohistochemical Scoring in Derivative Fibronectin Biomaterial Treated and Untreated Injured Tendons and Adhesions**
- 2.4 STATISTICAL ANALYSIS**

## **2.1 MATERIALS AND METHODS**

Unless otherwise stated all tissue culture materials were supplied by Gibco (Gibco, Paisley, UK) and Sigma (Sigma-Aldrich, Gillingham, UK), tissue culture plastics by Greiner (Greiner, Stonehouse, UK), and all chemicals used in this study were AnalaR grade, where available, and supplied by Sigma (Sigma-Aldrich, Gillingham, UK) and BDH (BDH Chemicals, Poole, UK). The source material for the derivative fibronectin biomaterial (DFn) and fibronectin control biomaterial (Fn control) was frozen cryoprecipitate (Bio Products Laboratory, Elstree, UK), derived from pooled human plasma from donors from the United States. Details of other suppliers of chemicals or compounds used are noted as and when appropriate within the text.

Primary fibroblast cell strains were obtained from New Zealand White (NZW) rabbit forepaws. All cell culture work was carried out in sterile class II laminar airflow hoods, (Laminar HB2448, Heraeus Instruments) and cells maintained in a Galaxy S incubator (Wolf Laboratories) at 37°C, humidified with a CO<sub>2</sub> concentration of 5%. All *in vivo* work was performed on NZW rabbit forepaws. All animal care and procedures complied with the UK Home Office “Guide for the Care and the Use of Laboratory Animals” 1996, under licence of the Department of Health.

## **2.2 IN VITRO METHODS**

### **2.2.1 Primary Rabbit Tissue Culture**

Routine tissue culture was performed in Normal Growth Media with 10% Fetal Calf Serum (FCS; referred to as 10% NGM in the text) and was made up as follows: Dulbecco's Modified Eagle's Medium (DMEM), 10% FCS, Penicillin-Streptomycin (100 units mL<sup>-1</sup> and 100 µg mL<sup>-1</sup>, respectively) and 2 mM L-Glutamine. Culture

media was stored at 4°C, used within 4 weeks and warmed in a 37°C water bath prior to use.

#### **2.2.1.1 Preparation of Explant Cultures**

Tendon core, tendon surface, synovial sheath, mobilised adhesion and immobilised adhesion cell strains were obtained using explant culture (Burt and McGrouther 1992) as follows.

NZW rabbit forepaws were removed following Schedule 1 Termination. Paws were wrapped in gauze moistened with phosphate buffered saline (PBS) and stored at 4°C prior to analysis, which was always within 48 hours of harvest. After shaving the paws, the epidermis and fatty tissue were removed using sterile forceps and a sterile scalpel. The digital flexor tendon-synovial complexes in unoperated samples, comprising tendon and synovial sheath, and peritendinous adhesions in operated samples (harvested at 2 weeks post injury), were removed en bloc under loupe magnification. The macroscopic appearance of the operated specimens was recorded.

The individual components of the tendon-synovial complex were carefully dissected out using a dissecting microscope, separating the flexor digitorum profundus (FDP) tendon from its enveloping sheath. The tendon was stripped of its surface using a scalpel, thus separating tendon surface from tendon core.

Each of the tissue types were thoroughly washed in sterile saline, then divided into 2-5 mm<sup>3</sup> pieces. All explants were then placed separately, according to their source of origin, into 25 cm<sup>2</sup> adherent tissue culture flasks with 5 mL of 10% NGM. The



tissue pieces were removed once fibroblasts were seen in culture. The flasks were incubated at 37°C for approximately 3 weeks; refreshing the media twice per week until approximately 80% of the surface area was covered with fibroblasts (80% confluence).

Cells were passaged as follows. The flasks were washed twice briefly with warmed versene. 1 mL of a 1:10 solution of trypsin: versene (final enzyme concentration of 0.25%) was added to the flasks, which were incubated at 37°C, until the cells had detached. The trypsin solution was neutralised with the addition of 4 mL 10% NGM. The cell suspensions were pelleted by centrifugation for 5 minutes at 1000 g and re-suspended in fresh 10% NGM, and sub-cultured on a split ratio of 1:3.

Media was refreshed twice weekly and cells were further sub-cultured routinely in a split-ratio of 1:3, by trypsinisation (as described above) on confluency. Only cells of passages 1-6 were used for experimentation.

#### **2.2.1.2 Cryogenic Storage**

Exponentially growing cells were trypsinised, pelleted by centrifugation (1000 g, 5 minutes) and re-suspended in 'freezing medium' (9 mL FCS and 1 mL Dimethyl Sulphoxide (DMSO; Sigma-Aldrich, Gillingham, UK)). Typically a confluent 75 cm<sup>2</sup> adherent tissue culture flask was re-suspended in 3 mL of freezing medium, which was then aliquoted into cryovials (1 mL per cryovial). Insulated cryovials were slowly frozen by placing insulated into a -80°C freezer for 24 hours before being transferred to liquid nitrogen for long-term storage.

Cells were retrieved from cryogenic storage by rapidly thawing the cryovials in a water bath at 37°C. The cell suspension was immediately transferred to a 15 mL labelled centrifuge tube. To this 9 mL of 10% NGM was added slowly, gently agitating the solution. The cells were then centrifuged (5 minutes at 1000 g), re-suspended in 10 mL of fresh 10% NGM, transferred to 75 cm<sup>2</sup> adherent tissue culture flasks and cultured as described in section 2.2.1.

### **2.2.1.3 Fixation of Tissues or Cells on Biomaterials**

In order to fix either tissues or cells on the biomaterials to enable maintenance of morphology, 10% neutral buffered formalin (Appendix I) was used unless otherwise stated.

Samples were processed using an enclosed automatic processing system (VIP 2000F/300E) programmed with the following processing schedule: 10% neutral buffered formalin for 2 hours at 40°C, 70% industrial methylated spirit (IMS) for 1 hour at 40°C, 90% IMS for 1 hour at 40°C, absolute IMS for 3 hours at 40°C, xylene (Merck, Poole, UK) for 4 hours at 40°C, paraffin wax for 3 hours at 60°C. Tissues were embedded in paraffin wax utilising the Tissue-Tek III. Blocks were cut using a microtome and sections were cut to 5 to 8 µm as appropriate.

## **2.2.2 Preparation of Derivative Fibronectin Biomaterial and Fibronectin Control**

Two types of Fn biomaterials were prepared for testing – the novel DFn and an adherent positive control (Fn control) as previously reported (Ejim, Blunn et al. 1993; Underwood, Afoke et al. 2001; Phillips, King et al. 2004). The initial stages of

production of these mats were identical, and based on the wet extrusion method previously described (Underwood, Afoke et al. 2001) which is detailed as follows.

#### **2.2.2.1 Cryoprecipitate Source Material**

The source material for the DFn and Fn control mats was frozen cryoprecipitate (Figure 2.1). Briefly, the frozen cryoprecipitate was thawed overnight at 4°C, hand shredded into small pieces, and dissolved in 20% Tris buffer at 37°C (0.05 mol L<sup>-1</sup> Tris (hydroxymethyl) aminomethane (Sigma-Aldrich, Gillingham, UK), 0.15 mol L<sup>-1</sup> NaCl, pH 7.4 in deionised water).

#### **2.2.2.2 Method for Heat Depletion of Fibrinogen**

The cryoprecipitate in Tris buffer solution was heated to between 52°C and 56°C in a microwave on a low setting to precipitate the fibrinogen in the process of heat depletion (Tsukada, Ying et al. 1995). The temperature was not allowed to exceed 56°C to avoid protein denaturation. The preparation was allowed to cool slightly at room temperature. The fibrinogen was filtered out using a sieve with a 2 mm pore size (Figure 2.2). The remaining solution was centrifuged at 3200 g in a swing-out rotor at 4°C for 10 minutes to remove the remaining fibrinogen.

#### **2.2.2.3 Method for Polyethylene Glycol Precipitation of Fibronectin**

Fn was precipitated from this solution at room temperature by adding 30% Polyethylene Glycol 3500 (Sigma-Aldrich, Gillingham, UK) (Homandberg 1987; Harding, Underwood et al. 2000; Underwood, Afoke et al. 2001; Phillips, King et al. 2004). The preparation was mixed gently and left for 30 minutes at 4°C. The contents were mixed again gently then centrifuged at 3200 g for 10 minutes

producing Fn pellets (Figure 2.3), which were kept and the supernatant was discarded.

#### **2.2.2.4 Shear Aggregation of Biomaterial**

The Fn pellets were then dissolved in urea ( $4 \text{ mol L}^{-1}$ ) as 1 mL urea per 1 g of pellet, producing a Fn solution after 2 hours on a roller mixer at  $37^{\circ}\text{C}$ . Urea transforms Fn from its compact conformation to its extended form (Homandberg 1987), facilitating its aggregation (Underwood, Afoke et al. 2001). The Fn was extruded using a 5 mL syringe on to a rotating rod at 10 revolutions per minute, forming thin-walled tubes by the process of shear aggregation (Phillips, King et al. 2004; Figure 2.4, Figure 2.5, Figure 2.6). The diameter of the tube was determined by the diameter of the rod on to which the biomaterial was applied. For the production of mats for *in vitro* testing 1 cm rods were used. For the production of biomaterials for *in vivo* testing 3 mm rods were used.

The biomaterial tubes were air dried, being divided into samples or mats of the required dimensions with a scalpel blade at 6 hours (before becoming brittle as a result of drying) for a total of 24 hours. The biomaterials were lyophilised in a high vacuum freeze dryer (Edwards, Sussex, UK) at  $-50^{\circ}\text{C}$ , 80 mbar vacuum pressure. Before use the mats were sterilised using a total dose of 28.6 kGray of  $\gamma$  irradiation. These were stored in sealed sterile tubes until use. 30 g of cold precipitate yielded 3 g of Fn, which was sufficient to produce 100 Fn mats weighing approximately 30 mg and measuring 1 cm x 1 cm.



**Figure 2.1** The cryoprecipitate raw material.



**Figure 2.2** The process of heat depletion resulted in the precipitation of fibrinogen, removing it from the biomaterial preparation.





**Figure 2.3** Fn pellets were produced following polyethylene glycol precipitation and centrifugation of the preparation.



**Figure 2.4** Shear aggregation of biomaterial onto a rotating rod.





**Figure 2.5** Air dried biomaterial tube prior to being cut into mats.

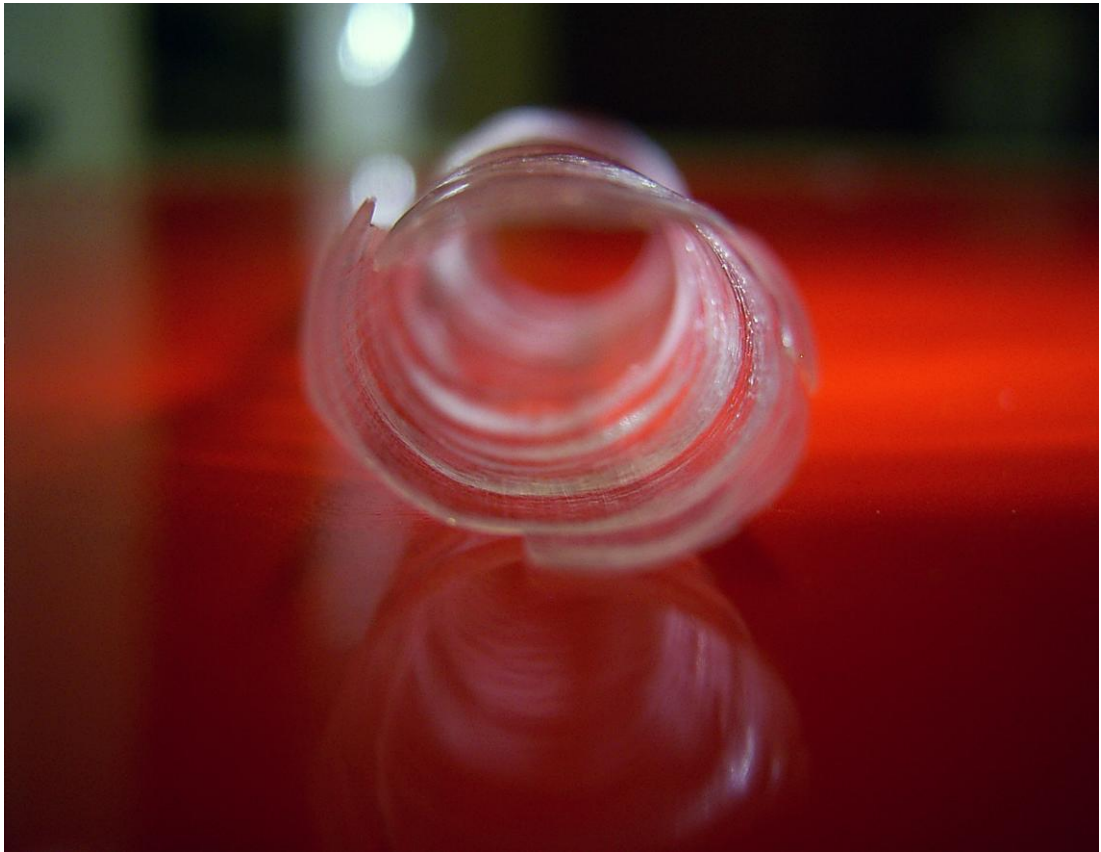


**Figure 2.6** Air dried biomaterial tube end-on showing thin wall.

#### **2.2.2.5 Preparation of Derivative Fibronectin Biomaterial and Fibronectin Control**

The production of DFn and Fn control mats differed by the latter subsequently undergoing a number of washing stages. The washing stages for the Fn control mats consisted firstly of elution for 24 hours in 0.1 mol L<sup>-1</sup> PBS at 4°C, followed by washing once in PBS at 4°C and then again in distilled water at room temperature. At each stage the elution was discarded.

Prior to any cell seeding both DFn and Fn control mats were briefly rehydrated for 30 minutes in 0.1 mol L<sup>-1</sup> PBS at 4°C. Where materials were used to coat glass cover slips these were applied directly and air dried in a sterile hood. The materials were stuck to the mats without difficulty.

#### **2.2.3 Protein Analysis of Derivative Fibronectin Biomaterial and Fibronectin Control**

To determine the protein content of the DFn and Fn control biomaterials a Titan Gel Immuno-electrophoresis kit (Helena Laboratories, Beaumont, USA) and a Radial Immunodiffusion Partigen® Plate (Dade Behring, Marburg, Germany) were used as follows.

##### **2.2.3.1 Immuno-electrophoresis Analysis of Biomaterial Composition**

The protein content of the solutions from the various stages of purification was analysed semi-quantitatively using a Titan Gel Immuno-electrophoresis (IEP) kit (Helena Laboratories, Beaumont, USA) as follows.

Immunoelectrophoresis combines two techniques, electrophoresis and immunodiffusion. In this two part procedure protein solutions (at 2  $\mu$ L per well) were first separated according to charge by electrophoresis on an agarose plate. The cryoprecipitate raw material dissolved in Tris 1:2 solution, the fibrinogen-depleted solution prior to the precipitation of Fn and the discarded supernatant after Fn precipitation were tested for their protein content.

Whole human serum (WHS) was used as a control. 2 drops of albumin marker was added to this. 100 mL of Electra® B<sub>1</sub> Buffer (Helena Laboratories, Beaumont, USA) was poured into each outer section of the chamber, with the supplied sponge wick being placed in each buffer-lined compartment. 2  $\mu$ L samples were applied to the plates, taking care not to damage the wells during sample application. The plates were immediately placed in the electrophoresis chamber, agarose side down, with the wells toward the cathode (negative terminal). The cover was placed on the electrophoresis chamber and allowed to equilibrate with the buffer for 60 seconds before applying the current. The plates were electrophoresed at 100 V for 45 minutes. Migration distance was verified by observing the position of the albumin marker.

The plates were removed from the chamber and placed on a flat surface, agarose side up. Then 25  $\mu$ L of each of the antisera to human Fn, human fibrinogen, and WHS were applied to the troughs in the plate. The plates were incubated at room temperature and allowed to diffuse for 24 hours. The plates were then placed in 0.85% saline for 6 hours, changing the saline every hour, to remove unbound protein. Plates were pressed-dry using blotters, and then dried at 60°C for 5 minutes.

The dry plate was placed in the IEP stain (Helena Laboratories, Beaumont, USA) for 4 minutes. The plate was then destained by washing in destain solution twice for a total of 60 seconds. The plates were again dried at 60°C for 5 minutes.

Precipitin arcs formed where a favourable antigen to antibody ratio existed, indicating that the protein complementary to the antiserum used was present in the test sample. The size and location of the arc were indications of the amount of total protein in the test sample, making this a semi-quantitative technique. Thick precipitin arcs closer to the antiserum trough indicated higher protein concentrations relative to control.

#### **2.2.3.2 Immunodiffusion Analysis of Biomaterial Composition**

The protein content of the solutions from the various stages of purification was analysed quantitatively utilising a radial immunodiffusion Partigen® plate as follows.

The Partigen® plate was left to stand at room temperature for 5 minutes prior to use to allow any condensed water to evaporate. Fn standards were used undiluted (283 mg L<sup>-1</sup>), as 25% (70.75 mg L<sup>-1</sup>) and as 50% (141.5 mg L<sup>-1</sup>) dilutions. Samples of cryoprecipitate raw material dissolved in Tris 1:2 solution, the fibrinogen-depleted solution prior to the precipitation of Fn, and the discarded supernatant following precipitation of the Fn were tested for their protein content. To bring the concentration of the samples to within the measuring range of the Partigen® plate the samples were used undiluted and in a 1:10 dilution in PBS and were applied at 20 µL per well. Plates were allowed to stand at room temperature for 3 days.

The gel contained a monospecific antiserum to human plasma Fn. The Fn formed immune complexes with the specific antibodies in the agarose gel of the Partigen® plates. These complexes became visible as precipitin rings (radial immunodiffusion). The diameter of the precipitin ring was directly proportional to the concentration of the relevant protein in the sample. The diameter of the precipitin rings was measured. This method has an accuracy of 0.1 mm to 0.2 mm with the plates viewed against a dark background with side illumination. The precipitin ring diameters of the standard dilutions were squared and the values were plotted against their concentrations. The line of best fit was used to calculate the concentrations of the samples tested based on their squared precipitin ring diameters, with the relevant factor for diluted solutions being taken into account.

#### **2.2.3.3 Determination of Degradability of the Derivative Fibronectin Biomaterial and Fibronectin Control**

The biodegradability of the DFn and Fn control was tested using colorimetric detection and quantitation of total protein in solution over 21 days as follows.

DFn and Fn control samples were placed in sterile Eppendorf Tubes (Fisher Scientific, Leicestershire, UK) containing 3 mL of one of the following: 10% NGM; PBS; or PBS containing the protease inhibitor Aprotinin ( $300 \text{ iu mL}^{-1}$ ). Aprotinin was included to test for proteases present in DFn. Experiments were performed in triplicate for both DFn and Fn control, which were maintained in solution at  $37^{\circ}\text{C}$  for 21 days. Protein loss from the biomaterials in solution was evaluated by taking  $10 \mu\text{L}$  samples at regular intervals over 21 days. These were immediately frozen at  $-20^{\circ}\text{C}$

for later simultaneous testing using a Bicinchoninic Acid (BCA) Protein Assay Reagent Kit (Pierce Biotechnology, Illinois, USA).

The colorimetric detection of protein uses the biuret reaction: this is the reduction of  $\text{Cu}^{2+}$  to  $\text{Cu}^{1+}$  by protein in an alkaline medium. The cuprous cation ( $\text{Cu}^{1+}$ ) is detected using a reagent containing BCA (Smith, Krohn et al. 1985). The chelation of 2 molecules of BCA with 1 cuprous ion forms a purple reaction product. This water-soluble complex exhibits a strong absorbance at 562 nm that is nearly linear with increasing protein concentrations over a broad working range (20 to 2000  $\mu\text{g mL}^{-1}$ ).

The protein concentration of the samples were determined and reported with reference to known bovine serum albumin (BSA) dilutions (from 0 to 2000  $\mu\text{g mL}^{-1}$ ) which were assayed alongside the test samples by comparing their absorbance at 562 nm. The same diluents were used to prepare the protein standards as the test samples.

The 10  $\mu\text{L}$  samples taken at regular intervals over 21 days and standards were placed into 96-well plates. 200  $\mu\text{L}$  of the BCA working reagent was added to each well. Plates were mixed on a plate shaker for 30 seconds. The plates were then covered and incubated at 37°C for 30 minutes. Plates were then allowed to cool to room temperature and the absorbance measured at 562 nm. The mean absorbance of the blank standard (0  $\mu\text{g mL}^{-1}$ ) replicates was subtracted from all the other individual standard and test samples.

In order to generate a standard curve the average blank corrected 562 nm measurement for each BSA standard was plotted against its concentration in

$\mu\text{g mL}^{-1}$ . The protein concentration of each test sample was determined using the standard curve. The absorbances of samples containing 10% NGM were corrected for the protein present in the FCS using biomaterial free samples in 10% NGM.

#### **2.2.4 Measurement of Cell Attachment to Derivative Fibronectin Biomaterial and Fibronectin Control**

Both DFn and Fn biomaterials were tested for their effects on synovial sheath fibroblast attachment in the following manner.

Samples (1 cm by 1 cm) of the DFn and Fn control mats were prepared as described in section 2.2.2, and then dried on glass cover slips. Experiments were performed in triplicate and repeated for 5 different fibroblast strains, representing 15 samples per group. Biomaterials were rehydrated prior to the addition of fibroblasts ( $1 \times 10^5$  in 1 mL 10% NGM) in 6-well plates. 15 plain (non treated) glass cover slips were also seeded with fibroblasts. All samples were incubated for 6 hours at 37°C.

##### **2.2.4.1 Immunostaining Protocol for $\alpha$ -Smooth Muscle Actin with Propidium Iodide Counter-Stain for Cells Attached to Biomaterials**

The medium was aspirated carefully and replaced with 2 mL of 10% formal saline (Appendix I). The samples were left overnight to fix at room temperature. The following day the cover slips were then carefully washed three times with PBS for 15 minutes. Just prior to staining, the PBS was replaced with 2 mL of ice cold Analar Grade Methanol (to permeabilise the cell membranes) for 1 hour at -20°C. The cover slips were then washed three times with PBS for a further 1 hour in total on a



Luckham R100 Rotatest Shaker orbital shaker (Luckham Ltd., Burgess Hill, United Kingdom).

Cover slips were stained with an immunofluorescent  $\alpha$ -smooth muscle actin ( $\alpha$ -SMA) stain to detect the presence of stress fibres, which are expressed by cells that have undergone activation as myofibroblasts (Harris, Stopak et al. 1981; Darby, Skalli et al. 1990), and with the fluorescent nuclear stain Propidium Iodide as a nuclear counter-stain as follows.

Cover slips were incubated with 500  $\mu$ L per well of dilute primary mouse Anti- $\alpha$ -SMA Antibody (1:1000 dilution of primary antibody in PBS; Sigma-Aldrich, Gillingham, UK) overnight at room temperature. Separate DFn and Fn coated cover slips used as negative controls were incubated in the same way but with 1 mL of PBS alone. The cover slips were then washed in their wells three times with PBS for 30 minutes in total before adding 2 mL of the secondary antibody, rabbit anti-mouse Fluorescein Isothiocyanate (as 1:400 dilution in PBS; Sigma-Aldrich, Gillingham, UK), with Propidium Iodide (25  $\mu$ g mL<sup>-1</sup>; Sigma-Aldrich, Gillingham, UK) as a nuclear counter-stain. Cover slips were left for 1 hour in a dark box to prevent photo-bleaching of the fluorescence.

Cover slips were washed three times in PBS for 30 minutes in total, in the dark at room temperature. Cover slips were then carefully placed on a slide with 2 drops of Vectashield Vector H-1000 Anti-Fade Mounting Medium (Vector Laboratories, Peterborough, UK) and covered with a further cover slip. These were then immediately viewed with a Zeiss Axioskop Optical Microscope (Carl Zeiss, Jena,

Germany) under an ultraviolet lamp and 5 random x40 high power microscopy fields per sample were captured as digital micrographs. Myofibroblasts, which were positive for  $\alpha$ -SMA demonstrated intracellular stress fibers that fluoresced bright green. Negative cells showed red nuclear staining only. The number of cell nuclei per microscopy field and the number of myofibroblasts were recorded for test (n=5) and control (n=5) groups, and mean values calculated.

### **2.2.5 Assessment of Synovial Sheath Fibroblast Migration into Derivative Fibronectin Biomaterial and Fibronectin Control**

The barrier properties of the DFn and Fn control were tested *in vitro* as follows.

DFn and Fn control samples were prepared and rehydrated as described in section 2.2.2. Fibroblasts ( $1 \times 10^5$  in 1 mL of 10% NGM) were added to the uppermost surface of the biomaterials and were allowed to attach for 24 hours at 37°C. Experiments were performed in triplicate and repeated for 3 separate synovial sheath fibroblast cell strains (n=3). Biomaterials were washed in PBS to remove unattached cells, and then fixed in formalin. During this process the orientation of the biomaterials was maintained, so that the surface that had been in contact with fibroblasts was known throughout. After paraffin embedding, 8  $\mu$ m sections were cut perpendicular to the seeded surface of the biomaterials using a microtome. The sections were then placed on glass slides, deparaffinised, and then stained with Haematoxylin and Eosin (H and E). The slides were then examined using light microscopy (Nikon Eclipse T5100, Nikon, Tokyo, Japan) for fibroblasts attached to, or having migrated beneath, the surface of the biomaterials.

#### **2.2.5.1 Haematoxylin and Eosin Staining of Seeded Biomaterials**

The sections were first deparaffinised as follows. The slides were pre-warmed in an incubator, and then immersed in two consecutive xylene baths (Merck, Poole, UK) for 5 minutes to remove wax. This was followed by immersion in absolute alcohol, 90% alcohol and 70% alcohol for 5 minutes each to remove the xylene. The slides were rehydrated in distilled water for 5 minutes.

The slides were then placed into a 1% solution of Harris Haematoxylin (BDH Chemicals, Poole, UK) and Eosin (BDH Chemicals, Poole, UK) and incubated at room temperature for approximately 15 minutes on a rotary shaker. The slides were washed thoroughly three times with distilled water (dH<sub>2</sub>O) before being examined by light microscopy.

#### **2.2.6 Determination of Synovial Sheath Fibroblast Viability on Derivative Fibronectin Biomaterial**

Synovial sheath fibroblasts were stained with Trypan Blue to determine viability as follows.

Fibroblasts ( $1 \times 10^5$  in 1 mL of 10% NGM) were plated into each of the wells of a 6-well culture plate and allowed to attach for 24 hours at 37°C. The culture plates were washed with 10% NGM to remove unattached cells. DFn was added to the wells of the culture plate, held apposed to the base of the plate by a metal ring and incubated at 37°C for 24 hours (Figure 2.7). The rings were then lifted out from the plates, any remaining biomaterial carefully removed and the solution aspirated. 2 mL of Trypan

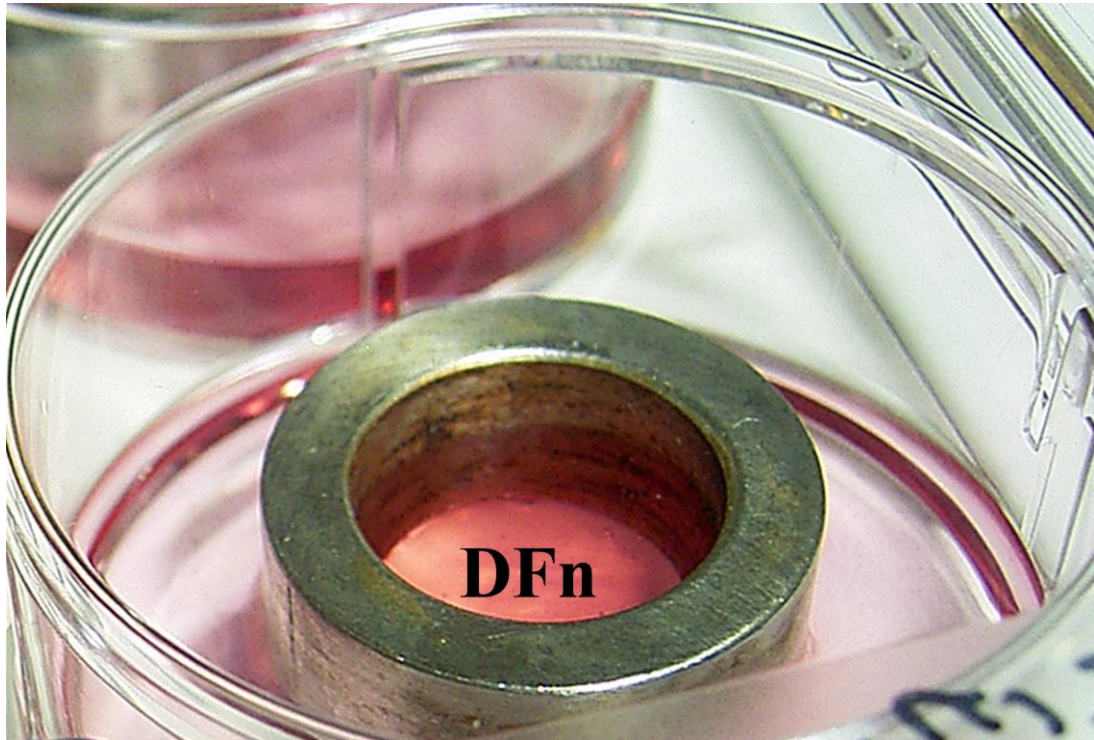


**Figure 2.7** Metal ring used to hold DFn apposed to plated cells.

Blue (0.4%) (Sigma-Aldrich, Gillingham, UK) was diluted 1:1 in 10% NGM and added to each well to determine cell viability.

### **2.2.7 Time Lapse Observation of Cells on Derivative Fibronectin Biomaterial**

In order to examine the interaction between synovial sheath fibroblasts and the DFn biomaterial time lapse images were produced as follows.

DFn was used to coat a glass cover slip as described in section 2.2.4. Fibroblasts ( $1 \times 10^5$  in 10% NGM) were loaded onto the biomaterial coated cover slip, which was maintained at 37°C on the stage of a Diaphot Inverted Stage Microscope (Nikon, Tokyo, Japan). Digital images of the edge of the biomaterial on the glass cover slip were taken over 24 hours.

### **2.2.8 Determination of Cell Attachment and Examination of Morphology of Cells on Collagen Type-I and Fibronectin**

In order to assess the attachment and morphology of fibroblasts derived from the tendon-synovial complex and adhesions to collagen type-I and Fn cells were first seeded on protein coated plates and then stained with crystal violet. Absorbance was determined as a measure of cell attachment and cell morphology was quantified using ImageJ software (US National Institutes of Health, Bethesda, USA) as follows.

#### **2.2.8.1 Adsorption of Collagen Type-I and Fibronectin**

Collagen type-I (First Link, Brierley Hill, United Kingdom) and Fn (Sigma-Aldrich, Poole, United Kingdom) were diluted in ice-cold PBS to obtain 0, 1, 2, 6, 12, 25 and 50  $\mu\text{g mL}^{-1}$  solutions. The solutions were then stored on ice, before adding 50  $\mu\text{L}$  per well of either collagen type-I or Fn solution to appropriate wells of high-binding Nunc MaxiSorp 96-well ELISA plates (Nunc, Paisley, United Kingdom). Each well was reproduced in quadruplicate. The plates were then incubated in a 37°C tissue culture incubator for 1 hour. The wells were aspirated and gently washed with PBS to remove unattached protein.

#### **2.2.8.2 Cell Seeding on Collagen Type-I and Fibronectin**

Cells at passage three or four were washed with Versene for 5 minutes at 37°C, then harvested using Accutase, then resuspended in DMEM with 0.01% BSA (to block non-specific cell adhesion to the 96-well plates). Cells were counted and centrifuged at 1000 g for 5 minutes. The supernatant was then removed and the cell pellet resuspended in 100  $\mu\text{L}$  DMEM with 0.01% BSA, to give  $1 \times 10^5$  cells  $\text{mL}^{-1}$ .

When the cells were ready for the assay the PBS was aspirated from the 96-well plates and then the cells were added and incubated for 1 hour at 37°C. 1 cell strain was tested per plate. Control wells contained PBS and DMEM with 0.01% BSA only without cells. The wells were washed twice using 100  $\mu\text{L}$  PBS using a fine needle vacuum to aspirate. Cell attachment was measured by crystal violet staining.

### **2.2.8.3 Crystal Violet Cell Adhesion Assay**

The culture medium was carefully aspirated using a fine needle vacuum and each well was gently washed twice with 100  $\mu$ L of PBS. Adherent cells were fixed and stained using 25  $\mu$ L crystal violet solution (0.5% crystal violet, 5% formal saline, 50% ethanol in dH<sub>2</sub>O, 0.85% sodium chloride) and incubated for 10 minutes at 37°C. The crystal violet was aspirated using a fine needle. The wells were washed twice with 400  $\mu$ L PBS, using a multichannel pipette to drip the solution onto the side wall whilst holding the plate at 45° to avoid dislodging attached cells. The wells were drained by inversion onto a paper towel.

100  $\mu$ L of 33% acetic acid was then added per well to elute the dye from the cells (Figure 2.8). The optical density was then read using a microplate reader at 595 nm. Cell-free wells were used as intra-plate background control measurements, which were subtracted from all well measurements for that plate. Absorbance was calculated as the mean of the corrected quadruplicate well values for each concentration for each matrix protein for the tendon-synovial complex cell groups and for the adhesion cell groups.

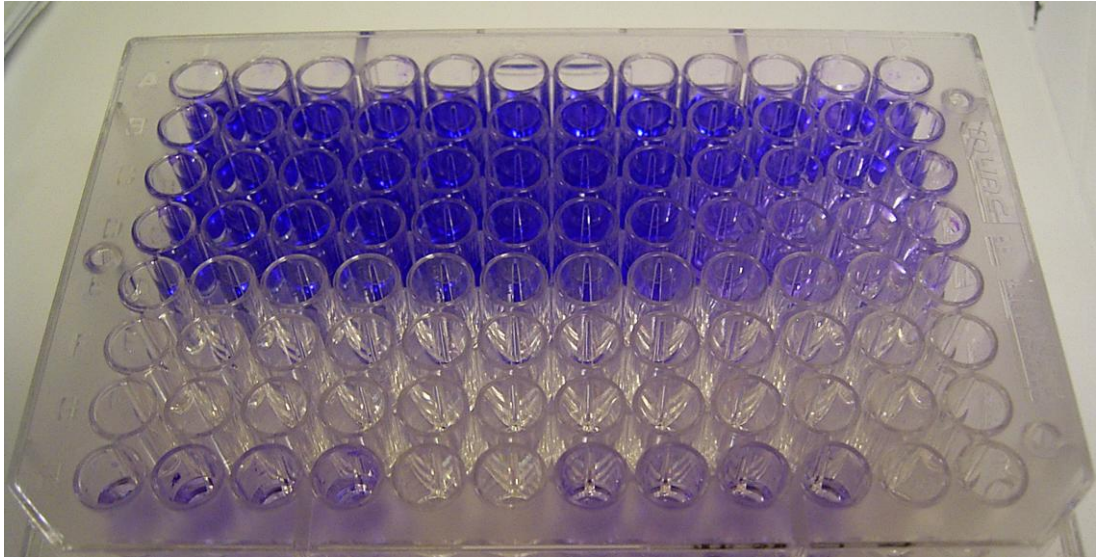


**Figure 2.8** Crystal violet cell adhesion assay.



#### **2.2.8.4 Morphological Assessment of Cells Attached to Collagen Type-I and Fibronectin**

To quantify cell area, perimeter and circularity, and to determine the proportion of elongated cells for the tendon-synovial complex cell groups and for the adhesion cell groups, images were processed as follows.

Digital images taken at random of the cells attached to either collagen type-I or Fn at  $25 \mu\text{g mL}^{-1}$  were captured using a x20 lens with a Zeiss Axioskop Inverted Optical Microscope (Carl Zeiss, Oberkochen, Germany). Cell area, perimeter and circularity were quantified using ImageJ software (Ng, Hinz et al. 2005; Papadopoulos, Spinelli et al. 2007). All cells in each image (typically 10 to 100 cells) were evaluated. Particle counting was used to determine the number of elongated or circular cells. In order to quantify cell area, perimeter and circularity for the different cell groups each digital micrograph image was first converted into a binary image using the threshold function with fixed limits determined from sample images. These were then despeckled, the watershed function applied to delineate apposed cells as shown in Figure 2.9, and processed using established macros (Ng, Hinz et al. 2005).

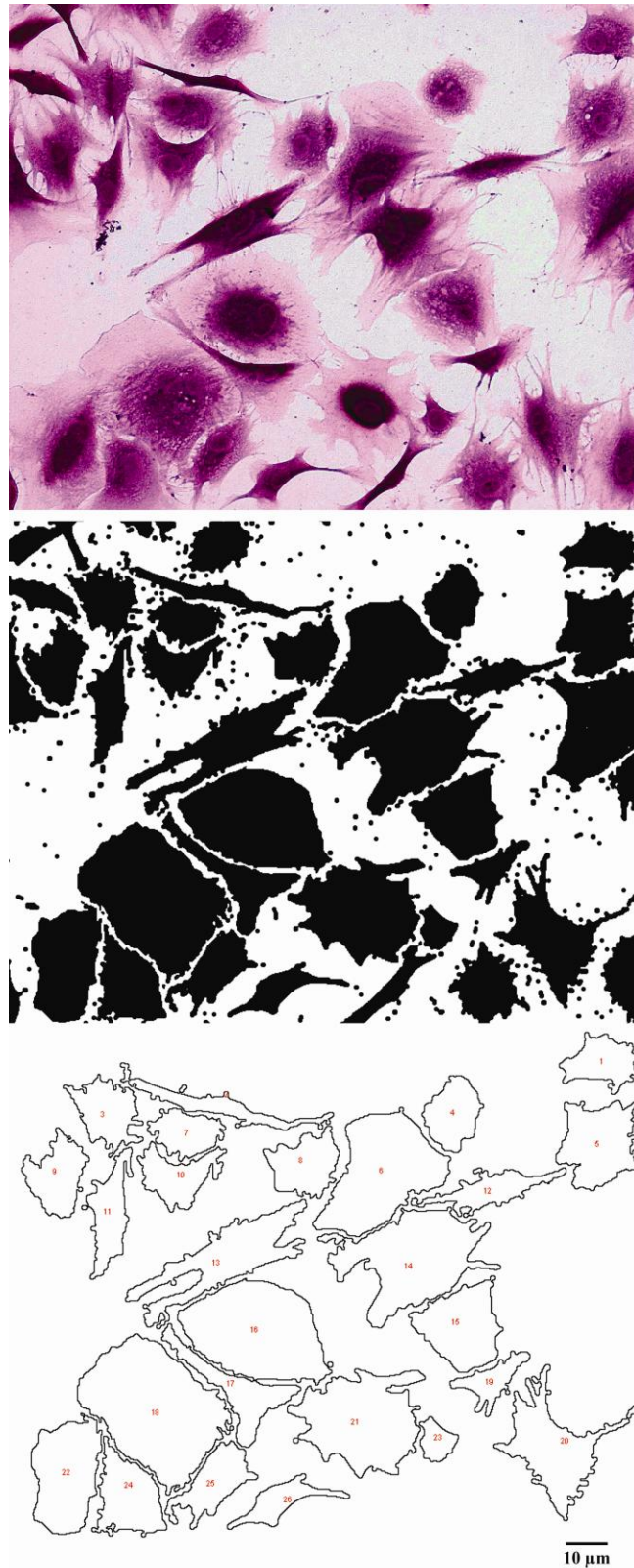


**Figure 2.9** Morphological assessment. (*Above*) Digital micrograph of tendon cells. Magnification x20. (*Centre*) Binary image in ImageJ. (*Below*) Outline image ready for data analysis.

## **2.3        *IN VIVO* METHODS**

### **2.3.1        Tendon Injury Model**

In order to create reproducible flexor tendon injuries while minimising the number of injury variables a partial tenotomy model was used as follows.

Surgery was conducted on digits 2 and 4 in a single paw (the right forepaw) in NZW male rabbits (2.4 - 3.3 kg) aged between 10 and 11 weeks under general anaesthesia with a Zeiss operating microscope (Carl Zeiss, Jena, Germany) using microsurgical operating instruments. Anaesthesia was induced by Hypnorm® (fentanyl-fluanisone 0.2 mL kg<sup>-1</sup>, im, Jansen Copenhagen, Denmark) and Diazepam (2 mL kg<sup>-1</sup>, iv, Phoenix Pharmaceuticals Ltd, Gloucester, United Kingdom). Oxygen was delivered by an anaesthetic mask flowing at 1 L per minute.

The palmar skin was shaved with electric clippers, prepared with chlorhexidine in alcohol and then isolated with sterile drapes. Minimally traumatic tissue handling was employed throughout the procedure. Conveniently the ‘dew claw’ identified the position of the apex of the incision, being just proximal to it (Figure 2.10). Care was made not to incise the dew claw to reduce irritation for the rabbit paw post operatively. A ‘V’ shaped incision proximal to the A1 pulley and the metacarpophalangeal joints gave access to the flexor digitorum profundus (FDP) tendons of digits 2 and 4 (Figure 2.11) avoiding direct injury to the synovial sheath. Once the FDP tendons were exposed, great care was taken to prevent desiccation of the tissue with frequent irrigation using 0.9% normal saline.

The flexor digitorum superficialis tendon was then excised, limiting adhesions to those formed between the FDP tendon and the sheath. Once the FDP tendon was free from surrounding tissue, gentle traction was applied with the aid of a skin hook. This flexed the digit concerned delivering part of the intrasynovial region of the tendon into the palmar wound.

A 1/3 thickness 5 mm long injury (Figure 2.12) was made (Jones, Burnett et al. 2002) with a No.15 scalpel blade (Swann-Morton Limited, Sheffield, UK). Partial tenotomies have been used in several rabbit models (Kakar, Khan et al. 1998; Akali, Khan et al. 1999; Khan, Kakar et al. 2000). On extending the digits the injured tendon was returned to the neutral position within the sheath. This approach circumvents the need for suture repair, thereby minimising the number of injury variables and allowing for immediate postoperative tendon mobilisation (Kubota, Manske et al. 1996; Chan, Fu et al. 1998).

Skin was closed using interrupted 4-0 nylon sutures. The wound was cleaned using gauze with iodine in alcohol and Cicatrin® (neomycin sulphate/ bacitracin zinc, GlaxoSmithKline, United Kingdom) antimicrobial powder applied. All animals received buprenorphine ( $0.025 \text{ mg kg}^{-1}$ , sc) as postoperative analgesia.



**Figure 2.10** The dew claw was just proximal to the apex of the incision. Care was taken not to injure it.

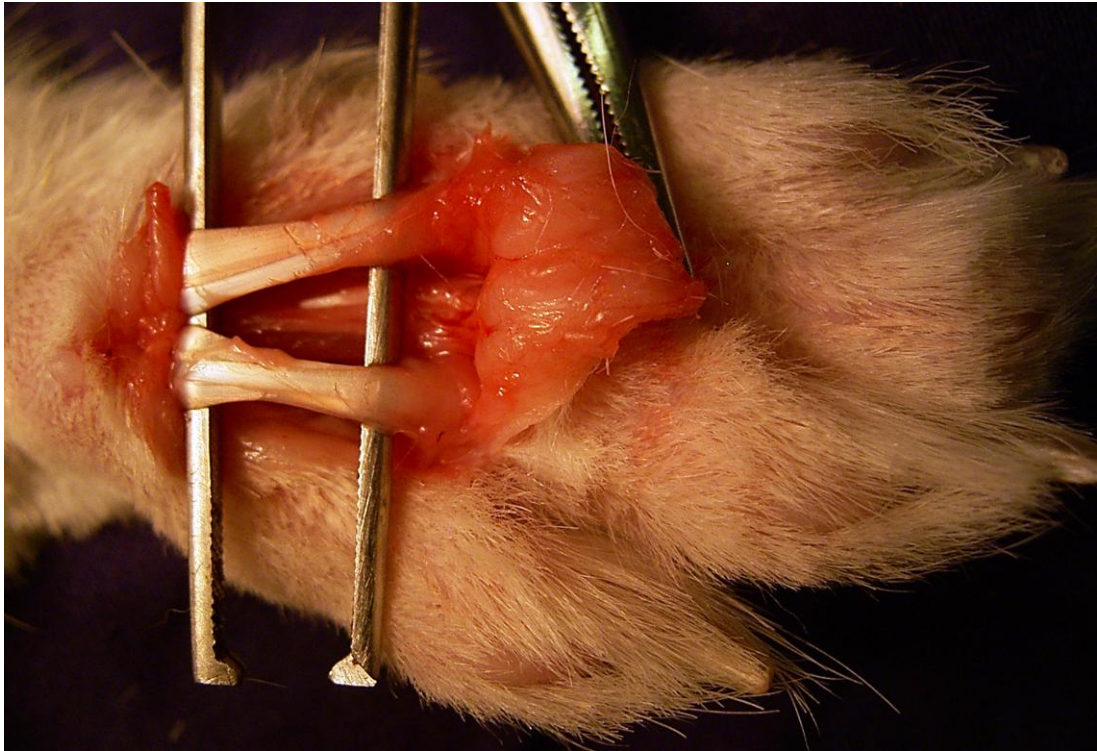


**Figure 2.11** The 'V' shaped incision gave good access to the FDP tendons of digits 2 and 4.





**Figure 2.12** Partial tenotomy injury in the intrasynovial portion of the FDP tendon in the rabbit prior to removal of the segment.

### **2.3.2 Investigation of the Effects of Derivative Fibronectin Biomaterial Treatment on Adhesions**

In this investigation, following creation of a partial tenotomy injury (section 2.3.1), rabbits were randomised to biomaterial treated or untreated injury groups. In the treatment group the DFn was introduced over a proximally placed temporary suture as a 10 mm long tube around the injured tendons in digits 2 and 4 of the right forepaw (Figures 2.13 and Figure 2.14). The injured untreated digits received 3 minutes air exposure, as this time was required to insert the material around the treated tendons.

In order to minimise the number of variables all injured FDP tendons were immobilised by proximal complete transection via the same incision (Jones, Burnett et al. 2002). After recovery, animals were allowed to move freely.

The animals were euthanised at 14 days and the right and left paws were harvested. Digits 2 and 4 of the left forepaw were harvested as unoperated controls. Digits were randomised to mechanical (section 2.3.2.1) or histological (section 2.3.4.1) and immunohistochemical assessments (section 2.3.4.2; Figure 2.15).





**Figure 2.13** Biomaterial tube insertion around the injured tendon using a temporary suture.

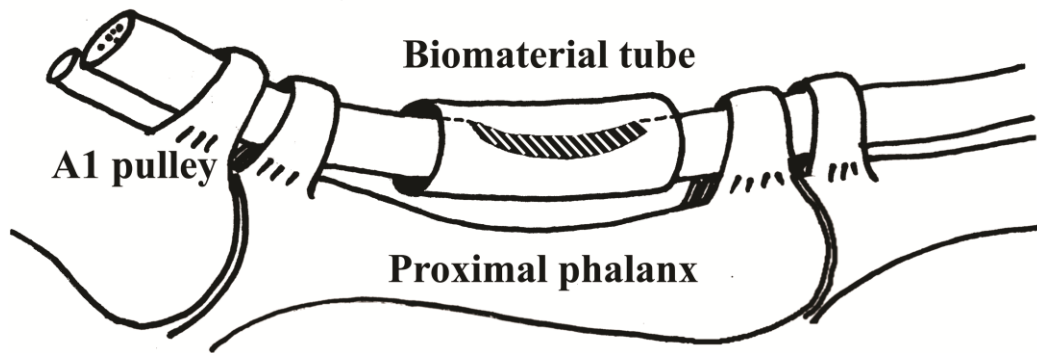


**Figure 2.14** Diagram of biomaterial *in situ* around tendon injury.

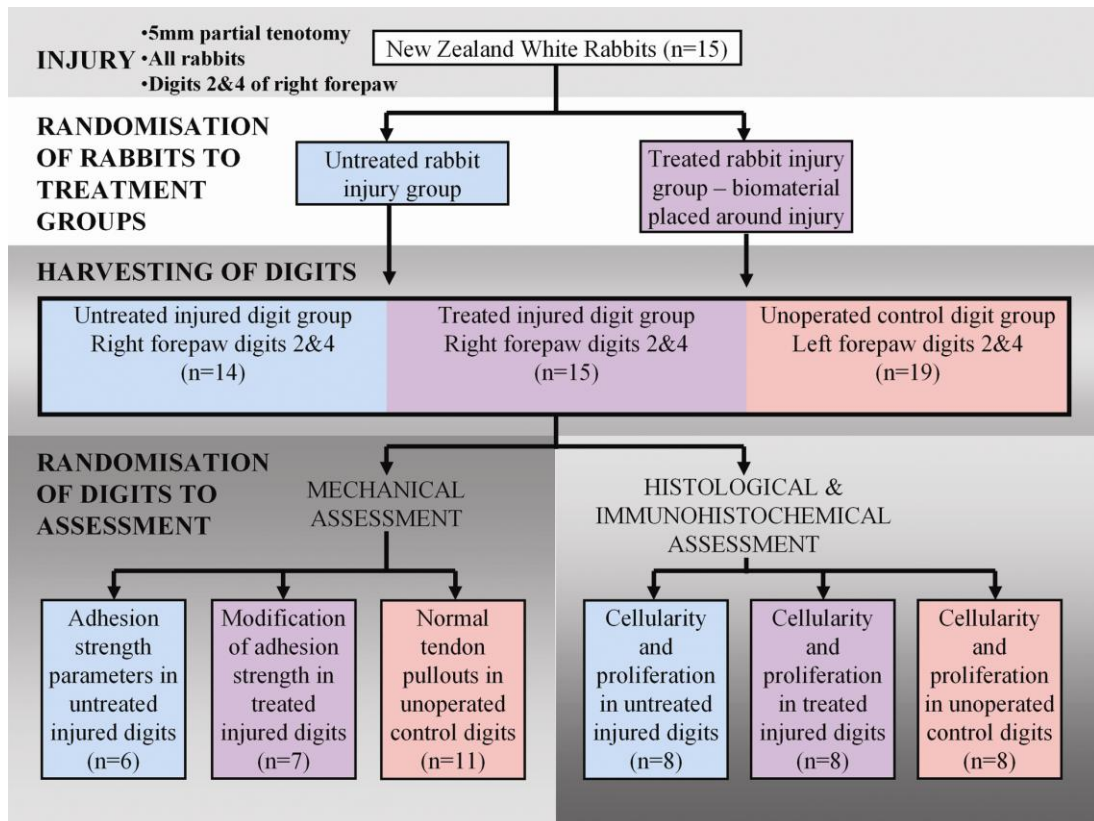


**Figure 2.15** Study design showing randomisation of animals having received a partial tendon injury to digits 2 and 4 of their right forepaw to biomaterial treated or untreated injury groups. Digits were harvested at 2 weeks, with subsequent randomisation of digit groups to either mechanical or histological and immunohistochemical scoring.

### **2.3.2.1 Mechanical Pullout Evaluation**

In order to assess the effects of DF<sub>n</sub> treatment on mean peak force required for tendon pullout and adhesion structural stiffness, digits were subjected to tensile testing as follows.

Forepaws were maintained in saline soaked gauze and freshly assessed. The incisions were reopened with the assistance of a Zeiss operating microscope. The digital claw was held using a clamp and the free proximal end of the cut FDP tendon was identified, transfixed with a silk 2/0 suture and secured to a tensile testing machine (Zwick Roell Group, Ulm, Germany; Figure 2.16). Vertical shear reducing pullouts were carried out at constant speed (2.5 mm per minute) to determine the force required to draw the tendon from its sheath with the tendon transected at its insertion just before assessment. This method allowed the tendon to lie freely within the sheath, disconnected at either end so that a force applied proximally would measure solely the strength of any adhesion between the tendon and the sheath. The applied force was increased until adhesions failed (force returning to zero Newtons (N)).

Untreated injured digits were used to determine adhesion strength. The treated injured digits were tested to investigate the material's effect on modifying adhesion strength. The restriction parameters were the mean peak force in N required for tendon pullout and the adhesion mean structural stiffness (determined in the linear portion of each force displacement curve, being the resistance of the adhesion to deflection by an applied force in  $\text{N m}^{-1}$ ).

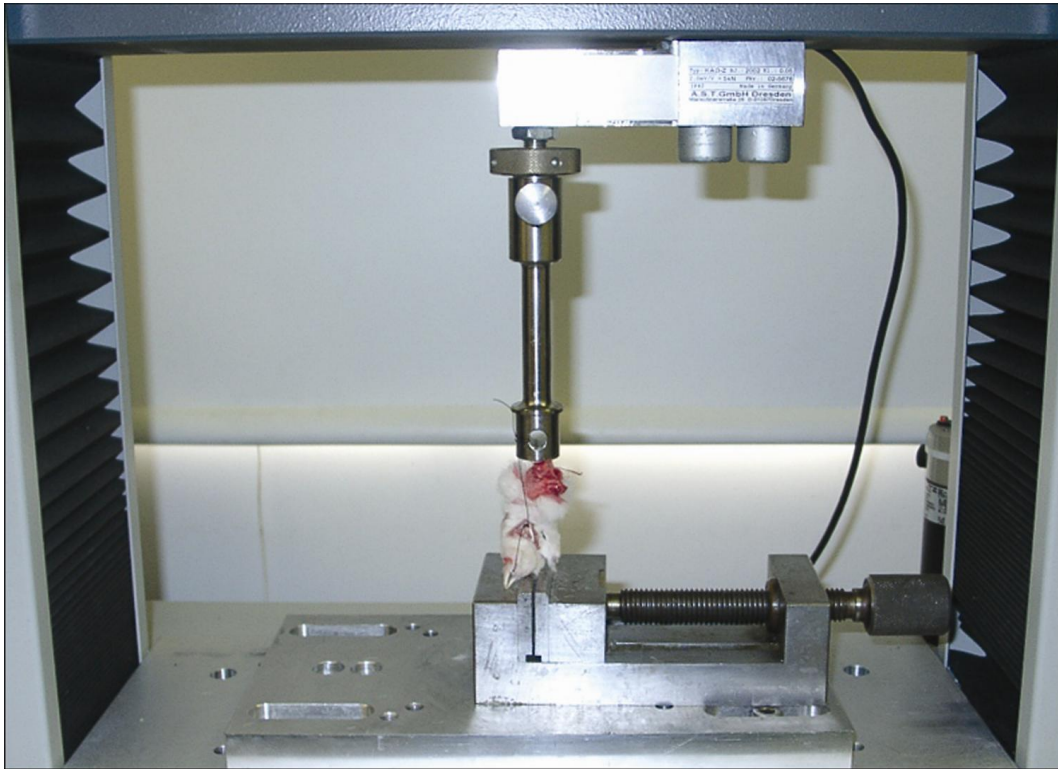


**Figure 2.16** Mechanical pullout assessment with the digital claw being held at one end and the FDP tendon of the same digit being held using a transfixion suture at the other.

To assess biomaterial degradation, it was recorded whether biomaterial was present macroscopically within the wound at the time of dissection of digits subjected to mechanical pullouts.

### **2.3.3 Investigation of the Effects of Mobilisation on the Hierarchical Biomechanical Properties of Adhesions**

In order to describe how mobilisation affects adhesion tissue organisation, to examine local strains in adhesions and to relate local tissue responses to gross restrictive parameters a hierarchical approach was used as follows (Figure 2.17). Digits 2 and 4 of the right forepaw were operated on in each animal (as described in section 2.3.1) in order to reduce numbers, although paired comparisons were not made.

#### **2.3.3.1 Mobilisation Regime for Injured Digits**

In order to examine the effects of mobilisation on injured tendons, rabbits were randomised to mobilised or immobilised injury groups as follows.

Tendons were immobilised by proximal complete transection via the same incision (Jones, Burnett et al. 2002). In those animals that were mobilised tendons were not transected, allowing normal digital excursion. After recovery, animals were allowed to move freely. The animals were euthanised at 14 days and the paws were harvested.

### **2.3.3.2 Sample Preparation**

Paws were wrapped in gauze moistened with PBS and stored at 4°C prior to analysis, which was always within 48 hours of harvest. The paw skin was excised and the tendon-adhesion-synovial complexes, comprising tendon, peritendinous adhesions and surrounding soft tissues, were removed en bloc from the phalanges of digits 2 and 4 under x3.5 loupe magnification. The macroscopic appearance of the specimens was recorded. Samples were kept moistened with PBS throughout subsequent testing.

### **2.3.3.3 Determination of Gross Adhesion Mechanics**

Gross mechanical testing, as represented by structural stiffness and the peak load at failure, provides an assessment of the overall material properties of a tissue.

Mobilised and immobilised samples were secured using a grip at each end separated by a fixed length of 15 mm, with the tendon being held at one end and the peritendinous tissues at the other (Figure 2.18). In this way, each sample was loaded in tension up to failure of the adhesion (connecting the fixed tendon and surrounding tissues) at a constant rate of 2.5 mm per minute, using the Bionix® 100 mechanical testing system (MTS Systems Limited, Cirencester, United Kingdom). The linear proportion of the resulting load-extension data yielded structural stiffness and the peak load represented the load at failure for the adhesion in each sample (Figure 2.18).

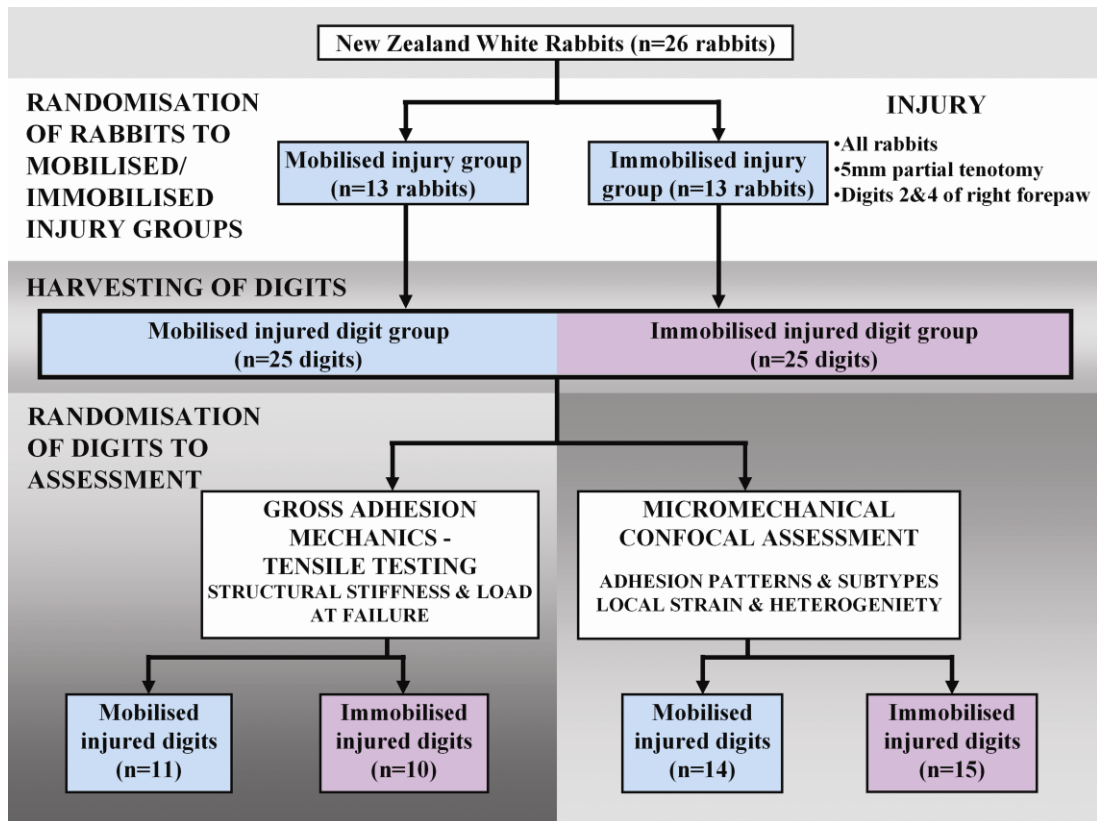


**Figure 2.17** Study design showing randomisation of digits to either gross tensile testing or to micromechanical assessment.



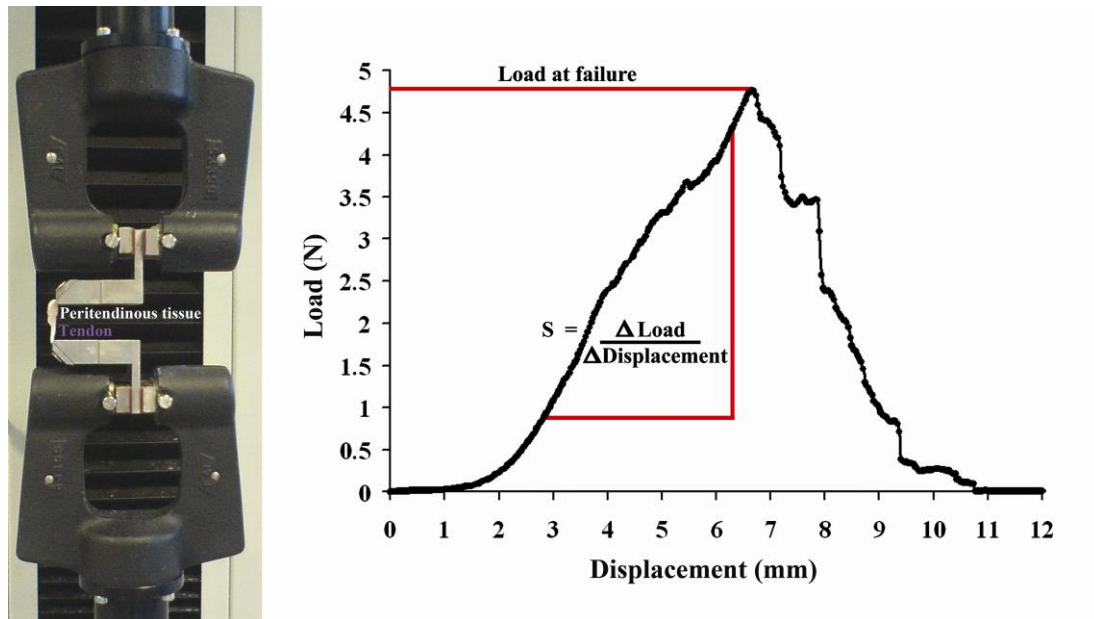


**Figure 2.18** Macromechanical testing of adhesions. (*Left*) Gross tensile testing system. (*Right*) Representative load-displacement curve for a test sample, showing load at failure and structural stiffness (S).

#### **2.3.3.4 Micromechanical Assessment**

In order to examine local tissue organisation and strain responses in tendon adhesions a straining system was used to apply load, using the fluorescently labelled cell nuclei as dynamic local strain markers as follows.

##### ***2.3.3.4.1 Straining System***

A custom designed tensile straining rig (Screen, Lee et al. 2003; Screen, Lee et al. 2004; Screen 2004; Cheng 2007) was used to apply load to the adhesions with the specimen being held in an identical manner to that during the gross tensile testing in section 2.3.3.3. The rig was mounted on the stage of an inverted TCS SP2 confocal laser scanning microscope (Leica Microsystems GmbH, Wetzlar, Germany; Figure 2.19). The design of the rig ensured that the specimen was located adjacent to the glass coverslip, enabling visualisation of cells within the tissue. The rig was driven by stepping linear actuators and controlled using LabVIEW™ (National Instruments UK Limited, Newbury, United Kingdom). A maximum displacement of 10% was applied at increments of  $75\ \mu\text{m} \pm 15\ \mu\text{m}$ , equivalent to a strain increment of 0.5% strain at a strain rate of 1.5% per minute (Screen, Lee et al. 2003). The 2 motors on either side of the rig moved simultaneously, ensuring that the central region of the sample remained within the microscopic field of view during the application of strain to facilitate cell tracking. Specimens were bathed in PBS in a chamber maintained at 37°C using heater pads.

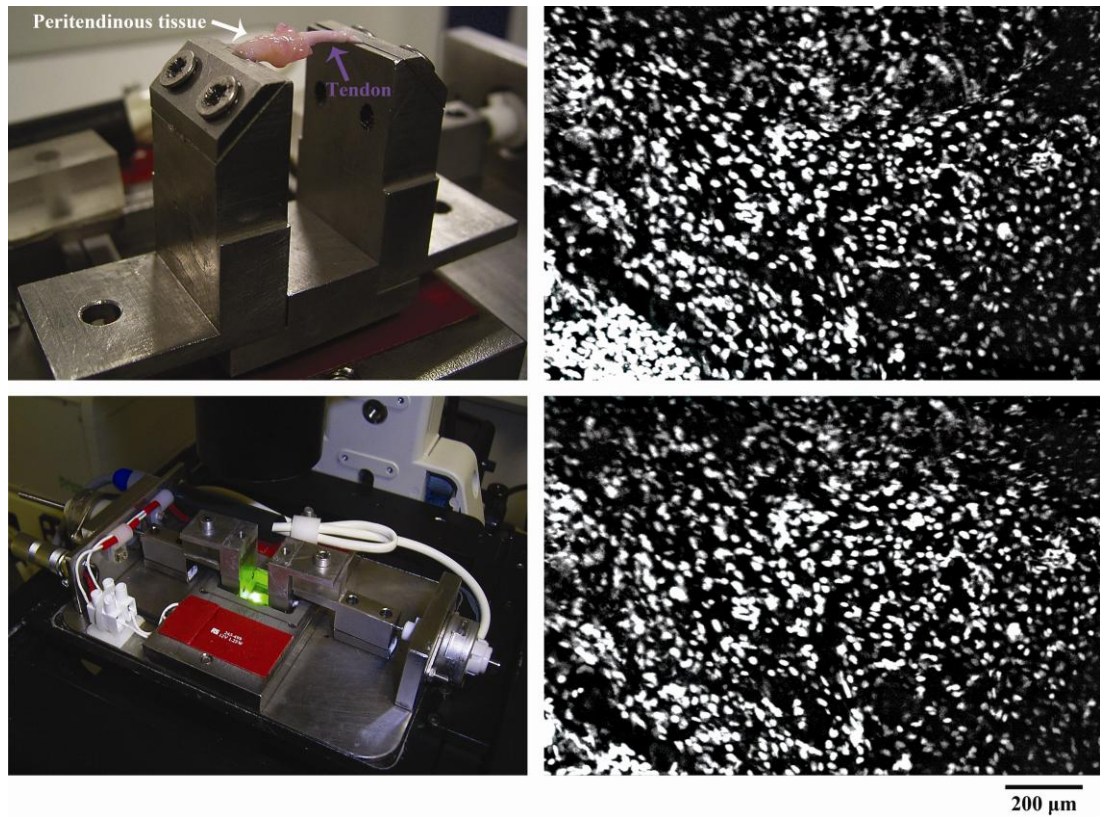


**Figure 2.19** Micromechanical testing of adhesions. (*Above left*) Micromechanical straining system with specimen held in tissue grips. (*Below left*) Custom designed rig on stage of inverted confocal laser microscope. (*Above right*) Digital confocal image of adhesion cell nuclei fluorescently labelled with ethidium homodimer-1: At 0% applied strain. (*Below right*) Digital confocal image at 10% applied strain. Magnification x10.

#### **2.3.3.4.2    *Confocal Microscopy***

Invasive imaging methods such as histology, and scanning electron microscopy, also lack real three-dimensional information and require long and harsh processing steps. Confocal microscopy has been an important advance in imaging, enabling the non-destructive visualisation of optically non-transparent specimens to produce high resolution images of tissue structure using fluorescent probes (Stephens and Allan 2003; Tan, Sendemir-Urkmez et al. 2004). The technique scans the specimen using a focused beam of light, collecting the fluorescence signal via a pinhole that rejects light from out of focus areas. In this way cell distribution and tissue architecture may be examined in real time or with time lapse imaging. It is therefore possible to make repeated observations within a single sample in response to mechanical stimuli (Tan, Sendemir-Urkmez et al. 2004). Local tissue mechanics may be reconstructed in three dimensions over time (Cukierman, Pankov et al. 2001; Voytik-Harbin, Rajwa et al. 2001). Confocal microscopy has been used to detect alterations in cell shape, in response to loading and increasing local tissue strain in articular cartilage (Guilak 1995; Guilak, Ratcliffe et al. 1995; Guilak, Tedrow et al. 2000), which may stimulate cell signalling events through calcium mediated pathways (Guilak 1994).

In this thesis confocal microscopy was used in combination with image processing software to examine local tissue strains in mobilised and immobilised adhesions. This was in order to analyse the effect of mobilisation on tendon adhesion tissue organisation, to quantify the local strain responses produced in adhesions to applied strain and to relate these micromechanical findings to gross restrictive parameters.

#### **2.3.3.4.3 *Confocal Assessment***

Samples were incubated in 20  $\mu$ M ethidium homodimer-1 (Invitrogen, Paisley, UK) in PBS for 1 hour at 37°C to label the cell nuclei fluorescently. The specimens were briefly rinsed in PBS, and then loaded into the straining rig as detailed in section 2.3.3.4.1. The confocal laser scanning microscope was used to visualise the adhesion cell nuclei, with a Plan Apo x10 magnification objective lens (Nikon, Kingston-Upon-Thames, United Kingdom) and the argon laser set at 10% power. The laser excitation wavelength was 488 nm and emission was detected above 586 nm.

Strain was applied following the method detailed in section 2.3.3.4.1. A population of cells within the adhesion were imaged at each strain increment, using the cell nuclei to ensure maintenance of the same focal depth (Figure 2.19). The image immediately preceding the first detectable cell movement was defined as 0% strain. Orthogonal directions ( $x$  and  $y$ ) were defined with the  $y$  axis being in the direction of the applied strain. Images were captured every 20 seconds.

#### **2.3.3.4.4 *Image Analysis***

By tracking the cell nuclei throughout the entire strain range it was possible to determine local strain values, using the nuclei as local strain markers as follows.

All of the digital confocal images for each sample were first centred on a reference nucleus using Adobe® Photoshop® CS4 (Adobe Systems Incorporated, San Jose, Calif.) with the assistance of the grid function. These images were then uploaded into the image analysis package Imaris® 6.1 (Bitplane AG, Zurich, Switzerland). The software was used to assign exact values of the  $x$  and  $y$  axis positions of the cell

nuclei in each of the images (Figure 2.20). The reference nucleus was assigned the position  $x = 0$ ,  $y = 0$  at all levels of strain. The tracking module of the software was then used to track the displacement of all the cell nuclei up to 10% applied strain (Figure 2.20). The resulting data were converted into a spreadsheet format for further processing.

#### **2.3.3.4.5 Data Analysis**

The distribution of the local strain across each sample was determined as follows.

Local strain was defined as the change in dimension along the y axis resulting from the applied displacement. Using the Cartesian co-ordinate system the distance of each peripheral nucleus from the central reference nucleus was measured at each applied strain and subsequently converted to local strain values using the formula (Cheng 2007):

$$\text{Local strain (\%)} = (y_2 - y_1) \times 100 / y_1$$

Where  $y_1$  and  $y_2$  are the distances between the position of the central reference nucleus and the peripheral nucleus in the y axis at 0% and 10% applied strain, respectively (Figure 2.21). By plotting the displacement of each peripheral nucleus,  $(y_2 - y_1)$ , against  $y_1$ , the slope represents the local strain for each adhesion sample.

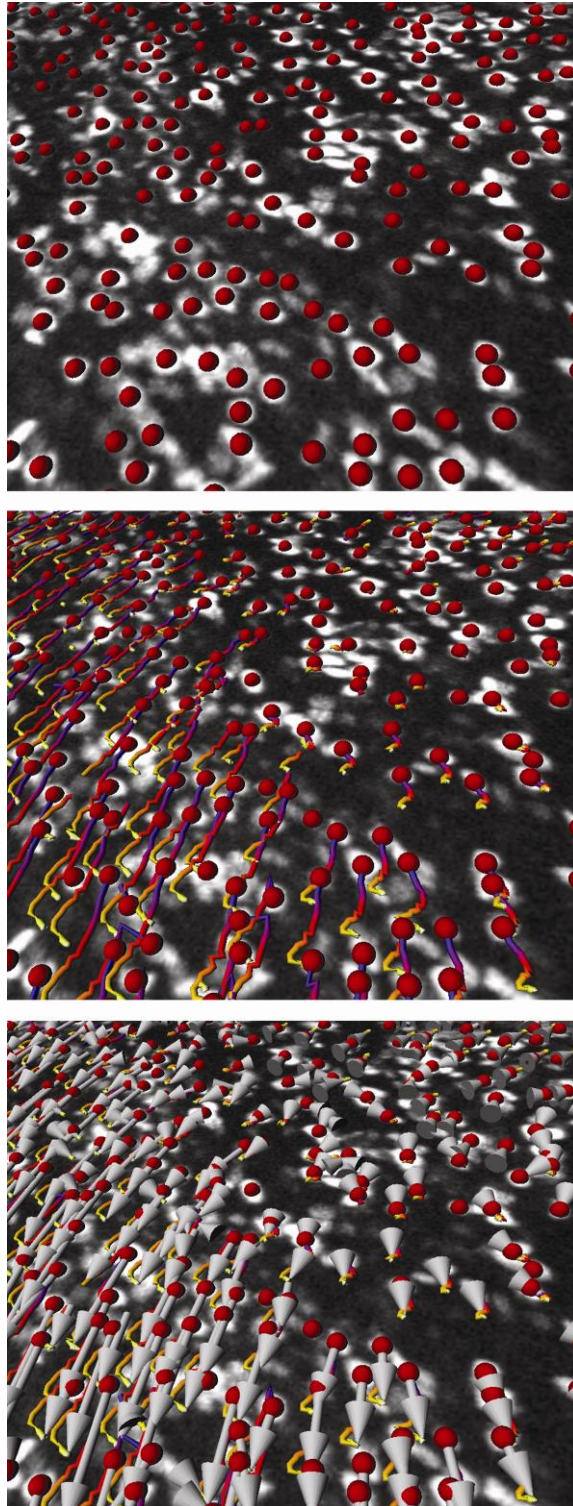


**Figure 2.20** Processed confocal images of adhesion cell nuclei. (*Above*) Cell nuclei identified by red spheres. (*Centre*) Tracks generated by nuclear displacement (blue at 0% strain: white at 10% strain). (*Below*) Geometric vector displacement over the range of applied strain shown as grey arrows.

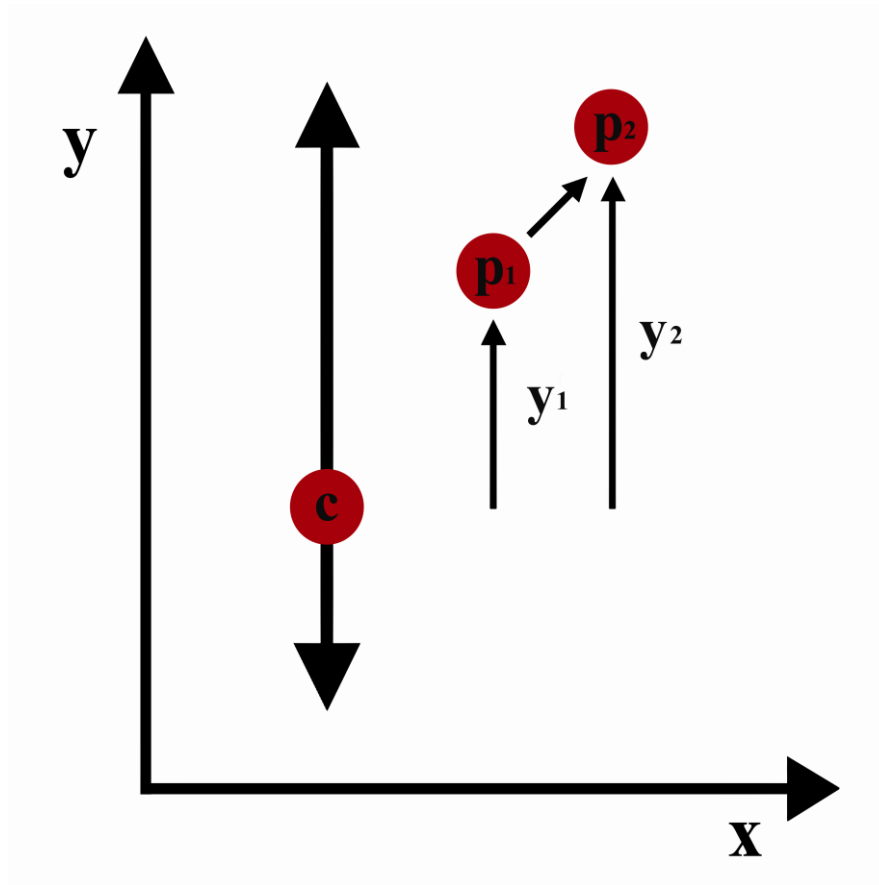


**Figure 2.21** Schematic of the measurements relevant to calculating local strain.  $y_1$  is the distance between the position of the central reference nucleus (c) and the peripheral nucleus ( $p_1$ ) in the y axis at 0% applied strain and  $y_2$  the distance between the position of the central reference nucleus and the peripheral nucleus ( $p_2$ ) in the y axis at the higher increment of applied strain. The direction of the applied strain is shown by the arrows centred on c.



## **2.3.4 Histology and Immunohistochemical Scoring in Derivative Fibronectin Biomaterial Treated and Untreated Injured Tendons and Adhesions**

Tendon and adhesion cellularity and cell proliferation were assessed to clarify the material's mechanism of action as follows.

### **2.3.4.1 Histological Scoring**

Digits were divided into halves in the sagittal plane, formalin fixed, decalcified in ethylenediamine tetraacetic acid (EDTA) for a total of 4 days and paraffin wax embedded. 3 longitudinal 5  $\mu$ m sections were cut from 3 longitudinal equally spaced zones within each half. The high number of sections enabled both haematoxylin and eosin (H and E) and immunohistochemical staining to be carried out, and ensured that sufficient specimens contained tendon. 1 representative sample was taken from each half digit and stained with H and E using the technique described in section 2.2.5.1.

The presence of adhesions on microscopic examination as a characteristic densely cellular band connecting tendon to the surrounding tissues (Figure 2.22) was recorded. Digital micrographs were uploaded into Adobe® Photoshop® for analysis. Cell counts from 1 sample from each half were used to provide mean digital counts. Tissue cellularity was quantified using the grid function, with the grid being placed so that its sides were parallel with the tissue surface. Cell counts were made in 10  $\mu$ m high rows from superficial to deep over a 200 x 200  $\mu$ m grid (Figure 2.23). For tendon the grid was placed in the zone of injury.

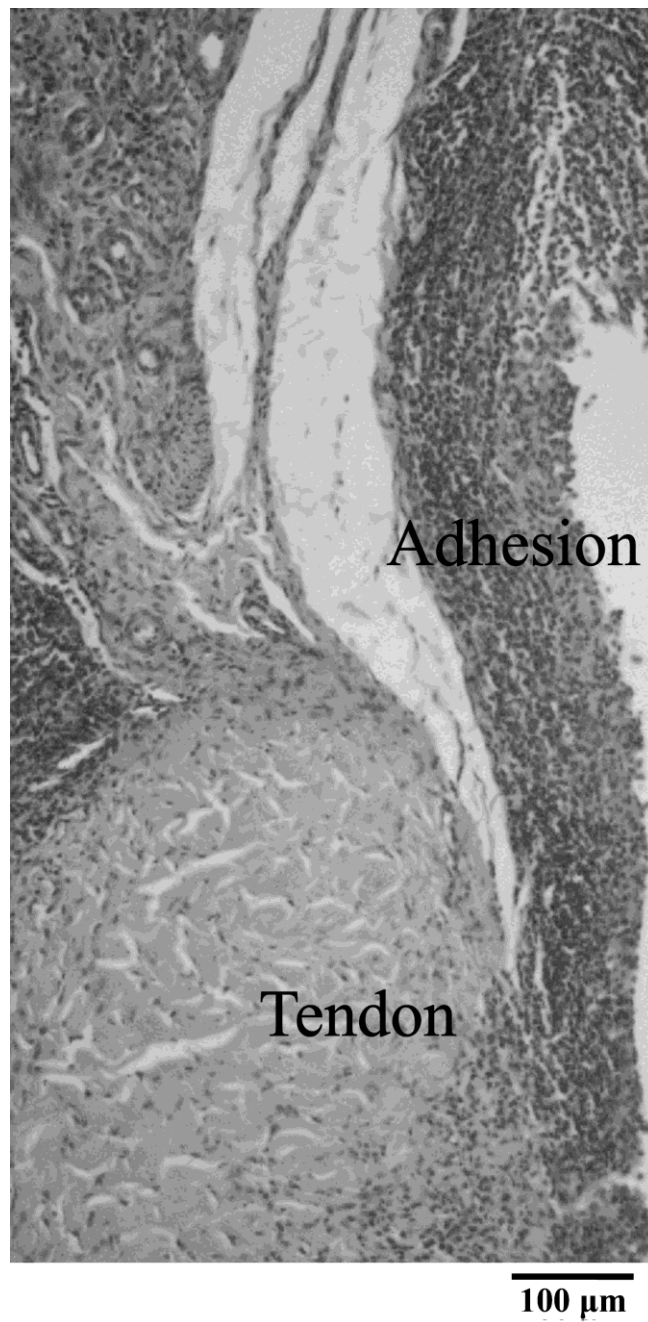


**Figure 2.22** Micrograph of an adhesion bridging interface between tendon and surrounding soft tissues. Magnification x10.

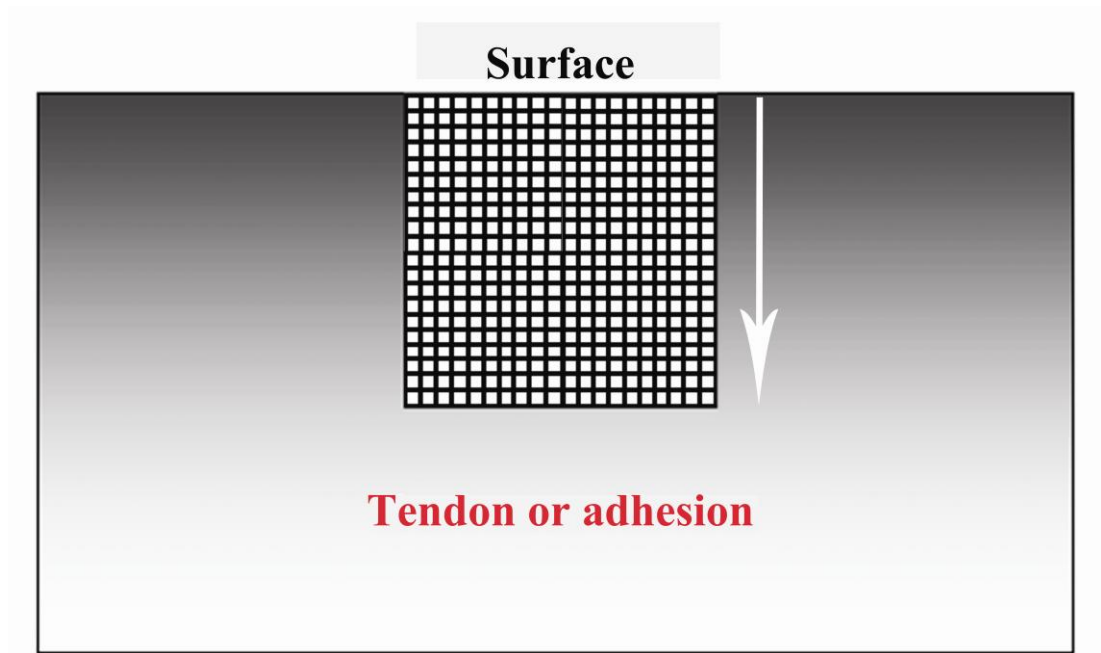


**Figure 2.23** The cellularity of tendon and adhesion tissue was quantified using cell counts over a 200 x 200  $\mu\text{m}$  grid. The grid was placed so that its sides were parallel with the tissue surface. Counts were made in 10  $\mu\text{m}$  high rows from the surface into the tissue substance. For tendon the grid was placed in the zone of injury.

A representative tendon or adhesion was assessed from each sample. Slides were scored independently by 3 observers. A similar technique has previously been used to study the surface cell response to tendon injury (Akali, Khan et al. 1999; Jones, Mudera et al. 2003).

#### **2.3.4.2 Immunohistochemical Detection of Ki-67 Antigen**

The number of proliferating cells in the sections was assessed by immunohistochemical detection of Ki-67 antigen, detecting all active stages of the cell cycle but not the G0 'resting' stage (Scott, Hall et al. 1991), as follows. This was then quantified using the grid technique described in section 2.3.4.1 (Figure 2.23). Slides were scored independently by 3 observers.

Firstly, slides were deparaffinised in xylene (Merck, Poole, UK) and then rehydrated in reducing percentages of ethanol, to distilled water as described in section 2.2.5.1. Endogenous peroxidases were then removed by soaking in a 3% fresh solution of hydrogen peroxide (Merck, Poole, UK; Appendix I) followed by a wash in the buffer PBS. The primary antibody was optimised for antigen retrieval by microwaving in sodium citrate buffer (Appendix I) for 10 minutes in two 5 minute bursts with a 5 minute break between. The slides were cooled in the sodium citrate buffer prior to incubation with the antibodies.

Slides were then placed in a humidity chamber and normal rabbit serum (Dako, High Wycombe, UK) was added to prevent non-specific staining (diluted 1:10 and left on the sections for 10 minutes at room temperature). This serum was then removed by

tapping off the excess and the primary antibody was layered on top at a 1:25 dilution in 1% BSA diluted in PBS.

Before doing the experiments the antibody dilution optimised by starting with the recommended manufacturer's dilution and then using a range either side. The sections from the control tissue were then assessed for intensity of staining and absence of non-specific staining. Incubation time was also optimised, along with incubation temperature, allowing specific staining with the lowest concentration of antibody but still providing intense specific staining. The incubation time for the primary antibody was 90 minutes at room temperature.

Following incubation, the primary antibody was washed off in two 3 minute washes with PBS. The secondary antibody was then applied in phosphate buffered saline-bovine serum albumin (PBS-BSA; Appendix I) containing a 10% dilution of normal human serum. The secondary antibody uses the primary antibody as its antigen; hence the mouse monoclonal primary (anti Ki67, Dako, High Wycombe, UK) would have a secondary antibody raised against the mouse (rabbit anti-mouse biotinylated antibody, Dako, High Wycombe, UK). This secondary had been biotinylated; i.e. biotin had been added chemically. It was added at a dilution of 1:200 and was left at room temperature for 45 minutes. The secondary antibody was then removed by two 3 minute washes in PBS. The streptavidin-biotin-horseradish peroxidase complex (Dako, High Wycombe, UK) was then made up in a dilution of 1:200 and layered onto the tissue and left at room temperature for 45 minutes. This was washed off and the slides then immersed in the chromogen 3, 3'-diaminobenzidine tetrahydrochloride (Sigma-Aldrich, Gillingham, UK; Appendix I). The slides were

left for 8 to 12 minutes until a colour had developed, and the reaction terminated by placing the slides in tap water. The slides were then counterstained in Mayer's haemalum (BDH, Poole, UK) and re-hydrated with grades of ethanol. They were cleared with xylene to allow the refractive index to come to 1 and then mounted in Depex (BDH, Poole, UK) and a cover slip added.

A positive control was included in each staining batch to ensure that the staining was successful. A negative control was also included in each staining run. In the negative controls the primary antibody was omitted and replaced by PBS in one reaction, and the secondary antibody replaced by PBS in another, to check for non-specific staining.

To ensure staining consistency and reproducibility all sections from different blocks were stained as a batch on the same day and the process was repeated four times. Results were analysed independently by 3 observers.

## **2.4 STATISTICAL ANALYSIS**

All statistical analysis was performed using Sigmastat for Windows, Version 2.0 (Jandel Scientific Corporation, San Rafael, USA). Data was analysed using Student's t-test, the unpaired t-test, the Mann-Whitney U test, or 2-way repeated measures ANOVA with the Tukey post-test or Dunnett's post-test as appropriate, with  $p < 0.05$  being judged as statistically significant.

# **CHAPTER 3**

## **RESULTS**

### **SHEAR-AGGREGATED FIBRONECTIN WITH ANTI- ADHESIVE PROPERTIES**

#### **3.1 INTRODUCTION**

##### **3.1.1 Aim**

#### **3.2 MATERIALS AND METHODS**

##### **3.2.1 Protein analysis of Derivative Fibronectin Biomaterial and Fibronectin Control**

##### **3.2.2 Biodegradability of Derivative Fibronectin Biomaterial and Fibronectin Control**

##### **3.2.3 Synovial Sheath Fibroblast Culture**

##### **3.2.4 Assessment of Fibroblast Attachment**

##### **3.2.5 Assessment of Migration**

##### **3.2.6 Fibroblast Viability Assessment**

##### **3.2.7 Time Lapse Assessment**

##### **3.2.8 Statistical Analysis**

#### **3.3 RESULTS**

##### **3.3.1 Protein Analysis of the Derivative Fibronectin Biomaterial and Fibronectin Control**

- 3.3.2 Biodegradability of the Derivative Fibronectin Biomaterial and Fibronectin Control**
- 3.3.3 Assessment of Fibroblast Attachment**
- 3.3.4 Assessment of Migration**
- 3.3.5 Fibroblast Viability Assessment**
- 3.3.6 Time Lapse Assessment**
- 3.4 DISCUSSION**
  - 3.4.1 Preventing Cell Attachment to Fibronectin: A Therapeutic Strategy**
  - 3.4.2 Cell Binding and Fibronectin**
  - 3.4.3 An Anti-Adhesive Biomaterial**
  - 3.4.4 Inhibitory Fragments Within the Fibronectin Molecule**
  - 3.4.5 Cryptic Anti-Adhesive Site and Exposure to Urea**
  - 3.4.6 The Anti-Adhesive Nature of the Derivative Fibronectin Biomaterial**
  - 3.4.7 Cryoprecipitate Contains Fibronectin Fragments**
  - 3.4.8 Inhibition of Myofibroblastic Conversion by the Derivative Fibronectin Biomaterial**
  - 3.4.9 Biomaterial Degradation**
  - 3.4.10 Barrier Effects of the Derivative Fibronectin Biomaterial**
  - 3.4.11 Summary**



### 3.1 INTRODUCTION

Biomaterials based on proteins, such as fibronectin (Fn), have the potential to guide cell and tissue behaviour during healing as a function of their unique mechanical and bioactive properties. Fn has been reported as a scaffold for the attachment of fibroblasts and the subsequent deposition of collagen. During production of shear aggregated Fn based biomaterials with adhesive properties, withdrawal of a washing step resulted in a derivative of the fibronectin biomaterial (DFn) with inhibitory properties (Djerkovic, Phillips et al. 2005). The properties of DFn have been investigated both *in vitro* (Branford, Brown et al. 2010; this Chapter) and *in vivo* (Branford, Mudera et al. 2008; Chapter 4).

The *in vitro* investigation tested DFn and its effects on aggressive adhesion forming cells, using rabbit flexor tendon synovial sheath fibroblasts. These cells were used as they are recognised as being active contributors to adhesion formation (Brigman, Hu et al. 1994; Khan, Occleston et al. 1997; Khan, Occleston et al. 1998; Ragoowansi, Khan et al. 2003). The stability of the biomaterial in solution was tested as a measure of its degradation. An ideal biomaterial would have the ability to undergo degradation, reducing its likelihood to stimulate further inflammation and adhesion formation. Attachment and infiltration of fibroblasts cultured with the DFn was examined, representing the biomaterial's anti-adhesive properties and ability to act as a physical barrier, respectively. Toxicity of the biomaterial on fibroblasts and stress fibre formation by fibroblasts seeded on the biomaterial were examined. Finally, the interaction between fibroblasts and the biomaterial was visualised using time lapse photography.

### **3.1.1 Aim**

To conduct an investigation into the properties of a DFn and its effects on aggressive adhesion forming cells *in vitro*, using synovial sheath fibroblasts.

## **3.2 MATERIALS AND METHODS**

### **3.2.1 Protein Analysis of Derivative Fibronectin Biomaterial and Fibronectin Control**

The protein content of the solutions from the various stages of production of the DFn and Fn control were analysed qualitatively using an immunoelectrophoresis kit (section 2.2.3.1) and quantitatively using immunodiffusion techniques (section 2.2.3.2).

### **3.2.2 Biodegradability of Derivative Fibronectin Biomaterial and Fibronectin Control**

Degradation of the DFn and Fn control materials in normal growth media with 10% fetal calf serum (FCS; referred to as 10% NGM in the text), phosphate buffered saline (PBS), or PBS containing the protease inhibitor Aprotinin was tested. This was achieved by evaluating protein loss in solution in samples taken over 21 days, which were tested using a Bicinchoninic Acid Protein Assay Reagent Kit, as measured as described in section 2.2.3.3.

### **3.2.3 Synovial Sheath Fibroblast Culture**

The synovial sheaths of the digital flexor tendons from 5 New Zealand white rabbit forepaws were dissected out using a dissecting microscope, thoroughly washed, then

divided into 2-5 mm<sup>3</sup> pieces and explant cultured to obtain their fibroblasts, as described in section 2.2.1.1.

### **3.2.4 Assessment of Fibroblast Attachment**

The attachment of synovial sheath fibroblasts to glass coated with the DFn biomaterial, relative to fibroblast attachment to uncoated and Fn control coated glass was assessed using a propidium iodide stain as a measure of cell counts, as detailed in section 2.2.4.1. The number of myofibroblasts was assessed using an immunofluorescent  $\alpha$ -smooth muscle actin ( $\alpha$ -SMA) stain, as detailed in section 2.2.4.1.

### **3.2.5 Assessment of Migration**

The infiltration of the biomaterials by fibroblasts was assessed by seeding synovial sheath cells onto DFn and Fn control, washing, formalin fixation and Haematoxylin and Eosin (H and E) staining as described in section 2.2.5. This was examined using light microscopy for fibroblasts attached to, or having migrated beneath, the surface of the biomaterials.

### **3.2.6 Fibroblast Viability Assessment**

Details of the assessment of the cytotoxicity of the DFn to fibroblasts exposed to it using Trypan Blue staining are outlined in section 2.2.6.

### **3.2.7 Time Lapse Assessment**

The interaction between synovial sheath fibroblasts and DFn over 24 hours was visualised using time lapse photography, as described in section 2.2.7.

### **3.2.8 Statistical Analysis**

Statistical analysis was used, using a p value of <0.05 as to be statistical significant. The different treatment groups were compared using the unpaired t-test as the data was normally distributed.

## **3.3 RESULTS**

### **3.3.1 Protein Analysis of the Derivative Fibronectin Biomaterial and Fibronectin Control**

#### **3.3.1.1 Immunoelectrophoresis**

The immunoelectrophoretic assessment demonstrated semiquantitatively that there were high levels of Fn or Fn protein fragments in both the cold precipitate raw material and the fibrinogen depleted solution (the solution from which both of the DFn and Fn control biomaterials are made, just prior to their shear aggregation). There was no detectable fibrinogen present in the biomaterial preparation following fibrinogen heat depletion. The assessment also demonstrated that both the dissolved DFn and Fn control biomaterials were Fn or Fn protein fragments, with no detectable fibrinogen. This was confirmed by the presence or absence of precipitation arcs to these antigens on the immunodiffusion test plate (Figure 3.1).

#### **3.3.1.2 Immunodiffusion**

A radial immunodiffusion assay was used to test the concentration of Fn proteins in the DFn and Fn control biomaterials following precipitation and washing. Data are presented as mean ( $\pm$  SD). By calculating the Fn concentrations from the diameter of known protein standards, the assay demonstrated a high concentration ( $1162 \pm 89$  mg L<sup>-1</sup>) of Fn or Fn protein fragments in the cold precipitate raw material Tris 1:2

solution, a high concentration ( $1467 \pm 123 \text{ mg L}^{-1}$ ) of these proteins in the fibrinogen-depleted solution prior to the precipitation of Fn, and only  $18 \pm 3 \text{ mg L}^{-1}$  of these proteins in the supernatant following precipitation of the biomaterial. This suggests that any fragments of Fn were largely incorporated into the DFn biomaterial.

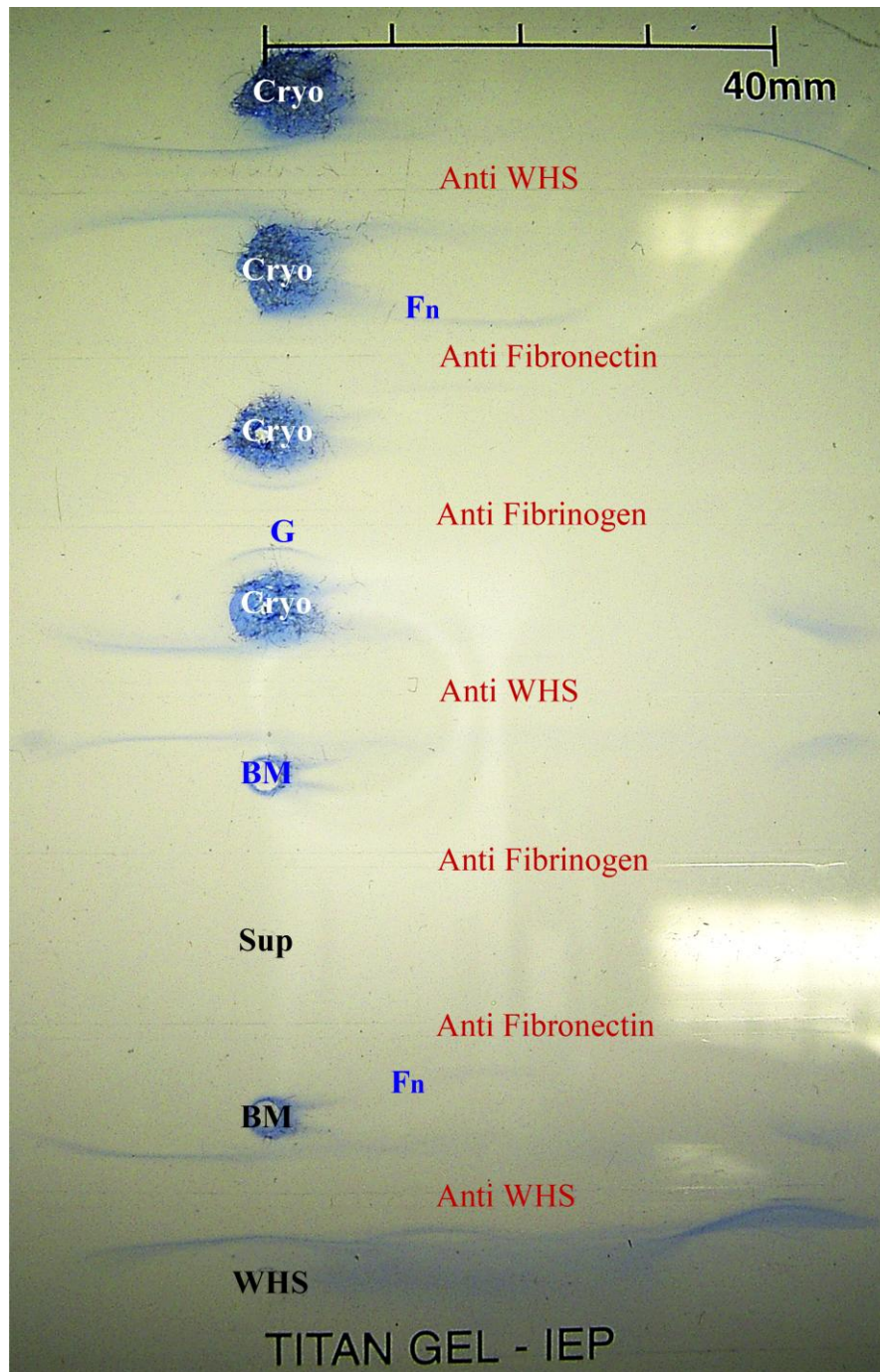


**Figure 3.1** Immunoelectrophoresis plate showing precipitin arcs for Fn and Fibrinogen (G). The raw material Cryoprecipitate (Cryo), the biomaterial in solution prior to precipitation (BM), the discarded supernatant after biomaterial precipitation (Sup) and a control Whole Human Serum (WHS) were tested against antisera to Whole Human Serum (Anti WHS), Fn (Anti Fibronectin), and Fibrinogen (Anti Fibrinogen).

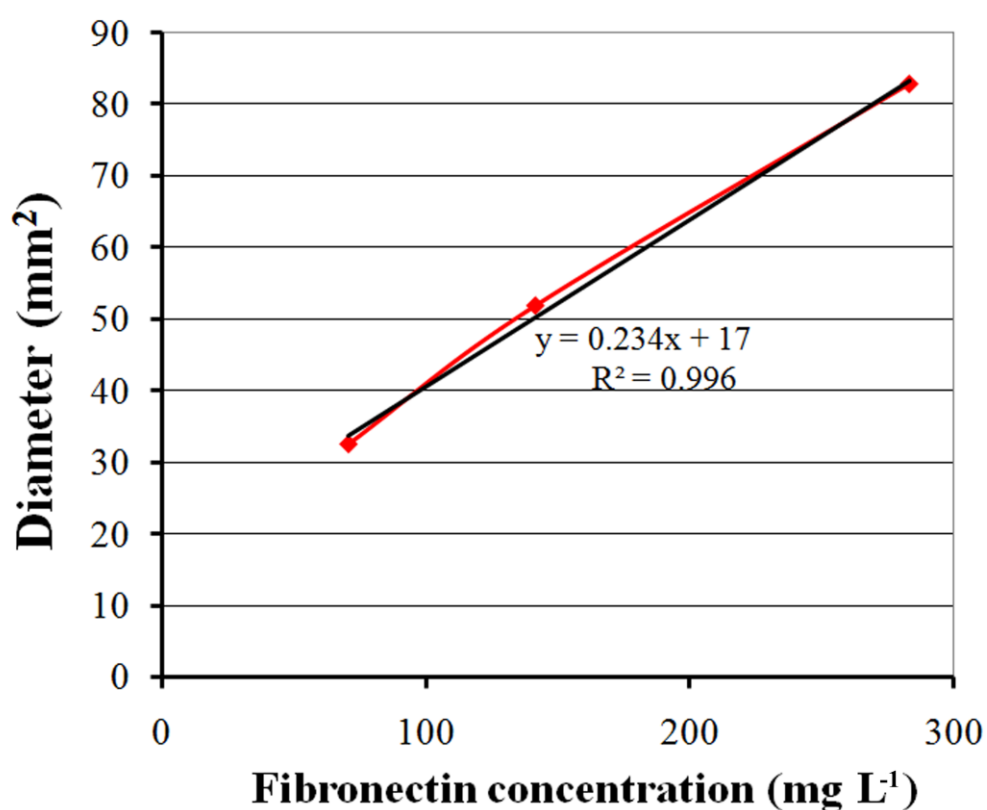


**Figure 3.2** Calculation of Fn concentration in solution from protein standards.

The line of best fit enables the Fn concentration of the test solutions to be calculated from the diameter of their precipitin rings. The 1:10 cold precipitate raw material Tris 1:2 solution, the 1:10 fibrinogen depleted solution and the discarded supernatant had mean precipitin ring diameters of 6.65 mm, 7.16 mm and 4.61 mm respectively. From the line of best fit ( $y = 0.234x + 17$ ) for the Fn protein standards this gives mean Fn concentrations of 1162, 1467 and 18 mg L<sup>-1</sup> respectively.

### **3.3.2 Biodegradability of the Derivative Fibronectin Biomaterial and Fibronectin Control**

In the next step DFn and Fn control biomaterials were assessed for stability, comparing their dissolution rates in PBS, PBS with Aprotinin (300 iu mL<sup>-1</sup>; a protease inhibitor, to test for proteases present in the DFn material), and 10% NGM. This last solution was used as it was the culture medium used in the cell attachment, cell migration, and cytotoxicity assays. Experiments were performed in triplicate for both DFn and Fn control biomaterials, which were maintained in the solutions at 37°C for 21 days. Protein loss from the biomaterials into solution was evaluated by taking samples at regular intervals over 21 days, tested using a Bicinchoninic Acid Protein Assay Reagent Kit (Pierce Biotechnology, Illinois, USA). Samples containing DMEM were corrected for the protein present in FCS.

As can be seen in Figure 3.3 both DFn and Fn control biomaterials were fully degradable, having dissolved 100% by 72 hours in PBS. There was no significant difference between the dissolution rates of DFn and Fn control materials in PBS. The resistance of DFn and Fn control biomaterials to protease dissolution was also tested by using Aprotinin. Data is presented as the mean percentage dissolution ( $\pm$  SD). Percentages only are presented for clarity of results. As can be seen in Figure 3.3 at this time point in Aprotinin (mats dissolved by 51%  $\pm$  17% and 63%  $\pm$  14% of their initial weight respectively,  $p=0.48$  unpaired t-test) or in DMEM (55%  $\pm$  24% and 71%  $\pm$  25% respectively,  $p\leq 0.92$  unpaired t-test). By 3 weeks there was no significant difference in dissolution between DFn and Fn control biomaterial in DMEM (88%  $\pm$  21% and 89  $\pm$  20% respectively,  $p\leq 0.97$  unpaired t-test) or in PBS containing Aprotinin (64%  $\pm$  21% and 77%  $\pm$  10% respectively  $p\leq 0.46$  unpaired t-



test). Adding Aprotinin to the PBS solution resulted in significantly less degradation for the DFn mats (36% less,  $p \leq 0.038$  unpaired t-test). However, this decrease was not significant for the Fn control mats (23% less,  $p \leq 0.079$  unpaired t-test). The rapid dissolution of the biomaterials when tested in PBS is likely to be due to proteases not eliminated from them during their production. Adding Aprotinin to the PBS solution resulted in significantly less degradation for the DFn biomaterial at 3 weeks. However this was not the case for the Fn control biomaterial. These results suggest that DFn, where soluble fragments are not eliminated during the final stages of production, contains higher levels of proteases than the Fn control where the soluble fragments are eliminated during washing. It follows that the release of proteolytic Fn fragments by DFn may partly be the result of the presence of these proteases. The reduced protein dissolution seen for both DFn and Fn control mats in DMEM relative to PBS may be due to anti-proteases present in the FCS (Paczek, Michalska et al. 2008).

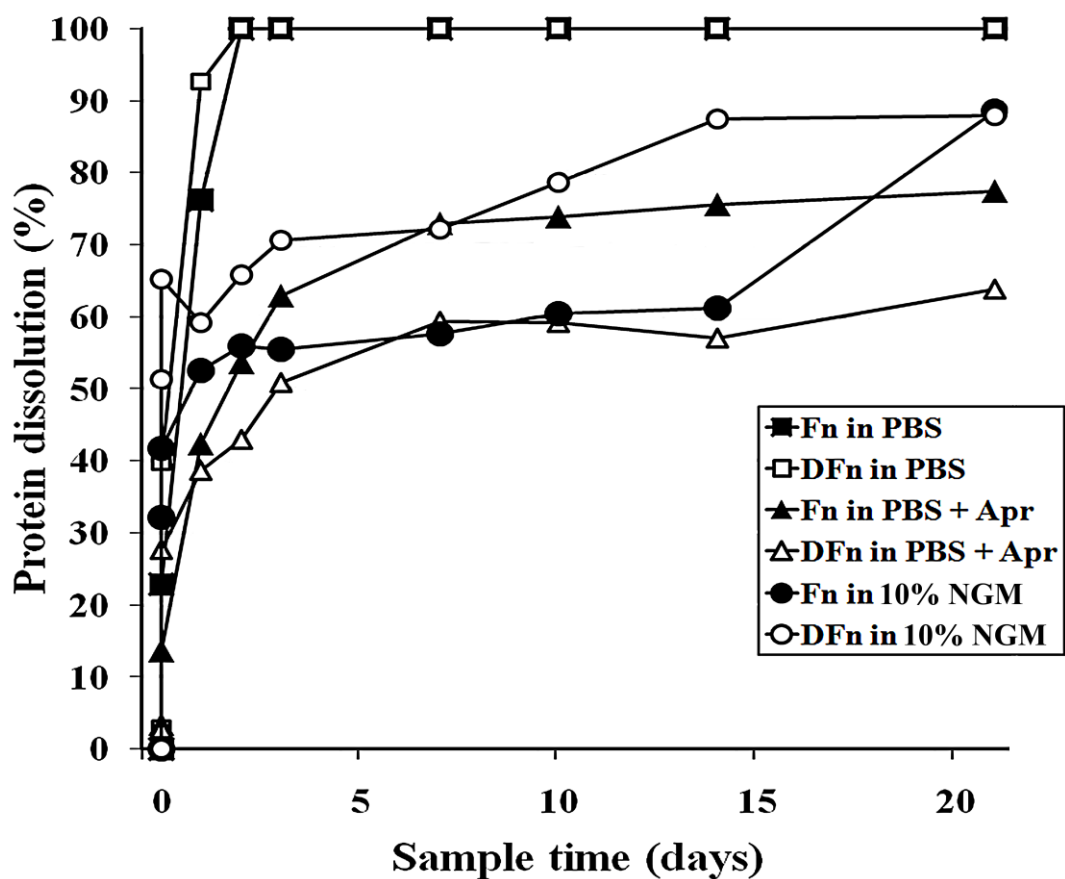


**Figure 3.3** Protein dissolution curves (n=3) for DFEn and FEn control biomaterials in 10% NGM, PBS and PBS with Aprotinin (300 iu mL<sup>-1</sup>; PBS + Apr) solutions. The dissolution curves for DFEn and FEn control in PBS were very similar. Data is presented as the mean percentage dissolution.

### 3.3.3 Assessment of Fibroblast Attachment

The attachment of fibroblasts to DFn and Fn control was tested by seeding ( $1 \times 10^5$ ) fibroblasts in 1mL 10% NGM on these materials. At 6 hours the unattached cells were washed off, and the remaining attached cells were fixed and stained. The fluorescent nuclear stain propidium iodide was used to facilitate cell counts. Fluorescein isothiocyanate (FITC)-labelled  $\alpha$ -SMA immunostaining was used to test for any alteration of synovial sheath fibroblasts to a more myofibroblastic lineage. The data are presented as mean cell counts per microscopy field ( $\pm$  SD). The results showed that there almost no fibroblasts attached to cover slips coated with DFn ( $0.1 \pm 0.0$ ) compared to cover slips coated with Fn control or to untreated glass ( $(23.6 \pm 10.0)$  and  $(20.8 \pm 10.0)$ ,  $p \leq 0.001$  and  $p \leq 0.002$  respectively), as shown in Figure 3.4. This showed that while fibroblasts attached to glass or the Fn control, DFn effectively eliminated cell attachment. There was no microscopic evidence of substantial cell death, indicating that toxicity did not contribute to this effect. As detected by  $\alpha$ -SMA staining there were  $2.0 \pm 0.7$  myofibroblasts per microscopy field on plain cover slips. No myofibroblasts were seen on the DFn or Fn control mats which were clearly less stiff than the glass cover slips (Figure 3.5).

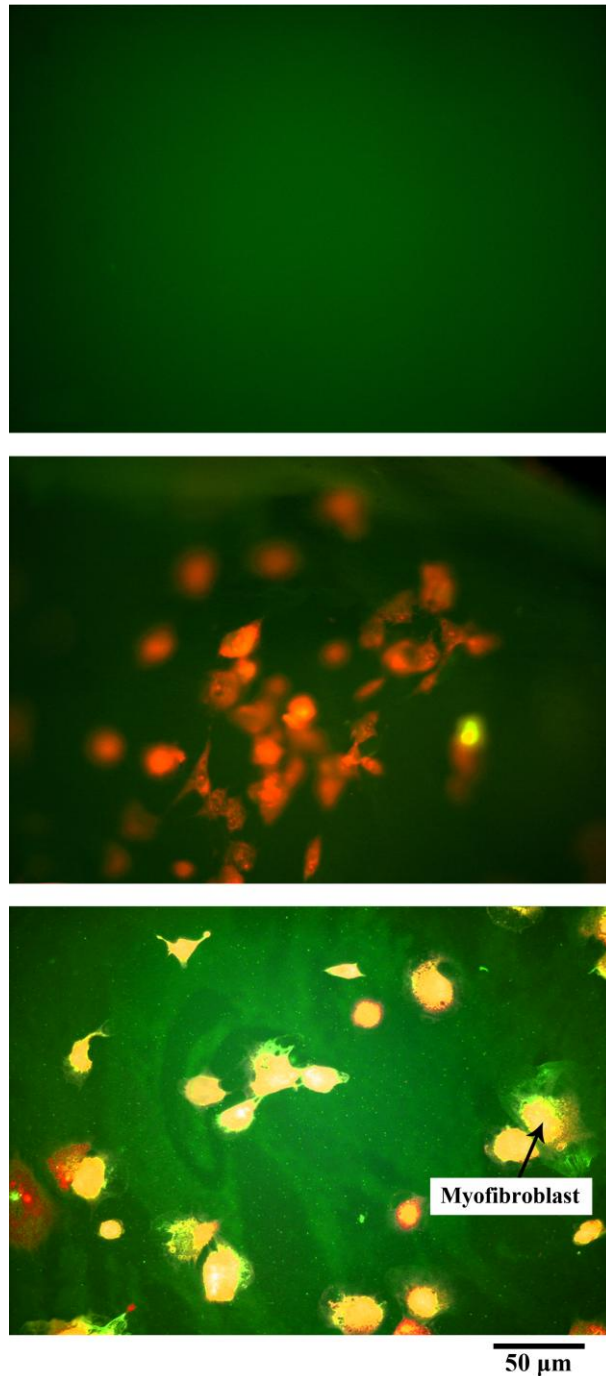


**Figure 3.4** Immunofluorescent micrographs of biomaterials cultured with fibroblasts after washing and  $\alpha$ -SMA and propidium iodide staining. (*Above*) DFn biomaterial. Note the absence of attached cells. (*Centre*) Fn control biomaterial. Cells were attached to the coated cover slips, but no myofibroblasts were seen. (*Below*) Plain glass cover slips. Attached cells were seen and some expressed  $\alpha$ -SMA (myofibroblast). Magnification x40.

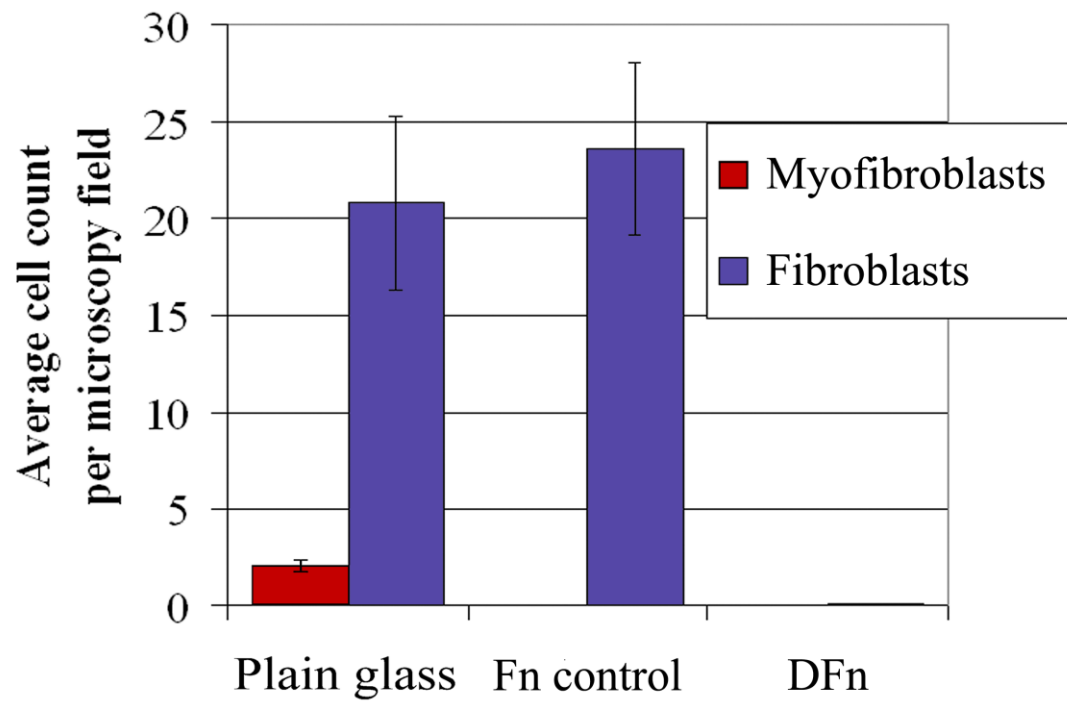


**Figure 3.5** Average attached fibroblast and myofibroblast cell counts per microscopy field to DFfn, Fn control and plain glass (with myofibroblasts staining positively for  $\alpha$ -SMA). The DFfn biomaterial coated cover slips (n=5) showed significantly fewer attached cells than Fn control biomaterial coated cover slips (n=5) or plain glass cover slips (n=5). The data are presented as mean cell counts per microscopy field ( $\pm$  SD).

### **3.3.4 Assessment of Migration**

The ability of fibroblasts seeded on the surface of the biomaterials (DFn and Fn control) to migrate into a three-dimensional structure was tested by incubating surface seeded materials for 24 hours. Experiments were performed in triplicate and repeated for 3 separate synovial sheath fibroblast cell strains (n=3). Fibroblasts were found deep within the Fn control biomaterial with the deepest cell seen at a depth of 70  $\mu\text{m}$ , but no fibroblasts were located either at the surface of, or within, the DFn biomaterial (Figure 3.6).

### **3.3.5 Fibroblast Viability Assessment**

Fibroblasts that had been plated into each of the wells of a 6-well culture plate and allowed to attach for 24 hours were placed in direct apposition with DFn for a further 24 hours. Experiments were performed in duplicate and repeated for 3 separate synovial sheath fibroblast cell strains (n=3). Cells were then stained with Trypan Blue to test cell viability. No Trypan Blue uptake was detected in DFn treated cells (Figure 3.7), indicating no loss of cell viability resulting from exposure to the DFn. In contrast to the cells in the attachment assay where no attachment was seen, a large number of cells that had already been plated did not appear to detach after exposure to the DFn. This is seen in Figure 3.7 where elongated and rounded cells are seen attached to the base of the culture well.

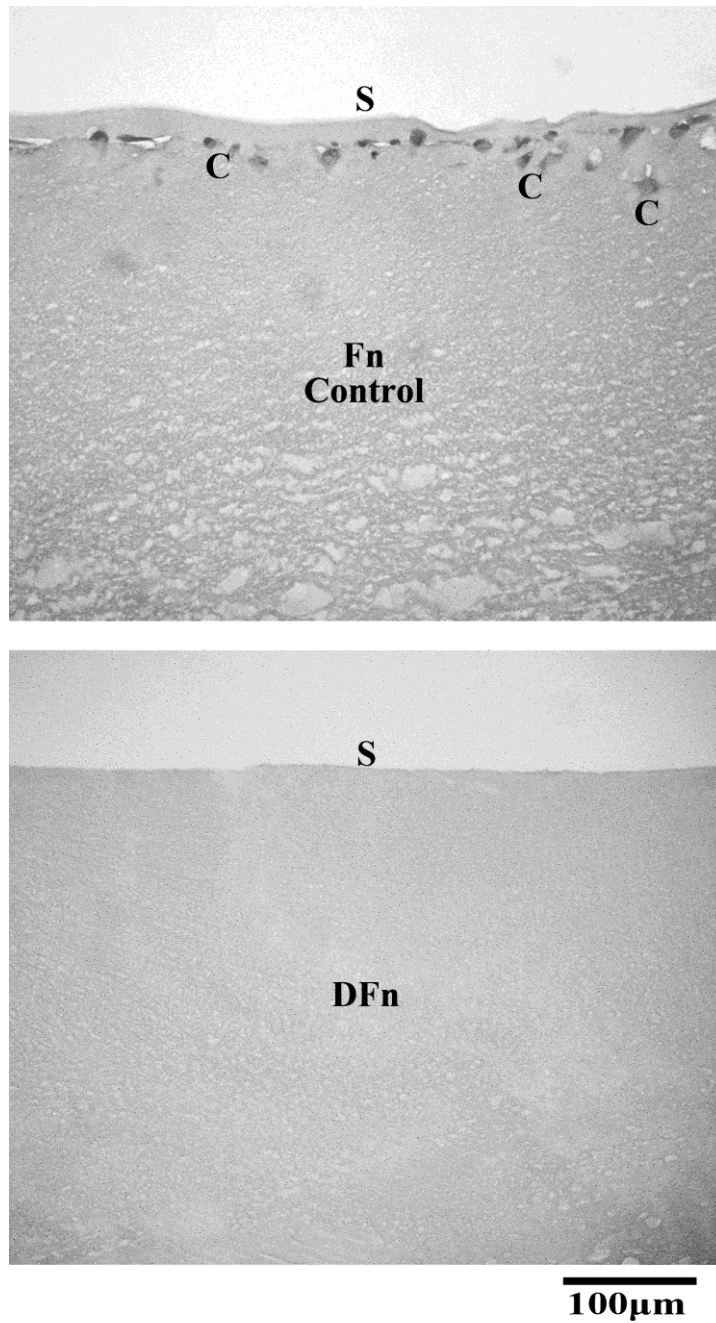


**Figure 3.6** Micrographs of biomaterials 24 hours after seeding with fibroblasts after washing and H and E staining. (*Above*) Fn control biomaterial. Cells (C) are evident at the material surface (S) with limited invasion by cells into the biomaterial substance. (*Below*) DFn biomaterial. No cells were seen at or below the biomaterial surface (S). Magnification x20.



**Figure 3.7** Micrograph demonstrating fibroblasts that have been exposed to a DFn biomaterial mat for 24 hours and stained with trypan blue. No dead cells were seen. Some of the cells assumed a rounded morphology (R), although many cells remained attached to the base of the culture well. Magnification x100.



### **3.3.6 Time Lapse Assessment**

Dynamic interaction between fibroblasts and the biomaterial was monitored directly using time lapse microscopy for 1 randomly selected synovial sheath cell strain. Following fibroblast ( $1 \times 10^5$ ) seeding and culture with the DFn biomaterial the majority of cells maintained rounded morphology with no cells attaching to the biomaterial (Figure 3.8). A minority of cells attached to the base of the culture well some distance from the DFn biomaterial. However, even these continuously shifted between bipolar and rounded morphologies, suggesting repeated attachment and detachment cycles in individual cells (Figure 3.9).

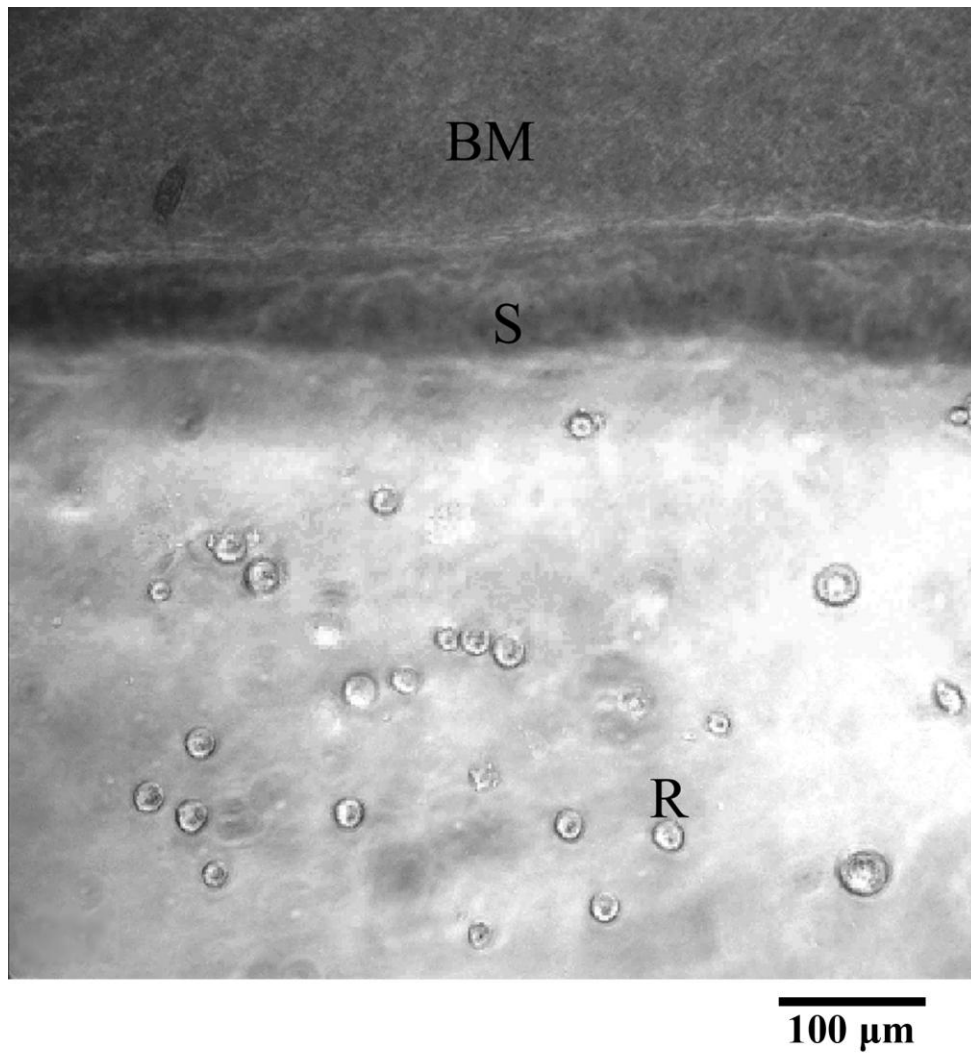


**Figure 3.8** Micrograph from the time lapse assessment of the interaction between cells and the DFn biomaterial at 6 hours. This demonstrates that no cells are attached to the DFn biomaterial (BM; seen in the top 1/3 of the image) and that those adjacent to the material generally assumed a more rounded morphology (R). Magnification x20.

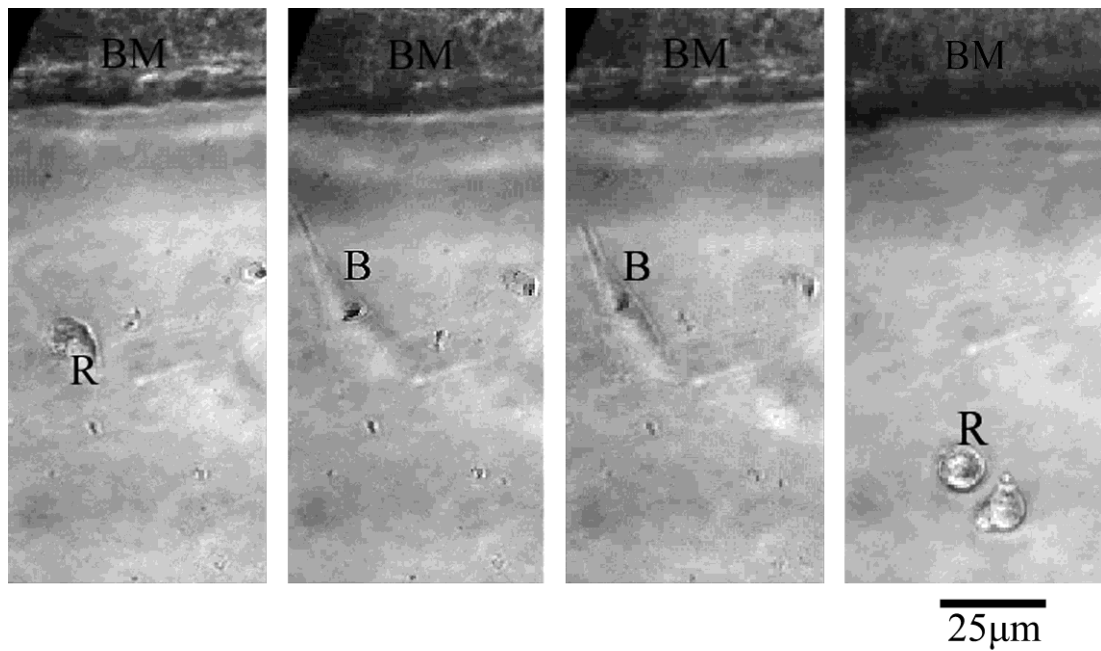


**Figure 3.9** Detail micrographs from the time lapse assessment of the interaction between cells and the DFn biomaterial. Cells did not attach to the biomaterial surface. Some of the cells that did attach appeared to continuously shift between bipolar (B) and rounded (R) morphologies as seen in the images above. (*Far left*) At 6 hours. (*Centre left*) At 12 hours. (*Centre right*) At 18 hours. (*Far right*) At 24 hours. These cells were not dead as they were seen to alternate between detaching and reattaching to the culture plates. In general, cells appeared to move away from the biomaterial surface over time. Scale as shown.

## **3.4 DISCUSSION**

### **3.4.1 Preventing Cell Attachment to Fibronectin: A Therapeutic Strategy**

Fn is a key cell adhesion glycoprotein secreted by wound fibroblasts, and is involved in organising cellular interactions with the extracellular matrix (ECM) in the healing surgical wound. An important component of the early healing process, Fn acts as biological adhesive. It promotes attachment and migration of fibroblasts on the ECM. It forms an intermediary scaffold for deposition of collagen by fibroblasts, eventually leading to the formation of adhesions (Grinnell 1984; Gelberman, Steinberg et al. 1991). It follows that preventing attachment of fibroblasts to the ECM in the days after injury is a potential strategy to interrupt the formation of fibrous adhesions.

### **3.4.2 Cell Binding and Fibronectin**

Cells bind to Fn via integrin and non-integrin receptors (Clark, An et al. 2003). Integrins are cell adhesion molecules that link the ECM to the cytoskeleton, enabling cells to respond to their external environment (Johansson, Svineng et al. 1997; van der Flier and Sonnenberg 2001). Blocking these receptors may influence aspects of cell behaviour such as attachment and migration. The answer to how this may be achieved may lie within the Fn molecule itself.

Fn has a central cell-binding domain, its predominant cell adhesive domain, recognised by most adherent cells via several integrin receptors. The activity of the central domain is attributed to the Arg-Gly-Asp (RGD) motif in the tenth type III module (Pierschbacher and Ruoslahti 1984; Ruoslahti 1996) and the synergistic

motif in the ninth type III module (Skorstengaard, Jensen et al. 1986). These cell adhesive sites are recognized by a cell adhesion receptor, the integrin  $\alpha 5 \beta 1$  (Hofer, Syfrig et al. 1990; Watanabe, Takahashi et al. 2000). The RGD sequence has a central role in cell adhesion biology as the prototype adhesion signal (Ruoslahti 1996; Meredith and Schwartz 1997). It has the capacity to support maximal fibroblast attachment (Clark, An et al. 2003) and is therefore a suitable target in modifying adhesion formation.

The carboxy-terminal domain (Hep 2) contains at least 6 major cell adhesive sites, which support heparin-dependent, RGD-independent cell adhesion (McCarthy, Skubitz et al. 1990). In addition, there are cell adhesive sites in the domain adjacent to the Hep 2 domain in the type III connecting segment, recognized by the integrin  $\alpha 4 \beta 1$  (Mould and Humphries 1991).

### **3.4.3 An Anti-Adhesive Biomaterial**

Plasma Fn aggregates from solution, under shear force, to form fibrous materials that have been previously reported for use in tissue engineering applications (Underwood, Afoke et al. 2001; Phillips, King et al. 2004). During development of these aggregates (the Fn control biomaterial in this study), the elimination of a single processing step resulted in a material which, in complete contrast, did not support cell attachment (i.e. the DFn biomaterial assessed here). The soluble fraction of the DFn biomaterial assessed in this study has been previously shown to contain a heterogeneous group of Fn fragments with inhibitory effects (Djerkovic, Phillips et al. 2005). After separation by affinity and molecular weight a heparin binding fraction less than 30 kDa significantly inhibited neurite growth without increasing

cell death *in vitro*. Results from immunoassays in the present study have confirmed that a soluble Fn protein was present in the DFn biomaterial.

The current *in vitro* investigation was designed to investigate the mechanism of action of the biomaterial, and indicates that the DFn biomaterial releases soluble Fn fragments that inhibit fibroblast attachment to any intact Fn. Although adhesive peptides can promote cell attachment when attached to a surface, when present in solution, they prevent attachment that would otherwise occur (Ruoslahti 1996). Alternatively, fragments of Fn may be acting as inhibitors to cell adhesion.

#### **3.4.4 Inhibitory Fragments Within the Fibronectin Molecule**

Proteolytic fragments of the Fn molecule, which may result from its digestion by wound proteases, and similar synthetic peptides have been shown to inhibit integrin mediated cellular processes, such as attachment, growth, differentiation of cells and contraction of the ECM (Fukai, Hasebe et al. 1997; Fukai, Mashimo et al. 1998; Fukai, Kamiya et al. 2000; Watanabe, Takahashi et al. 2000; Sethi, Mudera et al. 2002). Fn fragment competitive self inhibition through cell receptor blocking has been suggested previously (Brown 1983).

A number of adhesion inhibiting sequences, which may be contained within fragments of the Fn molecule, have been described. These include the RGD sequence within the central cell binding domain (Hautanen, Gailit et al. 1989; Ruoslahti 1996; Sethi, Mudera et al. 2002), the Y-T-I-V-I-A-L sequence (Fukai, Hasebe et al. 1997) and other sequences within the heparin-binding (Hep 2) domain (McCarthy, Skubitz et al. 1990; Mould and Humphries 1991; Wilke, Skubitz et al.

1991; Mooradian, McCarthy et al. 1992). The prevention of cell attachment has been investigated using synthetic peptides (Pierschbacher and Ruoslahti 1984; Yamada and Kennedy 1984; Hautanen, Gailit et al. 1989; McCarthy, Skubitz et al. 1990; Mould and Humphries 1991; Wilke, Skubitz et al. 1991; Mooradian, McCarthy et al. 1992; Ruoslahti 1996; Fukai, Hasebe et al. 1997; Sethi, Mudera et al. 2002) and by modifications in key sequences (Obara, Kang et al. 1988; Sakata, Sasatomi et al. 2000). Yamada and Kennedy found that for inhibition of fibroblast to Fn binding using synthetic peptides, Gly-Arg-Gly-Asp-Ser was found to be considerably more active than Arg-Gly-Asp-Ser. For both proteins, the inverted peptide sequence Ser-Asp-Gly-Arg was also moderately active, However, closely related peptides containing a transposition, a deletion, or a single conserved amino acid substitution were much less active at preventing fibroblast adhesion to Fn (Yamada and Kennedy 1987).

### **3.4.5 Cryptic Anti-Adhesive Site and Exposure to Urea**

Fukai and colleagues demonstrated that a 30 kDa Hep 2 fragment, which showed no significant effect on kidney cell attachment to Fn, suppressed cell adhesion after exposure to urea in a non-competitive fashion (Fukai, Takahashi et al. 1996). It suppressed cell adhesion when coated on a culture dish and when added as a soluble supplement. RGD-dependent cell adhesion was preferentially inhibited, with no significant binding of the Hep 2 fragment to Fn. The cryptic anti-adhesive activity of Fn was expressed upon conformational change and following proteolytic cleavage of the Hep 2 hydrophobic domain (Fukai, Takahashi et al. 1996; Watanabe, Takahashi et al. 2000). Interestingly, Fukai and colleagues showed that human plasma derived Fn, as used in the present study, which was purified without exposure to a

denaturant, such as urea, exhibited no central cell binding domain, amino-terminal fibrin-binding domain or carboxyl-terminal fibrin-binding (Hep 2) domain activity. By exposure to urea or surface adsorption, Fn showed central cell binding but not those of the other domains (Fukai, Ohtaki et al. 1995). Therefore competitive inhibition by Fn and its fragments may require conformational changes as occurs following exposure to urea.

### **3.4.6 The Anti-Adhesive Nature of the Derivative Fibronectin Biomaterial**

Either one or both of two possible processes that expose the anti-adhesive site of Fn or its fragments (Fukai, Hasebe et al. 1997) may therefore be occurring in the present study: a conformational change, resulting from preparation of the mats using urea, and proteolytic cleavage of the Fn molecule resulting from proteases present in the source material. The urea used during preparation of the DFn mats may have promoted their antiadhesive activity by inducing a conformational change in Fn or its fragments to reveal a cryptic antiadhesive site as previously described (Rocco, Carson et al. 1983; Fukai, Takahashi et al. 1996; Watanabe, Takahashi et al. 2000). The extreme sensitivity of interdomain sequences of Fn to proteolysis, by a broad range of proteases (Brown 1983), suggests that it would be rapidly split into partly active fragments by the presence of these, either by plasma proteases present in the material or by tissue proteinases that are known to be present in the inflammatory wound environment *in vivo* (Yamada 1983; Grinnell, Ho et al. 1992; Grinnell and Zhu 1994). Fn degradation products may lead to increased proteinase gene expression and release, which may lead to further protease-mediated matrix



fragmentation *in vivo* (Werb, Tremble et al. 1989; Homandberg, Meyers et al. 1992; Stack and Pizzo 1993).

In this investigation, time lapse studies confirmed that synovial sheath fibroblasts did not adhere to the material, and that cells in the area immediately adjacent to the dissolving DFn biomaterial maintained a rounded unattached morphology consistent with the idea that a released component was responsible.

### **3.4.7 Cryoprecipitate Contains Fibronectin Fragments**

Plasma cryoprecipitate is known to be rich in Fn (Scovill, Saba et al. 1978; Harding, Underwood et al. 2000; Underwood, Afoke et al. 2001; Phillips, King et al. 2004). In addition, Fn present in cryoprecipitate is known to be heavily degraded into Fn fragments (Ruoslahti, Hayman et al. 1981; Brown 1983). Cryoprecipitate is also known to be low in the protease inhibitor antithrombin III (Cosgriff, Hodgson et al. 1983), which may contribute to the activity of proteases contained within the DFn material. Qualitative and quantitative assessment of the DFn biomaterial in the present study confirmed that it is rich in such Fn fragments. The protein dissolution assessments in this study also suggest the DFn materials contain higher levels of proteases than the Fn control biomaterials, which may further increase their Fn fragment content, and result in exposure of cryptic antiadhesive sites by proteolytic cleavage.

The results in this investigation suggest that Fn fragments are the likely candidate component of the source cryoprecipitate that appear to give the DFn its ability to reduce fibroblast attachment. The decrease in cell adhesion found in the previous

studies was only due to competitive binding of cleaved Fn fragments onto cell receptors (Brown 1983; Yamada and Kennedy 1984). It is not clear from the present study whether the protein fragments were causing inhibition by acting in a competitive or non-competitive way. If the effect is only due to competitive binding by dissolved Fn fragments the anti-adhesive effect will only exert its effect while the DFn biomaterial is still dissolving.

#### **3.4.8 Inhibition of Myofibroblastic Conversion by the Derivative Fibronectin Biomaterial**

In this study no myofibroblasts were seen following fibroblast culture on either DFn or Fn control biomaterials. It would normally be expected in a population of *in vitro* fibroblasts that a proportion of cells would be myofibroblasts. Fn-derived antiadhesive peptides have previously been shown to suppress myofibroblastic conversion of rat hepatic stellate cells (Kato, Kamiya et al. 2001). Alternatively, this finding may be related to the biomaterial surfaces as such materials are far less stiff than plain glass, generating a low tension cell-environment, removing one of the factors thought to stimulate myofibroblast formation (Tomasek *et al.*, 2002). However, longer time frames need to be examined to determine if there is an increase in myofibroblast conversion over time in culture on DFn and Fn control. When myofibroblasts persist in fibrotic lesions they are believed to be responsible for excessive collagen production that leads to alteration of tissue architecture and ultimately to organ dysfunction. Myofibroblasts may promote clinically important adhesion formation. Preventing myofibroblast differentiation may therefore be a target mechanism for reducing fibrosis and adhesion formation.

### **3.4.9 Biomaterial Degradation**

Strategies that target fibroblast to Fn adhesion are likely to have their maximal effects on preventing adhesion formation during the inflammatory and fibroblastic phases of wound healing. It is during this time that fibroblast migration and provisional ECM deposition (the inflammatory phase), and consequent fibroblast proliferation and collagen deposition (the fibroblastic phase) predominate (Mutsaers, Bishop et al. 1997; Liakakos, Thomakos et al. 2001; Beredjikian 2003). These overlapping events last from days to weeks post injury. The biomaterial may only be required to be present during these early stages of wound healing. Presence of the biomaterial at later stages may contribute to further inflammation and adhesion formation. In this study, by 21 days the DFn material dissolved by 64% in PBS with Aprotinin and 88% in 10% NGM.

### **3.4.10 Barrier Effects of the Derivative Fibronectin Biomaterial**

The results of this investigation have shown that fibroblast cells were clearly able to attach and migrate into the Fn control biomaterial as has been previously reported (Ejim, Blunn et al. 1993; Phillips, King et al. 2004). This *in vitro* study has shown that fibroblasts did not migrate into the DFn biomaterial substance, confirming its suitability as a protein barrier. The absence of migration into the DFn biomaterial by fibroblasts may be due the material not supporting their attachment.

### **3.4.11 Summary**

The results of this investigation have shown that the DFn biomaterial has barrier properties and biodegrades to provide prolonged delivery of anti-adhesive factors, preventing the attachment of adhesion forming fibroblasts. This supports the idea

that the DFn biomaterial may be used to prevent adhesion formation at tissue interfaces. Importantly, the DFn biomaterial was not toxic to fibroblasts indicating that it is unlikely to cause a generalised loss of fibroblasts which might impair healing of adjacent tissues.

# **CHAPTER 4**

## **RESULTS**

### **A NOVEL BIOMIMETIC MATERIAL FOR ENGINEERING POSTSURGICAL ADHESION IN THE INJURED DIGITAL FLEXOR TENDON COMPLEX**

#### **4.1 INTRODUCTION**

##### **4.1.1 Aim**

#### **4.2 MATERIALS AND METHODS**

##### **4.2.1 Tendon Injury Model**

##### **4.2.2 Mechanical Evaluation**

##### **4.2.3 Histology and Immunohistochemical Scoring**

##### **4.2.4 Statistical Analysis**

#### **4.3 RESULTS**

##### **4.3.1 Mechanical Evaluation**

##### **4.3.2 Histology and Immunohistochemical Scoring**

#### **4.4 DISCUSSION**

##### **4.4.1 A Combined Mechanical and Histological Approach**

##### **4.4.2 Cellular Effects of the Biomaterial**

##### **4.4.3 A Mechanism for Differential Cellular Effects on Injured Tendon and the Synovial Surface**

##### **4.4.4 Suitability for Surgical Use**

#### **4.4.5      Summary**

## **4.1 INTRODUCTION**

Fibronectin (Fn) glycoprotein binds cell surfaces and numerous substances including collagen and fibrin (Ruoslahti, Hayman et al. 1982) and is a promoter of cell proliferation (Sottile, Hocking et al. 2000). During the development of Fn-based biomaterials to promote healing, a modification in the fabrication process resulted in scaffolds not supporting fibroblast attachment. Washing the materials abolished this anti-adhesive effect, suggesting that soluble Fn fragments were responsible (Branford, Brown et al. 2010). Short fragments may act as competitive inhibitors of cell-surface adhesion (Brown 1983) and the Fn molecule harbours anti-adhesive sites (Yamada and Kennedy 1984; Fukai, Takahashi et al. 1996; Fukai, Hasebe et al. 1997; Watanabe, Takahashi et al. 2000). Following injury to gliding tissue surfaces collagen is deposited by migrating cells to form stiff bridges. Cell attachment is a pre-requisite for migration (van der Flier and Sonnenberg 2001) and if cell attachment and migration is reduced this may prevent collagen deposition and fibrotic adhesion formation.

A rabbit model has been developed using the digital tendon-synovial complex in which the mechanical restriction is in a single axis. It was hypothesised that if interposed as barriers between the tissue interfaces then these constructs would block extracellular matrix (ECM) bridge deposition. These constructs would encourage tendon surface cellularity whilst preventing the attachment of migrating fibroblasts by acting as delivery vehicles for anti-adhesive fragments.

### **4.1.1 Aim**

To test the novel biomimetic material *in vivo* to determine its efficacy in reducing restrictive adhesion in a flexor tendon-synovial complex injury model.

## **4.2 MATERIALS AND METHODS**

### **4.2.1 Tendon Injury Model**

The deep flexor tendons of digits 2 and 4 in the right forepaw of 15 New Zealand White (NZW) rabbits were subjected to 5 mm long partial tenotomies as described in section 2.3.1. Animals were randomised to receive biomaterial tubes enveloping the tendon injuries or left untreated as set out in section 2.3.2.

### **4.2.2 Mechanical Evaluation**

Mechanical pullout studies were used to determine the gross mechanical parameters for DFn treated and untreated digits at 2 weeks post injury. Mean peak force and structural stiffness for the adhesions were calculated as described in section 2.3.2.1.

### **4.2.3 Histology and Immunohistochemical Scoring**

Tendon and adhesion surface cellularity and cell proliferation were assessed to clarify the material's mechanism of action. This was achieved using Haematoxylin and Eosin (H and E) staining (section 2.3.4.1) and immunohistochemical staining for Ki67 (section 2.3.4.2.), with cell counts being made over a 200 x 200 µm grid by 3 independent observers. Details of the analysis are set out in section 2.3.4.1.



#### **4.2.4 Statistical Analysis**

The mechanical and cellular data were assessed using the Mann-Whitney Rank Sum test as the data was non-parametrically distributed. Statistical analysis was used, using a p value of <0.05 as to be statistically significant.

### **4.3 RESULTS**

15 treated and 14 untreated injured digits were randomised to mechanical or histological assessment. Of the 7 treated injured tendons that were evaluated by pullout testing there was macroscopic evidence of the material in only 2 cases at 14 days, confirming reports that Fn biomaterials resorb *in vivo*.

#### **4.3.1 Mechanical Evaluation**

All 3 sets of pullout data are shown in Figure 4.1. Values are given below as the mean ( $\pm$  SD). Normal pullouts (uninjured, negative controls) had a mean peak pullout force of  $0.04 \pm 0.04$  Newtons (N; range 0.01 to 0.13 N; n=11; Figure 4.2).

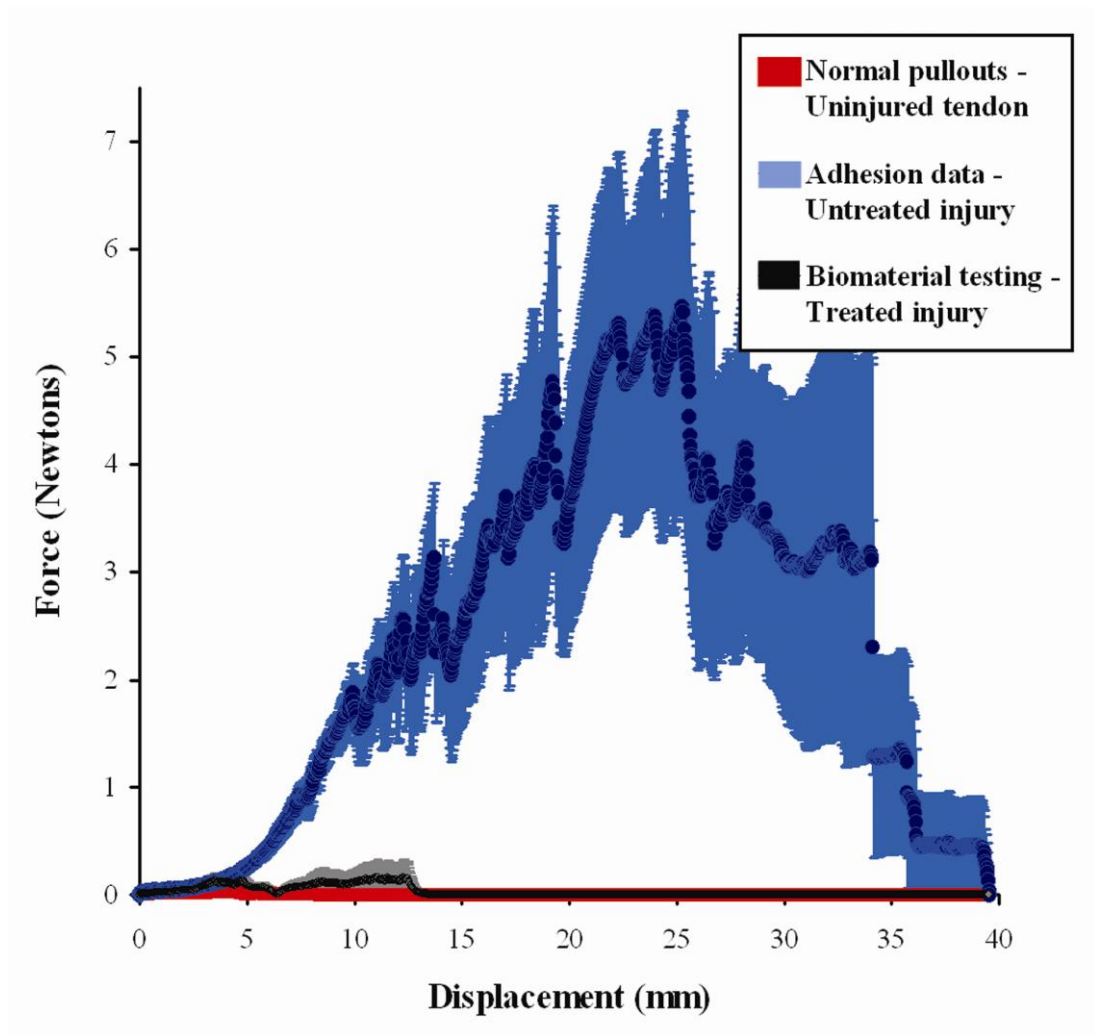


**Figure 4.1** This force displacement graph shows a reduced mean pullout force in the treated injured group (n=7) relative to the untreated injured control group (n=6) and uninjured digits (n=11). Pale shading indicates mean ( $\pm$  SEM).

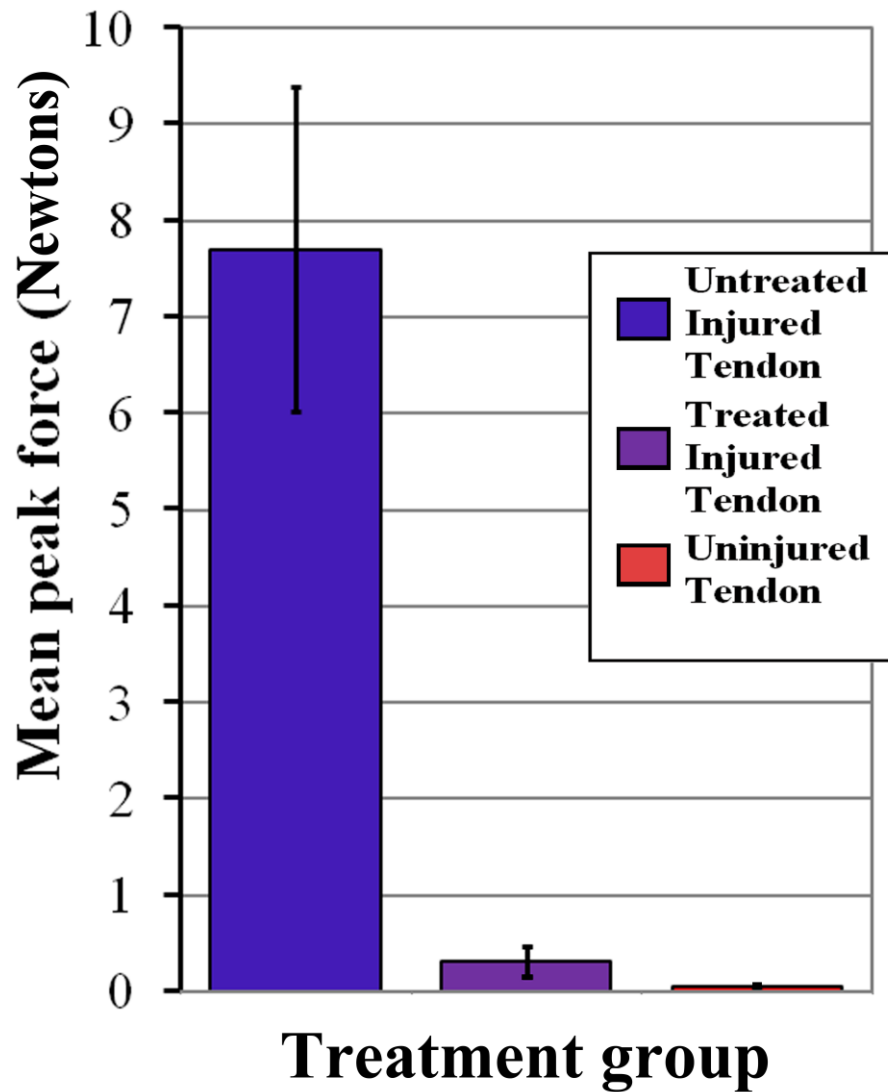


**Figure 4.2** A comparison of mean peak force required to overcome adhesions in untreated injured digits (n=6), DFn treated injured digits (n=7) and uninjured digits (n=11). The mean peak force required to overcome treated adhesions (treated injury) was not significantly different to that for normal pullouts (uninjured digits;  $p=0.174$ ) and was lower than for positive controls ( $p=0.001$ ). Error bars = SEM.

For the untreated injury group (positive control), the mean peak force required to overcome adhesions was  $7.70 \pm 4.14$  N (range 1.20 to 12.00 N; n=6; Figure 4.2). Their mean structural stiffness was  $628.02 \pm 139.84$  N m<sup>-1</sup>.

The mean peak force required to overcome treated adhesions (treated injury group) was  $0.31 \pm 0.41$  N (range 0.01 to 1.13 N; n=7; Figure 4.2). This was not significantly different to that for normal pullouts (uninjured digits; p=0.174) and was lower than for positive controls (untreated injured digits; p=0.001). The highest peak pullout force for the treated adhesions was lower than the lowest peak pullout force for positive controls. This indicates that the highest peak pullout force with the biomaterial was below the nominal threshold used to functionally define adhesion. Treating adhesions resulted in a significantly lower mean structural stiffness ( $39.60 \pm 38.60$  N m<sup>-1</sup>) than for positive controls (p=0.001). No tendons ruptured during testing.

### **4.3.2 Histology and Immunohistochemical Scoring**

As described in section 2.3.4, slides were scored independently by 3 observers and a consensus achieved.

#### **4.3.2.1 Histological Scoring**

Adhesions were present in all injured digits on histological examination. Uninjured tendons (n=8) showed a rapid decrease in cellularity from 0 to 30  $\mu$ m from their surface. Deeper than 30  $\mu$ m the cell counts levelled out (Figure 4.3).

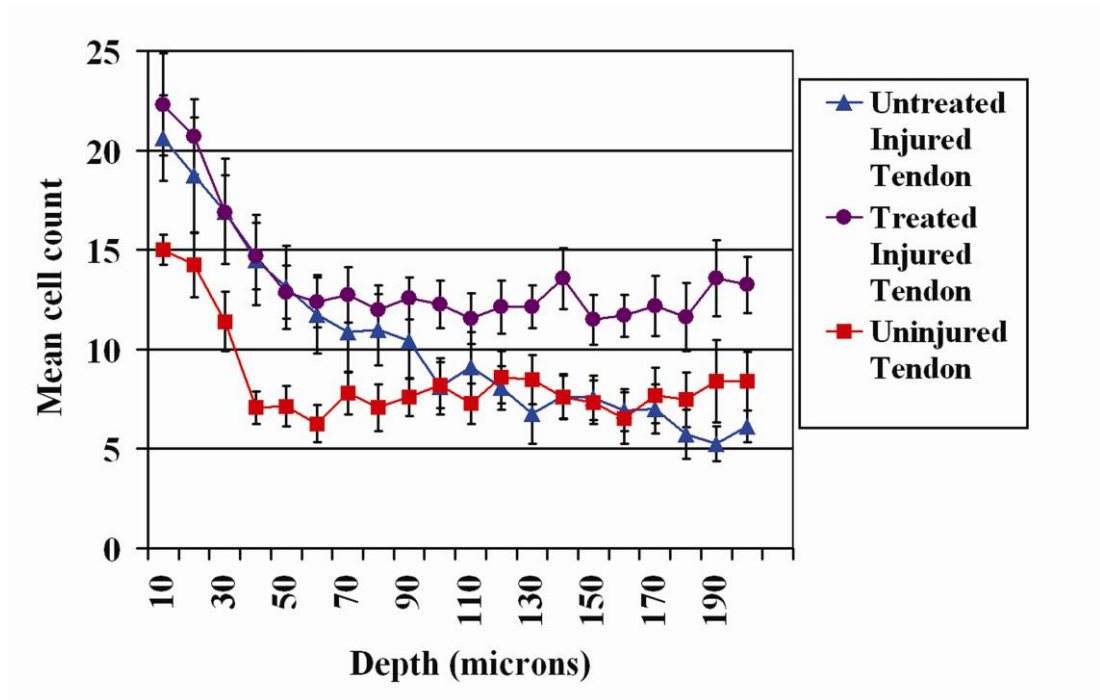


**Figure 4.3** A comparison of cell counts measured from the tendon surface in microns at 2 weeks post injury in treated injured digits (n=8), untreated injured digits (n=8) and negative control digits (n=8). Untreated injured tendons more cellular at their surface than uninjured control tendons ( $p=0.028$ ). Treated tendons were more cellular at their surface (first 10  $\mu\text{m}$ ) than uninjured controls ( $p=0.130$ ) and untreated injured digits ( $p=0.645$ ). Treated tendons were consistently significantly more cellular than their untreated counterparts deeper than 110  $\mu\text{m}$  ( $p\leq 0.05$ ). Error bars = SEM.

Untreated injured tendons (n=8) were 28% more cellular at their surface (0 to 10  $\mu\text{m}$ ) than uninjured tendons ( $p=0.028$ ). There was a more gradual decrease in cellularity than with uninjured digits (Figure 4.3).

Values are given as the mean ( $\pm$  SD). Treated injured tendons were 38% more cellular ( $22.3 \pm 7.3$  cells; n=8) at their surface (first 10  $\mu\text{m}$ ) than uninjured controls ( $16.2 \pm 2.2$  cells; n=8;  $p=0.130$ ), remaining hypercellular up to 200  $\mu\text{m}$  into their substance (Figure 4.3). There was an 8% increase in cellularity in the first 10  $\mu\text{m}$  as a result of treatment from  $20.6 \pm 6.1$  cells (n=8) to  $22.3 \pm 7.3$  cells (n=8;  $p=0.645$ ; Figure 4.3). Treated injured tendons were consistently significantly more cellular than their untreated injured counterparts deeper than 110  $\mu\text{m}$  where the curves levelled out ( $p \leq 0.05$ ). Examples of all 3 groups are shown in Figure 4.4.

The mean cell count following biomaterial testing in the most superficial 10 microns of the adhesion surface was reduced by 55% from  $18.7 \pm 4.7$  cells in the positive control adhesions (n=8) to  $8.4 \pm 4.7$  cells in treated samples (n=8;  $p=0.003$ ; Figure 4.5). Deeper than 50  $\mu\text{m}$  the cellularity of both groups reached a plateau, with treated adhesions being significantly more cellular ( $p < 0.001$ ). The untreated and treated injury groups are shown in Figure 4.6.

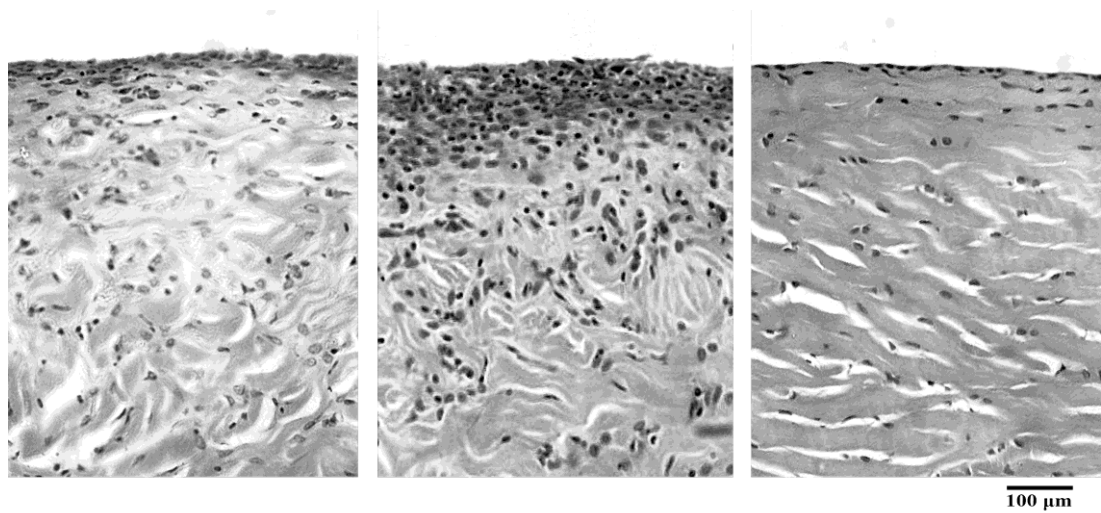


**Figure 4.4** H and E stain of tendon injury groups. (*Left*) Untreated injured tendon. (*Centre*) Treated injured tendon. (*Right*) Uninjured tendon. Treatment with the biomaterial did not reduce surface cellularity, and increased cellularity within the substance of the tendon following injury. Magnification x20.

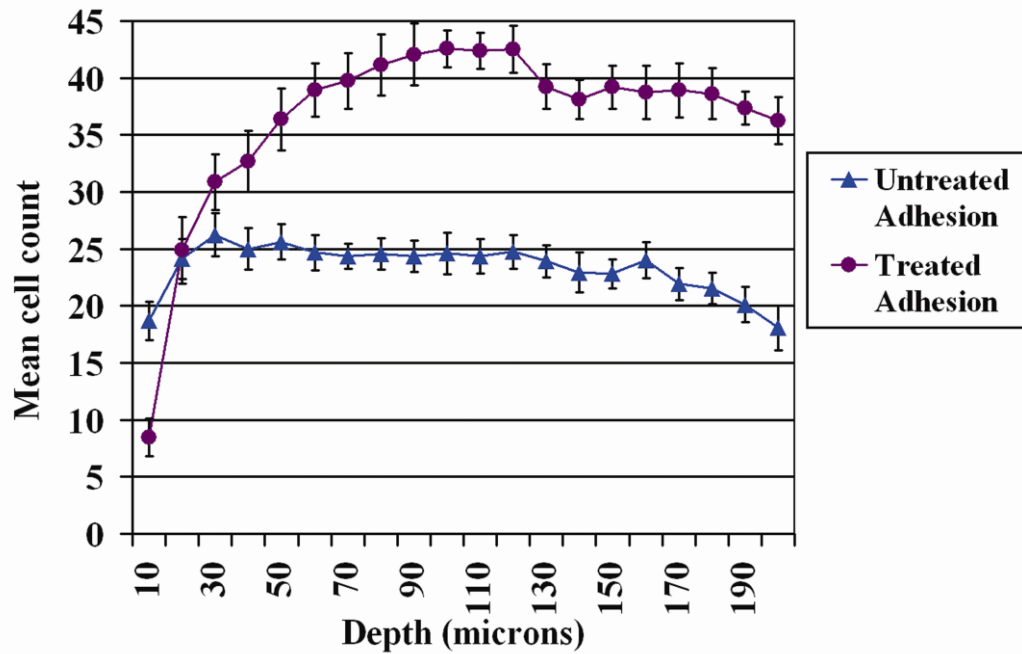


**Figure 4.5** A comparison of cell counts measured from the adhesion surface in microns in treated injured digits (n=8) and untreated injured digits (n=8). The mean cell count in the most superficial 10  $\mu$ m of the adhesion surface in treated injured digits was significantly reduced relative to untreated injured digits ( $p=0.003$ ). Deeper than 50  $\mu$ m, treated adhesions were significantly more cellular ( $p<0.001$ ). Error bars = SEM.



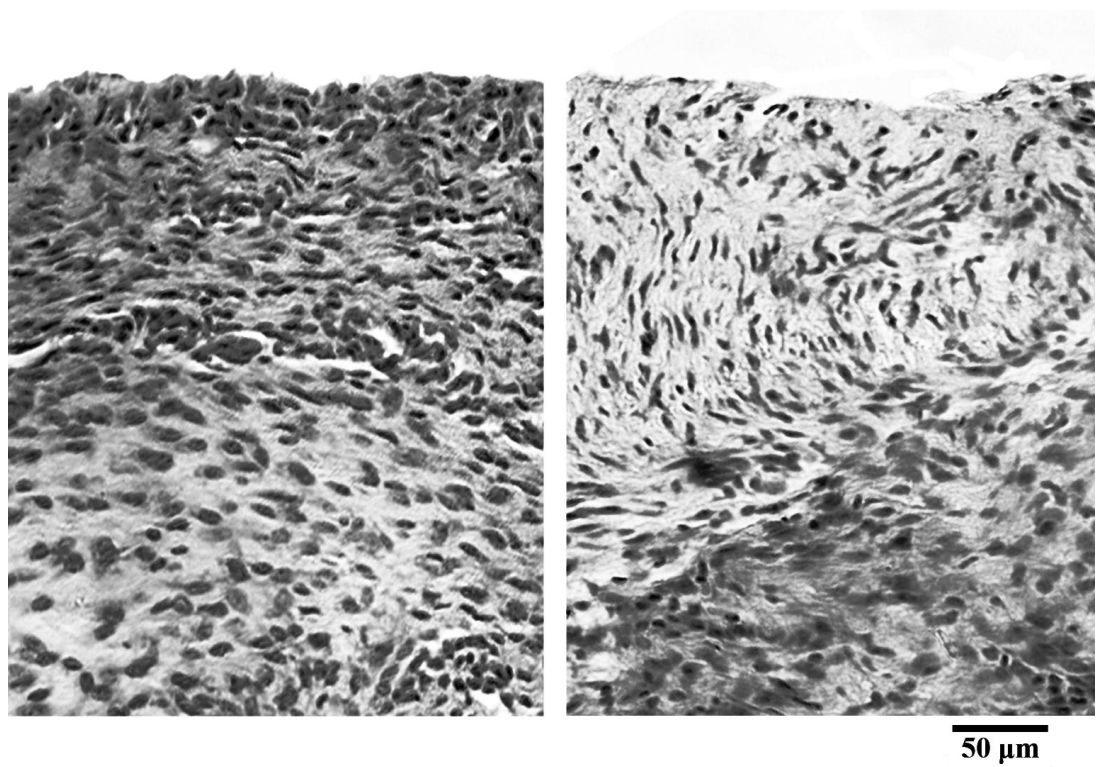


**Figure 4.6** H and E stain of adhesion groups. (*Left*) Untreated injured adhesion. (*Right*) Treated injured adhesion. Treatment with the biomaterial reduced the surface cellularity of adhesions. Treated adhesions were more cellular within their substance. Magnification x20.

#### **4.3.2.2 Immunohistochemical Scoring**

There was a significant reduction in the number of proliferating cells in the most superficial 10  $\mu\text{m}$  of the adhesions in the treated injured digits (n=8) relative to untreated injured controls (n=8;  $p<0.001$ ; Figure 4.7). Deeper than 50  $\mu\text{m}$  the situation was reversed with the number of proliferating cells in the treated adhesions being significantly increased ( $p\leq 0.007$ ). The hypercellularity and high number of Ki67 positive staining cells is evident within the bulk of the treated adhesions (Figure 4.8).

As would be expected, the number of proliferating cells in the untreated injured tendons (n=8; Figure 4.9) and treated injured tendons (n=8; Figure 4.10) was greater than that in the uninjured tendons. There was no significant difference in the number of Ki67 positive cells at the tendon surface or within the tendon substance comparing untreated injured tendons (n=8) and treated injured tendons (n=8; Figure 4.11). The differences in the different treatment groups and uninjured control tendons are shown in Figure 4.12.

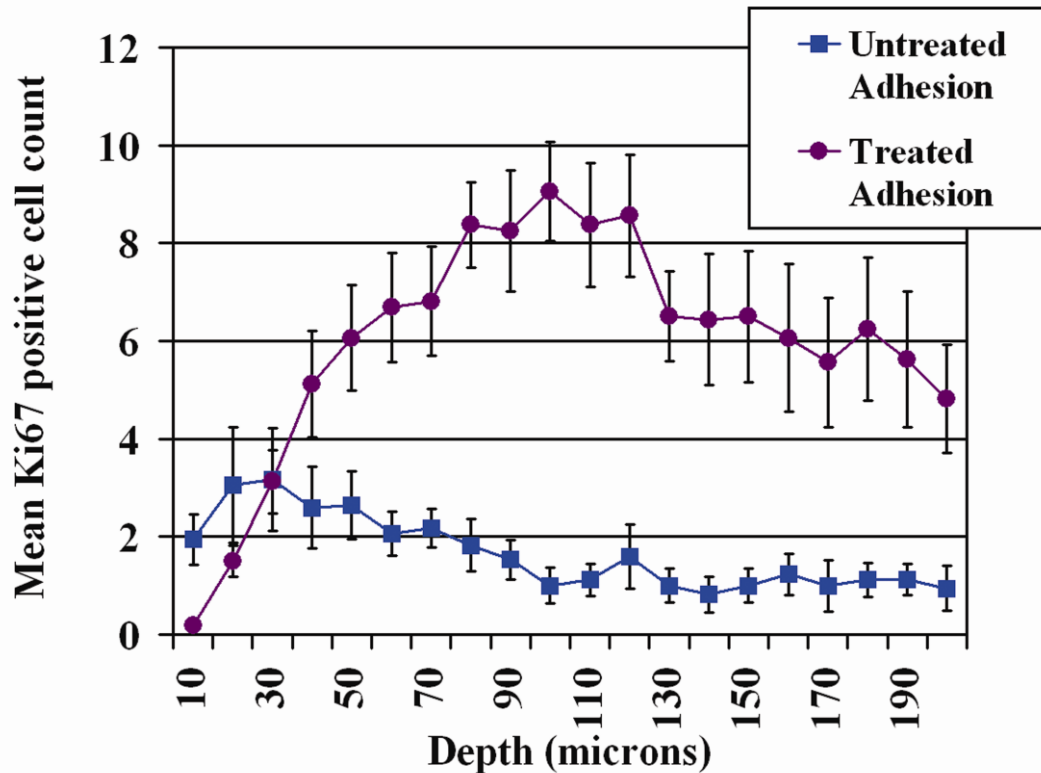


**Figure 4.7** A comparison of Ki67 positive cell counts measured from the adhesion surface in microns in treated injured digits (n=8) and untreated injured digits (n=8). There was a significant reduction in the number of proliferating cells in the most superficial 10  $\mu\text{m}$  of the adhesions in the treated injured digits relative to untreated injured controls ( $p < 0.001$ ). Deeper than 50  $\mu\text{m}$  the situation was reversed with the number of proliferating cells in the treated adhesions being significantly increased ( $p \leq 0.007$ ). Error bars = SEM.

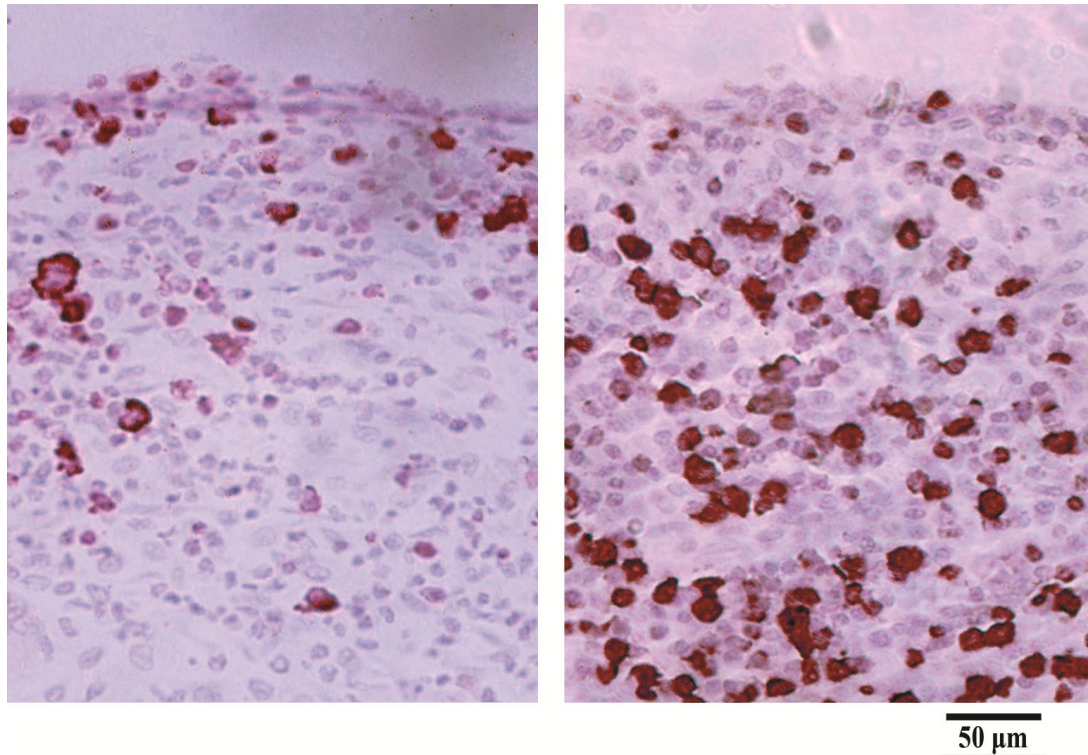


**Figure 4.8** Ki67 stained sections through adhesion surface. (*Left*) Untreated adhesion. (*Right*) Treated adhesion. These micrographs show increased staining and so cell division within the treated adhesions. There is reduced cell division in the treated adhesion surface, and increased cell division within the adhesion substance. Magnification x40.

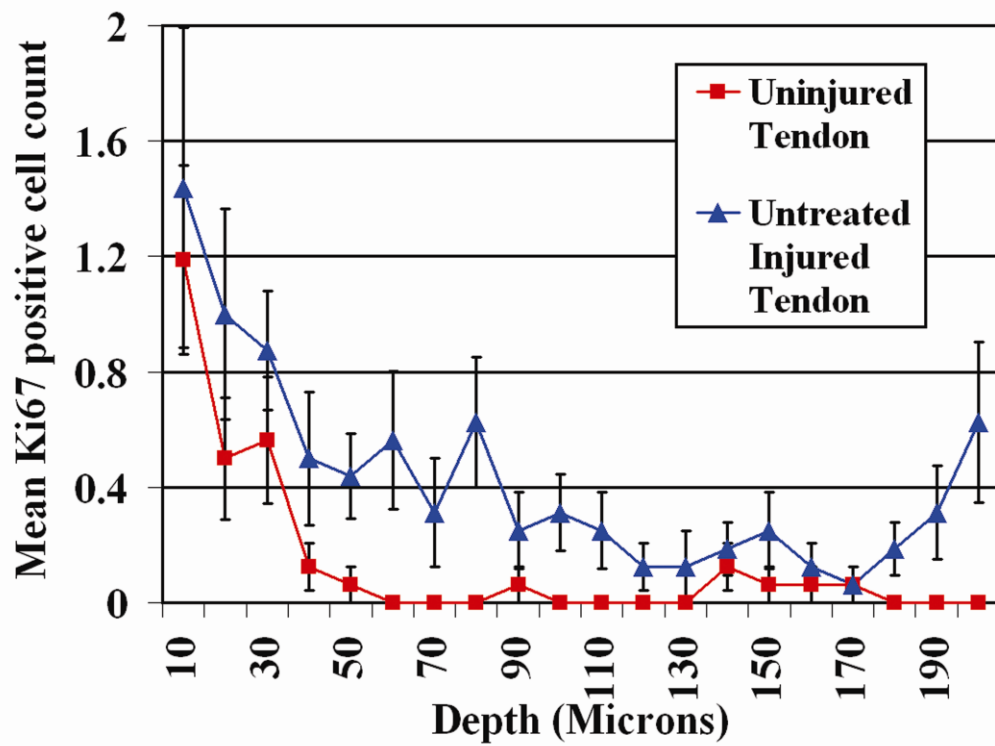


**Figure 4.9** A comparison of Ki67 positive cell counts measured from the tendon surface in microns in uninjured tendons (n=8) and untreated injured tendons (n=8). Error bars = SEM.

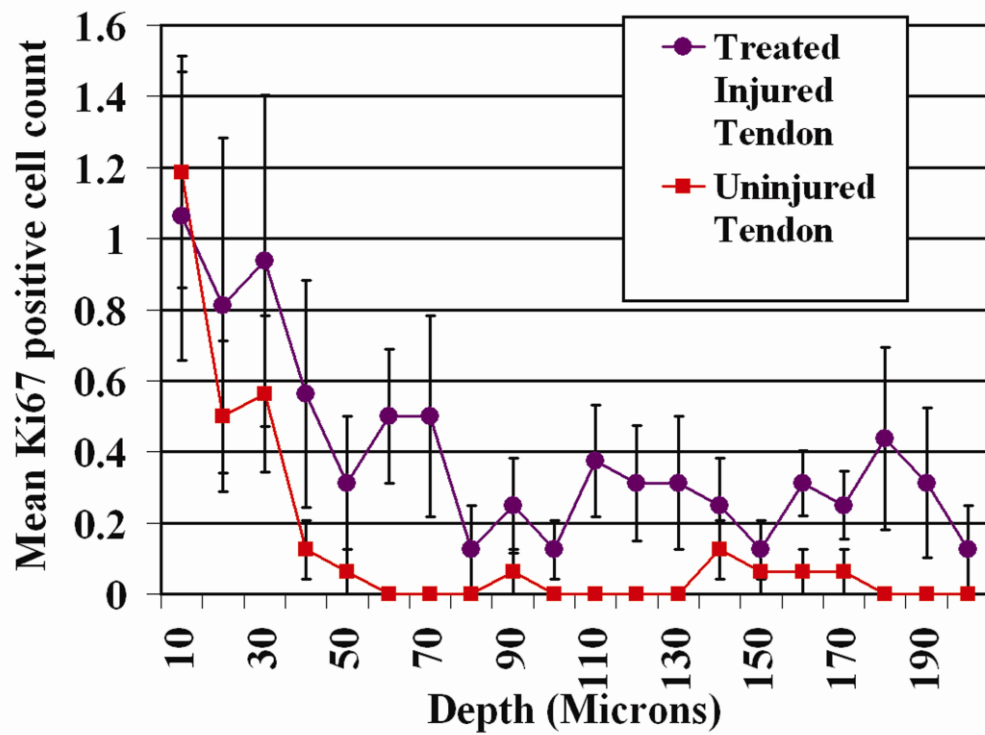


**Figure 4.10** Ki67 positive cell counts measured from the tendon surface in microns in uninjured tendons (n=8) and treated injured tendons (n=8). Error bars = SEM.

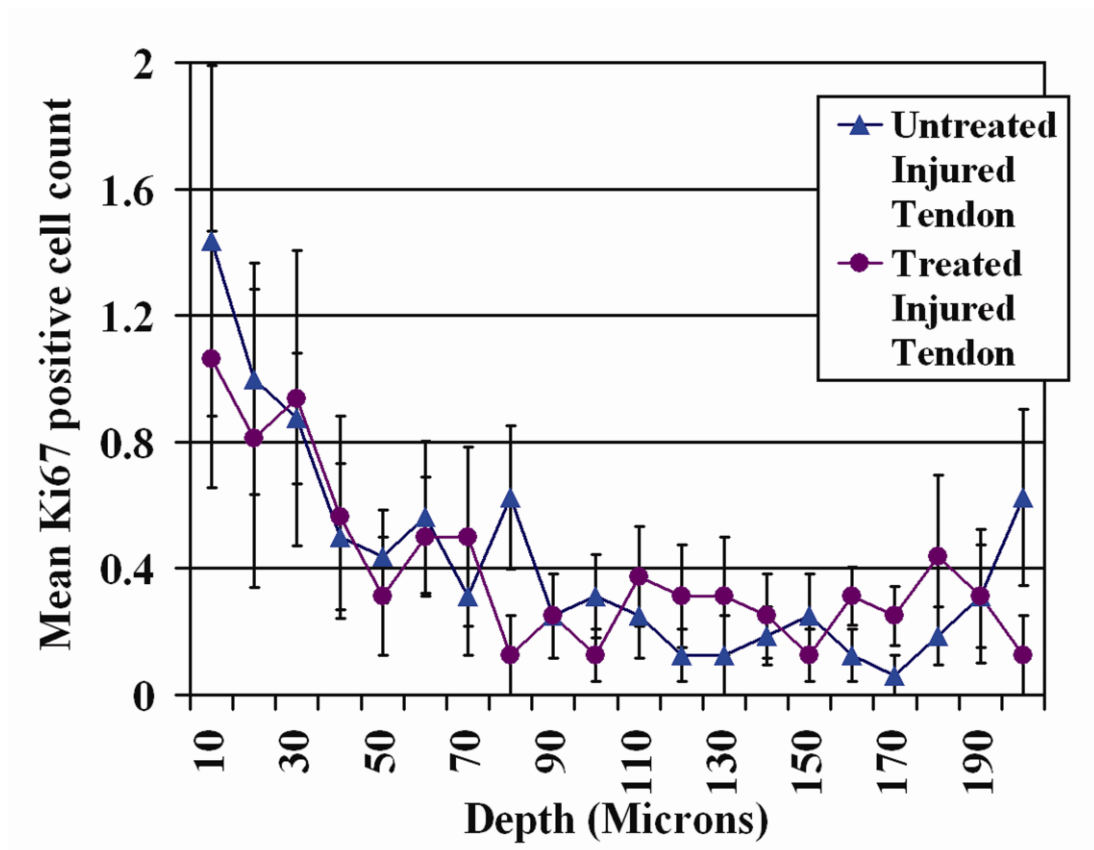


**Figure 4.11** Ki67 positive cell counts measured from the tendon surface in microns in untreated injured tendons (n=8) and treated injured tendons (n=8). Error bars = SEM.

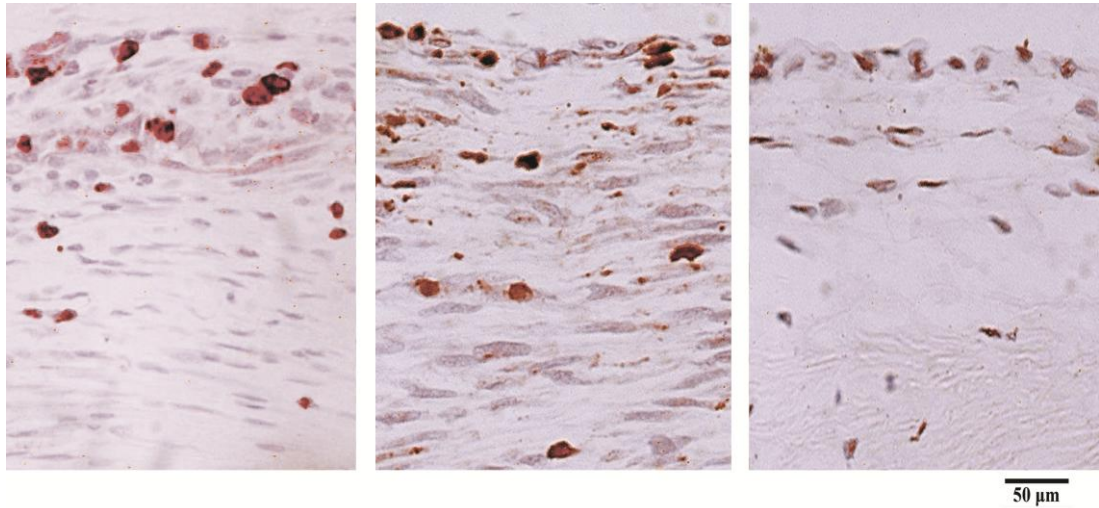


**Figure 4.12** Ki67 stained sections through tendon surface. (*Left*) Untreated injured tendon. (*Centre*) Treated injured tendon. (*Right*) Uninjured tendon. These micrographs show increased staining and so cell division within the injured tendons. There is no reduction in cell division at the treated injured tendon surface or within the tendon substance. Magnification x40.



## **4.4 DISCUSSION**

### **4.4.1 A Combined Mechanical and Histological Approach**

Much of the literature investigating adhesions is based on histological assessment, some using quantifiable methods (Akali, Khan et al. 1999). Few studies incorporate biomechanical and histopathological assessments (Strick, Filan et al. 2004). This study utilised a reproducible injury for quantification of the effects of the biomaterial in the zone of healing. The cellular response at the tendon surface has previously been described as ‘capping’ (Manske and Lesker 1984) or ‘thickening’ (Gelberman, Manske et al. 1984; Manske, Gelberman et al. 1984). In the present investigation the cellular responses at the tendon surface and adhesion surface were examined histologically to investigate the processes underlying adhesion formation. This has shown that the biomaterial produces a major reduction in the mechanical tethering of gliding interfaces by adhesions *in vivo*, although there was no difference in the incidence of adhesions between treated and untreated injury sites on histological examination.

### **4.4.2 Cellular Effects of the Biomaterial**

Cellular proliferation in response to injury is greater within the synovial sheath and tendon surface than within the tendon core (Kakar, Khan et al. 1998). The present study has demonstrated that the DFn biomaterial resulted in ‘adhesions’ that were significantly *less* cellular at their surface but were far *more* cellular over their bulk. This was reflected in the pattern of cell proliferation. The cellularity of the tendon surface was not reduced as a result of treatment. Treated injured tendons were consistently significantly more cellular than their untreated injured counterparts deeper within their substance. It is concluded that the biomaterial reduces the

strength of adhesions by diminishing the formation of *bridging* tissue connections by inducing adhesion surface cellular paucity. It achieves this without compromising tendon surface cellularity and while increasing the cellularity of the tendon core.

#### **4.4.3 A Mechanism for Differential Cellular Effects on Injured Tendon and the Synovial Surface**

Following injury provisional ECM is largely composed of Fn and collagen type-III collagen and supports cellular migration from tissue margins (Lorenz 2003). Fibroblasts predominate and a causative relation has been reported between Fn secretion and cell chemotaxis and adherence (Gelberman, Steinberg et al. 1991). As fibroblasts proliferate and migrate (Yamada 1996; Greiling and Clark 1997), they deposit an increasingly mature, mechanically functional collagen matrix (Stadelmann, Digenis et al. 1998).

Synovial sheath cells produce higher levels of Fn than tendon derived cells (Brigman, Hu et al. 1994), whereas tendon cells produce three times as much collagen *in vitro* than synovial sheath cells (Riederer-Henderson, Gauger et al. 1983). Tendon cells are therefore the foremost contributors of collagen (and tensile strength) to the repair (Gelberman, Amiel et al. 1992). It seems likely then that there is a *spatial* - from the synovial sheath to the tendon and a *temporal* ECM gradient progressing from Fn-rich to collagen-rich tissue. If the anti-adhesive Fn biomaterial releases Fn fragments at the collagenous gliding surface then cell adhesion and migration within tendon would be preserved but reduced at the synovial surface. This would reduce the ability of fibroblasts to lay down collagen across the interface. Hence adhesion would be reduced but tendon repair sustained.

A key study provides support for this, suggesting that human fibroblasts have differential properties when attaching to ECM proteins (Shimo-Oka, Hasegawa et al. 1988). The production of a Fn fragment following trypsinisation inhibited fibroblasts from attaching and spreading onto Fn, without inhibiting attachment to collagen. This is the result of competitive binding site inhibition and of fibroblasts having different protein binding sites (Brown 1983; Shimo-Oka, Hasegawa et al. 1988). RGD peptides inhibit cell attachment and migration on Fn without concomitant effect on collagen binding and migration (Oharazawa, Ibaraki et al. 2005). The collagen binding domain of Fn is spatially distinct from its cell binding (RGD) domains (Ruoslahti, Hayman et al. 1980), suggesting a further mechanism for a differential effect on tissue cellularity.

The biomaterial has been shown to dissolve *in vitro* producing a heterogeneous group of fragments (Djerkovic, Phillips et al. 2005; Branford, Brown et al. 2010). Certain Fn fragments prevent cell adhesion and auto-inhibit Fn function (Yamada and Kennedy 1984; Fukai, Takahashi et al. 1996; Fukai, Hasebe et al. 1997; Watanabe, Takahashi et al. 2000; Yamada 2000). Both Fn (Sottile, Hocking et al. 2000) and Fn fragments (Zlatopol'skii, Chubukina et al. 1989; Zlatopol'skii, Chubukina et al. 1992) promote cell proliferation. The hypercellularity within the tissue substance may be explained by the dual proproliferative and anti-adhesive action of Fn fragments. That is, encouraging proliferation of deeper, attached cells and causing detachment of cells with poorer attachments at the adhesion surface. This suggests that in the location of the biomaterial, fibroblasts experience competitive inhibition for occupancy of their integrins reducing their overall ability to bind to the ECM and to migrate. It may be suggested that this reduction in motility

contributes to the difference in surface cellularity and in fewer ECM attachments with less mechanical integration at the gliding interface.

#### **4.4.4 Suitability for Surgical Use**

Zone 2 repairs are within a tight profibrotic tunnel and therefore anti-adhesive materials should not be bulky. The biomaterial rapidly assumes a gelatinous consistency in solution, facilitating its placement, which would be simplest as a spray on product.

It is likely that the material will be effective in sutured transected tendon injuries as the resultant increased inflammatory cascade may be targeted by the material's cellular effects on dampening the adhesion surface response as shown in this study. The biomaterial may be of particular use in non compliant patients as its effects were so significant in the immobilised setting.

#### **4.4.5 Summary**

The goal of adhesion tissue engineering is to reduce connective tissue formation across gliding interfaces whilst promoting anastomosis between injured surfaces. This *in vivo* study has shown that the anti-adhesive biomaterial significantly reduces restrictive adhesion formation and modifies cellular reactions in the wound milieu. The *in vitro* (Chapter 3) and *in vivo* investigations suggest that this would be due to the biomaterial's engineering properties providing a physical barrier that delivers both anti-adhesive and pro-proliferative fragments around the injured tendon synovial complex. The material was not cytotoxic as demonstrated by an absence of non viable cells after exposure to the material (Branford, Brown et al. 2010; Chapter

3). These findings may pave the way for a clinical study to use a biomaterial mat to reduce adhesion formation after tendon repair. In addition, this simple tendon model would be applicable to a much wider context for the testing of anti-adhesion treatments.

**CHAPTER 5**

**RESULTS**

**RELATING STRUCTURE TO HIERARCHICAL**

**MECHANICS OF IMMOBILISED AND MOBILISED**

**FLEXOR TENDON ADHESIONS**

**5.1 INTRODUCTION**

**5.1.1 Aims**

**5.2 MATERIALS AND METHODS**

**5.2.1 Gross Adhesion Mechanics**

**5.2.2 Micromechanical Assessment**

**5.2.3 Image Analysis**

**5.2.4 Data Analysis**

**5.2.5 Statistical Analysis**

**5.3 RESULTS**

**5.3.1 Gross Adhesion Mechanics**

**5.3.2 Micromechanical Assessment**

**5.4 DISCUSSION**

**5.4.1 A Hierarchical Approach to Adhesion Assessment**

**5.4.2 Local Strains in Adhesions Cannot be Inferred from  
Applied Strain**

- 5.4.3 Mobilisation Favours Dynamic Patterns with Higher Local Strain**
- 5.4.4 Mobilisation Favours Tissue Heterogeneity**
- 5.4.5 Summary**

## 5.1 INTRODUCTION

The composition of living tissues is less important in determining their mechanical behaviour under stress than the organisation of their component parts, with component subtype and topology being critical (Tanaka, Al-Jamal et al. 2001). In addition, tissues that have a hierarchical structure need to be studied at micro- and macrostructural levels in order to understand their intrinsic behaviour (Katz, Misra et al. 2007). At a microstructural level, the local strains seen in tissues are strongly dependent on the associations between the cells and the surrounding extracellular matrix (ECM) (Screen 2004). The degree of structural heterogeneity within tissues may also alter their response to load and lead to mechanical failure (Zioupou, Gresle et al. 2008), which may be particularly relevant to tendon adhesions. Structural organisation is a dynamic entity and is revealed by the application of stress. The difficulty lies in how to visualise dynamic structural organisation and heterogeneity at a local level and how to quantify local tissue stress-strain responses to applied loads.

Examinations of flexor tendon adhesions, previously described as either ‘loose’ or ‘dense’ (Masuda, Ishii et al. 2002), have generally followed assessment of the integrity of the healing tendon itself. Relatively few studies, however, have investigated the dynamic nature of these adhesions. This has been due, in part, to the lack of suitable techniques that were sensitive to dynamic micromechanics.

This study tests the hypothesis that adhesions are non-uniform and that their behaviour is a function of their organisation and their local strain responses to applied stress. As tendon mobilisation is a well recognised modulator of the quality



of adhesion formation, both immobilised and mobilised tendon adhesions were investigated. Adhesions were analysed using a hierarchical approach, with randomisation to either gross tensile testing, or to micromechanical assessment using defined strain regimes applied to the adhesions where the movement of fluorescently labelled cell nuclei, acting as dynamic markers, was visualised using real time confocal microscopy. Cellular organisation and local strain responses were assigned values using image analysis software.

### **5.1.1 Aims**

- To describe how immobilised and mobilised tendon adhesion tissues are organised.
- To examine the relationship between the local strains produced in adhesions and the applied strain.
- To relate the micromechanical findings to gross restrictive parameters.

## **5.2 MATERIALS AND METHODS**

### **5.2.1 Gross Adhesion Mechanics**

11 mobilised and 10 immobilised adhesion samples were assessed using tensile testing to obtain structural stiffness and peak load values as described in section 2.3.3.3.

### **5.2.2 Micromechanical Assessment**

A custom designed tensile straining rig was used to apply a defined strain regime to 14 mobilised and 15 immobilised adhesion samples as detailed in section 2.3.3.4.1.

The movement of adhesion cell nuclei was visualised using real-time confocal microscopy as described in section 2.3.3.4.3.

### **5.2.3 Image Analysis**

The image analysis software Imaris® 6.1 was used to determine the exact  $x$  and  $y$  axis positions of each of the adhesion cell nuclei in each of the images throughout the entire strain range, relative to the position of a central reference nucleus. The tracking module of the software was then used to track the displacement of all the cell nuclei up to 10% applied strain. Details of this are set out in section 2.3.3.4.4.

### **5.2.4 Data Analysis**

Local strains were determined for each sample, using the nuclei as local strain markers. This was achieved by plotting the displacement of each peripheral nucleus (over the entire strain range) against its original distance from the reference nucleus prior to the application of strain. The slope of the graph represents the local strain for each adhesion sample. Details of this process are described in section 2.3.3.4.5.

### **5.2.5 Statistical Analysis**

Statistical analysis was used, with  $p < 0.05$  being judged as statistically significant. Both the structural stiffness and load at failure of the mobilised and immobilised groups were compared using the Mann-Whitney U test, as the data were non-parametrically distributed. The micromechanical data were assessed using the unpaired t-test (the data were normally distributed).

## **5.3 RESULTS**

Of the original 52 digits, 2 were discarded due to the poor quality of the dissected specimens. Prior to harvest, digits were randomised to either immobilisation (n=25) or mobilisation (n=25). These digits were further randomised to either tensile testing (n=21) or to confocal assessment (n=29). Macroscopically, the immobilised peritendinous adhesions were pale, fibrotic and surrounded the injured tendon, whereas the mobilised adhesions were more translucent, pliable and less extensive (Figure 5.1).

### **5.3.1 Gross Adhesion Mechanics**

The combined load displacement data for both mobilised (n=11) and immobilised (n=10) specimens are shown in Figure 5.2 (Table 5.1). The structural stiffness of immobilised adhesions was 140% of that of mobilised adhesions ( $p=0.010$ ). The corresponding value for the load at failure was 160% ( $p=0.049$ ). Although the adhesions failed during testing, the tendons themselves were not observed to fail.

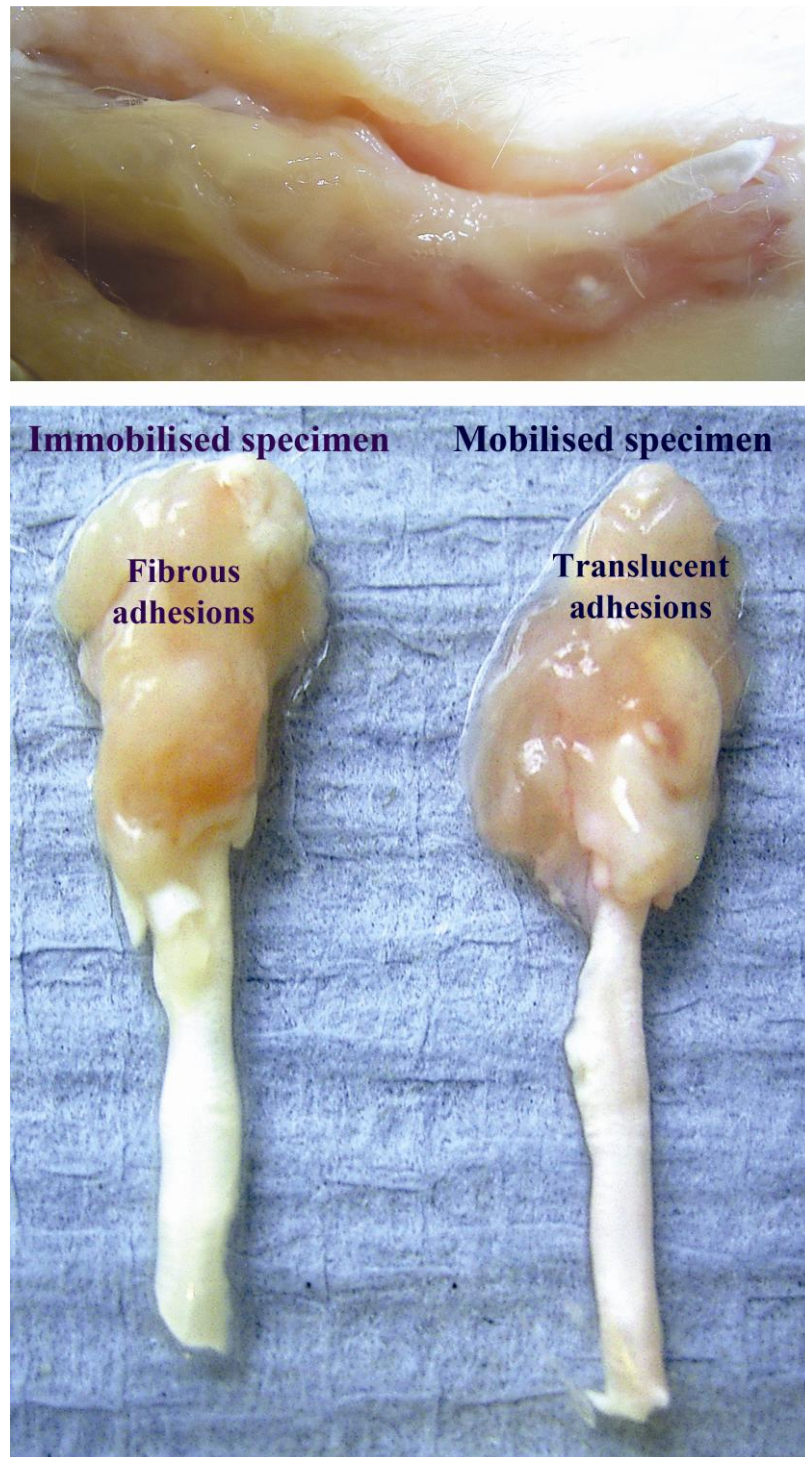


**Figure 5.1** Dissection of tendon-adhesion-synovial complexes at 14 days. *(Above)* In situ specimen prior to isolation. *(Below left)* Immobilised specimen demonstrating whiter, fibrous peritendinous tissue completely encasing the tendon. *(Below right)* Mobilised specimen showing translucent, pliable adhesions with visible tendon.

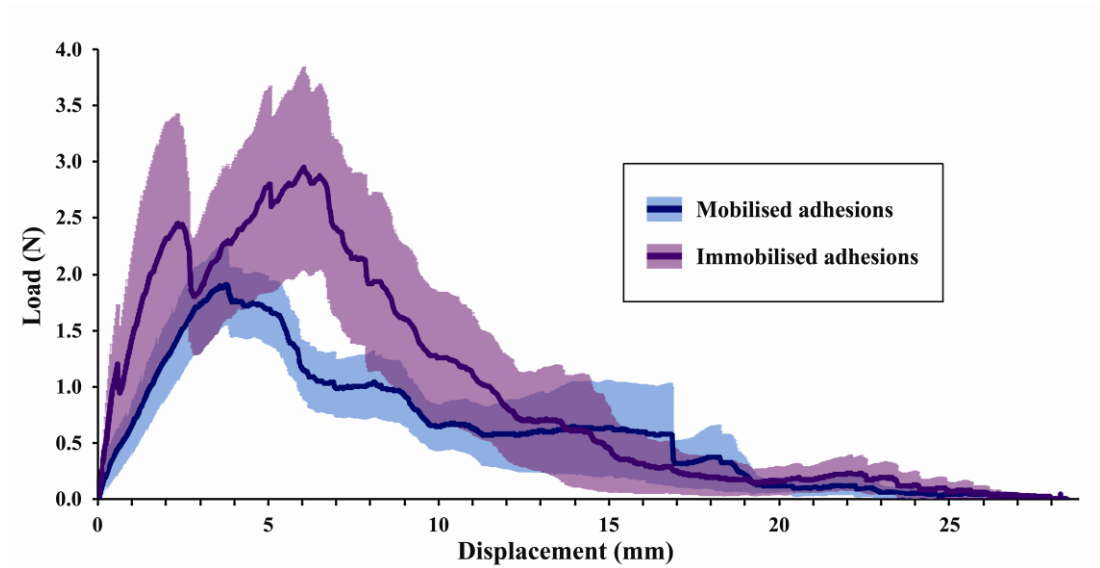


**Figure 5.2** Load displacement graph for mobilised adhesions (n=11) and immobilised (n=10) adhesions. The immobilised adhesions' structural stiffness was 140% of that for the mobilised adhesions ( $p=0.010$ ). The load at failure of the immobilised adhesions was 160% of that of the mobilised adhesions ( $p=0.049$ ). Pale shading indicates mean ( $\pm$  SEM).

<b>Integrity of Adhesion</b>	<b>Mobilised (n=11)</b>	<b>Immobilised (n=10)</b>
<b>Structural Stiffness</b> (N mm <sup>-1</sup> )	840 (640 – 990)	1200 (910 – 1700)
<b>Load at Failure (N)</b>	2.7 (1.7 – 3.7)	4.2 (3.6 – 6.9)

**Table 5.1** Mobilised versus immobilised adhesions: Comparison of structural stiffness and load at failure. Results are expressed as median (interquartile range).

## 5.3.2 Micromechanical Assessment

### 5.3.2.1 Confocal Assessment

The rig successfully strained the specimens with no slippage. Adhesions could be readily identified from other component tissues by their densely packed arrangement of cell nuclei as seen in Figure 5.3. The confocal images were reconstructed as movies of the cellular displacement over the entire strain regimen. The images in the movies detailed below are centred on the adhesion, and represent the entire imaged region of the specimen, at x10 magnification. When interpreting the movies the applied strain is in the vertical axis. This may be conceptualised in terms of a digit being extended in this direction, with visualisation of the deformation of the adhesion under applied strain. A variety of dynamic adhesion patterns were noted in both adhesion groups, with the imaged region of each specimen exhibiting a single pattern of local strain. These may be designated as:

- Stretch (See **Additional Illustrative Digital Material, Video 5.1**, which demonstrates the stretching dynamic pattern for a mobilised adhesion tissue sample, where adhesion cell nuclei become increasingly separated in the axis of the applied strain; See **Additional Illustrative Digital Material, Video 5.2**, which demonstrates the stretching dynamic pattern for an immobilised adhesion tissue sample, where adhesion cell nuclei become increasingly separated, although less than for the mobilised adhesion sample, reflecting lower local strain);
- Compress (See **Additional Illustrative Digital Material, Video 5.3**, which demonstrates the compressing dynamic adhesion pattern, where adhesion cell nuclei become increasingly approximated to each other);

- Shear (See **Additional Illustrative Digital Material, Video 5.4**, which demonstrates the shearing dynamic adhesion pattern, where groups of adhesion cell nuclei move perpendicularly to each other);
- Random (See **Additional Illustrative Digital Material, Video 5.5**, which demonstrates the random dynamic adhesion pattern, where adhesion cell nuclei appear to move at random);
- Tear (See **Additional Illustrative Digital Material, Video 5.6**, which demonstrates the tearing dynamic adhesion pattern).

#### **5.3.2.2 Image Analysis**

Typical graphs of local strain for both mobilised and immobilised adhesion samples are shown in Figure 5.4. The corresponding mean local strain data at 10% applied strain for both groups are presented in Figure 5.5 (Table 5.2), revealing considerable differences. The mean local strain for mobilised adhesions was 325% of that of the immobilised adhesions (3.83% (n=14) and 1.18% (n=15) respectively). However, due to the variability, these differences were not statistically significant (p=0.310). The spread of mean local strain values for mobilised adhesions, represented by the standard deviation (SD), was twice that of the immobilised adhesions (8.86% and 4.28% respectively).



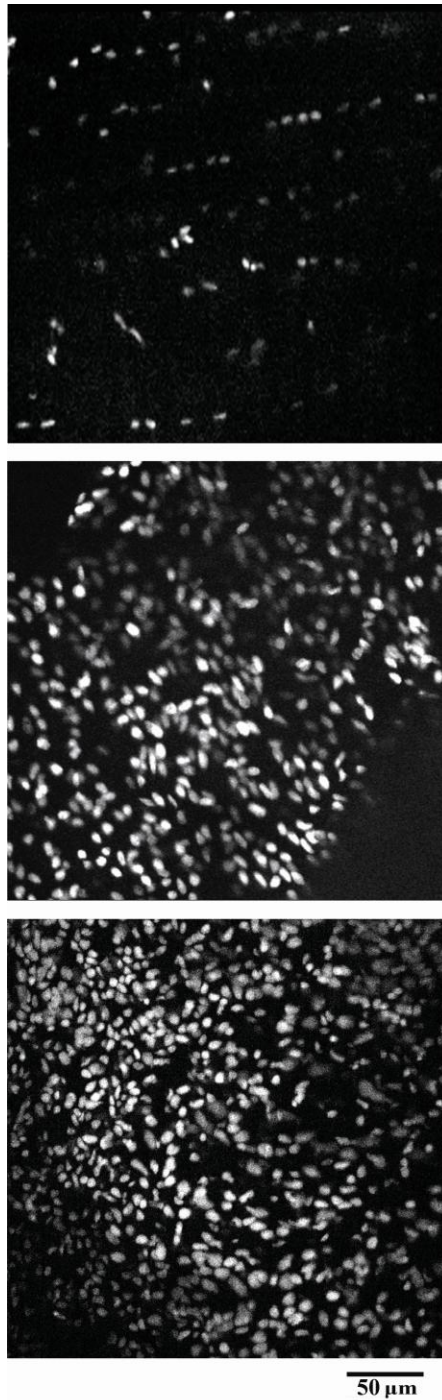


**Figure 5.3** Confocal images showing characteristic appearance of component tissues in specimens. (*Above*) Tendon core cell nuclei appear as long, narrow, non-overlapping lines. (*Centre*) Tendon surface cell arrangement, with evenly distributed cells. (*Below*) Adhesions could be readily identified from other component tissues by their densely packed arrangement of cell nuclei. Magnification x10.

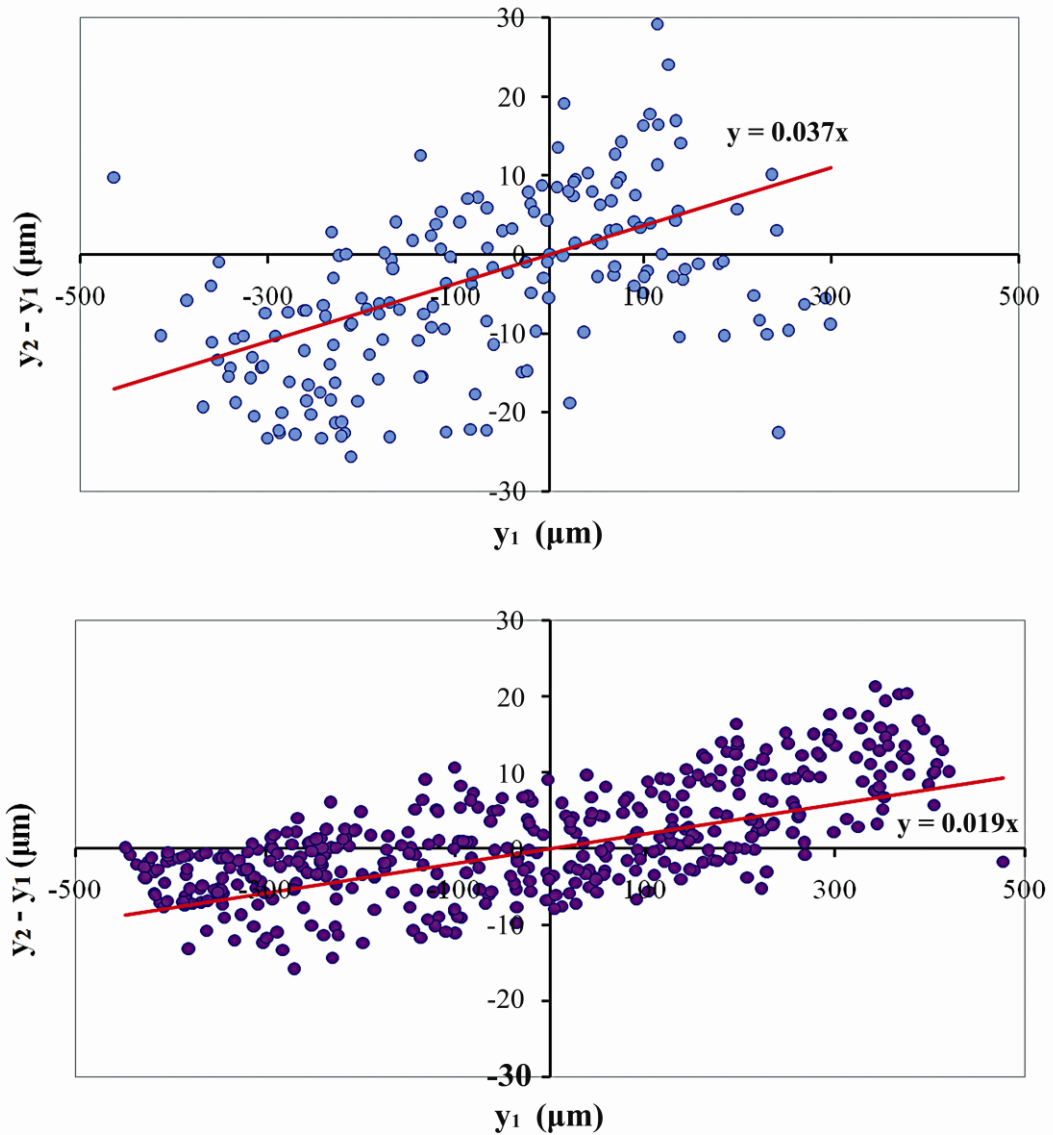


**Figure 5.4** Example graphs of the local strain for adhesion samples at 10% applied strain. The displacement of each peripheral nucleus,  $(y_2 - y_1)$ , was plotted against  $y_1$ , where  $y_1$  is the distance between the position of the central reference nucleus and the peripheral nucleus in the  $y$  axis at 0% applied strain and  $y_2$  is this distance at 10% applied strain. The gradient of the line of best fit was equal to the local strain for the adhesion sample. (*Above*) Mobilised adhesion with 3.7% local strain. (*Below*) Immobilised adhesion with 1.9% local strain.

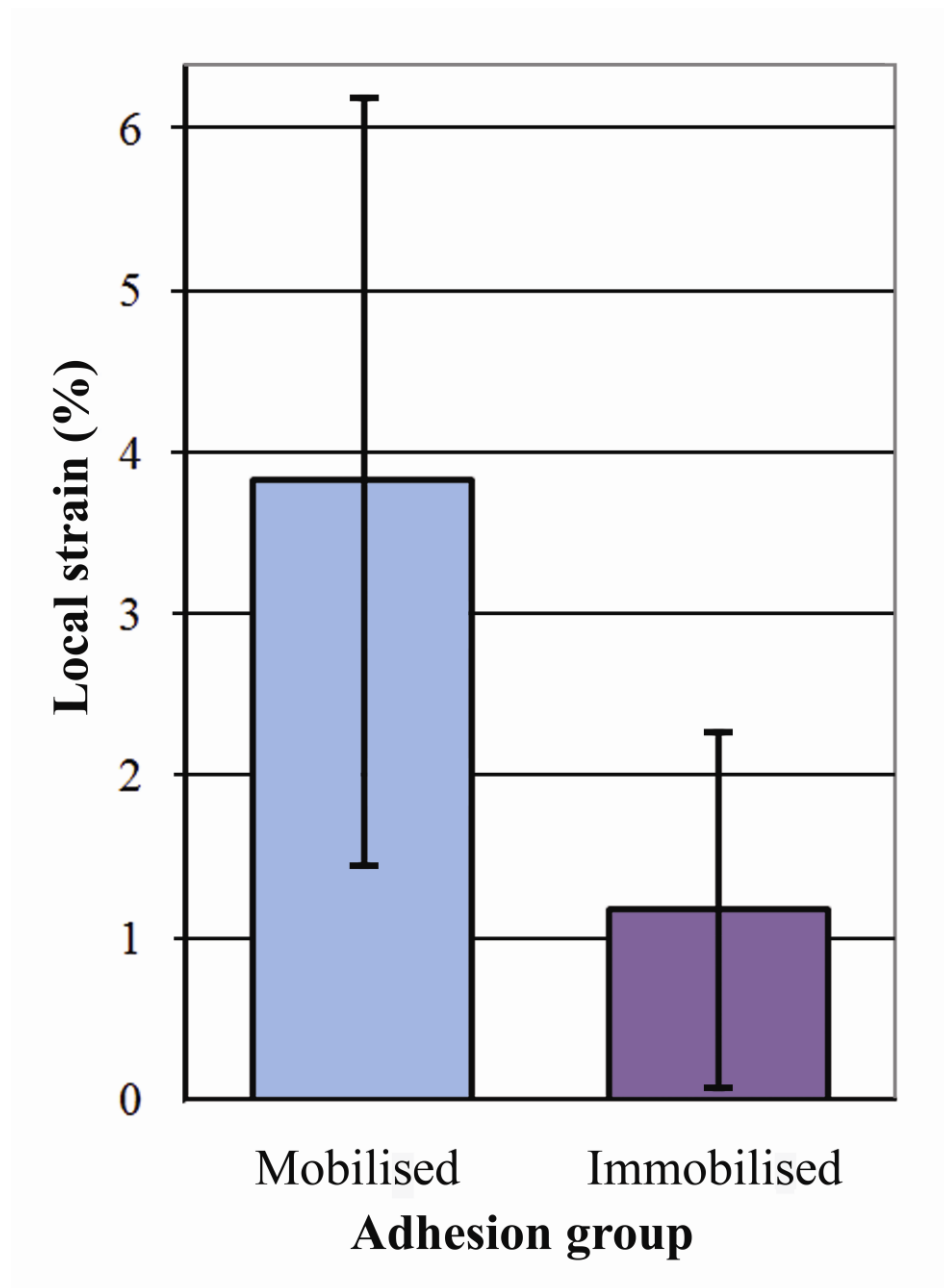


**Figure 5.5** Graphical comparison of mean local strain values at 10% applied strain for mobilised (n=14) and immobilised (n=15) adhesion samples. Error bars = SEM.

The local strain data were further analysed into five regional patterns (Table 5.3). Although the numbers associated with each pattern were relatively small, certain trends could be noted. For example, the local strains for mobilised adhesions were considerably higher than their immobilised counterparts, in both stretched and compressed regions, with fold increases of two and five, respectively. The random type of adhesion pattern had relatively low mean local strain values for both adhesion groups.

The SD for each sample, calculated from the movement of each of the peripheral nuclei, represented the spread of local strains and, hence, the heterogeneity of the micromechanical response at an intercellular level. The data for all movement patterns suggest a similar magnitude of distribution, between 7 and 8%.

	<b>Mobilised (n=14)</b>	<b>Immobilised (n=15)</b>
<b>Local Strain (%)</b>	3.83 ± 8.86	1.18 ± 4.28

**Table 5.2** Comparison of mean local strain values at 10% applied strain for mobilised (n=14) and immobilised (n=15) adhesion samples. Results are presented as mean local strain (%; ± SD).

<b>Regional Pattern</b>	<b>Mobilised (n=14) or Immobilised (n=15)</b>	<b>Number (n)</b>	<b>Mean Local Strain (%)</b>	<b>Mean Spread (SD) (%)</b>
Stretch	Mobilised	9	6.42	7.74
Stretch	Immobilised	7	2.90	7.45
Compress	Mobilised	1	-10.08	7.59
Compress	Immobilised	2	-2.06	7.27
Shear	Mobilised	2	2.06	8.65
Shear	Immobilised	4	2.44	7.04
Random	Mobilised	1	0.68	8.05
Random	Immobilised	2	-1.17	7.26
Tear	Mobilised	1	-5.37	8.58
Tear	Immobilised	0		

**Table 5.3** Frequency and mean local strain of regional patterns seen in mobilised and immobilised adhesions.

## **5.4 DISCUSSION**

### **5.4.1 A Hierarchical Approach to Adhesion Assessment**

This investigation adopted a hierarchical multiscale approach to examine the mechanical behaviour of digital flexor tendon adhesions. Both immobilised and mobilised tendon adhesions were assessed, employing an established flexor tendon injury model (Jones, Burnett et al. 2002; Branford, Mudera et al. 2008). Macroscopically, the immobilised adhesions were more fibrous in nature compared with their mobilised counterparts. Macromechanical testing demonstrated that immobilised adhesions had significantly higher values for structural stiffness and load at failure than mobilised adhesions (Table 5.1). The micromechanical assessment of adhesions employed a confocal laser microscope to visualise the movement of cell nuclei to examine local tissue organisation and local strain responses to applied stress. Different dynamic adhesion patterns (stretch, compress, shear, random and tear) were observed in both adhesion groups. Mobilised adhesions exhibited over a three-fold higher local strain than their immobilised counterparts (Table 5.2). Although the difference in mean local strain was not statistically significant due to the high variability of the data, the considerable change in the observed magnitude of the local strain suggests that the mobilised adhesions were more easily deformed by an applied force. This would be useful in the clinical setting as the adhesion would be more likely to deform and then fail.

### **5.4.2 Local Strains in Adhesions Cannot be Inferred from Applied Strain**

Confocal microscopy enables very accurate dynamic assessments to be made of the local strain fields between cells and within tissues, in viable and unprocessed

samples (Arnoczky, Lavagnino et al. 2002; Screen, Lee et al. 2003; Bruehlmann, Hulme et al. 2004; Screen, Lee et al. 2004; Screen 2004; Cheng 2007). Screen and colleagues previously examined the local strain in tendons using confocal microscopy, and found that local strains within a tendon fascicle were consistently smaller than the applied strain, never exceeding 1.2%, for a maximum applied strain of 8% (Screen, Lee et al. 2004; Screen 2004). By comparing these results with the data obtained in the present Chapter, this suggests that when strain is applied to immobilised adhesions, which exhibit low local strain, there may be greater deformation of the tendon itself, increasing the risk of tendon rupture. By contrast, when strain is applied to mobilised adhesions, which exhibit higher local strain values, the adhesions are more likely to deform and fail. However, although the increase in local strain following mobilisation may be partly responsible for the lower macromechanical structural stiffness of mobilised adhesions, the relation between local strain and gross adhesion mechanics is likely to be more complex. Indeed previous studies estimating bulk strain and local tissue strain using confocal techniques have found low levels of correlation between them (Schinagl, Gurskis et al. 1997; Arnoczky, Lavagnino et al. 2002). In the present investigation, the finding that different dynamic adhesion patterns occur, each with differences in their local strain values suggest that local strains within the tendon-adhesion-synovial complex cannot be inferred from the applied strain during gross mechanical testing.

#### **5.4.3 Mobilisation Favours Dynamic Patterns with Higher Local Strain**

Interrelated biochemical and biomechanical changes are seen in tendons as a result of increased or decreased applied loads (Gelberman, Amiel et al. 1981; Woo,



Gelberman et al. 1981; Amiel, Woo et al. 1982; Gelberman, Woo et al. 1982; Woo, Gomez et al. 1982; Gelberman, Vande Berg et al. 1983; Gelberman, Manske et al. 1986; Hitchcock, Light et al. 1987; Hannafin, Arnoczky et al. 1995; Kubota, Manske et al. 1996; Lin, Cardenas et al. 2004). However, much of the work on tendon adhesions has been secondary to that of the investigation of tendons themselves. For example, it is not clear why the tensile strength of mobilised adhesions is not increased following mobilisation in a similar manner to that of the tendon. From the results of this investigation it appears that injured adhesions appear to respond to mobilisation by local ECM remodelling to form dynamic patterns which exhibit higher local strains. This is a useful adaptation as the adhesion becomes less restrictive to glide and is more likely to fail. The lower local strain values for the immobilised adhesions seen in this investigation may reflect increases in neo-tissue deposition and/or collagen cross-linking (Masuda, Ishii et al. 2002).

#### **5.4.4 Mobilisation Favours Tissue Heterogeneity**

The spread of mean local strain values for mobilised adhesions was twice that of the immobilised adhesions, reflecting their greater heterogeneity, which may be associated with the presence of tissue subunits with differing mechanical properties. It seems likely that the micromechanical environment within each of the subunits is relatively uniform, as demonstrated by the similar range of local strain values. Thus heterogeneity within the mobilised adhesions may be due to a greater variety of different subunit types forming following mobilisation. It may be hypothesised that, due to their increased heterogeneity, mobilised adhesions contain points of weakness which are prone to failure.

### 5.4.5 Summary

This investigation has demonstrated that immobilised and mobilised adhesions differ at both micro- and macromechanical levels, supporting the need for a hierarchical approach to their evaluation. The confocal microscopy assessments described, using fibroblast nuclei as dynamic markers, have provided an accurate measure of local adhesion organisation and local strain responses to applied stress. This is the first investigation to describe the micromechanical changes in mobilised and immobilised tendon adhesions following injury, providing insight into the specific influence of *in vivo* loading on adhesion ECM remodelling. The increased local strain values and heterogeneity seen in the mobilised adhesions may explain why they are less restrictive *in vivo* than immobilised adhesions: adhesions may fail in localised areas corresponding to more readily deformed subunit patterns. It may be hypothesised that anti-adhesion treatments should favour the formation of sites either expressing increased local strain responses or those predisposed to heterogeneity and localised mechanical failure. These findings are fundamental to providing a better understanding of the micromechanical building blocks that are responsible for the overall dynamic response of flexor tendon adhesions, which is so critical to tendon function.

**CHAPTER 6**

**RESULTS**

**ATTACHMENT OF INTRINSIC AND EXTRINSIC**

**TENDON CELLS AND ADHESION CELLS TO**

**COLLAGEN AND FIBRONECTIN**

**6.1 INTRODUCTION**

**6.1.1 Aims**

**6.2 MATERIALS AND METHODS**

**6.2.1 Preparation of Explant Cultures**

**6.2.2 Cell Adhesion Assay**

**6.2.3 Cell Adhesion Assessment**

**6.2.4 Morphological Assessment**

**6.2.5 Statistical Analysis**

**6.3 RESULTS**

**6.3.1 Cell Adhesion Assessment**

**6.3.2 Morphological Assessment**

**6.4 DISCUSSION**

**6.4.1 Selectivity in Tendon Healing**

**6.4.2 Intrinsic Cells Show Greater Attachment to Collagen and  
Fibronectin**

- 6.4.3 Mobilisation Increases Cell Attachment and Favours Elongated Cellular Morphology**
- 6.4.4 A New Therapeutic Strategy: Selectively Preventing Extrinsic Cell Attachment to Fibronectin**
- 6.4.5 Summary**

## **6.1 INTRODUCTION**

Strickland has stated that it is impossible to isolate intrinsic and extrinsic contributions to flexor tendon healing in the clinical setting (Strickland 2000). With regard to anti-adhesion strategies it is unlikely that any barrier entirely prevents all cellular migration. In addition, current biochemical treatments are non-specific to cells of different origins. Treatments may reduce the adhesion response at the expense of impairing healing in the tendon, thereby favouring tendon rupture (Golash, Kay et al. 2003). A new strategic approach to modifying tendon healing is required. The results from Chapters 3 and 4 have demonstrated that, by using a biomaterial that reduces cell attachment, it may be possible to selectively target postsurgical adhesions without compromising tendon cellularity (Branford, Mudera et al. 2008; Branford, Brown et al. 2010).

The attachment profile of cells of the flexor tendon-synovial complex to the components of the extracellular matrix (ECM) and the effects of mobilisation on the attachment of peritendinous adhesion cells has not previously been reported. As tendon mobilisation is known to improve tensile strength in tendons and fewer adhesions (Gelberman, Woo et al. 1982; Gelberman and Manske 1985; Gelberman, Botte et al. 1986), cells from both immobilised and mobilised tendon adhesions were investigated.

Cell shape is a function of cell behaviour and reflects the distribution of focal adhesion complexes and therefore cell attachment (Singhvi, Kumar et al. 1994; Wang, Jia et al. 2003; McBeath, Pirone et al. 2004; Yang, Crawford et al. 2004; Lee, Jones et al. 2006; Li, Li et al. 2008). A morphological investigation was therefore

also conducted. The attachment of tendon core, tendon surface, synovial sheath, mobilised adhesion and immobilised adhesion cells to collagen and fibronectin (Fn) was investigated using both attachment assays and morphometric analysis.

### **6.1.1 Aims**

- To determine if there is a difference in cell attachment between the cells of different origins from within the digital tendon-synovial complex to collagen and Fn *in vitro*.
- To determine if mobilisation has an effect on the attachment of cells contributing to tendon adhesion formation.

## **6.2 MATERIALS AND METHODS**

### **6.2.1 Preparation of Explant Cultures**

5 New Zealand White (NZW) rabbit right forepaws were dissected to isolate the components of the deep digital flexor tendon-synovial complex (tendon core, tendon surface, and synovial sheath), which were explanted separately in 10% NGM, as described in section 2.2.1.1. A further 10 animals were subjected to deep flexor tendon injuries as set out in section 2.3.1. Animals were then randomised to either mobilisation or immobilisation as detailed in section 2.3.3.1. The resultant adhesions were harvested at 2 weeks and explant cultured as described in section 2.2.1.1.

### **6.2.2 Cell Adhesion Assay**

Collagen type-I or Fn were adsorbed at 0, 1, 2, 6, 12, 25 and 50  $\mu\text{g mL}^{-1}$  onto Nunc MaxiSorp 96-well ELISA plates as described in section 2.2.8.1. The different cell

groups were seeded onto the coated plates and adherent cells fixed and stained using crystal violet solution as detailed in section 2.2.8.3.

### **6.2.3 Cell Adhesion Assessment**

Bound crystal violet was dissolved in acetic acid. Absorbance, representing cell attachment, was measured in a microplate reader as detailed in section 2.2.8.3.

### **6.2.4 Morphological Assessment**

Digital images taken at random of the cells attached to either collagen type-I or Fn at  $25 \mu\text{g mL}^{-1}$  were captured using a Zeiss Axioskop Inverted Optical Microscope. Cell area, perimeter and circularity were quantified using ImageJ software as set out in section 2.2.8.4. The proportion of elongated or circular cells was quantified using particle counting as described in section 2.2.8.4.

### **6.2.5 Statistical Analysis**

Statistical analysis was used, using a p value of  $<0.05$  as to be statistically significant. The cell attachment data was compared using the 2-way analysis of variance (ANOVA) with the Tukey post-test. The quantitative morphological data was compared using Student's t-test for the adhesion cell groups (the Mann Whitney U Test was used when the data was not normally distributed). A 2-way analysis of variance (ANOVA) with Dunnett's post-test for the tendon-synovial complex cell groups.

## **6.3 RESULTS**

A total of 30 digits were explanted and included in the investigation (digits 2 and 4 from 15 NZW rabbit forepaws). This represents 5 cell strains (n=5) for each of tendon core, tendon surface, synovial sheath, mobilised adhesion and immobilised adhesion cell groups. These cell strains were tested for both cell attachment to collagen type-I and Fn using a crystal violet assay. Cell morphology when attached to these proteins was assessed using ImageJ, an image analysis and processing program. Results are shown separately for the tendon-synovial complex cell groups and for the adhesion cell groups. Representative micrographs and their processed images are shown in Figures 6.1, 6.2, 6.3, and 6.4.

### **6.3.1 Cell Adhesion Assessment**

Absorbance of crystal violet, representing cell attachment, was measured in quadruplicate in a microplate reader at 595 nm. Corrected values were expressed for each matrix protein for the tendon-synovial complex cell groups and for the adhesion cell groups.

#### **6.3.1.1 Tendon-Synovial Complex Cell Groups**

Cell attachment for each of the tendon core, tendon surface, and synovial sheath cell groups (all n=5) to protein-coated culture wells at 0 to 50  $\mu\text{g mL}^{-1}$  is shown for collagen type-I in Figure 6.5 (Table 6.1) and for Fn in Figure 6.6 (Table 6.2). Results indicate that cell attachment was greatest for tendon core cells and lowest for synovial sheath cells for both collagen type-I and Fn for all concentrations tested. The attachment of tendon surface cells was consistently between that of tendon core and synovial sheath cell groups. The difference in the mean absorbance values,



representing cell attachment, to both collagen type-I and Fn among the different cell groups was statistically significant ( $p<0.001$ ), after allowing for effects of differences in concentration.

#### **6.3.1.2 Adhesion Cell Groups**

Cell attachment for mobilised ( $n=5$ ) and immobilised adhesion cell groups ( $n=5$ ) to protein-coated culture wells at 0 to 50  $\mu\text{g mL}^{-1}$  is shown for collagen type-I in Figure 6.7 (Table 6.3) and for Fn in Figure 6.8 (Table 6.4). Results indicate that cell attachment was greater for mobilised adhesion cells than for immobilised adhesion cells both on collagen type-I and Fn at all concentrations tested. The difference in the mean absorbance values, representing cell attachment, to both collagen type-I and Fn between mobilised and immobilised groups was statistically significant ( $p<0.001$ ), after allowing for effects of differences in concentration.

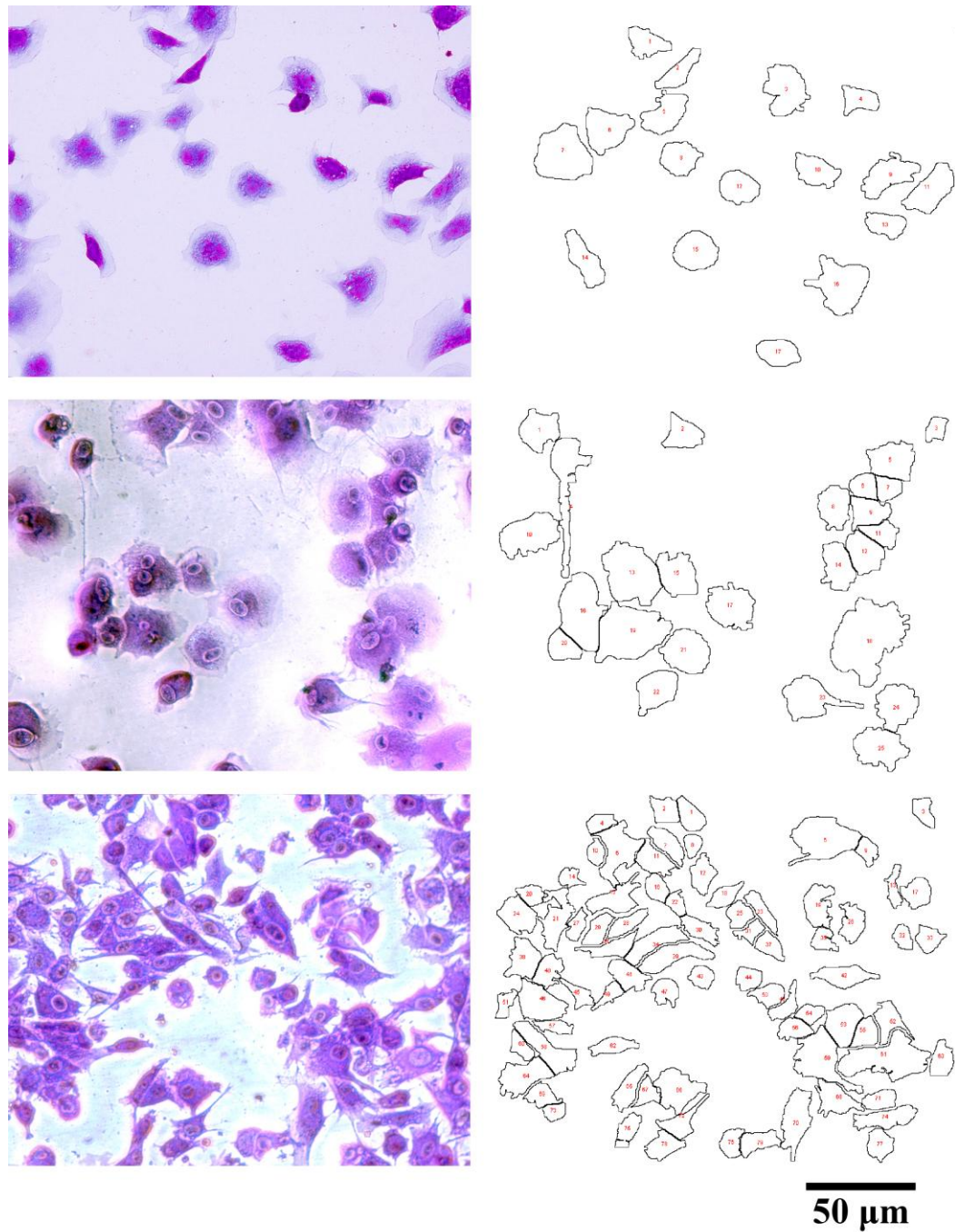


**Figure 6.1** Representative micrographs of tendon-synovial cell groups attached to collagen type-I. Processed images using ImageJ are shown on the right. The cell outlines are delineated for quantitative analysis. (*Above*) Tendon sheath cells. (*Centre*) Tendon surface cells. (*Below*) Tendon core cells. Attachment is greatest for cells from the tendon core, and least for cells derived from the synovial sheath. Magnification x20.

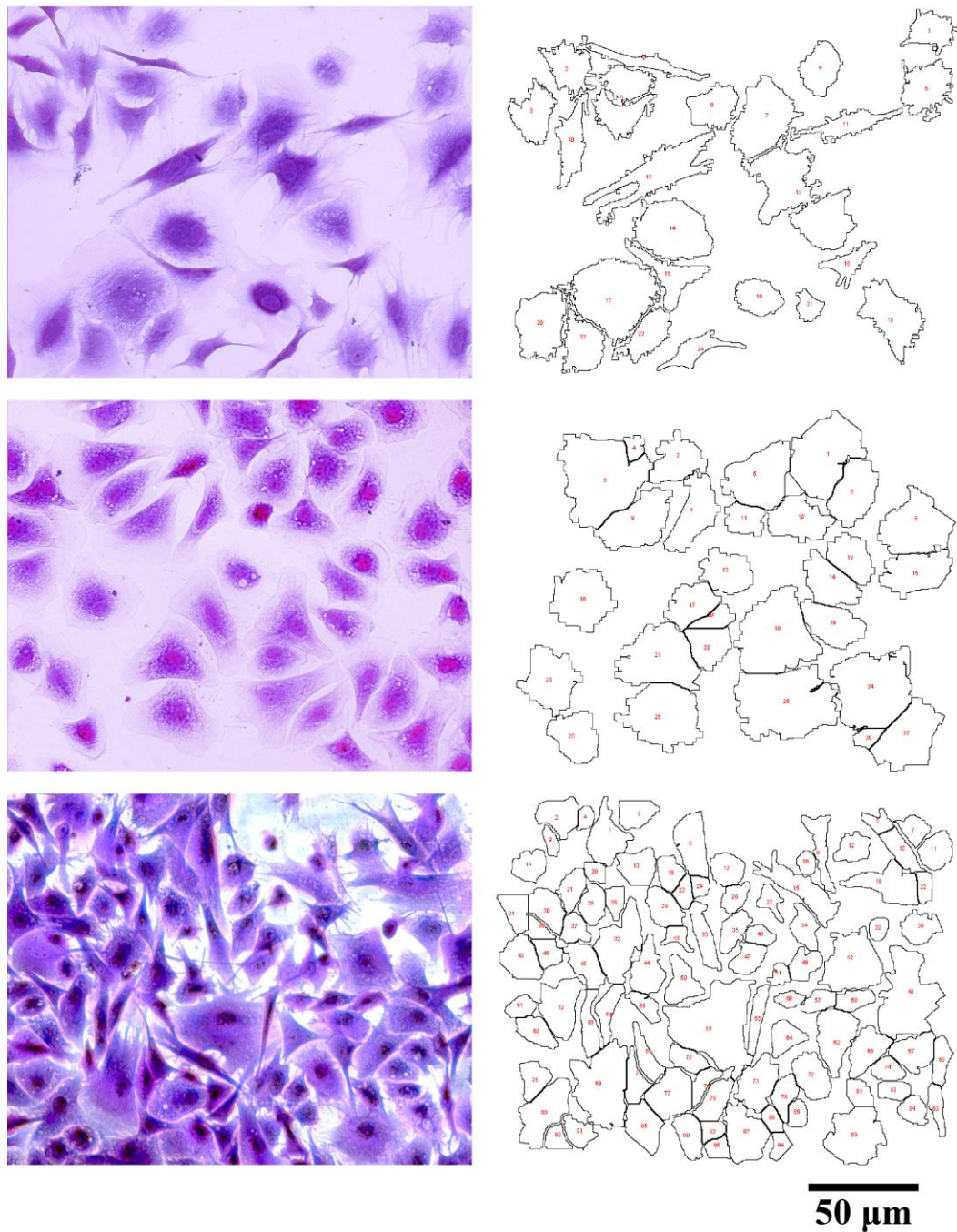


**Figure 6.2** Representative micrographs of tendon-synovial cell groups attached to Fn. Their processed images using ImageJ are shown on the right. (*Above*) Tendon sheath cells. (*Centre*) Tendon surface cells. (*Below*) Tendon core cells. Attachment is greatest for cells from the tendon core, and least for cells derived from the synovial sheath. Magnification x20.



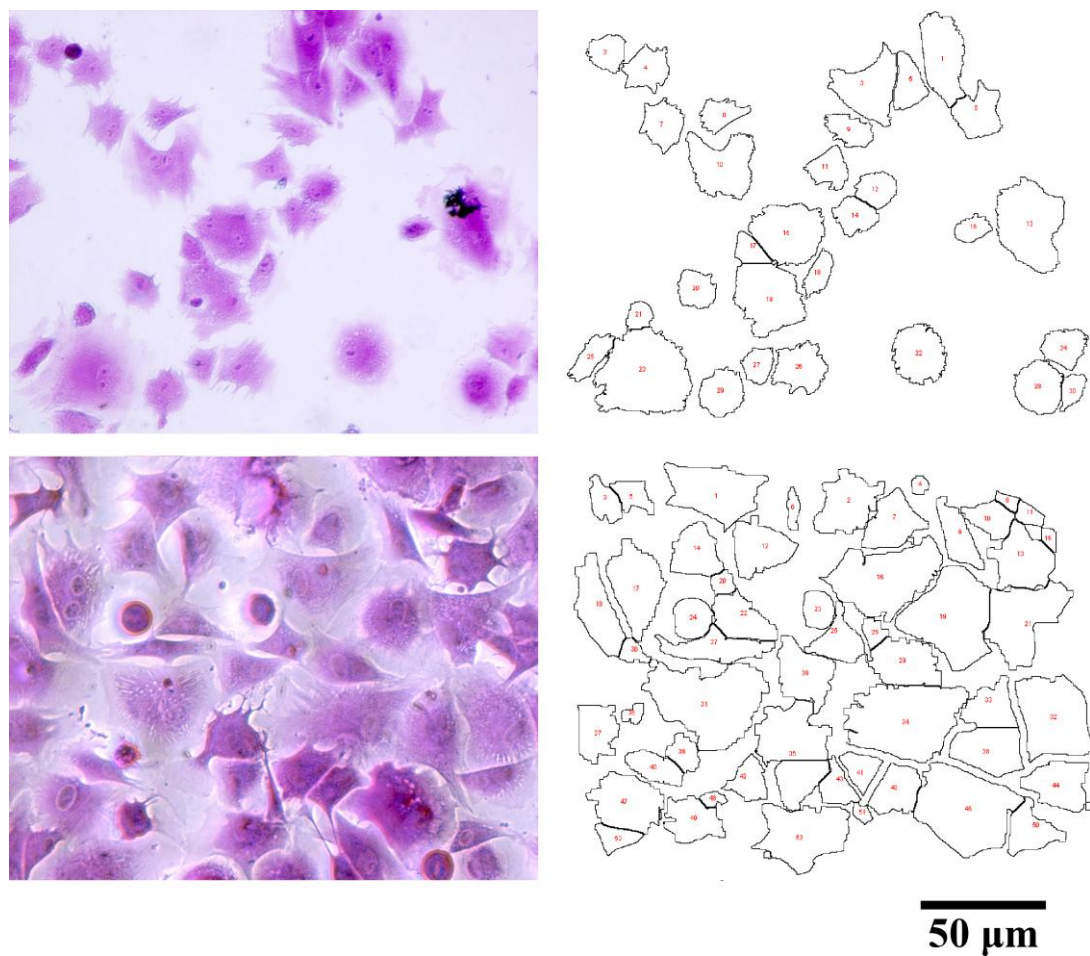


**Figure 6.3** Representative micrographs of adhesion cell groups attached to collagen type-I. Their processed images using ImageJ are shown on the right. (*Above*) Immobilised adhesion cells. (*Below*) Mobilised adhesion cells. Mobilisation increases cell attachment and increases the proportion of elongated cells. Magnification x20.

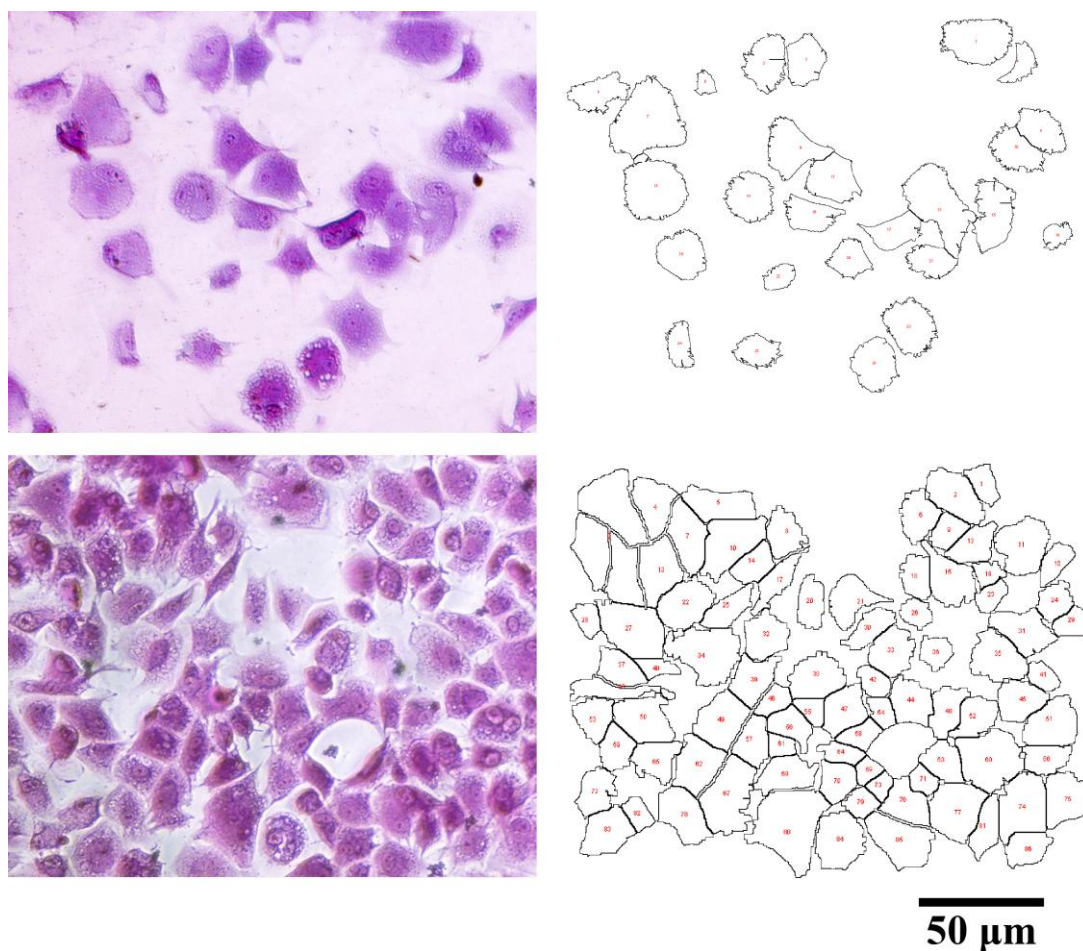


**Figure 6.4** Representative micrographs of adhesion cell groups attached to Fn. Their processed images using ImageJ are shown on the right. (*Above*) Immobilised adhesion cells. (*Below*) Mobilised adhesion cells. Mobilisation increases cell attachment and increases the proportion of elongated cells. Magnification x20.

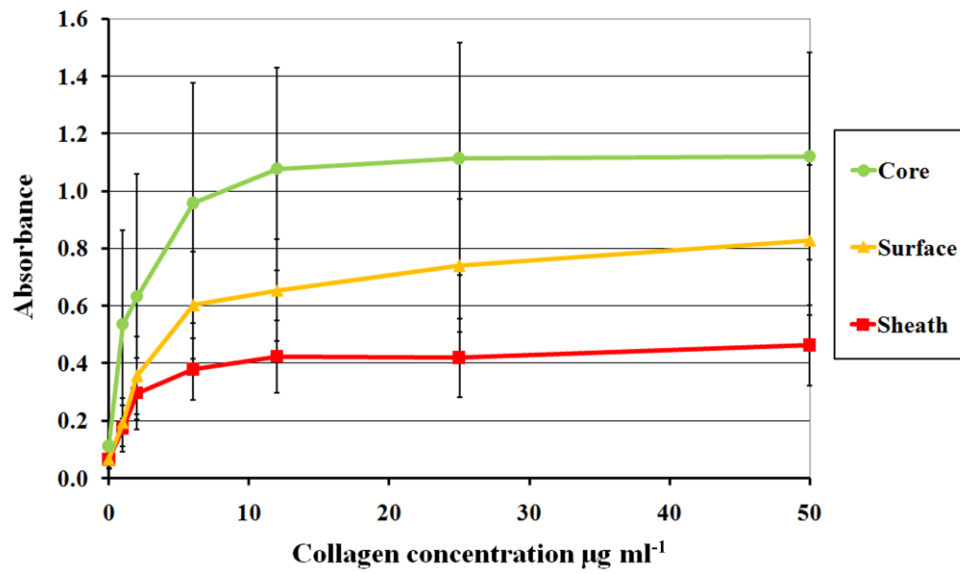


**Figure 6.5** Graph of attachment of tendon-synovial complex cell groups (all n=5) to collagen type-I. There was a statistically significant difference in cell attachment to collagen type-I among the different cell groups ( $p<0.001$ ). Error bars = SEM.

Conc. $\mu\text{g ml}^{-1}$ Cell Group	0	1	2	6	12	25	50
Core (n=5)	0.111	0.537	0.632	0.958	1.077	1.113	1.121
	$\pm$	$\pm$	$\pm$	$\pm$	$\pm$	$\pm$	$\pm$
	0.017	0.328	0.428	0.418	0.353	0.404	0.361
Surface (n=5)	0.067	0.194	0.358	0.603	0.654	0.740	0.829
	$\pm$	$\pm$	$\pm$	$\pm$	$\pm$	$\pm$	$\pm$
	0.033	0.084	0.134	0.186	0.177	0.232	0.260
Sheath (n=5)	0.065	0.174	0.296	0.379	0.424	0.419	0.463
	$\pm$	$\pm$	$\pm$	$\pm$	$\pm$	$\pm$	$\pm$
	0.027	0.081	0.125	0.108	0.125	0.137	0.140

**Table 6.1** Cell attachment for tendon-synovial complex cell groups to collagen type-I. Data are presented as mean absorbance ( $\pm$  SEM).

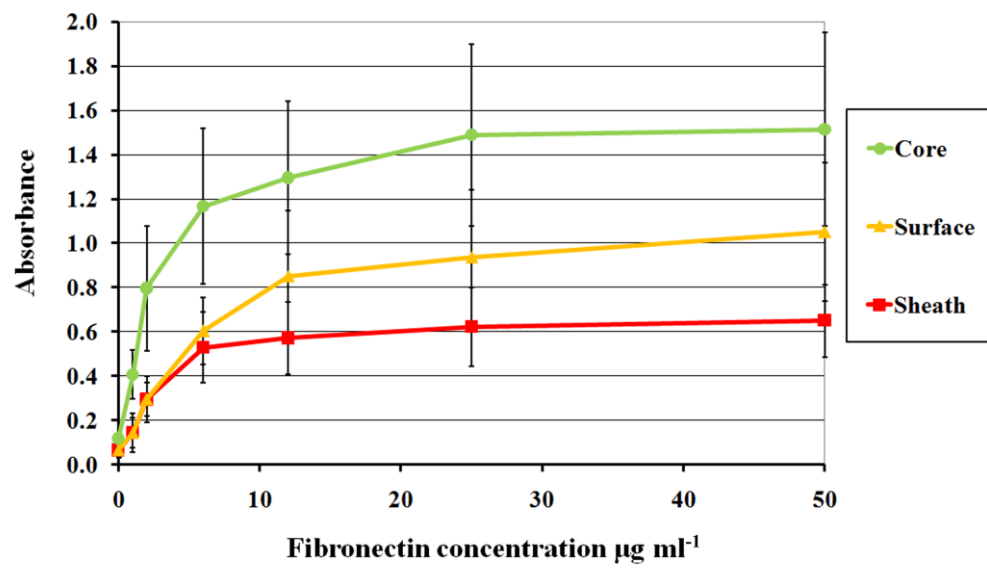


**Figure 6.6** Graph of attachment of tendon-synovial complex cell groups (all n=5) to Fn. There was a statistically significant difference in cell attachment to Fn among the different cell groups ( $p < 0.001$ ). Error bars = SEM.



Conc. $\mu\text{g ml}^{-1}$ Cell Group	0	1	2	6	12	25	50
Core (n=5)	0.117	0.406	0.796	1.167	1.295	1.488	1.514
	$\pm$	$\pm$	$\pm$	$\pm$	$\pm$	$\pm$	$\pm$
	0.017	0.111	0.281	0.351	0.346	0.411	0.438
Surface (n=5)	0.066	0.144	0.294	0.604	0.850	0.937	1.050
	$\pm$	$\pm$	$\pm$	$\pm$	$\pm$	$\pm$	$\pm$
	0.034	0.087	0.103	0.151	0.295	0.305	0.312
Sheath (n=5)	0.064	0.143	0.293	0.528	0.571	0.621	0.649
	$\pm$	$\pm$	$\pm$	$\pm$	$\pm$	$\pm$	$\pm$
	0.027	0.066	0.076	0.159	0.165	0.179	0.164

**Table 6.2** Cell attachment for tendon-synovial complex cell groups to Fn. Data are presented as mean absorbance ( $\pm$  SEM).

### **6.3.2 Morphological Assessment**

The morphology of the crystal violet cells was assessed after the cells had attached to collagen type I and Fn coated plates.

#### **6.3.2.1 Tendon-Synovial Complex Cell Groups**

Cell area (Table 6.5), cell perimeter (Table 6.6), cell circularity (Table 6.7) and percentage elongated morphology (Table 6.8) for each of the tendon core, tendon surface, and synovial sheath cell groups (all n=5) attached to collagen type-I and Fn are shown in Figure 6.9 and Figure 6.10, respectively. Comparing morphology data for the different cell groups attached to collagen type-I and Fn there were no statistically significant differences in cell area, cell perimeter, cell circularity or percentage of cells with an elongated morphology.

#### **6.3.2.2 Adhesion Cell Groups**

Cell area (Table 6.9), cell perimeter (Table 6.10), cell circularity (Table 6.11) and percentage elongated morphology (Table 6.12) for each of the mobilised and immobilised adhesion cell groups (all n=5) attached to collagen type-I and Fn are shown in Figure 6.11 and Figure 6.12, respectively.

For cells attached to collagen type-I, when compared to mobilised adhesion cells, immobilised adhesion cells had a 26% greater area ( $p=0.069$ ), a 6% greater perimeter ( $p=0.733$ ) and were 8% more circular ( $p=0.300$ ). Mobilised adhesions expressed 300% more cells with an elongated morphology relative to immobilised adhesions ( $p=0.004$ ), which was highly significant.

For cells attached to Fn, when compared to mobilised adhesion cells, immobilised adhesion cells had a 9% greater area ( $p=0.717$ ), a 1% greater perimeter ( $p=0.974$ ) and were 6% 'more circular' ( $p=0.440$ ). Mobilised adhesions had 68% more cells with elongated morphology relative to immobilised adhesions ( $p=0.046$ ) when attached to Fn.

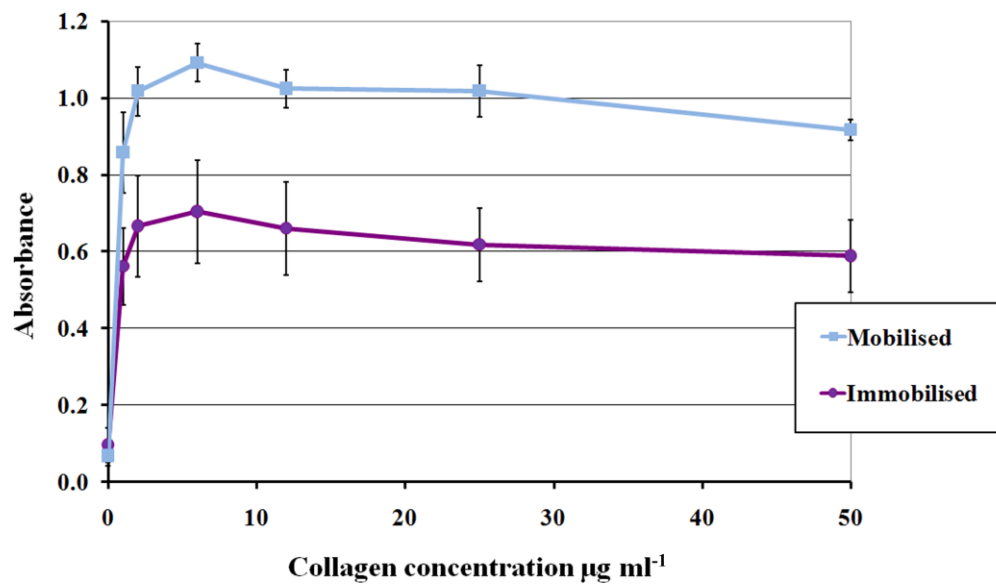


**Figure 6.7** Graph of attachment of mobilised and immobilised adhesion cell groups (all n=5) to collagen type-I. There was a statistically significant difference in cell attachment to collagen type-I between the 2 cell groups ( $p < 0.001$ ). Error bars = SEM.

Conc. $\mu\text{g ml}^{-1}$ Cell Group	0	1	2	6	12	25	50
<b>Mobilised</b>  <b>(n=5)</b>	0.068	0.858	1.017	1.092	1.024	1.018	0.916
	$\pm$	$\pm$	$\pm$	$\pm$	$\pm$	$\pm$	$\pm$
	0.026	0.105	0.064	0.049	0.050	0.067	0.028
<b>Immobilised</b>  <b>(n=5)</b>	0.096	0.561	0.666	0.704	0.661	0.618	0.588
	$\pm$	$\pm$	$\pm$	$\pm$	$\pm$	$\pm$	$\pm$
	0.044	0.101	0.132	0.135	0.121	0.094	0.094

**Table 6.3** Cell attachment for mobilised and immobilised adhesion cell groups to collagen type-I. Data are presented as mean absorbance ( $\pm$  SEM).

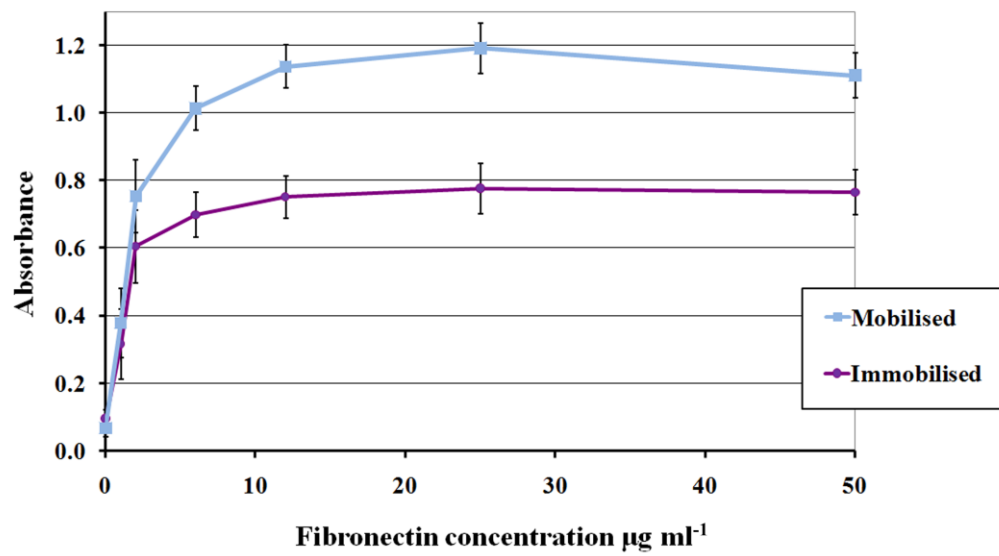


**Figure 6.8** Graph of attachment of mobilised and immobilised adhesion cell groups (all  $n=5$ ) to Fn. There was a statistically significant difference in cell attachment to Fn between the 2 cell groups ( $p<0.001$ ). Error bars = SEM.

Conc. $\mu\text{g ml}^{-1}$ Cell Group	0	1	2	6	12	25	50
<b>Mobilised</b>  <b>(n=5)</b>	0.068 $\pm$ 0.026	0.378 $\pm$ 0.103	0.754 $\pm$ 0.064	1.013 $\pm$ 0.049	1.137 $\pm$ 0.050	1.192 $\pm$ 0.067	1.111 $\pm$ 0.028
<b>Immobilised</b>  <b>(n=5)</b>	0.096 $\pm$ 0.026	0.316 $\pm$ 0.103	0.605 $\pm$ 0.108	0.699 $\pm$ 0.065	0.751 $\pm$ 0.063	0.777 $\pm$ 0.074	0.765 $\pm$ 0.066

**Table 6.4** Cell attachment for mobilised and immobilised adhesion cell groups to Fn. Data are presented as mean absorbance ( $\pm$  SEM).

<b>Cell Area (<math>\mu\text{m}^2</math>)</b>	<b>Core (n=5)</b>	<b>Surface (n=5)</b>	<b>Sheath (n=5)</b>
<b>Collagen type-I</b>	513.7 $\pm$ 54.3	433.1 $\pm$ 68.2	408.7 $\pm$ 94.5
<b>Fibronectin</b>	825.5 $\pm$ 222.7	1017.4 $\pm$ 347.7	629.8 $\pm$ 113.7

**Table 6.5** Cell area for tendon-synovial complex cell groups attached to collagen type-I and Fn. Values are expressed as mean cell area ( $\pm$  SEM).



<b>Cell Perimeter (μm)</b>	<b>Core (n=5)</b>	<b>Surface (n=5)</b>	<b>Sheath (n=5)</b>
<b>Collagen type-I</b>	101.5 ± 7.8	92.2 ± 9.4	91.7 ± 13.4
<b>Fibronectin</b>	135.5 ± 23.7	135.6 ± 21.0	116.3 ± 14.9

**Table 6.6** Cell perimeter for tendon-synovial complex cell groups attached to collagen type-I and Fn. Values are expressed as mean cell perimeter (± SEM).

<b>Cell Circularity</b>	<b>Core (n=5)</b>	<b>Surface (n=5)</b>	<b>Sheath (n=5)</b>
<b>Collagen type-I</b>	0.569 $\pm$ 0.034	0.618 $\pm$ 0.029	0.614 $\pm$ 0.044
<b>Fibronectin</b>	0.527 $\pm$ 0.034	0.577 $\pm$ 0.037	0.578 $\pm$ 0.044

**Table 6.7** Cell circularity for tendon-synovial complex cell groups attached to collagen type-I and Fn. Values are expressed as mean cell circularity ( $\pm$  SEM).

<b>Percentage Elongated Morphology (%)</b>	<b>Core (n=5)</b>	<b>Surface (n=5)</b>	<b>Sheath (n=5)</b>
<b>Collagen type-I</b>	14.7 ± 4.9	15.6 ± 4.5	22.2 ± 5.4
<b>Fibronectin</b>	24.1 ± 5.2	12.3 ± 2.3	37.6 ± 7.4

**Table 6.8** Percentage elongated morphology for tendon-synovial complex cell groups attached to collagen type-I and Fn. Values are expressed as mean percentage elongated morphology ( $\pm$  SEM).

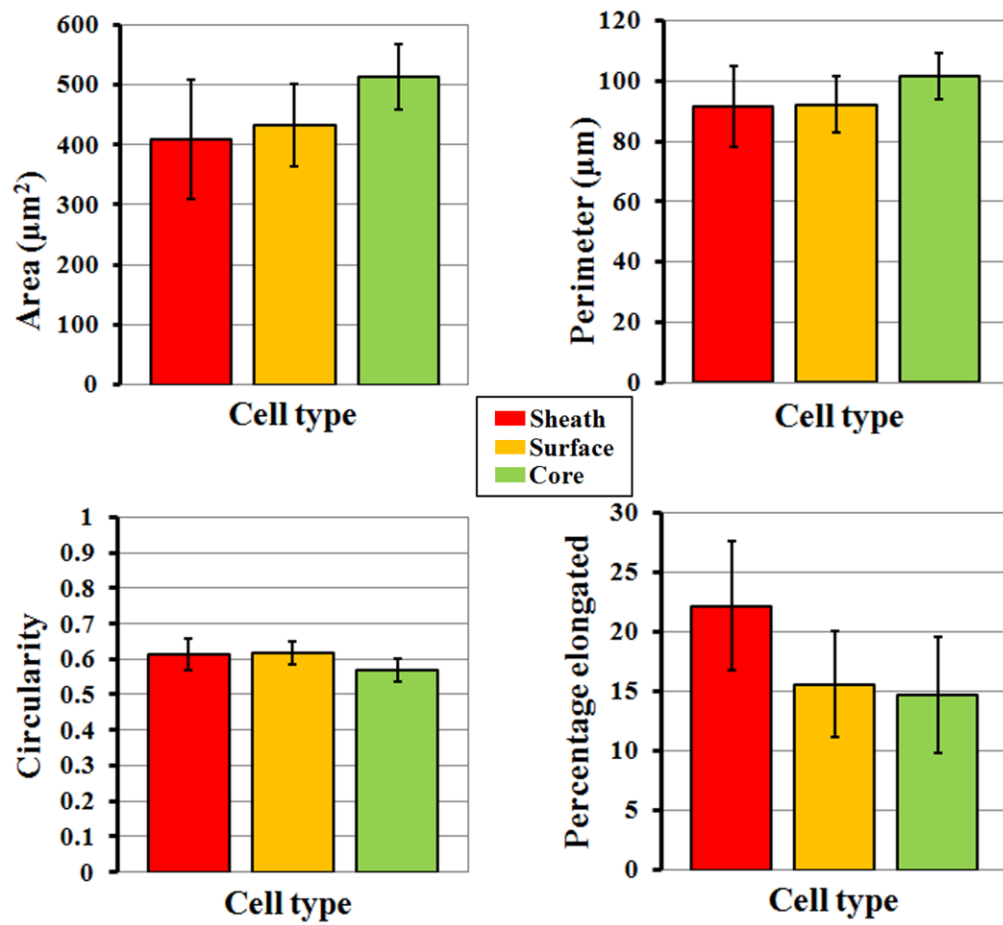


**Figure 6.9** Graphs of morphology of cells attached to collagen type-I. Results are shown for tendon core, tendon surface, and synovial sheath cell groups (all n=5). *(Above left)* Cell area. *(Above right)* Cell perimeter. *(Below left)* Cell circularity. *(Below right)* Percentage elongated morphology. Error bars = SEM.

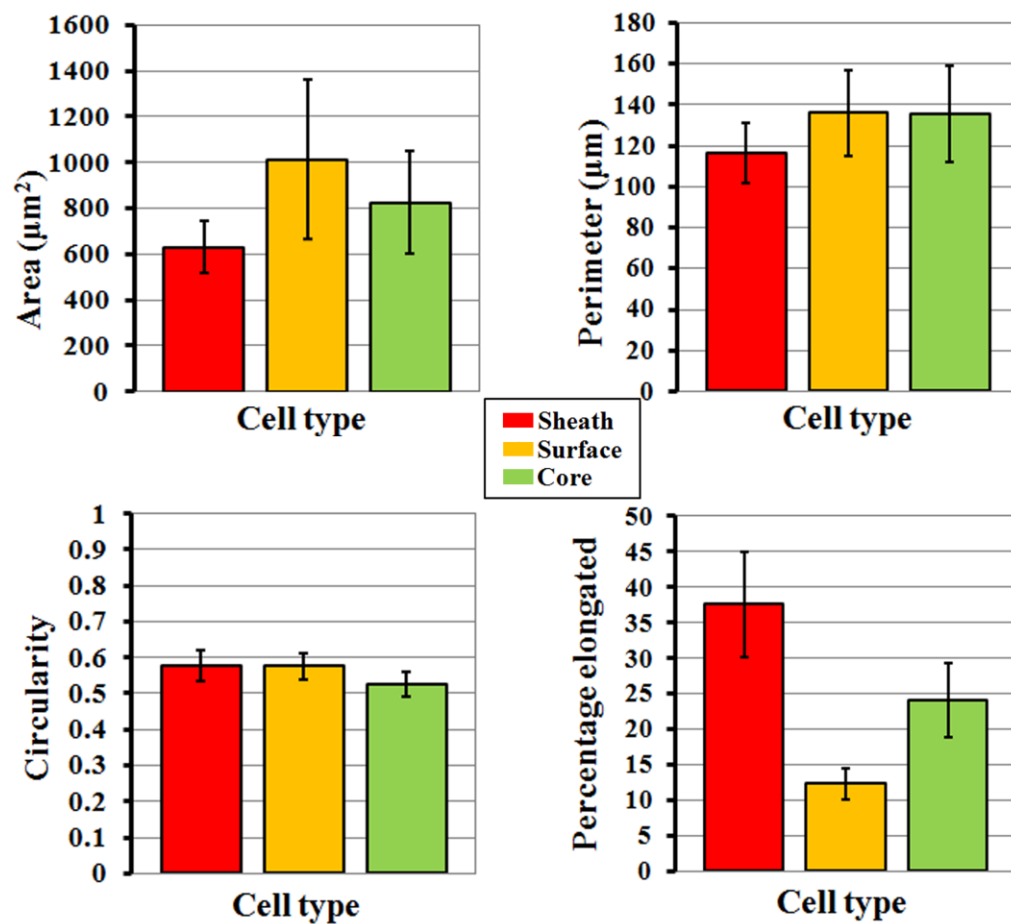


**Figure 6.10** Graphs of morphology of cells attached to Fn. Results are shown for tendon core, tendon surface, and synovial sheath cell groups (all n=5). (*Above left*) Cell area. (*Above right*) Cell perimeter. (*Below left*) Cell circularity. (*Below right*) Percentage elongated morphology. Error bars = SEM.

<b>Cell Area (<math>\mu\text{m}^2</math>)</b>	<b>Immobilised Adhesion (n=5)</b>	<b>Mobilised Adhesion (n=5)</b>
<b>Collagen type-I</b>	286.0 $\pm$ 54.3	226.1 $\pm$ 40.4
<b>Fibronectin</b>	362.5 $\pm$ 58.3	334.1 $\pm$ 48.2

**Table 6.9** Cell area for mobilised and immobilised adhesion cell groups attached to collagen type-I and Fn. Values are expressed as mean cell area ( $\pm$  SEM).

<b>Cell Perimeter (<math>\mu\text{m}</math>)</b>	<b>Immobilised Adhesion (n=5)</b>	<b>Mobilised Adhesion (n=5)</b>
<b>Collagen type-I</b>	71.3 $\pm$ 7.8	67.5 $\pm$ 7.0
<b>Fibronectin</b>	83.4 $\pm$ 8.7	82.4 $\pm$ 6.4

**Table 6.10** Cell perimeter for mobilised and immobilised adhesion cell groups attached to collagen type-I and Fn. Values are expressed as mean cell perimeter ( $\pm$  SEM).

<b>Cell Circularity</b>	<b>Immobilised Adhesion (n=5)</b>	<b>Mobilised Adhesion (n=5)</b>
<b>Collagen type-I</b>	0.665 ± 0.034	0.615 ± 0.029
<b>Fibronectin</b>	0.627 ± 0.031	0.593 ± 0.028

**Table 6.11** Cell circularity for mobilised and immobilised adhesion cell groups attached to collagen type-I and Fn. Values are expressed as mean cell circularity ( $\pm$  SEM).



<b>Percentage Elongated Morphology (%)</b>	<b>Immobilised Adhesion (n=5)</b>	<b>Mobilised Adhesion (n=5)</b>
<b>Collagen type-I</b>	10.4 ± 2.6	41.6 ± 7.3
<b>Fibronectin</b>	24.8 ± 5.5	41.6 ± 1.5

**Table 6.12** Percentage elongated morphology for mobilised and immobilised adhesion cell groups attached to collagen type-I and Fn. Values are expressed as mean percentage elongated morphology ( $\pm$  SEM).

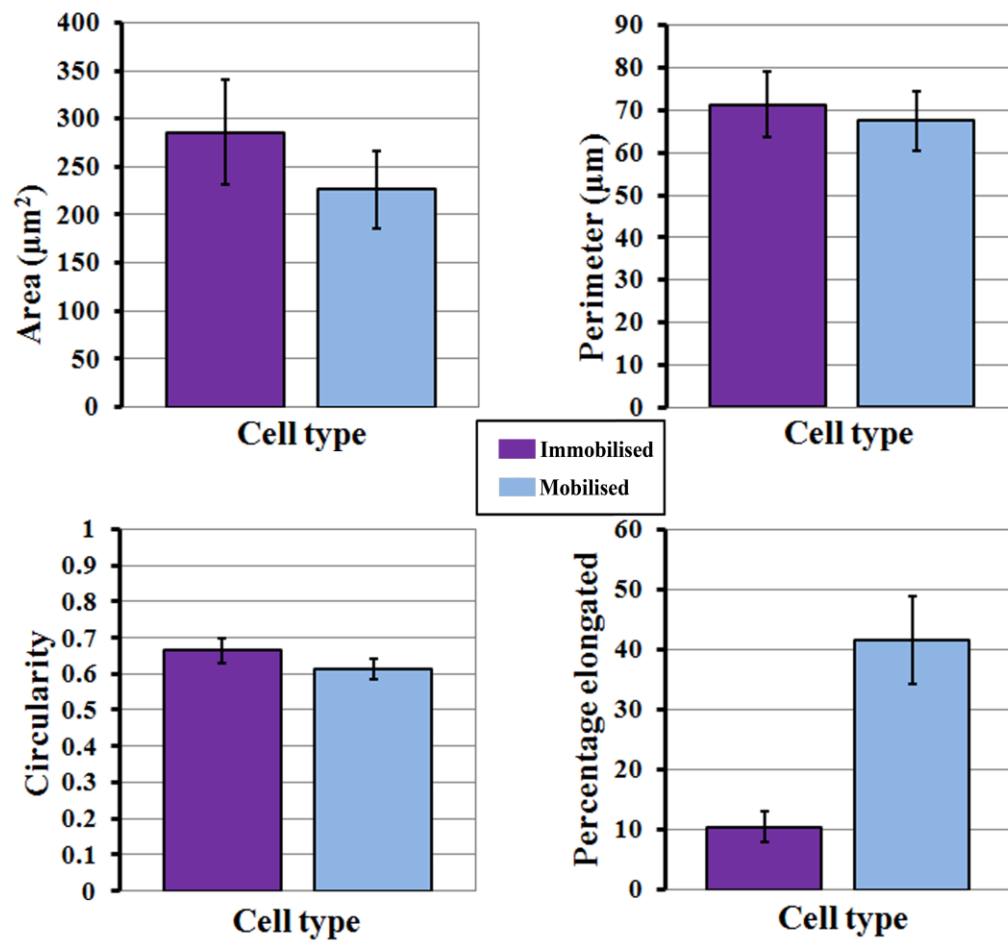


**Figure 6.11** Graphs of morphology of cells attached to collagen type-I. Results are shown for mobilised and immobilised adhesion cell groups (all  $n=5$ ). (*Above left*) Cell area. (*Above right*) Cell perimeter. (*Below left*) Cell circularity. (*Below right*) Percentage elongated morphology. Mobilised adhesions expressed significantly more cells with an elongated morphology relative to immobilised adhesions ( $p=0.004$ ). Error bars = SEM.

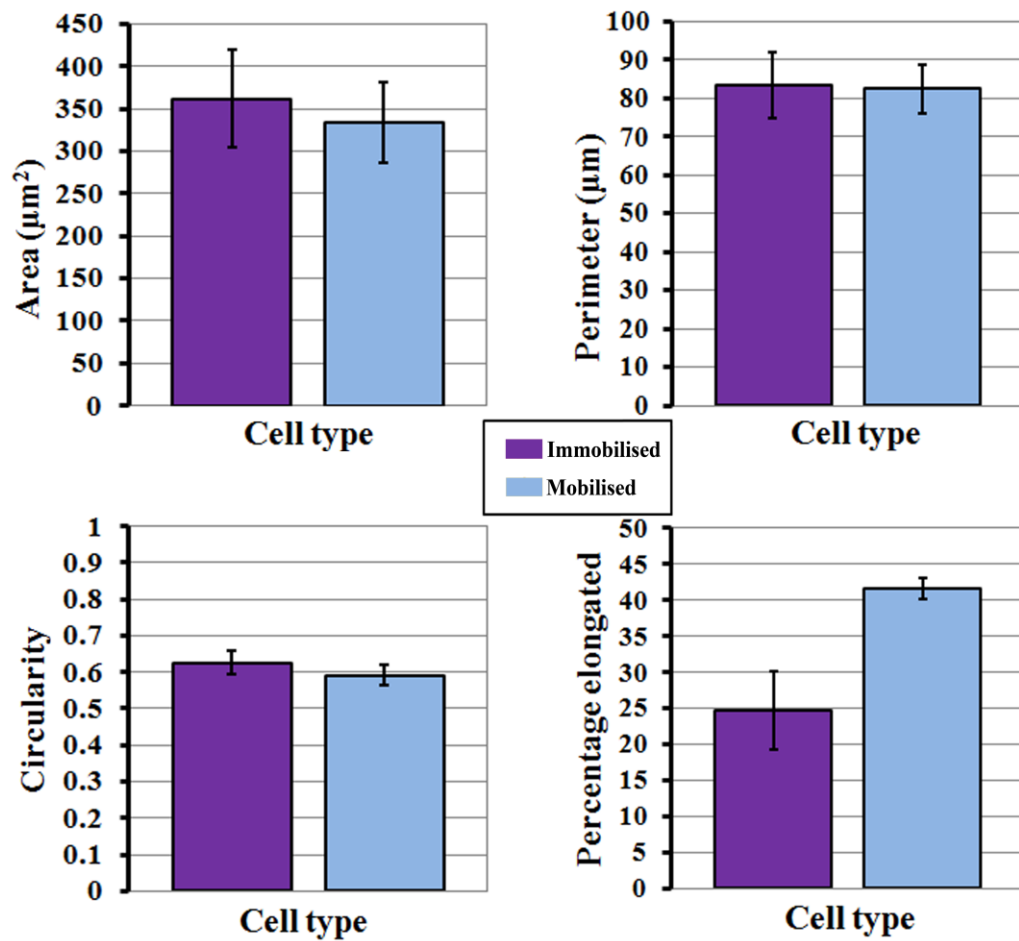


**Figure 6.12** Graphs of morphology of cells attached to Fn. (*Above left*) Cell area. (*Above right*) Cell perimeter. (*Below left*) Cell circularity. (*Below right*) Percentage elongated morphology for mobilised and immobilised adhesion cell groups (all n=5). Mobilised adhesions expressed significantly more cells with an elongated morphology relative to immobilised adhesions (p=0.046). Error bars = SEM.

## **6.4 DISCUSSION**

### **6.4.1 Selectivity in Tendon Healing**

Various strategies to modify flexor tendon adhesion formation have previously been investigated. These may be categorised as either biochemical agents (for example non steroidal anti-inflammatory agents, 5-fluorouracil, and mannose-6-phosphate) (Bates, Morrow et al. 2006; Zhao, Zobitz et al. 2009; Tan, Nourbakhsh et al. 2010) or physical barriers (such as polytetrafluoroethylene, ADCON®, and phospholipid polymer hydrogel) (Hanff and Hagberg 1998; Golash, Kay et al. 2003; Ishiyama, Moro et al. 2010). However, no ideal treatment exists at present and none are used routinely following tendon repair. The difficulty with this clinical problem lies in how to selectively favour intrinsic tendon healing, in order to reduce the risk of tendon rupture, while reducing the formation of restrictive adhesions (Lin, Cardenas et al. 2004). The treatment strategies previously described are not specific in selecting for cells of a particular origin. The results of Chapters 2 and 3 have demonstrated, that using a novel biomaterial that appears to reduce cell attachment, it may be possible to target postsurgical adhesions without compromising tendon cellularity (Branford, Mudera et al. 2008; Branford, Brown et al. 2010).

This investigation adopted a quantitative scientific approach to examine the attachment of the different cellular components of the tendon-synovial complex and adhesions to collagen type-I and Fn. There were two aims to this investigation. Firstly, to determine if there is a difference in cell attachment between the cells of different origins from within the digital tendon-synovial complex to collagen and Fn. Secondly, to determine if mobilisation has an effect on the attachment of cells contributing to tendon adhesion formation. Crystal violet based attachment assays

and quantitative morphometric analyses of cell size and shape using image analysis software were employed.

#### **6.4.2      Intrinsic Cells Show Greater Attachment to Collagen and Fibronectin**

The attachment of intrinsic tendon cells (tendon core cells and tendon surface cells) was statistically significantly higher than that of extrinsic tendon cells (synovial sheath cells). This was the case for attachment to both collagen type-I and Fn, at all concentrations tested. This difference in attachment was not reflected in changes in cell morphology with regard to cell area, perimeter or percentage of cells with an elongated or circular morphology on either collagen type-I or Fn.

Wong and colleagues have also shown that the greatest activity following tendon injury occurs in the tissues surrounding the tendons (Wong, Lui et al. 2009). The flexor tendon synovial sheath demonstrates a vigorous inflammatory response post-injury to the flexor tendon (Khan, Edwards et al. 1996). Cell proliferation in response to injury is greater within the synovial sheath than within the tendon itself (Kakar, Khan et al. 1998). Previous studies suggest that synovial sheath fibroblasts contribute actively to adhesion formation (Brigman, Hu et al. 1994; Khan, Edwards et al. 1996; Khan, Occleston et al. 1997; Kakar, Khan et al. 1998; Klein, Pham et al. 2001; Ragoowansi, Khan et al. 2003). This is the result of their high proliferative level, their capacity to degrade the ECM (facilitating the process of cell migration), and their ability to contract a collagen lattice. In the present study, the cells that have previously been recognised as being the most aggressively adhesion forming cells, (that is the synovial sheath fibroblasts), expressed lowest attachment to both collagen

type-I and Fn. Khan and colleagues demonstrated that synovial sheath fibroblasts are more active migrators than tendon fibroblasts (Khan, Occleston et al. 1998). Cell migration is regulated through cell-substratum adhesive interactions. Although cell attachment is a prerequisite for migration (van der Flier and Sonnenberg 2001), at high adhesiveness forces are insufficient to break cell-substratum attachments, leaving cells incapable of locomotion (Huttenlocher, Sandborg et al. 1995). At lower adhesiveness cytoskeletal forces are roughly in balance with adhesion so that traction can be maintained at the cell front while it can be disrupted at the cell rear (DiMilla, Stone et al. 1993). This permits net cell body movement. The synovial sheath cells, being more active migrators, therefore show lower attachment than tendon cells. The implication of the results of this Chapter are that as the synovial sheath cells are the least avidly attached, then the prevention of the attachment of these cells may therefore be a suitable selective biological therapeutic target.

The results of this investigation confirm the results of a previous study where tendon synovial sheath fibroblasts had a lower attachment efficiency than did tendon cells (Riederer-Henderson, Gauger et al. 1983). However, the authors examined attachment to tissue culture plastic and not to ECM proteins. The study did not examine all the components of the tendon-synovial complex and did not assess adhesion cells or the effect of mobilisation on cell phenotype. However, such studies augment existing data that not all fibroblasts have identical phenotypes. The variation in phenotypic expression of tendon-synovial complex fibroblasts has not been extensively investigated, and this information may prove useful for optimising repair strategies (Sharma and Maffulli 2005).

### **6.4.3 Mobilisation Increases Cell Attachment and Favours Elongated Cellular Morphology**

The effect of mobilisation on tendon healing is well documented: adhesions are reduced and tendon tensile properties are enhanced (Gelberman, Woo et al. 1982; Gelberman, Manske et al. 1986; Kubota, Manske et al. 1996). Mobilisation may result in increased cellular activity, collagen and glycosaminoglycan content in tendons, whereas immobilisation may cause increased collagen degradation and a reduction in proline and sulphate incorporation (Gelberman, Amiel et al. 1981; Amiel, Woo et al. 1982; Gelberman, Woo et al. 1982; Woo, Gomez et al. 1982; Vailas, Pedrini et al. 1985; Gelberman, Manske et al. 1986; Hannafin, Arnoczky et al. 1995; Kubota, Manske et al. 1996; Yasuda and Hayashi 1999). However, the effect of mobilisation on cell attachment has not been previously investigated.

The results of this investigation have shown that the attachment of cells derived from mobilised adhesions was statistically significantly higher than that of cells derived from immobilised adhesions. This was seen for attachment to both collagen type-I and Fn, at all concentrations tested. Mobilised adhesion cells expressed a statistically significantly greater percentage of elongated cells to both collagen type-I and Fn than did immobilised adhesion cells. When compared with cells derived from mobilised adhesions, immobilised adhesion cells had a 26% and 9% greater area when attached to collagen type-I and Fn respectively. Although these differences were not statistically significant, they approached significance for collagen type-I. Synovial sheath fibroblasts have previously been shown to be larger than tendon cells (Ragoowansi, Khan et al. 2003). The results from the present investigation appear to confirm that synovial sheath cells contribute disproportionately to

adhesions, and therefore tendon healing, when digits are immobilised, as demonstrated by the larger size and poorer attachment of the adhesion cells. Conversely, intrinsic cells appear to be favoured in mobilised adhesions, where cells were smaller, more elongated and showed higher attachment.

Previous studies have shown that cell attachment and morphology is related to cell fate, gene expression and protein production, implying cell shape-based regulation of cellular function (Singhvi, Kumar et al. 1994; McBeath, Pirone et al. 2004; Lee, Jones et al. 2006). Li and colleagues have shown that elongated human tendon cells expressed 65% higher collagen type-I than circular cells with the same cell area (Li, Li et al. 2008). The authors proposed that this indicated that tendon cells *in vivo*, which assume an elongated shape in normal tendons, have an “optimal shape” to perform their major function, that is, to synthesise collagen type-I. By producing collagen type-I, tendon cells *in vivo* function to maintain, repair and remodel the tendon matrix (Yang, Crawford et al. 2004). Li and colleagues demonstrated that elongated cells have focal adhesions that were concentrated at their two ends. They also showed that in circular cells focal adhesions were uniformly distributed along the circumference of the cell (Li, Li et al. 2008). The observation that cell shape determines the distribution of focal adhesion complex formation may explain why these elongated tendon cells produce aligned collagen matrix *in vitro* and *in vivo* (Wang, Jia et al. 2003; Li, Li et al. 2008). The results from this Chapter have shown that mobilisation favours the formation of elongated cells, which may explain why mobilised tendons demonstrate improved tensile properties.



#### **6.4.4 A New Therapeutic Strategy: Selectively Preventing Extrinsic Cell Attachment to Fibronectin**

Previous studies suggest that tendon synovial sheath cells secrete Fn, in contrast to tendon fibroblasts (Banes, Link et al. 1988; Brigman, Hu et al. 1994). Conversely, synovial sheath cells produce less collagen than do tendon cells (Riederer-Henderson, Gauger et al. 1983). Therefore, there appears to be a gradient from a Fn rich to a collagen rich environment from the synovial sheath to the tendon itself. Berglund and colleagues have identified spatial and temporal-specific aspects to the healing process in a rabbit flexor tendon injury model (Berglund, Reno et al. 2006), supporting this concept. It may be proposed that preventing attachment of poorly adherent extrinsic cells to Fn may be a suitable target for selective inhibition within the tendon healing complex. This may explain the results of Chapter 4 that demonstrated significant reduction in the restrictive nature of postsurgical adhesions following treatment without compromising tendon cellularity (Branford, Mudera et al. 2008). As demonstrated in Chapter 3, this was achieved using a biomaterial that appears to prevent the attachment of fibroblasts to Fn (Branford, Brown et al. 2010).

#### **6.4.5 Summary**

Flexor tendon adhesion formation continues to be a significant and unsolved problem. Other than by using rehabilitative regimes, the selection of intrinsic tendon healing over extrinsic tendon healing has escaped previous therapeutic strategies. This is the first study to demonstrate that attachment of intrinsic tendon cells and mobilised adhesion cells is significantly higher to both collagen type-I and Fn than their respective extrinsic tendon cell and immobilised adhesion counterparts. Mobilised adhesion cells expressed a statistically significantly greater percentage of

elongated type cells attached to both collagen type-I and Fn than did mobilised adhesion cells. This study suggests that the differential avidity of cell attachment within the healing tendon-synovial complex is a potential therapeutic target when developing novel anti-adhesive strategies. It may be proposed that this approach may favour intrinsic cell contributions to tendon healing while minimising extrinsic tendon cell contributions. This may ultimately reduce formation of restrictive adhesions without compromising tendon healing. The model developed allows for a robust basis with which to assess the efficacy of potential anti-adhesion strategies in differentially affecting cell attachment. Novel treatments may be introduced into this system by topical application over the protein coated plates before the cells are seeded.

# **CHAPTER 7**

## **DISCUSSION**

### **7.1 INTRODUCTION**

### **7.2 MAJOR FINDINGS AND CRITIQUE OF METHODOLOGIES**

#### **7.2.1 Shear-Aggregated Fibronectin with Anti-Adhesive Properties**

#### **7.2.2 A Novel Biomimetic Material for Engineering Postsurgical Adhesion in the Injured Digital Flexor Tendon**

#### **7.2.3 Relating Structure to Hierarchical Mechanics of Immobilised and Mobilised Flexor Tendon Adhesions**

#### **7.2.4 The Attachment of Intrinsic and Extrinsic Tendon Cells and Adhesion Cells to Collagen and Fibronectin**

### **7.3 NOVEL APPROACHES TO THE ASSESSMENT AND STRATEGIC MODIFICATION OF FLEXOR TENDON ADHESION FORMATION**

#### **7.3.1 Assessment of Adhesions**

#### **7.3.2 Modification of Adhesions**

### **7.4 FUTURE WORK**

### **7.5 GENERAL SUMMARY**

## **7.1 INTRODUCTION**

Despite adhesion formation being a significant problem in reconstructive hand surgery, there were currently no anti-adhesive treatments in widespread clinical use at the time of commencing this thesis (Strickland 2005). Mobilisation of injured flexor tendons remains the only clinically useful method to produce improved tendon healing and reduced adhesion formation (Woo, Gelberman et al. 1981; Gelberman, Vande Berg et al. 1983; Gelberman, Manske et al. 1986; Hitchcock, Light et al. 1987; Feehan and Beauchene 1990; Khanna, Gougoulis et al. 2009). Although cyclical strain applied to cultured tendon cells can enhance cell proliferation and extracellular matrix (ECM) production (Riboh, Chong et al. 2008), the precise mechanism for how adhesions are modified by mobilisation is unknown. Treatments are required that mimic, complement and augment the beneficial effects of mobilisation. Protein based biomaterials demonstrate ability to guide cell and tissue behaviour during healing as a function of the complex interplay that exists between their mechanical and bioactive properties (Maskarinec and Tirrell 2005; Brown and Phillips 2007). Precisely through the selectivity in their effects, protein biomaterials may provide a solution to the almost ubiquitous drawback of many anti-adhesive strategies: that dampening the adhesion response results in reduced healing at the tendon injury site.

## **7.2 MAJOR FINDINGS AND CRITIQUE OF METHODOLOGIES**

A novel micromechanical assessment technique was developed in this thesis to examine the effect of mobilisation on tendon adhesions. Tissue organisation and local strain responses produced to applied strain were examined. These findings were related to gross restrictive parameters. The effect of mobilisation on the attachment of adhesion cells to the ECM has not previously been investigated and is assessed in this thesis. The attachment of intrinsic and extrinsic tendon cells to components of the ECM was also assessed. A novel derivative fibronectin biomaterial (DFn) with anti-adhesive effects was tested for its effects on cell attachment *in vitro* and in reducing restrictive adhesion, while preserving tendon surface cellularity, *in vivo*.

A rabbit flexor tendon-synovial complex injury model was used in this thesis. The use of human tendons was precluded from study due to their limited availability and the poor quality of surgically removed specimens. In humans, fresh specimens are often traumatised or degenerative. The rabbit model is comparable to man both in terms of cellular behaviour during healing and structural anatomy. The deep flexors of the forepaw were chosen over the hindpaw due to their accessibility and to their being functionally closer to human hand tendons (Jones, Ladhani et al. 2000; Ngo, Pham et al. 2001; Harrison, Jones et al. 2003; Henn, Kuo et al. 2010; Tan, Nourbakhsh et al. 2010). A partial tenotomy window was used as it avoids the need for suture repair, thereby minimising the number of injury variables (Kubota, Manske et al. 1996; Chan, Fu et al. 1998; Jones, Mudera et al. 2003). This injury also conveniently allows for immediate postoperative mobilisation. Where required, immobilisation was achieved using a proximal division of the flexor digitorum

profundus (FDP) tendon as in a previous flexor tendon adhesion model (Jones, Burnett et al. 2002).

### **7.2.1 Shear-Aggregated Fibronectin with Anti-Adhesive Properties**

The investigation of the novel DFn biomaterial *in vitro* has shown that it biodegrades to provide a prolonged delivery of anti-adhesive factors, preventing the attachment of adhesion forming synovial sheath fibroblasts (Branford, Brown et al. 2010). The qualitative and quantitative assessments of the biomaterial indicate that anti-adhesive fibronectin (Fn) fragments are responsible for this effect. This may be the result of a conformational change in the protein during production, resulting from preparation of the mats using urea, or proteolytic cleavage of the Fn molecule resulting from proteases present in the cryoprecipitate source material. It is not clear from the results of this investigation whether the protein fragments were causing inhibition by acting in a competitive or non-competitive way. However, if the effect is due to competitive binding by dissolved Fn fragments the anti-adhesive effect will only exert its effect while the DFn biomaterial is still dissolving. Time lapse studies confirmed that synovial sheath fibroblasts did not adhere to the material. The DFn biomaterial did not cause cell death indicating that it is unlikely to impair healing in the adjacent tendon *in vivo*. These findings support the idea that DFn biomaterial may be used to prevent adhesion formation at tissue interfaces as a bioactive mechanical barrier.

Myofibroblasts were not seen following culture on either DFn or Fn control biomaterials. This may be due to suppression of myofibroblastic conversion by Fn-

derived peptides (Kato, Kamiya et al. 2001). Alternatively, this finding may be because the biomaterial surfaces are less stiff than plain glass, with an associated lower tension cell-environment, removing one of the stimulating factors in myofibroblast differentiation (Tomasek *et al.*, 2002). However, longer time frames need to be examined to determine if there is an increase in myofibroblastic conversion over time in culture on DF<sub>n</sub>.

### **7.2.2 A Novel Biomimetic Material for Engineering Postsurgical Adhesion in the Injured Digital Flexor Tendon**

The *in vivo* investigation into the effects of the DF<sub>n</sub> biomaterial showed a significant reduction in adhesion strength following treatment (Figure 4.1). The mean peak force required to overcome adhesions was reduced from 7.7 Newtons (N) to 0.3 N (Figure 4.2). The mean structural stiffness was reduced from 628 N m<sup>-1</sup> to 40 N m<sup>-1</sup>. There was a 55% fall in the cellularity at the surface of the adhesions (Figure 4.5), which was also reflected in the pattern of cell proliferation. Importantly, the cellularity of the tendon surface was not reduced as a result of treatment. Treated tendons were significantly more cellular than their untreated counterparts deeper within their substance. The tensile strength of the tendons themselves was not examined directly as this would have required a doubling of the number of animals used in the study. Further, this study was primarily assessing adhesion strength. However, none of the treated tendons ruptured during testing.

The DF<sub>n</sub> material had suitable mechanical properties allowing it to be handled and inserted into a wound *in vivo* for surgical application (Underwood, Afoke et al. 2001; Branford, Mudera et al. 2008). However, only 2 out of 7 DF<sub>n</sub> treated tendons had

any macroscopic evidence of the material at 14 days. The biodegradability of the material is likely to be an advantage, reducing the risk of stimulating further inflammation and adhesion formation.

Although the biomaterial was only tested in a partial tenotomy model where tendons did not require suture, it is likely that the material will be effective in sutured transected tendon injuries. The increased inflammatory cascade as a result of suturing may be targeted by the material's cellular effects, with dampening of the adhesion surface cellular response.

### **7.2.3 Relating Structure to Hierarchical Mechanics of Immobilised and Mobilised Flexor Tendon Adhesions**

This thesis adopted a hierarchical approach to examine the mechanical behaviour of immobilised and mobilised digital flexor tendon adhesions. Macroscopically, the immobilised adhesions were more fibrous compared with the mobilised adhesions. Macromechanical testing demonstrated that immobilised adhesions had significantly higher values for structural stiffness and load at failure, than mobilised adhesions (Table 5.1). The structural stiffness of immobilised adhesions was 140% of that of mobilised adhesions. The corresponding value for the load at failure was 160%. The micromechanical assessment of adhesions employed a confocal laser microscope to visualise the movement of cell nuclei to examine local tissue organisation and local strain responses to applied stress. Cellular organisation and local strain responses were assigned values using image analysis software. The mean local strain for mobilised adhesions was 325% of that of the immobilised adhesions. This suggests that mobilised adhesions were more easily deformed by an applied force. However,



due to the variability, the differences in local strain values were not statistically significant. An unexpectedly high range of dynamic local adhesion patterns (stretch, compress, shear, random and tear) were observed in both adhesion groups. This may account for the high variability in local strain values. With more time available it would have been interesting to perform more local strain assessments to delineate local adhesion organisation more completely.

#### **7.2.4 The Attachment of Intrinsic and Extrinsic Tendon Cells and Adhesion Cells to Collagen and Fibronectin**

The investigation of cell attachment adopted a quantitative scientific approach to examine the attachment of the different cellular components of the tendon-synovial complex and adhesions to collagen type-I and Fn. The attachment of intrinsic tendon cells (tendon core and tendon surface cells) was statistically significantly higher than that of extrinsic tendon cells (synovial sheath cells) to both collagen type-I and Fn. The attachment of cells derived from mobilised adhesions was statistically significantly higher than that of cells derived from immobilised adhesions to both collagen type-I and Fn.

The results from this thesis have also shown that mobilisation favours the formation of elongated cells, which may in part explain why mobilised tendons demonstrate improved tensile properties. Li and colleagues have shown that elongated human tendon cells expressed 65% higher collagen type I than circular cells with the same cell area (Li, Li et al. 2008).

## **7.3 NOVEL APPROACHES TO THE ASSESSMENT AND STRATEGIC MODIFICATION OF FLEXOR TENDON ADHESION FORMATION**

### **7.3.1 Assessment of Adhesions**

#### **7.3.1.1 Mechanical Assessment**

Few studies investigating flexor tendon adhesions incorporate both biomechanical and histopathological assessments (Isik, Ozturk et al. 1999; Strick, Filan et al. 2004; Thomopoulos, Kim et al. 2010). The investigation of the effects of the biomaterial *in vivo* utilised a reproducible injury for quantification of the effects of the biomaterial in the zone of healing using both tensiometer pullout and histopathological assessments. This enabled the mechanical effects of biomaterial treatment to be correlated to tissue cellularity and cell proliferation.

This investigation has demonstrated that immobilised and mobilised adhesions differ at both micro- and macromechanical levels, supporting the need for a hierarchical approach to understand their behaviour (Katz, Misra et al. 2007). The confocal microscopy assessments described, using fibroblast nuclei as dynamic markers, have provided an accurate measure of local adhesion organisation and local strain responses to applied stress. Structural organisation is a dynamic entity and is only revealed by the application of stress. The local strains seen in tissues are strongly dependent on the associations between the cells and the ECM (Screen 2004). This is the first investigation to describe the micromechanical changes in mobilised and immobilised tendon adhesions following injury, providing insight into the specific influence of *in vivo* loading on adhesion ECM remodelling. Increased local strain values and heterogeneity seen in the mobilised adhesions may explain why they are

less restrictive *in vivo* than immobilised adhesion. From the results of this thesis it appears that adhesions may fail in localised areas corresponding to more readily deformed subunit patterns. It is known that structural heterogeneity within tissues may alter their response to load and lead to mechanical failure (Zioupos, Gresle et al. 2008). These findings are fundamental to providing a better understanding of the micromechanical building blocks that are responsible for the overall dynamic response of flexor tendon adhesions, which is critical to tendon glide and function.

#### **7.3.1.2 Assessment of Cell Attachment**

The results of this thesis have shown that the attachment of tendon core and tendon surface cells were statistically significantly higher than that of synovial sheath cells to both collagen type-I and Fn. The results of this investigation confirm the results of a previous study where synovial sheath fibroblasts had a lower attachment efficiency than did tendon cells (Riederer-Henderson, Gauger et al. 1983). However, the authors examined attachment to tissue culture plastic and not to ECM proteins. The study did not examine tendon cell attachment and did not assess adhesion cells or the effect of mobilisation on cell phenotype. It is clear that subpopulations of fibroblasts have differing phenotypes (Khan, Occleston et al. 1998; Ragoowansi, Khan et al. 2003). Targeting such differences in the phenotypic expression of tendon and synovial sheath fibroblasts may prove useful for optimising future repair strategies that have a selective effect on wound healing (Sharma and Maffulli 2005). In this thesis mobilisation of injured digits resulted in greater attachment of adhesion cells to collagen type-I and Fn.

These findings suggest that one possible pathway for the beneficial effects of mobilisation in adhesions is in favouring the attachment and therefore contribution of intrinsic cells, which demonstrate greater attachment than extrinsic cells.

The results from this thesis suggest that the differential avidity of cell attachment within the healing tendon-synovial complex is a potential therapeutic target when developing novel anti-adhesive strategies. It may be proposed that it may be possible to favour intrinsic cell contributions to tendon healing while minimising extrinsic tendon cell contributions. This may ultimately reduce the formation of restrictive adhesions without compromising tendon healing.

### **7.3.2 Modification of Adhesions**

The effect of mobilisation on cell attachment has not been previously determined. Cell attachment is a prerequisite for migration (van der Flier and Sonnenberg 2001) and if cell attachment and migration is reduced this may prevent collagen deposition and fibrotic adhesion formation. The present work confirms that it is possible to reduce the restrictive nature of fibrous adhesion using a cell attachment based approach, without compromising tendon cellularity. In this way, the effect of mobilisation on differential healing in the tendon synovial-complex may be replicated. In the location of the DF<sub>n</sub> biomaterial it may be proposed that fibroblasts experience competitive inhibition for occupancy of their integrins, reducing their overall ability to bind to the ECM and to migrate. Inducing adhesion surface cellular paucity reduces strength of adhesions by diminishing ECM attachments, preventing the formation of *bridging* tissue connections.

The selectivity of the protein based treatment may be understood using a matrix based approach. Previous studies suggest that synovial sheath cells secrete greater quantities of Fn than tendon fibroblasts (Banes, Link et al. 1988; Brigman, Hu et al. 1994). Conversely, synovial sheath cells produce less collagen than do tendon cells (Riederer-Henderson, Gauger et al. 1983). Previous authors have identified spatial and temporal-specific aspects to the healing process in a rabbit flexor tendon injury model (Berglund, Reno et al. 2006). The authors demonstrated using the reverse transcription polymerase chain reaction that there was a shift in collagen expression with a marked increase in type-III mRNA levels in both the tendon and tendon synovial sheath, with the greatest increase being seen in the tendon itself. Berglund and colleagues have also shown using similar techniques that collagen type-I is higher in the flexor tendon than in its synovial sheath (Berglund, Wiig et al. 2004). There appears to be a gradient from a Fn rich to a collagen rich environment from the synovial sheath to the tendon itself. Wong and colleagues investigated collagen type-I production in a mouse tendon injury model and found that the peak in production was later for tendon than in peritendinous tissues (Wong, Lui et al. 2009). This confirms that collagen synthesis in tendon and subcutaneous tissues is temporally different. It seems likely then that there is a *spatial* ECM gradient - from the synovial sheath to the tendon, and a *temporal* ECM gradient progressing from Fn-rich to collagen-rich tissue. In an *in vivo* canine study comparing Fn levels in injured tendons subjected to passive motion and immobilised controls there were higher levels of Fn in the mobilised tendon synovial-complex tissues (Amiel, Gelberman et al. 1991). Mobilisation may result in augmentation of the ECM gradients seen in the healing tendon. Ragoowansi and colleagues have demonstrated that synovial sheath cells produce greater amounts of matrix metalloproteinase

(MMP)-2 and MMP-9 when compared to tendon core cells (Ragoowansi, Khan et al. 2003). It has been proposed that there is flooding of the healing wound milieu with Fn following mobilisation (Amiel, Gelberman et al. 1991). This may result in competitive self inhibition (Brown 1983) and reduced synovial sheath cell attachment to the ECM as the synovial sheath is already exposed to a higher level of Fn than the tendon itself (Banes, Link et al. 1988; Brigman, Hu et al. 1994). Alternatively, increased Fn levels, combined with the increased MMP activity that has been observed in the synovial sheath cells *in vitro* (Ragoowansi, Khan et al. 2003) may result in proteolytic Fn fragments being produced which have been shown to inhibit cell-ECM binding (Yamada and Kennedy 1984; Fukai, Takahashi et al. 1996; Fukai, Hasebe et al. 1997; Watanabe, Takahashi et al. 2000; Yamada 2000). Watanabe and colleagues have shown that MMP-2 may play a particularly important role in generating biologically active ECM fragments (Watanabe, Takahashi et al. 2000). Certain Fn peptides can inhibit cell attachment and migration on Fn without concomitant effect on collagen binding (Oharazawa, Ibaraki et al. 2005). If this observation is combined with the presence of the spatial Fn gradient it would follow that extrinsic cell attachment may be selectively inhibited in the peritendinous tissues following mobilisation. In this way mobilisation may share a common pathway with the action of the DFn biomaterial in the *in vivo* study (Branford, Mudera et al. 2008; Chapter 4). If the DFn biomaterial releases Fn fragments at the collagenous tendon surface then cell adhesion would be maintained, but reduced at the predominantly Fn-based adhesion surface. This would reduce the ability of fibroblasts to attach, migrate and lay down collagen across the interface. Hence adhesion would be reduced but tendon repair sustained.

Shimo-Oka and colleagues demonstrated that human fibroblasts have differential properties when attaching to ECM proteins (Shimo-Oka, Hasegawa et al. 1988). The authors showed that the production of a Fn fragment following trypsinisation inhibited fibroblasts from attaching and spreading on to Fn, without inhibiting attachment to collagen. In a more recent study, the authors demonstrated that RGD peptides inhibit cell attachment and migration on Fn without concomitant effect on collagen binding and migration (Oharazawa, Ibaraki et al. 2005). This is likely to be due to the collagen binding domain of Fn being spatially distinct from its cell binding (RGD) domains (Ruoslahti, Hayman et al. 1980), suggesting a further mechanism for a differential effect on tissue cellularity.

It may be proposed that preventing the attachment of the poorly adherent extrinsic cells to Fn may be a suitable target for selective inhibition within the tendon healing complex. This may explain the results of Chapter 4 that demonstrated a significant reduction in the restrictive nature of postsurgical adhesions following treatment, associated with a significant decrease in adhesion surface cellularity, without compromising tendon cellularity (Branford, Mudera et al. 2008).

Increased cellularity was seen within both the adhesion and tendon tissue during *in vivo* DFn testing. This may be the result of the pro-proliferative action of Fn fragments (Zlatopol'skii, Chubukina et al. 1989; Zlatopol'skii, Chubukina et al. 1992). Cells deeper within the tendon may be protected by having more of their ECM binding sites occupied. Alternatively, cells deep within the tissues may not be exposed to such high levels of anti-adhesive fragments, partly due to the dissolved anti-adhesive fragments going into the systemic circulation. The effects of the anti-

adhesive fragments may also be diminished by the presence of other proteins from the surgical wound.

Tendon fibroblasts are highly sensitive to their mechanical environment, detecting strain during tissue loading (Asundi and Rempel 2008). Fibroblasts respond through mechanotransduction pathways, transducing mechanical into chemical information (Gillard, Reilly et al. 1979; Slack, Flint et al. 1984; Abrahamsson 1991; Khan, Edwards et al. 1996; McNeilly, Banes et al. 1996; Screen, Lee et al. 2003; Chiquet, Gelman et al. 2009). These signals are integrated with growth factor derived stimuli to achieve specific changes in gene expression to remodel the ECM. Strain-induced changes in biomechanical properties are likely to be the result of changes in ECM production and MMP activity, secondary to strain-induced changes in growth factor and cytokine production (Zeichen, van Griensven et al. 2000; Archambault, Tsuzaki et al. 2002; Webb, Hitchcock et al. 2006). Mechanical strengthening most likely results from increased collagen type-I production through transforming growth factor beta-1 (TGF $\beta$ -1) and connective tissue growth factor (CTGF). ECM adhesion contacts are now recognised as the major sites of crosstalk between mechanical and chemical stimuli (Chiquet, Gelman et al. 2009). For fibroblasts, production of the ECM is a prominent response to changes in mechanical load. Integrin-containing cell-ECM adhesion contacts are essential for force transmission from the ECM to the cytoskeleton. For these reasons using a cell-ECM attachment based approach to the problem of adhesion formation is useful if progress in developing anti-adhesive treatments is to be made.



## 7.4 FUTURE WORK

These findings may pave the way for a clinical study to use the DFn biomaterial to reduce adhesion formation after tendon repair. However, further studies need to be carried out assessing DFn treated sutured transected tendons that are mobilised to relate the treatment to the clinical situation. Longer time points need to be assessed to determine whether abolishing the initial adhesion response dampens the entire response or whether it is merely delayed. However, therapeutic benefit is likely in either case.

In future work it would be interesting to stain the *in vivo* specimens for  $\alpha$ -smooth muscle actin ( $\alpha$ -SMA) to determine the presence of myofibroblasts, which contribute to excessive fibrosis in healing tissues (Desmouliere, Chaponnier et al. 2005). Ragoowansi and colleagues demonstrated that synovial sheath fibroblasts demonstrated greater amounts of intra-cellular  $\alpha$ -SMA than tendon core cells, implying that synovial sheath fibroblasts play an active role in adhesion formation and should be specifically targeted to inhibit or treat tendon adhesions (Ragoowansi, Khan et al. 2003).

In future work, the anti-adhesive DFn biomaterial could be separated into fractions according to heparin or gelatin binding affinity, and by ultrafiltration according to molecular weight. Each of these fractions could be tested for their effects *in vitro* and *in vivo*. However, it is likely that the DFn biomaterial is a heterogeneous mix of fragments which may act synergistically or in combination. Alternatively the material may only have its effects while the solid material is dissolving and may not possess anti-adhesive properties in soluble form.

The attachment model developed in this thesis allows for testing the efficacy of potential anti-adhesion strategies in differentially affecting cell attachment to various ECM proteins. Novel treatments may be introduced into this system by topical application over the protein coated plates before the cells are seeded onto the proteins. Other substances with a similar effect to the DFn biomaterial, without the stigma of being derived from a blood product could be tested. For example, epigallocatechin-3-gallate (EGCG), a constituent of green tea, has been shown to have an effect on TGF $\beta$ -1-stimulated wound contraction (Klass, Branford et al. 2010). Hung and colleagues have shown that EGCG inhibits fibroblast to Fn binding (Hung, Huang et al. 2005). It appears to bind to Fn but not to collagen and therefore possesses selective properties in inhibiting cell adhesion to ECM components. Similarly the quantitative hierarchical mechanical and histopathological models used in this thesis could be used to test anti-adhesive treatments, introduced at the time of injury, for their effects on adhesion formation.

Peptides of Fn also have effects on cells other than fibroblasts that are found in the surgical site, for example promotion of chemotaxis and adhesion of monocytes (Clark, Wikner et al. 1988; Chung and Kao 2009), and promotion of phagocyte activity (Czop and Austen 1982). It would be interesting to determine if these had beneficial effects on reducing post-surgical wound infection, which is a potential cause of worsening adhesions.

In future studies selective matrix based approaches may be combined with cytokine-based strategies to provide further selectivity in tendon healing. Fu and colleagues found that in the presence of TGF- $\beta$ 1, the gene expression of procollagen type-I was

promoted in tendon fibroblasts anchored to a collagen type-I matrix, but not in those with Fn anchorage (Fu, Wong et al. 2005). Klass and colleagues demonstrated a differential response in rabbit endotenon, epitenon and synovial sheath in cells in collagen type-I gene expression in response to TGF- $\beta$ 1 *in vitro* (Klass, Rolfe et al. 2009).

In future work, bilayered scaffolds, with an inner adherent mesenchymal stem cell seeded layer and an outer anti-adhesive layer, could be tissue engineered in bioreactors with cyclic strain regimes. These could have cytokines incorporated then implanted and tested *in vivo*.

There are several plastic reconstructive surgical applications where the lines of investigation used in the present study may be useful. Tissue engineering is likely to play an ever increasing role in future plastic surgery research and is pervaded by principles of mechanotransduction. The techniques described in the present study have broad application to healing tissues subject to distortion under strain. The dynamic assessment of the organisation of healing tissues, especially where they are under applied load, would be suitably applied to investigating cutaneous scarring, and also in ligament and muscle healing. Such approaches would be readily transferrable to other areas of hand surgery, for example, in assessing novel therapeutic strategies in Dupuytren's disease. Outside the field of plastic surgery such approaches are relevant to assessing dynamic healing tissues as occur following cardiac injury, or post surgical intra-abdominal adhesions, where the mechanical properties of these tissues under shear stress are critical to function. The tendon models described in this thesis would be applicable to a much wider context for the

testing of anti-adhesion treatments, due to the commonality of the process of adhesion formation at different anatomical sites.

Proposed future studies:

- Various topical anti-adhesive treatments could be tested for their differential effects on matrix attachment using the models described in this thesis
- Further micromechanical assessments could be made, at slightly lower magnification, to try to understand how the individual dynamic adhesions patterns fit together to form higher order adhesions
- A bilayered tissue-engineered biomaterial could be developed with an adhesive inner (tendon surface) layer seeded with mesenchymal stem cells and an outer anti-adhesive (synovial) layer: Cytokines could be incorporated into these materials to further enhance selectivity in tendon healing, with the materials being conditioned in bioreactors prior to implantation *in vivo*

## **7.5 GENERAL SUMMARY**

This thesis presents a series of studies, used to develop a quantitative assessment of adhesion formation using biomechanical, histopathological, biological and dynamic cellular approaches in a rabbit flexor tendon-synovial complex injury model. The hypotheses challenged within this thesis were:

- Mobilisation results in increased intrinsic cell attachment and reduced extrinsic cell attachment in adhesions
- Mobilisation has a favourable effect on the local strain responses of adhesions to applied stress, which reduces the restrictive nature of the adhesions

- Selectively blocking cell-ECM attachment mimics the effects of mobilisation by selectively inducing adhesion surface cellular paucity. This reduces ECM deposition and fibrotic adhesion formation without compromising tendon cellularity

A model system was developed, enabling the microanalysis of local strain fields within rabbit tendon adhesions, using the cell nuclei as dynamic strain markers. The system was used in conjunction with macromechanical analysis, in order to examine the mechanisms by which tendon adhesions are modified by mobilisation. The attachment of tendon-synovial complex cells and mobilised and immobilised adhesion cells to collagen and Fn was examined *in vitro*. A novel protein based anti-adhesive biomaterial was investigated *in vitro* and *in vivo* to determine its effects on adhesion formation.

These studies led to the following conclusions:

- Mobilisation favours intrinsic cell attachment to the ECM relative to that of extrinsic cells and therefore intrinsic contributions to healing
- Mobilisation results in three-fold higher local strain values and increased heterogeneity in adhesions. The increased heterogeneity may provide a mechanism for localised mechanical failure due to altered local strain patterns and therefore points of weakness in mobilised adhesions
- Immobilised and mobilised adhesions differ at both micro- and macromechanical levels, supporting the need for a hierarchical approach to understand their behaviour

- A matrix based approach preventing cell-Fn attachment may mimic the effects of mobilisation by selectively reducing adhesion cellularity while maintaining tendon cellularity

The hypotheses stated above are therefore accepted. Accordingly, it would appear that the local strain and ECM environment of fibroblasts in tendon adhesions is complex. Improving the understanding of how these local phenomena are linked together will enable the selective manipulation of healing in a way that further favours recovery of tensile strength in tendons while reducing restrictive adhesion formation.

## REFERENCES

- Abrahamsson, S. O. (1991). "Matrix metabolism and healing in the flexor tendon. Experimental studies on rabbit tendon." *Scand J Plast Reconstr Surg Hand Surg Suppl* **23**: 1-51.
- Abrahamsson, S. O. (1997). "Similar effects of recombinant human insulin-like growth factor-I and II on cellular activities in flexor tendons of young rabbits: experimental studies in vitro." *J Orthop Res* **15**(2): 256-62.
- Abrahamsson, S. O., G. Lundborg, et al. (1991). "Long-term explant culture of rabbit flexor tendon: effects of recombinant human insulin-like growth factor-I and serum on matrix metabolism." *J Orthop Res* **9**(4): 503-15.
- Ahmed, Z. and R. A. Brown (1999). "Adhesion, alignment, and migration of cultured Schwann cells on ultrathin fibronectin fibres." *Cell Motil Cytoskeleton* **42**(4): 331-43.
- Ahmed, Z., S. Underwood, et al. (2000). "Low concentrations of fibrinogen increase cell migration speed on fibronectin/fibrinogen composite cables." *Cell Motil Cytoskeleton* **46**(1): 6-16.
- Akali, A., U. Khan, et al. (1999). "Decrease in adhesion formation by a single application of 5-fluorouracil after flexor tendon injury." *Plast Reconstr Surg* **103**(1): 151-8.
- Akeson, W. H., D. Amiel, et al. (1977). "Collagen cross-linking alterations in joint contractures: changes in the reducible cross-links in periarticular connective tissue collagen after nine weeks of immobilization." *Connect Tissue Res* **5**(1): 15-9.

- Akhouayri, O., M. H. Lafage-Proust, et al. (1999). "Effects of static or dynamic mechanical stresses on osteoblast phenotype expression in three-dimensional contractile collagen gels." *J Cell Biochem* **76**(2): 217-30.
- Akiyama, S. K., E. Hasegawa, et al. (1985). "The interaction of fibronectin fragments with fibroblastic cells." *J Biol Chem* **260**(24): 13256-60.
- Amiel, D., W. H. Akeson, et al. (1983). "Stress deprivation effect on metabolic turnover of the medial collateral ligament collagen. A comparison between nine- and 12-week immobilization." *Clin Orthop Relat Res*(172): 265-70.
- Amiel, D., R. Gelberman, et al. (1991). "Fibronectin in healing flexor tendons subjected to immobilization or early controlled passive motion." *Matrix* **11**(3): 184-9.
- Amiel, D., K. Ishizue, et al. (1989). "Hyaluronan in flexor tendon repair." *J Hand Surg [Am]* **14**(5): 837-43.
- Amiel, D., S. L. Woo, et al. (1982). "The effect of immobilization on collagen turnover in connective tissue: a biochemical-biomechanical correlation." *Acta Orthop Scand* **53**(3): 325-32.
- Aoki, M., H. Kubota, et al. (1997). "Biomechanical and histologic characteristics of canine flexor tendon repair using early postoperative mobilization." *J Hand Surg [Am]* **22**(1): 107-14.
- Aota, S., M. Nomizu, et al. (1994). "The short amino acid sequence Pro-His-Ser-Arg-Asn in human fibronectin enhances cell-adhesive function." *J Biol Chem* **269**(40): 24756-61.
- Archambault, J., M. Tsuzaki, et al. (2002). "Stretch and interleukin-1 $\beta$  induce matrix metalloproteinases in rabbit tendon cells in vitro." *J Orthop Res* **20**(1): 36-9.



- Arnaout, M. A., S. L. Goodman, et al. (2002). "Coming to grips with integrin binding to ligands." *Curr Opin Cell Biol* **14**(5): 641-51.
- Arnoczky, S. P., M. Lavagnino, et al. (2002). "In situ cell nucleus deformation in tendons under tensile load; a morphological analysis using confocal laser microscopy." *J Orthop Res* **20**(1): 29-35.
- Assoian, R. K. (1997). "Control of the G1 phase cyclin-dependent kinases by mitogenic growth factors and the extracellular matrix." *Cytokine Growth Factor Rev* **8**(3): 165-70.
- Asundi, K. R. and D. M. Rempel (2008). "MMP-1, IL-1beta, and COX-2 mRNA expression is modulated by static load in rabbit flexor tendons." *Ann Biomed Eng* **36**(2): 237-43.
- Banes, A. J., K. Donlon, et al. (1988). "Cell populations of tendon: a simplified method for isolation of synovial cells and internal fibroblasts: confirmation of origin and biologic properties." *J Orthop Res* **6**(1): 83-94.
- Banes, A. J., G. Horesovsky, et al. (1999). "Mechanical load stimulates expression of novel genes in vivo and in vitro in avian flexor tendon cells." *Osteoarthritis Cartilage* **7**(1): 141-53.
- Banes, A. J., G. W. Link, et al. (1988). "Tendon synovial cells secrete fibronectin in vivo and in vitro." *J Orthop Res* **6**(1): 73-82.
- Banes, A. J., M. Tsuzaki, et al. (1995). "Mechanoreception at the cellular level: the detection, interpretation, and diversity of responses to mechanical signals." *Biochem Cell Biol* **73**(7-8): 349-65.
- Bates, S. J., E. Morrow, et al. (2006). "Mannose-6-phosphate, an inhibitor of transforming growth factor-beta, improves range of motion after flexor tendon repair." *J Bone Joint Surg Am* **88**(11): 2465-72.

- Becker, H., M. F. Graham, et al. (1981). "Intrinsic tendon cell proliferation in tissue culture." *J Hand Surg [Am]* **6**(6): 616-9.
- Beredjikian, P. K. (2003). "Biologic aspects of flexor tendon laceration and repair." *J Bone Joint Surg Am* **85-A**(3): 539-50.
- Berglund, M., C. Reno, et al. (2006). "Patterns of mRNA expression for matrix molecules and growth factors in flexor tendon injury: differences in the regulation between tendon and tendon sheath." *J Hand Surg Am* **31**(8): 1279-87.
- Berglund, M., M. Wiig, et al. (2004). "Assessment of mRNA levels for matrix molecules and TGF-  $\beta$ 1 in rabbit flexor and peroneus tendons reveals regional differences in steady-state expression." *J Hand Surg [Br]* **29**(2): 165-9.
- Berry, C. C., J. C. Shelton, et al. (2003). "Influence of external uniaxial cyclic strain on oriented fibroblast-seeded collagen gels." *Tissue Eng* **9**(4): 613-24.
- Bhavsar, D., D. Shettko, et al. (2010). "Encircling the tendon repair site with collagen-GAG reduces the formation of postoperative tendon adhesions in a chicken flexor tendon model." *J Surg Res* **159**(2): 765-71.
- Birdsell, D. C., E. R. Tustanoff, et al. (1966). "Collagen production in regenerating tendon." *Plast Reconstr Surg* **37**(6): 504-11.
- Bouten, C. V., M. M. Knight, et al. (2001). "Compressive deformation and damage of muscle cell subpopulations in a model system." *Ann Biomed Eng* **29**(2): 153-63.
- Boyes, J. H. (1950). "Flexor-tendon grafts in the fingers and thumb; an evaluation of end results." *J Bone Joint Surg Am* **32-A**(3): 489-99; passim.

- Boyes, J. H. (1955). "Evaluation of results of digital flexor tendon grafts." *Am J Surg* **89**(6): 1116-9.
- Braga, V. (2000). "The crossroads between cell-cell adhesion and motility." *Nat Cell Biol* **2**(10): E182-4.
- Branford, O. A., V. Mudera, et al. (2008). "A novel biomimetic material for engineering postsurgical adhesion using the injured digital flexor tendon-synovial complex as an in vivo model." *Plast Reconstr Surg* **121**(3): 781-93.
- Branford, O. A., R. A. Brown, et al. (2010). "Shear-aggregated fibronectin with anti-adhesive properties." *J Tissue Eng Regen Med* **5**(1): 20-31.
- Brigman, B. E., P. Hu, et al. (1994). "Fibronectin in the tendon-synovial complex: quantitation in vivo and in vitro by ELISA and relative mRNA levels by polymerase chain reaction and northern blot." *J Orthop Res* **12**(2): 253-61.
- Brown, R. A. (1983). "Failure of fibronectin as an opsonin in the host defence system: a case of competitive self inhibition?" *Lancet* **2**(8358): 1058-60.
- Brown, R. A., G. W. Blunn, et al. (1994). "Preparation of orientated fibrous mats from fibronectin: composition and stability." *Biomaterials* **15**(6): 457-64.
- Brown, R. A. and J. B. Phillips (2007). "Cell responses to biomimetic protein scaffolds used in tissue repair and engineering." *Int Rev Cytol* **262**: 75-150.
- Bruehlmann, S. B., P. A. Hulme, et al. (2004). "In situ intercellular mechanics of the bovine outer annulus fibrosus subjected to biaxial strains." *J Biomech* **37**(2): 223-31.
- Buck-Gramcko, D., F. E. Dietrich, et al. (1976). "[Evaluation criteria in follow-up studies of flexor tendon therapy]." *Handchirurgie* **8**(2): 65-9.

- Burrill, P. H., I. Bernardini, et al. (1981). "Effect of serum, fibronectin, and laminin on adhesion of rabbit intestinal epithelial cells in culture." *J Supramol Struct Cell Biochem* **16**(4): 385-92.
- Burt, A. and D. A. McGrouther (1992). Production and use of skin cell cultures in therapeutic situation. *Animal Cell Biotechnology*. R. E. Spier and J. B. Griffiths. New York, Academic Press 158-68.
- Butler, D. L., E. S. Grood, et al. (1984). "Effects of structure and strain measurement technique on the material properties of young human tendons and fascia." *J Biomech* **17**(8): 579-96.
- Calderwood, D. A. (2004). "Talin controls integrin activation." *Biochem Soc Trans* **32**(Pt3): 434-7.
- Calderwood, D. A., S. J. Shattil, et al. (2000). "Integrins and actin filaments: reciprocal regulation of cell adhesion and signaling." *J Biol Chem* **275**(30): 22607-10.
- Canty, E. G. and K. E. Kadler (2005). "Procollagen trafficking, processing and fibrillogenesis." *J Cell Sci* **118**(Pt 7): 1341-53.
- Carlstedt, C. A., K. Madsen, et al. (1986). "Biomechanical and biochemical studies of tendon healing after conservative and surgical treatment." *Arch Orthop Trauma Surg* **105**(4): 211-5.
- Carpenter, J. E., S. Thomopoulos, et al. (1999). "Animal models of tendon and ligament injuries for tissue engineering applications." *Clin Orthop Relat Res*(367 Suppl): S296-311.
- Carter, W. G., H. Rauvala, et al. (1981). "Studies on cell adhesion and recognition. II. The kinetics of cell adhesion and cell spreading on surfaces coated with

- carbohydrate-reactive proteins (glycosidases and lectins) and fibronectin." *J Cell Biol* **88**(1): 138-48.
- Castellani, P., A. Siri, et al. (1986). "Transformed human cells release different fibronectin variants than do normal cells." *J Cell Biol* **103**(5): 1671-7.
- Chan, B. P., S. C. Fu, et al. (1998). "Pyridinoline in relation to ultimate stress of the patellar tendon during healing: an animal study." *J Orthop Res* **16**(5): 597-603.
- Chang, J., D. Most, et al. (1998). "Molecular studies in flexor tendon wound healing: the role of basic fibroblast growth factor gene expression." *J Hand Surg [Am]* **23**(6): 1052-8.
- Chang, J., R. Thunder, et al. (2000). "Studies in flexor tendon wound healing: neutralizing antibody to TGF-beta1 increases postoperative range of motion." *Plast Reconstr Surg* **105**(1): 148-55.
- Chen, C. H., Y. Cao, et al. (2008). "Tendon healing in vivo: gene expression and production of multiple growth factors in early tendon healing period." *J Hand Surg Am* **33**(10): 1834-42.
- Chen, C. H., Y. L. Zhou, et al. (2009). "Effectiveness of microRNA in Down-regulation of TGF-beta gene expression in digital flexor tendons of chickens: in vitro and in vivo study." *J Hand Surg Am* **34**(10): 1777-84 e1.
- Chen, H., B. W. Bernstein, et al. (2000). "Regulating actin-filament dynamics in vivo." *Trends Biochem Sci* **25**(1): 19-23.
- Cheng, V. T. C., Screen, H. R. C. (2007). "The micro-structural strain response of tendon." *J Mater Sci* **42**: 8957-8965.

- Chiquet, M., L. Gelman, et al. (2009). "From mechanotransduction to extracellular matrix gene expression in fibroblasts." *Biochim Biophys Acta* **1793**(5): 911-20.
- Chung, A. S. and W. J. Kao (2009). "Fibroblasts regulate monocyte response to ECM-derived matrix: the effects on monocyte adhesion and the production of inflammatory, matrix remodeling, and growth factor proteins." *J Biomed Mater Res A* **89**(4): 841-53.
- Churei, Y., T. Yoshizu, et al. (1999). "Flexor tendon repair in a rabbit model using a "core" of extensor retinaculum with synovial membrane. An experimental study." *J Hand Surg [Br]* **24**(3): 267-71.
- Clark, R. A., J. Q. An, et al. (2003). "Fibroblast migration on fibronectin requires three distinct functional domains." *J Invest Dermatol* **121**(4): 695-705.
- Clark, R. A., N. E. Wikner, et al. (1988). "Cryptic chemotactic activity of fibronectin for human monocytes resides in the 120-kDa fibroblastic cell-binding fragment." *J Biol Chem* **263**(24): 12115-23.
- Constantine, K. L., S. A. Brew, et al. (1992). "<sup>1</sup>H-n.m.r. studies of the fibronectin 13 kDa collagen-binding fragment. Evidence for autonomous conserved type I and type II domain folds." *Biochem J* **283** ( Pt 1): 247-54.
- Copie, V., Y. Tomita, et al. (1998). "Solution structure and dynamics of linked cell attachment modules of mouse fibronectin containing the RGD and synergy regions: comparison with the human fibronectin crystal structure." *J Mol Biol* **277**(3): 663-82.
- Cosgriff, T. M., L. A. Hodgson, et al. (1983). "The antithrombin III content of cryoprecipitate prepared from blood collected with and without heparin." *Vox Sang* **44**: 98-101.

- Cukierman, E., R. Pankov, et al. (2001). "Taking cell-matrix adhesions to the third dimension." *Science* **294**(5547): 1708-12.
- Czop, J. K. and K. F. Austen (1982). "Augmentation of phagocytosis by a specific fibronectin fragment that links particulate activators to the fibronectin adherence receptor of human monocytes." *J Immunol* **129**(6): 2678-81.
- Damsky, C. H. and D. Ilic (2002). "Integrin signaling: it's where the action is." *Curr Opin Cell Biol* **14**(5): 594-602.
- Danen, E. H. and K. M. Yamada (2001). "Fibronectin, integrins, and growth control." *J Cell Physiol* **189**(1): 1-13.
- Darby, I., O. Skalli, et al. (1990). "Alpha-smooth muscle actin is transiently expressed by myofibroblasts during experimental wound healing." *Lab Invest* **63**(1): 21-9.
- de Wit, T., D. de Putter, et al. (2009). "Auto-crosslinked hyaluronic acid gel accelerates healing of rabbit flexor tendons in vivo." *J Orthop Res* **27**(3): 408-15.
- Desmouliere, A., C. Chaponnier, et al. (2005). "Tissue repair, contraction, and the myofibroblast." *Wound Repair Regen* **13**(1): 7-12.
- DiMilla, P. A., J. A. Stone, et al. (1993). "Maximal migration of human smooth muscle cells on fibronectin and type IV collagen occurs at an intermediate attachment strength." *J Cell Biol* **122**(3): 729-37.
- Djerkovic, G. S., J. B. Phillips, et al. (2005). "Soluble heparin binding fraction from fibronectin tissue engineered scaffold inhibits neuronal growth: 2nd World Congress on Regenerative Medicine, Leipzig, Germany, May 18-20, 2005. ." *Int J Artif Organs* **28**: 284.

- Dogramaci, Y., A. Kalac, et al. (2010). "Effects of a single application of extractum cepae on the peritendinous adhesion: an experimental study in rabbits." *Ann Plast Surg* **64**(3): 338-41.
- Douglas, T., S. Heinemann, et al. (2006). "Fibrillogenesis of collagen types I, II, and III with small leucine-rich proteoglycans decorin and biglycan." *Biomacromolecules* **7**(8): 2388-93.
- Ejim, O. S., G. W. Blunn, et al. (1993). "Production of artificial-orientated mats and strands from plasma fibronectin: a morphological study." *Biomaterials* **14**(10): 743-8.
- Enwemeka, C. S., N. I. Spielholz, et al. (1988). "The effect of early functional activities on experimentally tenotomized Achilles tendons in rats." *Am J Phys Med Rehabil* **67**(6): 264-9.
- Eskeland, G., T. Eskeland, et al. (1977). "The ultrastructure of normal digital flexor tendon sheath and of the tissue formed around silicone and polyethylene implants in man." *J Bone Joint Surg Br* **59**(2): 206-12.
- Feehan, L. M. and J. G. Beauchene (1990). "Early tensile properties of healing chicken flexor tendons: early controlled passive motion versus postoperative immobilization." *J Hand Surg [Am]* **15**(1): 63-8.
- Felsenfeld, D. P., P. L. Schwartzberg, et al. (1999). "Selective regulation of integrin-cytoskeleton interactions by the tyrosine kinase Src." *Nat Cell Biol* **1**(4): 200-6.
- Ferguson, R. E. and B. Rinker (2006). "The use of a hydrogel sealant on flexor tendon repairs to prevent adhesion formation." *Ann Plast Surg* **56**(1): 54-8.



- Fong, K. D., M. C. Trindade, et al. (2005). "Microarray analysis of mechanical shear effects on flexor tendon cells." *Plast Reconstr Surg* **116**(5): 1393-404; discussion 1405-6.
- Frykman, E., S. Jacobsson, et al. (1993). "Fibrin sealant in prevention of flexor tendon adhesions: an experimental study in the rabbit." *J Hand Surg [Am]* **18**(1): 68-75.
- Fu, S. C., Y. P. Wong, et al. (2005). "TGF-beta1 reverses the effects of matrix anchorage on the gene expression of decorin and procollagen type I in tendon fibroblasts." *Clin Orthop Relat Res*(431): 226-32.
- Fukai, F., S. Hasebe, et al. (1997). "Identification of the anti-adhesive site buried within the heparin-binding domain of fibronectin." *J Biochem (Tokyo)* **121**(2): 189-92.
- Fukai, F., S. Kamiya, et al. (2000). "The fibronectin-derived anti-adhesive peptide III14-2 suppresses adhesion and apoptosis of leukemic cell lines through down-regulation of protein-tyrosine phosphorylation." *Cell Mol Biol (Noisy-le-grand)* **46**(1): 145-52.
- Fukai, F., M. Mashimo, et al. (1998). "Modulation of apoptotic cell death by extracellular matrix proteins and a fibronectin-derived antiadhesive peptide." *Exp Cell Res* **242**(1): 92-9.
- Fukai, F., M. Ohtaki, et al. (1995). "Release of biological activities from quiescent fibronectin by a conformational change and limited proteolysis by matrix metalloproteinases." *Biochemistry* **34**(36): 11453-9.
- Fukai, F., H. Takahashi, et al. (1996). "Fibronectin harbors anticell adhesive activity." *Biochem Biophys Res Commun* **220**(2): 394-8.

- Furlow, L. T., Jr. (1976). "The role of tendon tissues in tendon healing." *Plast Reconstr Surg* **57**(1): 39-49.
- Galbraith, C. G., K. M. Yamada, et al. (2002). "The relationship between force and focal complex development." *J Cell Biol* **159**(4): 695-705.
- Geiger, B., J. P. Spatz, et al. (2009). "Environmental sensing through focal adhesions." *Nat Rev Mol Cell Biol* **10**(1): 21-33.
- Gelberman, R. H., D. Amiel, et al. (1981). "The influence of protected passive mobilization on the healing of flexor tendons: a biochemical and microangiographic study." *Hand* **13**(2): 120-8.
- Gelberman, R. H., D. Amiel, et al. (1992). "Genetic expression for type I procollagen in the early stages of flexor tendon healing." *J Hand Surg [Am]* **17**(3): 551-8.
- Gelberman, R. H., M. J. Botte, et al. (1986). "The excursion and deformation of repaired flexor tendons treated with protected early motion." *J Hand Surg [Am]* **11**(1): 106-10.
- Gelberman, R. H., M. I. Boyer, et al. (1999). "The effect of gap formation at the repair site on the strength and excursion of intrasynovial flexor tendons. An experimental study on the early stages of tendon-healing in dogs." *J Bone Joint Surg Am* **81**(7): 975-82.
- Gelberman, R. H. and P. R. Manske (1985). "Factors influencing flexor tendon adhesions." *Hand Clin* **1**(1): 35-42.
- Gelberman, R. H., P. R. Manske, et al. (1986). "Flexor tendon repair." *J Orthop Res* **4**(1): 119-28.
- Gelberman, R. H., P. R. Manske, et al. (1984). "Flexor tendon repair in vitro: a comparative histologic study of the rabbit, chicken, dog, and monkey." *J Orthop Res* **2**(1): 39-48.

- Gelberman, R. H., J. A. Nunley, 2nd, et al. (1991). "Influences of the protected passive mobilization interval on flexor tendon healing. A prospective randomized clinical study." *Clin Orthop Relat Res*(264): 189-96.
- Gelberman, R. H., D. Steinberg, et al. (1991). "Fibroblast chemotaxis after tendon repair." *J Hand Surg [Am]* **16**(4): 686-93.
- Gelberman, R. H., J. S. Vande Berg, et al. (1983). "Flexor tendon healing and restoration of the gliding surface. An ultrastructural study in dogs." *J Bone Joint Surg Am* **65**(1): 70-80.
- Gelberman, R. H., S. L. Woo, et al. (1982). "Effects of early intermittent passive mobilization on healing canine flexor tendons." *J Hand Surg Am* **7**(2): 170-5.
- Gelberman, R. H., S. L. Woo, et al. (1982). "Effects of early intermittent passive mobilization on healing canine flexor tendons." *J Hand Surg [Am]* **7**(2): 170-5.
- Gemba, T., J. Valbracht, et al. (2002). "Focal adhesion kinase and mitogen-activated protein kinases are involved in chondrocyte activation by the 29-kDa amino-terminal fibronectin fragment." *J Biol Chem* **277**(2): 907-11.
- Gildner, C. D., A. L. Lerner, et al. (2004). "Fibronectin matrix polymerization increases tensile strength of model tissue." *Am J Physiol Heart Circ Physiol* **287**(1): H46-53.
- Gillard, G. C., H. C. Reilly, et al. (1979). "The influence of mechanical forces on the glycosaminoglycan content of the rabbit flexor digitorum profundus tendon." *Connect Tissue Res* **7**(1): 37-46.
- Golash, A., A. Kay, et al. (2003). "Efficacy of ADCON-T/N after primary flexor tendon repair in Zone II: a controlled clinical trial." *J Hand Surg [Br]* **28**(2): 113-5.

- Gomez, M. (1995). "The physiology and biochemistry of soft tissue healing. In: Griffin, L. (Ed.), Rehabilitation of the injured knee, 2nd Edition. Mosby Company, St. Louis, MO." 34-44.
- Grays (1989). Gray's Anatomy. New York, Churchill Livingstone.
- Greiling, D. and R. A. Clark (1997). "Fibronectin provides a conduit for fibroblast transmigration from collagenous stroma into fibrin clot provisional matrix." *J Cell Sci* **110** ( Pt 7): 861-70.
- Grinnell, F. (1984). "Fibronectin and wound healing." *J Cell Biochem* **26**(2): 107-16.
- Grinnell, F., C. H. Ho, et al. (1992). "Degradation of fibronectin and vitronectin in chronic wound fluid: analysis by cell blotting, immunoblotting, and cell adhesion assays." *J Invest Dermatol* **98**(4): 410-6.
- Grinnell, F. and M. Zhu (1994). "Identification of neutrophil elastase as the proteinase in burn wound fluid responsible for degradation of fibronectin." *J Invest Dermatol* **103**(2): 155-61.
- Guan, J. L. (1997). "Role of focal adhesion kinase in integrin signaling." *Int J Biochem Cell Biol* **29**(8-9): 1085-96.
- Guan, J. L., J. E. Trevithick, et al. (1991). "Fibronectin/integrin interaction induces tyrosine phosphorylation of a 120-kDa protein." *Cell Regul* **2**(11): 951-64.
- Guilak, F. (1995). "Compression-induced changes in the shape and volume of the chondrocyte nucleus." *J Biomech* **28**(12): 1529-41.
- Guilak, F., Donahue, H.J., Zell, R., Grande, D.A., McLeod, K.J., and Rubin, C.T. (1994). "Deformation-induced calcium signaling in articular chondrocytes. In: Cell Mechanics and Cellular Engineering, eds. V.C. Mow, F. Guilak, R. Tran-Son-Tay, and R.M. Hochmuth." Springer-Verlag, New York: 380-397.

- Guilak, F., A. Ratcliffe, et al. (1995). "Chondrocyte deformation and local tissue strain in articular cartilage: a confocal microscopy study." *J Orthop Res* **13**(3): 410-21.
- Guilak, F., J. R. Tedrow, et al. (2000). "Viscoelastic properties of the cell nucleus." *Biochem Biophys Res Commun* **269**(3): 781-6.
- Haddad, R., T. S. Peltz, et al. (2010). "The relationship between gap formation and grip-to-grip displacement during cyclic testing of repaired flexor tendons." *J Biomech* **43**(14): 2835-8.
- Hagberg, L. and B. Gerdin (1992). "Sodium hyaluronate as an adjunct in adhesion prevention after flexor tendon surgery in rabbits." *J Hand Surg [Am]* **17**(5): 935-41.
- Halikis, M. N., P. R. Manske, et al. (1997). "Effect of immobilization, immediate mobilization, and delayed mobilization on the resistance to digital flexion using a tendon injury model." *J Hand Surg [Am]* **22**(3): 464-72.
- Hand, A. S. f. S. o. t. (1976). Clinical assessment committee report. Aurora, Colorado.
- Hanff, G. and L. Hagberg (1998). "Prevention of restrictive adhesions with expanded polytetrafluoroethylene diffusible membrane following flexor tendon repair: an experimental study in rabbits." *J Hand Surg [Am]* **23**(4): 658-64.
- Hannafin, J. A., S. P. Arnoczky, et al. (1995). "Effect of stress deprivation and cyclic tensile loading on the material and morphologic properties of canine flexor digitorum profundus tendon: an in vitro study." *J Orthop Res* **13**(6): 907-14.
- Harding, S. I., A. Afoke, et al. (2002). "Engineering and cell attachment properties of human fibronectin-fibrinogen scaffolds for use in tissue engineered blood vessels." *Bioprocess Biosyst Eng* **25**(1): 53-9.

- Harding, S. I., S. Underwood, et al. (2000). "Assessment of cell alignment by fibronectin multi-fibre cables capable of large scale production." *Bioprocess Eng* **22**(2): 159-164.
- Harris, A. K., D. Stopak, et al. (1981). "Fibroblast traction as a mechanism for collagen morphogenesis." *Nature* **290**(5803): 249-51.
- Harrison, R. K., M. E. Jones, et al. (2003). "Mapping of vascular endothelium in the human flexor digitorum profundus tendon." *J Hand Surg [Am]* **28**(5): 806-13.
- Harrison, R. K., V. Mudera, et al. (2003). "Synovial sheath cell migratory response to flexor tendon injury: an experimental study in rats." *J Hand Surg [Am]* **28**(6): 987-93.
- Hausmann, J. T., G. Vekszler, et al. (2009). "Biomechanical comparison of modified Kessler and running suture repair in 3 different animal tendons and in human flexor tendons." *J Hand Surg Am* **34**(1): 93-101.
- Hautanen, A., J. Gailit, et al. (1989). "Effects of modifications of the RGD sequence and its context on recognition by the fibronectin receptor." *J Biol Chem* **264**(3): 1437-42.
- Hayashi, M. and K. M. Yamada (1981). "Differences in domain structures between plasma and cellular fibronectins." *J Biol Chem* **256**(21): 11292-300.
- Hayashi, M. and K. M. Yamada (1983). "Domain structure of the carboxyl-terminal half of human plasma fibronectin." *J Biol Chem* **258**(5): 3332-40.
- Healy, C., K. J. Mulhall, et al. (2007). "The effect of thermal preconditioning of the limb on flexor tendon healing." *J Hand Surg Eur Vol* **32**(3): 289-95.
- Henn, R. F., 3rd, C. E. Kuo, et al. (2010). "Augmentation of Zone II Flexor Tendon Repair Using Growth Differentiation Factor 5 in a Rabbit Model." *J Hand Surg Am* **35**(11): 1825-32.

- Hitchcock, T. F., T. R. Light, et al. (1987). "The effect of immediate constrained digital motion on the strength of flexor tendon repairs in chickens." *J Hand Surg [Am]* **12**(4): 590-5.
- Hofer, U., J. Syfrig, et al. (1990). "Identification and characterization of a dimeric chicken fibronectin receptor. Subunit-specific monoclonal antibodies to the putative chicken alpha 5 beta 1 integrin." *J Biol Chem* **265**(24): 14561-5.
- Hohenester, E. and J. Engel (2002). "Domain structure and organisation in extracellular matrix proteins." *Matrix Biol* **21**(2): 115-28.
- Holmdahl, L. (1999). "Making and covering of surgical footprints." *Lancet* **353**(9163): 1456-7.
- Homandberg, G. A. (1987). "Characterization of the interactions of an amino-terminal fibronectin fragment with the native molecule: implications for polymerization of fibronectin." *Biopolymers* **26**(12): 2087-98.
- Homandberg, G. A., R. Meyers, et al. (1992). "Fibronectin fragments cause chondrolysis of bovine articular cartilage slices in culture." *J Biol Chem* **267**(6): 3597-604.
- Huang, H., R. D. Kamm, et al. (2004). "Cell mechanics and mechanotransduction: pathways, probes, and physiology." *Am J Physiol Cell Physiol* **287**(1): C1-11.
- Humphries, J. D., A. Byron, et al. (2006). "Integrin ligands at a glance." *J Cell Sci* **119**(Pt 19): 3901-3.
- Hung, C. F., T. F. Huang, et al. (2005). "(-)-Epigallocatechin-3-gallate, a polyphenolic compound from green tea, inhibits fibroblast adhesion and migration through multiple mechanisms." *J Cell Biochem* **96**(1): 183-97.

- Huttenlocher, A., R. R. Sandborg, et al. (1995). "Adhesion in cell migration." *Curr Opin Cell Biol* **7**(5): 697-706.
- Huveneers, S., H. Truong, et al. (2008). "Binding of soluble fibronectin to integrin alpha5 beta1 - link to focal adhesion redistribution and contractile shape." *J Cell Sci* **121**(Pt 15): 2452-62.
- Hynes, R. O. (1990). *Fibronectins*. New York, Springer-Verlag.
- Hynes, R. O. (2009). "The extracellular matrix: not just pretty fibrils." *Science* **326**(5957): 1216-9.
- Hynes, R. O. and K. M. Yamada (1982). "Fibronectins: multifunctional modular glycoproteins." *J Cell Biol* **95**(2 Pt 1): 369-77.
- Ingber, D. (1991). "Integrins as mechanochemical transducers." *Curr Opin Cell Biol* **3**(5): 841-8.
- Ishiyama, N., T. Moro, et al. (2010). "The prevention of peritendinous adhesions by a phospholipid polymer hydrogel formed in situ by spontaneous intermolecular interactions." *Biomaterials* **31**(14): 4009-16.
- Isik, S., S. Ozturk, et al. (1999). "Prevention of restrictive adhesions in primary tendon repair by HA-membrane: experimental research in chickens." *Br J Plast Surg* **52**(5): 373-9.
- Iwuagwu, F. C. and D. A. McGrouther (1998). "Early cellular response in tendon injury: the effect of loading." *Plast Reconstr Surg* **102**(6): 2064-71.
- James, R., G. Kesturu, et al. (2008). "Tendon: biology, biomechanics, repair, growth factors, and evolving treatment options." *J Hand Surg Am* **33**(1): 102-12.
- Jeekel, H. (1997). "Cost implications of adhesions as highlighted in a European study." *Eur J Surg Suppl* **163**(579): 43-5.



- Johansson, S., G. Svineng, et al. (1997). "Fibronectin-integrin interactions." *Front Biosci* **2**: d126-46.
- Jokinen, J., E. Dadu, et al. (2004). "Integrin-mediated cell adhesion to type I collagen fibrils." *J Biol Chem* **279**(30): 31956-63.
- Jones, M. E., S. Burnett, et al. (2002). "The role of human-derived fibrin sealant in the reduction of postoperative flexor tendon adhesion formation in rabbits." *J Hand Surg [Br]* **27**(3): 278-82.
- Jones, M. E., K. Ladhani, et al. (2000). "Flexor tendon blood vessels." *J Hand Surg [Br]* **25**(6): 552-9.
- Jones, M. E., V. Mudera, et al. (2003). "The early surface cell response to flexor tendon injury." *J Hand Surg [Am]* **28**(2): 221-30.
- Jozsa, L., Kannus, P. (1997). "Human tendons: Anatomy, Physiology and Pathology. Human Kinetics, Champaign, IL."
- Juncosa-Melvin, N., K. S. Matlin, et al. (2007). "Mechanical stimulation increases collagen type I and collagen type III gene expression of stem cell-collagen sponge constructs for patellar tendon repair." *Tissue Eng* **13**(6): 1219-26.
- Kakar, S., U. Khan, et al. (1998). "Differential cellular response within the rabbit tendon unit following tendon injury." *J Hand Surg [Br]* **23**(5): 627-32.
- Kato, R., S. Kamiya, et al. (2001). "The fibronectin-derived antiadhesive peptides suppress the myofibroblastic conversion of rat hepatic stellate cells." *Exp Cell Res* **265**(1): 54-63.
- Katz, B. Z. and K. M. Yamada (1997). "Integrins in morphogenesis and signaling." *Biochimie* **79**(8): 467-76.

- Katz, B. Z., E. Zamir, et al. (2000). "Physical state of the extracellular matrix regulates the structure and molecular composition of cell-matrix adhesions." *Mol Biol Cell* **11**(3): 1047-60.
- Katz, J. L., A. Misra, et al. (2007). "Multiscale mechanics of hierarchical structure/property relationships in calcified tissues and tissue/material interfaces." *Mater Sci Eng A Struct Mater* **27**(3): 450-468.
- Katzel, E. B., M. Wolenski, et al. (2010). "Impact of Smad3 loss of function on scarring and adhesion formation during tendon healing." *J Orthop Res*.
- Khan, U., J. C. Edwards, et al. (1996). "Patterns of cellular activation after tendon injury." *J Hand Surg [Br]* **21**(6): 813-20.
- Khan, U., S. Kakar, et al. (2000). "Modulation of the formation of adhesions during the healing of injured tendons." *J Bone Joint Surg Br* **82**(7): 1054-8.
- Khan, U., N. L. Occleston, et al. (1997). "Single exposures to 5-fluorouracil: a possible mode of targeted therapy to reduce contractile scarring in the injured tendon." *Plast Reconstr Surg* **99**(2): 465-71.
- Khan, U., N. L. Occleston, et al. (1998). "Differences in proliferative rate and collagen lattice contraction between endotenon and synovial fibroblasts." *J Hand Surg [Am]* **23**(2): 266-73.
- Khanna, A., N. Gougoulas, et al. (2009). "Modalities in prevention of flexor tendon adhesion in the hand: what have we achieved so far?" *Acta Orthop Belg* **75**(4): 433-44.
- King, V. R., M. Henseler, et al. (2003). "Mats made from fibronectin support oriented growth of axons in the damaged spinal cord of the adult rat." *Exp Neurol* **182**(2): 383-98.

- Kitis, P. T., N. Buker, et al. (2009). "Comparison of two methods of controlled mobilisation of repaired flexor tendons in zone 2." *Scand J Plast Reconstr Surg Hand Surg* **43**(3): 160-5.
- Kitsis, C. K., P. J. Wade, et al. (1998). "Controlled active motion following primary flexor tendon repair: a prospective study over 9 years." *J Hand Surg [Br]* **23**(3): 344-9.
- Kjaer, M. (2004). "Role of extracellular matrix in adaptation of tendon and skeletal muscle to mechanical loading." *Physiol Rev* **84**(2): 649-98.
- Klass, B. R., O. A. Branford, et al. (2010). "The effect of epigallocatechin-3-gallate, a constituent of green tea, on transforming growth factor-beta1-stimulated wound contraction." *Wound Repair Regen* **18**(1): 80-8.
- Klass, B. R., K. J. Rolfe, et al. (2009). "In vitro flexor tendon cell response to TGF-beta1: a gene expression study." *J Hand Surg Am* **34**(3): 495-503.
- Klein, M. B., H. Pham, et al. (2001). "Flexor tendon wound healing in vitro: the effect of lactate on tendon cell proliferation and collagen production." *J Hand Surg [Am]* **26**(5): 847-54.
- Kubota, H., P. R. Manske, et al. (1996). "Effect of motion and tension on injured flexor tendons in chickens." *J Hand Surg [Am]* **21**(3): 456-63.
- Kulick, M. I., R. Brazlow, et al. (1984). "Injectable ibuprofen: preliminary evaluation of its ability to decrease peritendinous adhesions." *Ann Plast Surg* **13**(6): 459-67.
- Kulick, M. I., S. Smith, et al. (1986). "Oral ibuprofen: evaluation of its effect on peritendinous adhesions and the breaking strength of a tenorrhaphy." *J Hand Surg [Am]* **11**(1): 110-20.

- Kurkinen, M., A. Vaheri, et al. (1980). "Sequential appearance of fibronectin and collagen in experimental granulation tissue." *Lab Invest* **43**(1): 47-51.
- LaFlamme, S. E., S. K. Akiyama, et al. (1992). "Regulation of fibronectin receptor distribution." *J Cell Biol* **117**(2): 437-47.
- Lane, J. M., F. W. Bora, Jr., et al. (1975). "cis-hydroxyproline limits work necessary to flex a digit after tendon injury." *Clin Orthop Relat Res*(109): 193-200.
- Larson, B. J., M. T. Longaker, et al. (2010). "Scarless fetal wound healing: a basic science review." *Plast Reconstr Surg* **126**(4): 1172-80.
- Lauffenburger, D. A. and A. F. Horwitz (1996). "Cell migration: a physically integrated molecular process." *Cell* **84**(3): 359-69.
- Lee, D. A. and D. L. Bader (1997). "Compressive strains at physiological frequencies influence the metabolism of chondrocytes seeded in agarose." *J Orthop Res* **15**(2): 181-8.
- Lee, H. (1990). "Double loop locking suture: a technique of tendon repair for early active mobilization. Part II: Clinical experience." *J Hand Surg [Am]* **15**(6): 953-8.
- Lee, J. Y., C. Jones, et al. (2006). "Analysis of local tissue-specific gene expression in cellular micropatterns." *Anal Chem* **78**(24): 8305-12.
- Li, F., B. Li, et al. (2008). "Cell shape regulates collagen type I expression in human tendon fibroblasts." *Cell Motil Cytoskeleton* **65**(4): 332-41.
- Liakakos, T., N. Thomakos, et al. (2001). "Peritoneal adhesions: etiology, pathophysiology, and clinical significance. Recent advances in prevention and management." *Dig Surg* **18**(4): 260-73.
- Lin, T. W., L. Cardenas, et al. (2004). "Biomechanics of tendon injury and repair." *J Biomech* **37**(6): 865-77.

- Lin, Y. L., H. Moolenaar, et al. (2006). "Effect of microcurrent electrical tissue stimulation on equine tenocytes in culture." *Am J Vet Res* **67**(2): 271-6.
- Lindsay, W. K. and F. G. Walker (1961). "The effect of an antihistamine (promethazine) on digital flexor tendon healing in the chicken." *Plast Reconstr Surg* **28**: 634-48.
- Lister, G. D., H. E. Kleinert, et al. (1977). "Primary flexor tendon repair followed by immediate controlled mobilization." *J Hand Surg [Am]* **2**(6): 441-51.
- Liu, S., D. A. Calderwood, et al. (2000). "Integrin cytoplasmic domain-binding proteins." *J Cell Sci* **113** ( Pt 20): 3563-71.
- Liu, Y., A. Skardal, et al. (2008). "Prevention of peritendinous adhesions using a hyaluronan-derived hydrogel film following partial-thickness flexor tendon injury." *J Orthop Res* **26**(4): 562-9.
- Lorenz, H. P. a. M. T. L. (2003). "Wounds: Biology, Pathology, and Management." In: *Surgery: Scientific Basis and Current Practice*. Norton JA, Bollinger RR, Chang AE, Lowry SF, Mulvihill SJ, Pass HI and Thompson RW (eds.), Springer-Verlag, New York, 2000.(Chapter 7): Pages 77-88.
- Lundborg, G. (1976). "Experimental flexor tendon healing without adhesion formation--a new concept of tendon nutrition and intrinsic healing mechanisms. A preliminary report." *Hand* **8**(3): 235-8.
- Lundborg, G., S. Holm, et al. (1980). "The role of the synovial fluid and tendon sheath for flexor tendon nutrition. An experimental tracer study on diffusional pathways in dogs." *Scand J Plast Reconstr Surg* **14**(1): 99-107.
- Lundborg, G. and F. Rank (1978). "Experimental intrinsic healing of flexor tendons based upon synovial fluid nutrition." *J Hand Surg [Am]* **3**(1): 21-31.

- Lundborg, G., F. Rank, et al. (1985). "Intrinsic tendon healing. A new experimental model." *Scand J Plast Reconstr Surg* **19**(2): 113-7.
- Lutz, R., T. Sakai, et al. (2010). "Pericellular fibronectin is required for RhoA-dependent responses to cyclic strain in fibroblasts." *J Cell Sci* **123**(Pt 9): 1511-21.
- Maeda, E., J. C. Shelton, et al. (2009). "Differential regulation of gene expression in isolated tendon fascicles exposed to cyclic tensile strain in vitro." *J Appl Physiol* **106**(2): 506-12.
- Magnusson, M. K. and D. F. Mosher (1998). "Fibronectin: structure, assembly, and cardiovascular implications." *Arterioscler Thromb Vasc Biol* **18**(9): 1363-70.
- Malaviya, P., D. L. Butler, et al. (1998). "In vivo tendon forces correlate with activity level and remain bounded: evidence in a rabbit flexor tendon model." *J Biomech* **31**(11): 1043-9.
- Manske, P. R., R. H. Gelberman, et al. (1985). "Flexor tendon healing." *Hand Clin* **1**(1): 25-34.
- Manske, P. R., R. H. Gelberman, et al. (1984). "Intrinsic flexor-tendon repair. A morphological study in vitro." *J Bone Joint Surg Am* **66**(3): 385-96.
- Manske, P. R. and P. A. Lesker (1984). "Biochemical evidence of flexor tendon participation in the repair process--an in vitro study." *J Hand Surg [Br]* **9**(2): 117-20.
- Manske, P. R. and P. A. Lesker (1984). "Histologic evidence of intrinsic flexor tendon repair in various experimental animals. An in vitro study." *Clin Orthop Relat Res*(182): 297-304.
- Manske, P. R., P. A. Lesker, et al. (1985). "Intrinsic restoration of the flexor tendon surface in the nonhuman primate." *J Hand Surg [Am]* **10**(5): 632-7.

- Maskarinec, S. A. and D. A. Tirrell (2005). Protein engineering approaches to biomaterials design. *Curr Opin Biotechnol.* **16**: 422-6.
- Mass, D. P. and R. Tuel (1989). "Human flexor tendon participation in the in vitro repair process." *J Hand Surg [Am]* **14**(1): 64-71.
- Mass, D. P. and R. J. Tuel (1990). "Participation of human superficialis flexor tendon segments in repair in vitro." *J Orthop Res* **8**(1): 21-34.
- Mass, D. P. and R. J. Tuel (1991). "Intrinsic healing of the laceration site in human superficialis flexor tendons in vitro." *J Hand Surg [Am]* **16**(1): 24-30.
- Masuda, K., S. Ishii, et al. (2002). "Biochemical analysis of collagen in adhesive tissues formed after digital flexor tendon injuries." *J Orthop Sci* **7**(6): 665-71.
- Matthew, C., M. J. Moore, et al. (1987). "A quantitative ultrastructural study of collagen fibril formation in the healing extensor digitorum longus tendon of the rat." *J Hand Surg [Br]* **12**(3): 313-20.
- Matthews, P. and H. Richards (1974). "The repair potential of digital flexor tendons. An experimental study." *J Bone Joint Surg Br* **56-B**(4): 618-25.
- Matthews, P. and H. Richards (1975). "The repair reaction of flexor tendon within the digital sheath." *Hand* **7**(1): 27-9.
- Matthews, P. and H. Richards (1976). "Factors in the adherence of flexor tendon after repair: an experimental study in the rabbit." *J Bone Joint Surg Br* **58**(2): 230-6.
- May, E. J. and K. L. Silfverskiold (1993). "Rate of recovery after flexor tendon repair in zone II. A prospective longitudinal study of 145 digits." *Scand J Plast Reconstr Surg Hand Surg* **27**(2): 89-94.
- Mayne, R. and R. G. Brewton (1993). "New members of the collagen superfamily." *Curr Opin Cell Biol* **5**(5): 883-90.

- McBeath, R., D. M. Pirone, et al. (2004). "Cell shape, cytoskeletal tension, and RhoA regulate stem cell lineage commitment." *Dev Cell* **6**(4): 483-95.
- McCarthy, J. B., A. P. Skubitz, et al. (1990). "RGD-independent cell adhesion to the carboxy-terminal heparin-binding fragment of fibronectin involves heparin-dependent and -independent activities." *J Cell Biol* **110**(3): 777-87.
- McNeilly, C. M., A. J. Banes, et al. (1996). "Tendon cells in vivo form a three dimensional network of cell processes linked by gap junctions." *J Anat* **189** (Pt 3): 593-600.
- Mentzel, M., H. Hoss, et al. (2000). "The effectiveness of ADCON-T/N, a new anti-adhesion barrier gel, in fresh divisions of the flexor tendons in Zone II." *J Hand Surg [Br]* **25**(6): 590-2.
- Menzies, D. and H. Ellis (1990). "Intestinal obstruction from adhesions--how big is the problem?" *Ann R Coll Surg Engl* **72**(1): 60-3.
- Menzies, D., M. Parker, et al. (2001). "Small bowel obstruction due to postoperative adhesions: treatment patterns and associated costs in 110 hospital admissions." *Ann R Coll Surg Engl* **83**(1): 40-6.
- Meredith, J. E., Jr. and M. A. Schwartz (1997). "Integrins, adhesion and apoptosis." *Trends Cell Biol* **7**(4): 146-50.
- Messina, A. (1992). "The double armed suture: tendon repair with immediate mobilization of the fingers." *J Hand Surg [Am]* **17**(1): 137-42.
- Michalopoulos, G. K. (2007). "Liver regeneration." *J Cell Physiol* **213**(2): 286-300.
- Millward-Sadler, S. J., M. O. Wright, et al. (2000). "Mechanotransduction via integrins and interleukin-4 results in altered aggrecan and matrix metalloproteinase 3 gene expression in normal, but not osteoarthritic, human articular chondrocytes." *Arthritis Rheum* **43**(9): 2091-9.



- Millward-Sadler, S. J., M. O. Wright, et al. (2000). "Altered electrophysiological responses to mechanical stimulation and abnormal signalling through  $\alpha 5 \beta 1$  integrin in chondrocytes from osteoarthritic cartilage." *Osteoarthritis Cartilage* **8**(4): 272-8.
- Miyamoto, S., B. Z. Katz, et al. (1998). "Fibronectin and integrins in cell adhesion, signaling, and morphogenesis." *Ann N Y Acad Sci* **857**: 119-29.
- Mooney, D. J., R. Langer, et al. (1995). "Cytoskeletal filament assembly and the control of cell spreading and function by extracellular matrix." *J Cell Sci* **108** ( Pt 6): 2311-20.
- Mooradian, D. L., J. B. McCarthy, et al. (1992). "Rabbit corneal epithelial cells adhere to two distinct heparin-binding synthetic peptides derived from fibronectin." *Invest Ophthalmol Vis Sci* **33**(11): 3034-40.
- Mould, A. P. and M. J. Humphries (1991). "Identification of a novel recognition sequence for the integrin  $\alpha 4 \beta 1$  in the COOH-terminal heparin-binding domain of fibronectin." *Embo J* **10**(13): 4089-95.
- Mould, A. P., A. Komoriya, et al. (1991). "The CS5 peptide is a second site in the IIICS region of fibronectin recognized by the integrin  $\alpha 4 \beta 1$ . Inhibition of  $\alpha 4 \beta 1$  function by RGD peptide homologues." *J Biol Chem* **266**(6): 3579-85.
- Munevar, S., Y. L. Wang, et al. (2001). "Distinct roles of frontal and rear cell-substrate adhesions in fibroblast migration." *Mol Biol Cell* **12**(12): 3947-54.
- Munro, I. R., W. K. Lindsay, et al. (1970). "A synchronous study of collagen and mucopolysaccharide in healing flexor tendons of chickens." *Plast Reconstr Surg* **45**(5): 493-501.

- Murrell, G. A., E. G. Lilly, 3rd, et al. (1994). "Effects of immobilization on Achilles tendon healing in a rat model." *J Orthop Res* **12**(4): 582-91.
- Mutsaers, S. E., J. E. Bishop, et al. (1997). "Mechanisms of tissue repair: from wound healing to fibrosis." *Int J Biochem Cell Biol* **29**(1): 5-17.
- Nagai, T., N. Yamakawa, et al. (1991). "Monoclonal antibody characterization of two distant sites required for function of the central cell-binding domain of fibronectin in cell adhesion, cell migration, and matrix assembly." *J Cell Biol* **114**(6): 1295-305.
- Namba, J., K. Shimada, et al. (2007). "Modulation of peritendinous adhesion formation by alginate solution in a rabbit flexor tendon model." *J Biomed Mater Res B Appl Biomater* **80**(1): 273-9.
- Ng, C. P., B. Hinz, et al. (2005). "Interstitial fluid flow induces myofibroblast differentiation and collagen alignment in vitro." *J Cell Sci* **118**(Pt 20): 4731-9.
- Ngo, M., H. Pham, et al. (2001). "Differential expression of transforming growth factor-beta receptors in a rabbit zone II flexor tendon wound healing model." *Plast Reconstr Surg* **108**(5): 1260-7.
- Nykvist, P., H. Tu, et al. (2000). "Distinct recognition of collagen subtypes by alpha(1)beta(1) and alpha(2)beta(1) integrins. Alpha(1)beta(1) mediates cell adhesion to type XIII collagen." *J Biol Chem* **275**(11): 8255-61.
- Nyska, M., S. Porat, et al. (1987). "Decreased adhesion formation in flexor tendons by topical application of enriched collagen solution--a histological study." *Arch Orthop Trauma Surg* **106**(3): 192-4.

- Obara, M., M. S. Kang, et al. (1988). "Site-directed mutagenesis of the cell-binding domain of human fibronectin: separable, synergistic sites mediate adhesive function." *Cell* **53**(4): 649-57.
- Oharazawa, H., N. Ibaraki, et al. (2005). "Inhibitory effects of Arg-Gly-Asp (RGD) peptide on cell attachment and migration in a human lens epithelial cell line." *Ophthalmic Res* **37**(4): 191-6.
- Ozboluk, S., Y. Ozkan, et al. (2010). "The effects of human amniotic membrane and periosteal autograft on tendon healing: experimental study in rabbits." *J Hand Surg Eur Vol* **35**(4): 262-8.
- Paczek, L., W. Michalska, et al. (2008). "Trypsin, elastase, plasmin and MMP-9 activity in the serum during the human ageing process." *Age Ageing* **37**(3): 318-23.
- Palecek, S. P., J. C. Loftus, et al. (1997). "Integrin-ligand binding properties govern cell migration speed through cell-substratum adhesiveness." *Nature* **385**(6616): 537-40.
- Palmes, D., H. U. Spiegel, et al. (2002). "Achilles tendon healing: long-term biomechanical effects of postoperative mobilization and immobilization in a new mouse model." *J Orthop Res* **20**(5): 939-46.
- Pankov, R., E. Cukierman, et al. (2000). "Integrin dynamics and matrix assembly: tensin-dependent translocation of alpha(5)beta(1) integrins promotes early fibronectin fibrillogenesis." *J Cell Biol* **148**(5): 1075-90.
- Pankov, R. and K. M. Yamada (2002). "Fibronectin at a glance." *J Cell Sci* **115**(Pt 20): 3861-3.
- Papadopoulos, F., M. Spinelli, et al. (2007). "Common tasks in microscopic and ultrastructural image analysis using ImageJ." *Ultrastruct Pathol* **31**(6): 401-7.

- Park, J. C., B. J. Park, et al. (2001). "Comparative study on motility of the cultured fetal and neonatal dermal fibroblasts in extracellular matrix." *Yonsei Med J* **42**(6): 587-94.
- Parsons, J. T. (2003). "Focal adhesion kinase: the first ten years." *J Cell Sci* **116**(Pt 8): 1409-16.
- Parsons, M., E. Kessler, et al. (1999). "Mechanical load enhances procollagen processing in dermal fibroblasts by regulating levels of procollagen C-proteinase." *Exp Cell Res* **252**(2): 319-31.
- Peacock, E. E., Jr. (1965). "Some Technical Aspects and Results of Flexor Tendon Repair." *Surgery* **58**: 330-42.
- Peacock, E. E., Jr. and J. W. Madden (1969). "Some studies on the effects of beta-aminopropionitrile in patients with injured flexor tendons." *Surgery* **66**(1): 215-23.
- Peck, F. H., C. A. Bucher, et al. (1998). "A comparative study of two methods of controlled mobilization of flexor tendon repairs in zone 2." *J Hand Surg [Br]* **23**(1): 41-5.
- Phillips, G. F., D. A. McGrouther, et al. (1985). "Finger mobility following flexor tendon repair." *J Hand Surg [Br]* **10**(3): 337-9.
- Phillips, J. B., V. R. King, et al. (2004). "Fluid shear in viscous fibronectin gels allows aggregation of fibrous materials for CNS tissue engineering." *Biomaterials* **25**(14): 2769-79.
- Pierschbacher, M. D. and E. Ruoslahti (1984). "Cell attachment activity of fibronectin can be duplicated by small synthetic fragments of the molecule." *Nature* **309**(5963): 30-3.

- Pierschbacher, M. D. and E. Ruoslahti (1984). "Variants of the cell recognition site of fibronectin that retain attachment-promoting activity." *Proc Natl Acad Sci U S A* **81**(19): 5985-8.
- Potenza, A. D. (1962). "Tendon healing within the flexor digital sheath in the dog." *J Bone Joint Surg Am* **44-A**: 49-64.
- Potenza, A. D. (1963). "Critical Evaluation of Flexor-Tendon Healing and Adhesion Formation within Artificial Digital Sheaths." *J Bone Joint Surg Am* **45**: 1217-33.
- Potenza, A. D. (1964). "The Healing of Autogenous Tendon Grafts within the Flexor Digital Sheath in Dogs." *J Bone Joint Surg Am* **46**: 1462-84.
- Potenza, A. D. and M. C. Herte (1982). "The synovial cavity as a "tissue culture in situ"--science or nonsense?" *J Hand Surg [Am]* **7**(2): 196-9.
- Priestley, J. V., M. S. Ramer, et al. (2002). "Stimulating regeneration in the damaged spinal cord." *J Physiol Paris* **96**(1-2): 123-33.
- Qin, Z., M. J. Buehler, et al. (2010). "A multi-scale approach to understand the mechanobiology of intermediate filaments." *J Biomech* **43**(1): 15-22.
- Ragoowansi, R., U. Khan, et al. (2003). "Differences in morphology, cytoskeletal architecture and protease production between zone II tendon and synovial fibroblasts in vitro." *J Hand Surg [Br]* **28**(5): 465-70.
- Regent, M., E. Planus, et al. (2010). "Specificities of beta(1) integrin signaling in the control of cell adhesion and adhesive strength." *Eur J Cell Biol*.
- Riboh, J., A. K. Chong, et al. (2008). "Optimization of flexor tendon tissue engineering with a cyclic strain bioreactor." *J Hand Surg Am* **33**(8): 1388-96.

- Riederer-Henderson, M. A., A. Gauger, et al. (1983). "Attachment and extracellular matrix differences between tendon and synovial fibroblastic cells." *In Vitro* **19**(2): 127-33.
- Riveline, D., E. Zamir, et al. (2001). "Focal contacts as mechanosensors: externally applied local mechanical force induces growth of focal contacts by an mDial1-dependent and ROCK-independent mechanism." *J Cell Biol* **153**(6): 1175-86.
- Rocco, M., M. Carson, et al. (1983). "Dependence of the shape of the plasma fibronectin molecule on solvent composition. Ionic strength and glycerol content." *J Biol Chem* **258**(23): 14545-9.
- Rosales, C., V. O'Brien, et al. (1995). "Signal transduction by cell adhesion receptors." *Biochim Biophys Acta* **1242**(1): 77-98.
- Ross, R. (1975). "Connective tissue cells, cell proliferation and synthesis of extracellular matrix-a review." *Philos Trans R Soc Lond B Biol Sci* **271**(912): 247-59.
- Rosso, F., A. Giordano, et al. (2004). "From cell-ECM interactions to tissue engineering." *J Cell Physiol* **199**(2): 174-80.
- Rowlatt, U. (1979). "Intrauterine wound healing in a 20 week human fetus." *Virchows Arch A Pathol Anat Histol* **381**(3): 353-61.
- Ruoslahti, E. (1996). "RGD and other recognition sequences for integrins." *Annu Rev Cell Dev Biol* **12**: 697-715.
- Ruoslahti, E., E. G. Hayman, et al. (1980). "Molecular interactions of fibronectin." *Prog Clin Biol Res* **41**: 821-8.
- Ruoslahti, E., E. G. Hayman, et al. (1981). "Alignment of biologically active domains in the fibronectin molecule." *J Biol Chem* **256**(14): 7277-81.

- Ruoslahti, E., E. G. Hayman, et al. (1982). "Fibronectin: purification, immunochemical properties, and biological activities." *Methods Enzymol* **82 Pt A**: 803-31.
- Russell, J. E. and P. R. Manske (1990). "Collagen synthesis during primate flexor tendon repair in vitro." *J Orthop Res* **8**(1): 13-20.
- Sakata, N., Y. Sasatomi, et al. (2000). "Possible involvement of altered RGD sequence in reduced adhesive and spreading activities of advanced glycation and product-modified fibronectin to vascular smooth muscle cells." *Connect Tissue Res* **41**(3): 213-28.
- Salter, D. M., J. E. Robb, et al. (1997). "Electrophysiological responses of human bone cells to mechanical stimulation: evidence for specific integrin function in mechanotransduction." *J Bone Miner Res* **12**(7): 1133-41.
- Salti, N. I., R. J. Tuel, et al. (1993). "Effect of hyaluronic acid on rabbit profundus flexor tendon healing in vitro." *J Surg Res* **55**(4): 411-5.
- Samiric, T., M. Z. Ilic, et al. (2004). "Characterisation of proteoglycans and their catabolic products in tendon and explant cultures of tendon." *Matrix Biol* **23**(2): 127-40.
- Santas, A. J., J. A. Peterson, et al. (2002). "Alternative splicing of the IIIICS domain in fibronectin governs the role of the heparin II domain in fibrillogenesis and cell spreading." *J Biol Chem* **277**(16): 13650-8.
- Savage, R. and G. Risitano (1989). "Flexor tendon repair using a "six strand" method of repair and early active mobilisation." *J Hand Surg [Br]* **14**(4): 396-9.
- Schinagl, R. M., D. Gurskis, et al. (1997). "Depth-dependent confined compression modulus of full-thickness bovine articular cartilage." *J Orthop Res* **15**(4): 499-506.

- Schnabel, L. V., M. E. Lynch, et al. (2009). "Mesenchymal stem cells and insulin-like growth factor-I gene-enhanced mesenchymal stem cells improve structural aspects of healing in equine flexor digitorum superficialis tendons." *J Orthop Res* **27**(10): 1392-8.
- Schor, S. L., I. Ellis, et al. (1996). "Subpopulations of fetal-like gingival fibroblasts: characterisation and potential significance for wound healing and the progression of periodontal disease." *Oral Dis* **2**(2): 155-66.
- Schultz, G. S. and A. Wysocki (2009). "Interactions between extracellular matrix and growth factors in wound healing." *Wound Repair Regen* **17**(2): 153-62.
- Schwartz, M. A. (2001). "Integrin signaling revisited." *Trends Cell Biol* **11**(12): 466-70.
- Schwarzbauer, J. E. (1991). "Fibronectin: from gene to protein." *Curr Opin Cell Biol* **3**(5): 786-91.
- Scott, R. J., P. A. Hall, et al. (1991). "A comparison of immunohistochemical markers of cell proliferation with experimentally determined growth fraction." *J Pathol* **165**(2): 173-8.
- Scovill, W. A., T. M. Saba, et al. (1978). "Opsonic alpha2 surface binding glycoprotein therapy during sepsis." *Ann Surg* **188**(4): 521-9.
- Screen, H. R., D. A. Lee, et al. (2003). "Development of a technique to determine strains in tendons using the cell nuclei." *Biorheology* **40**(1-3): 361-8.
- Screen, H. R., D. A. Lee, et al. (2004). "An investigation into the effects of the hierarchical structure of tendon fascicles on micromechanical properties." *Proc Inst Mech Eng H* **218**(2): 109-19.



- Screen, H. R., J. C. Shelton, et al. (2005). "Cyclic tensile strain upregulates collagen synthesis in isolated tendon fascicles." *Biochem Biophys Res Commun* **336**(2): 424-9.
- Screen, H. R. C., Bader, D. L., Lee, D. A., Shelton, J. C. (2004). "Local strain measurement within tendon." *Strain* **40**(4): 157-163.
- Sekiguchi, K., A. Siri, et al. (1985). "Differences in domain structure between human fibronectins isolated from plasma and from culture supernatants of normal and transformed fibroblasts. Studies with domain-specific antibodies." *J Biol Chem* **260**(8): 5105-14.
- Sethi, K. K., V. Mudera, et al. (2002). "Contraction-mediated pinocytosis of RGD-peptide by dermal fibroblasts: inhibition of matrix attachment blocks contraction and disrupts microfilament organisation." *Cell Motil Cytoskeleton* **52**(4): 231-41.
- Sethi, K. K., I. V. Yannas, et al. (2002). "Evidence for sequential utilization of fibronectin, vitronectin, and collagen during fibroblast-mediated collagen contraction." *Wound Repair Regen* **10**(6): 397-408.
- Sharma, P. and N. Maffulli (2005). "Tendon injury and tendinopathy: healing and repair." *J Bone Joint Surg Am* **87**(1): 187-202.
- Sharma, P. and N. Maffulli (2006). "Biology of tendon injury: healing, modeling and remodeling." *J Musculoskelet Neuronal Interact* **6**(2): 181-90.
- Shattil, S. J., C. Kim, et al. (2010). "The final steps of integrin activation: the end game." *Nat Rev Mol Cell Biol* **11**(4): 288-300.
- Shelton, J. C., D. L. Bader, et al. (2003). "Mechanical conditioning influences the metabolic response of cell-seeded constructs." *Cells Tissues Organs* **175**(3): 140-50.

- Shimo-Oka, T., Y. Hasegawa, et al. (1988). "Differential properties of attachment of human fibroblasts to various extracellular matrix proteins." *Cell Struct Funct* **13**(6): 515-24.
- Siddiqi, N. A., Y. Hamada, et al. (1995). "Effects of hydroxyapatite and alumina sheaths on postoperative peritendinous adhesions in chickens." *J Appl Biomater* **6**(1): 43-53.
- Silfverskiold, K. L., E. J. May, et al. (1993). "Factors affecting results after flexor tendon repair in zone II: a multivariate prospective analysis." *J Hand Surg [Am]* **18**(4): 654-62.
- Singer, II, S. Scott, et al. (1988). "Cell surface distribution of fibronectin and vitronectin receptors depends on substrate composition and extracellular matrix accumulation." *J Cell Biol* **106**(6): 2171-82.
- Singhvi, R., A. Kumar, et al. (1994). "Engineering cell shape and function." *Science* **264**(5159): 696-8.
- Skoog, T. and B. H. Persson (1954). "An experimental study of the early healing of tendons." *Plast Reconstr Surg* (1946) **13**(5): 384-99.
- Skorstengaard, K., M. S. Jensen, et al. (1986). "Purification and complete primary structures of the heparin-, cell-, and DNA-binding domains of bovine plasma fibronectin." *Eur J Biochem* **154**(1): 15-29.
- Slack, C., M. H. Flint, et al. (1984). "The effect of tensional load on isolated embryonic chick tendons in organ culture." *Connect Tissue Res* **12**(3-4): 229-47.
- Small, J. O., M. D. Brennen, et al. (1989). "Early active mobilisation following flexor tendon repair in zone 2." *J Hand Surg [Br]* **14**(4): 383-91.

- Smith, P. K., R. I. Krohn, et al. (1985). "Measurement of protein using bicinchoninic acid." *Anal Biochem* **150**(1): 76-85.
- Sottile, J., D. C. Hocking, et al. (2000). "Fibronectin polymerization stimulates cell growth by RGD-dependent and -independent mechanisms." *J Cell Sci* **113 Pt 23**: 4287-99.
- Spalazzi, J. P., M. C. Vyner, et al. (2008). "Mechanoactive scaffold induces tendon remodeling and expression of fibrocartilage markers." *Clin Orthop Relat Res* **466**(8): 1938-48.
- Speer, D. P., S. Feldman, et al. (1985). "The control of peritendinous adhesions using topical beta-aminopropionitrile base." *J Surg Res* **38**(3): 252-7.
- Stack, M. S. and S. V. Pizzo (1993). "Modulation of tissue plasminogen activator-catalyzed plasminogen activation by synthetic peptides derived from the amino-terminal heparin binding domain of fibronectin." *J Biol Chem* **268**(25): 18924-8.
- Stadelmann, W. K., A. G. Digenis, et al. (1998). "Physiology and healing dynamics of chronic cutaneous wounds." *Am J Surg* **176**(2A Suppl): 26S-38S.
- Stark, H. H., J. H. Boyes, et al. (1977). "The use of paratenon, polyethylene film, or silastic sheeting to prevent restricting adhesions to tendons in the hand." *J Bone Joint Surg Am* **59**(7): 908-13.
- Stephens, D. J. and V. J. Allan (2003). "Light microscopy techniques for live cell imaging." *Science* **300**(5616): 82-6.
- Stopak, D., N. K. Wessells, et al. (1985). "Morphogenetic rearrangement of injected collagen in developing chicken limb buds." *Proc Natl Acad Sci U S A* **82**(9): 2804-8.

- Strauch, B. and W. de Moura (1985). "Digital flexor tendon sheath: an anatomic study." *J Hand Surg [Am]* **10**(6 Pt 1): 785-9.
- Streeter, H. B. and D. A. Rees (1987). "Fibroblast adhesion to RGDS shows novel features compared with fibronectin." *J Cell Biol* **105**(1): 507-15.
- Strick, M. J., S. L. Filan, et al. (2004). "Adhesion formation after flexor tendon repair: a histologic and biomechanical comparison of 2- and 4-strand repairs in a chicken model." *J Hand Surg [Am]* **29**(1): 15-21.
- Strickland, J. W. (1985). "Results of flexor tendon surgery in zone II." *Hand Clin* **1**(1): 167-79.
- Strickland, J. W. (2000). "Development of flexor tendon surgery: twenty-five years of progress." *J Hand Surg [Am]* **25**(2): 214-35.
- Strickland, J. W. (2005). "The scientific basis for advances in flexor tendon surgery." *J Hand Ther* **18**(2): 94-110; quiz 111.
- Strickland, J. W. and S. V. Glogovac (1980). "Digital function following flexor tendon repair in Zone II: A comparison of immobilization and controlled passive motion techniques." *J Hand Surg [Am]* **5**(6): 537-43.
- Sung, K. L., D. E. Whittemore, et al. (1996). "Signal pathways and ligament cell adhesiveness." *J Orthop Res* **14**(5): 729-35.
- Takai, S., S. L. Woo, et al. (1991). "The effects of frequency and duration of controlled passive mobilization on tendon healing." *J Orthop Res* **9**(5): 705-13.
- Tan, V., A. Nourbakhsh, et al. (2010). "Effects of nonsteroidal anti-inflammatory drugs on flexor tendon adhesion." *J Hand Surg Am* **35**(6): 941-7.

- Tan, W., A. Sendemir-Urkmez, et al. (2004). "Structural and functional optical imaging of three-dimensional engineered tissue development." *Tissue Eng* **10**(11-12): 1747-56.
- Tanaka, R., R. Al-Jamal, et al. (2001). "Maturation changes in extracellular matrix and lung tissue mechanics." *J Appl Physiol* **91**(5): 2314-21.
- Tang, J. B., D. Shi, et al. (1996). "Biomechanical and histologic evaluation of tendon sheath management." *J Hand Surg [Am]* **21**(5): 900-8.
- Thomopoulos, S., H. M. Kim, et al. (2010). "The effects of exogenous basic fibroblast growth factor on intrasynovial flexor tendon healing in a canine model." *J Bone Joint Surg Am* **92**(13): 2285-93.
- Thompson, J. N. and S. A. Whawell (1995). "Pathogenesis and prevention of adhesion formation." *Br J Surg* **82**(1): 3-5.
- Tipton, C. M., A. C. Vailas, et al. (1986). "Experimental studies on the influences of physical activity on ligaments, tendons and joints: a brief review." *Acta Med Scand Suppl* **711**: 157-68.
- Tseng, Y., K. M. An, et al. (2002). "Microheterogeneity controls the rate of gelation of actin filament networks." *J Biol Chem* **277**(20): 18143-50.
- Tsukada, H., X. Ying, et al. (1995). "Ligation of endothelial alpha v beta 3 integrin increases capillary hydraulic conductivity of rat lung." *Circ Res* **77**(4): 651-9.
- Tulla, M., O. T. Pentikainen, et al. (2001). "Selective binding of collagen subtypes by integrin alpha 1I, alpha 2I, and alpha 10I domains." *J Biol Chem* **276**(51): 48206-12.
- Underwood, S., A. Afoke, et al. (2001). "Wet extrusion of fibronectin-fibrinogen cables for application in tissue engineering." *Biotechnol Bioeng* **73**(4): 295-305.

- Vailas, A. C., V. A. Pedrini, et al. (1985). "Patellar tendon matrix changes associated with aging and voluntary exercise." *J Appl Physiol* **58**(5): 1572-6.
- van der Flier, A. and A. Sonnenberg (2001). "Function and interactions of integrins." *Cell Tissue Res* **305**(3): 285-98.
- Velling, T., J. Risteli, et al. (2002). "Polymerization of type I and III collagens is dependent on fibronectin and enhanced by integrins  $\alpha 11\beta 1$  and  $\alpha 2\beta 1$ ." *J Biol Chem* **277**(40): 37377-81.
- Voytik-Harbin, S. L., B. Rajwa, et al. (2001). "Three-dimensional imaging of extracellular matrix and extracellular matrix-cell interactions." *Methods Cell Biol* **63**: 583-97.
- Wang, J. H. (2006). "Mechanobiology of tendon." *J Biomech* **39**(9): 1563-82.
- Wang, J. H., F. Jia, et al. (2003). "Cell orientation determines the alignment of cell-produced collagenous matrix." *J Biomech* **36**(1): 97-102.
- Wang, N., J. P. Butler, et al. (1993). "Mechanotransduction across the cell surface and through the cytoskeleton." *Science* **260**(5111): 1124-7.
- Wang, Z., R. J. Collighan, et al. (2010). "RGD-independent cell adhesion via a tissue transglutaminase-fibronectin matrix promotes fibronectin fibril deposition and requires syndecan-4/2 and  $\{\alpha\}5\{\beta\}1$  integrin co-signalling." *J Biol Chem*.
- Watanabe, K., H. Takahashi, et al. (2000). "Interaction with heparin and matrix metalloproteinase 2 cleavage expose a cryptic anti-adhesive site of fibronectin." *Biochemistry* **39**(24): 7138-44.
- Webb, K., R. W. Hitchcock, et al. (2006). "Cyclic strain increases fibroblast proliferation, matrix accumulation, and elastic modulus of fibroblast-seeded polyurethane constructs." *J Biomech* **39**(6): 1136-44.

- Werb, Z., P. M. Tremble, et al. (1989). "Signal transduction through the fibronectin receptor induces collagenase and stromelysin gene expression." *J Cell Biol* **109**(2): 877-89.
- Whitby, D. J. and M. W. Ferguson (1991). "The extracellular matrix of lip wounds in fetal, neonatal and adult mice." *Development* **112**(2): 651-68.
- Whitworth, I. H., R. A. Brown, et al. (1995). "Orientated mats of fibronectin as a conduit material for use in peripheral nerve repair." *J Hand Surg [Br]* **20**(4): 429-36.
- Wierzbicka-Patynowski, I. and J. E. Schwarzbauer (2003). "The ins and outs of fibronectin matrix assembly." *J Cell Sci* **116**(Pt 16): 3269-76.
- Wilke, M. S., A. P. Skubitz, et al. (1991). "Human keratinocytes adhere to two distinct heparin-binding synthetic peptides derived from fibronectin." *J Invest Dermatol* **97**(3): 573-9.
- Williams, D. F., J. Black, et al. (1992). Consensus report of second conference on definitions in biomaterials. In: *Biomaterial-tissue interfaces.*, Amsterdam, Elsevier.
- Wojciak-Stothard, B., M. Denyer, et al. (1997). "Adhesion, orientation, and movement of cells cultured on ultrathin fibronectin fibers." *In Vitro Cell Dev Biol Anim* **33**(2): 110-7.
- Wong, J. K., Y. H. Lui, et al. (2009). "The cellular biology of flexor tendon adhesion formation: an old problem in a new paradigm." *Am J Pathol* **175**(5): 1938-51.
- Woo, S. L., R. H. Gelberman, et al. (1981). "The importance of controlled passive mobilization on flexor tendon healing. A biomechanical study." *Acta Orthop Scand* **52**(6): 615-22.

- Woo, S. L., M. A. Gomez, et al. (1982). "Mechanical properties of tendons and ligaments. II. The relationships of immobilization and exercise on tissue remodeling." *Biorheology* **19**(3): 397-408.
- Wozniak, M. A., K. Modzelewska, et al. (2004). "Focal adhesion regulation of cell behavior." *Biochim Biophys Acta* **1692**(2-3): 103-19.
- Xia, C., X. Yang, et al. (2009). "[Effects of TGF-beta1 neutralizing antibody on collagen production and adhesion formation of flexor tendon]." *Zhongguo Xiu Fu Chong Jian Wai Ke Za Zhi* **23**(6): 698-703.
- Xie, R. G., Y. Cao, et al. (2008). "The gliding force and work of flexion in the early days after primary repair of lacerated flexor tendons: an experimental study." *J Hand Surg Eur Vol* **33**(2): 192-6.
- Xu, Y., S. Gurusiddappa, et al. (2000). "Multiple binding sites in collagen type I for the integrins alpha1beta1 and alpha2beta1." *J Biol Chem* **275**(50): 38981-9.
- Yamada, K. M. (1983). "Cell surface interactions with extracellular materials." *Annu Rev Biochem* **52**: 761-99.
- Yamada, K. M. (2000). "Fibronectin peptides in cell migration and wound repair." *J Clin Invest* **105**(11): 1507-9.
- Yamada, K. M., S. K. Akiyama, et al. (1985). "Recent advances in research on fibronectin and other cell attachment proteins." *J Cell Biochem* **28**(2): 79-97.
- Yamada, K. M. and D. W. Kennedy (1984). "Dualistic nature of adhesive protein function: fibronectin and its biologically active peptide fragments can autoinhibit fibronectin function." *J Cell Biol* **99**(1 Pt 1): 29-36.
- Yamada, K. M. and D. W. Kennedy (1987). "Peptide inhibitors of fibronectin, laminin, and other adhesion molecules: unique and shared features." *J Cell Physiol* **130**(1): 21-8.



- Yamada, K. M., R. Pankov, et al. (2003). "Dimensions and dynamics in integrin function." *Braz J Med Biol Res* **36**(8): 959-66.
- Yamada, K. M. a. R. A. F. C. (1996). "Provisional Matrix." In *Molecular and Cellular Biology of Wound Repair* (ed. R. Clark). Plenum Press: 51-93.
- Yamada, M. and T. Okigaki (1983). "Promotion of epithelial cell adhesion on collagen by proteins from rat embryo fibroblasts." *Cell Biol Int Rep* **7**(12): 1115-21.
- Yamamoto, E., D. Kogawa, et al. (2005). "Effects of the frequency and duration of cyclic stress on the mechanical properties of cultured collagen fascicles from the rabbit patellar tendon." *J Biomech Eng* **127**(7): 1168-75.
- Yang, G., R. C. Crawford, et al. (2004). "Proliferation and collagen production of human patellar tendon fibroblasts in response to cyclic uniaxial stretching in serum-free conditions." *J Biomech* **37**(10): 1543-50.
- Yasuda, K. and K. Hayashi (1999). "Changes in biomechanical properties of tendons and ligaments from joint disuse." *Osteoarthritis Cartilage* **7**(1): 122-9.
- Yilmaz, E., M. Avci, et al. (2010). "The Effect of Seprafilm on Adhesion Formation and Tendon Healing After Flexor Tendon Repair in Chicken." *Orthopedics*: 164-170.
- Zaidel-Bar, R., C. Ballestrem, et al. (2003). "Early molecular events in the assembly of matrix adhesions at the leading edge of migrating cells." *J Cell Sci* **116**(Pt 22): 4605-13.
- Zamir, E., B. Z. Katz, et al. (1999). "Molecular diversity of cell-matrix adhesions." *J Cell Sci* **112** ( Pt 11): 1655-69.
- Zamir, E., M. Katz, et al. (2000). "Dynamics and segregation of cell-matrix adhesions in cultured fibroblasts." *Nat Cell Biol* **2**(4): 191-6.

- Zardi, L., B. Carnemolla, et al. (1985). "Elution of fibronectin proteolytic fragments from a hydroxyapatite chromatography column. A simple procedure for the purification of fibronectin domains." *Eur J Biochem* **146**(3): 571-9.
- Zavahir, F., D. A. McGrouther, et al. (2001). "A study of the cellular response to orientated fibronectin material in healing extensor rat tendon." *J Mater Sci Mater Med* **12**(10-12): 1005-11.
- Zeichen, J., M. van Griensven, et al. (2000). "The proliferative response of isolated human tendon fibroblasts to cyclic biaxial mechanical strain." *Am J Sports Med* **28**(6): 888-92.
- Zhang, Q., T. Sakai, et al. (1999). "Functional beta1-integrins release the suppression of fibronectin matrix assembly by vitronectin." *J Biol Chem* **274**(1): 368-75.
- Zhao, C., S. L. Moran, et al. (2007). "An analysis of factors associated with failure of tendon repair in the canine model." *J Hand Surg Am* **32**(4): 518-25.
- Zhao, C., Y. L. Sun, et al. (2010). "Effects of a lubricin-containing compound on the results of flexor tendon repair in a canine model in vivo." *J Bone Joint Surg Am* **92**(6): 1453-61.
- Zhao, C., M. E. Zobitz, et al. (2009). "Surface treatment with 5-fluorouracil after flexor tendon repair in a canine in vivo model." *J Bone Joint Surg Am* **91**(11): 2673-82.
- Zioupou, P., M. Gresle, et al. (2008). "Fatigue strength of human cortical bone: age, physical, and material heterogeneity effects." *J Biomed Mater Res A* **86**(3): 627-36.
- Zlatopol'skii, A. D., A. N. Chubukina, et al. (1989). "The effect of fibronectin fragments on proliferative activity of fibroblasts." *Biokhimiia* **54**(1): 74-80.

Zlatopol'skii, A. D., A. N. Chubukina, et al. (1992). "Heparin-binding fibronectin fragments containing cell-binding domains and devoid of hep2 and gelatin-binding domains promote human embryo fibroblast proliferation." *Biochem Biophys Res Commun* **183**(2): 383-9.

## **APPENDIX**

### **APPENDIX I: SOLUTIONS AND PROTOCOLS**

#### **DIAMINOBENZIDINE (DAB) SOLUTION**

1. Add 180 mg of 3, 3'-diaminobenzidine tetrahydrochloride to 270 mL distilled water
2. 30 mL Tris-buffered saline
3. 1 mL imidazole solution
4. Add 120 µL hydrogen peroxide just before use

#### **FORMAL SALINE**

For 10% formal saline:

40% formaldehyde 100 mL

Sodium chloride 9 g

Water 900 mL

#### **IMIDAZOLE SOLUTION**

(Merck, Poole, UK)

For 0.1M imidazole solution:

Add 0.681 g imidazole to 100 mL distilled water

Store at 4°C

#### **NEUTRAL BUFFERED FORMALIN**

For 10% neutral buffered formalin:

40% formaldehyde 100 mL

Distilled water 900 mL

Sodium dihydrogen phosphate monohydrate 4 g

Disodium hydrogen phosphate anhydrous 6.5 g

## **HYDROGEN PEROXIDE SOLUTION**

For 3% hydrogen peroxide solution:

Add 10 mL 30% hydrogen peroxide to 90 mL distilled water

## **NORMAL HUMAN SERUM**

1. Withdraw 9 mL of blood into serum tube
2. Allow to clot for 1 hour at room temperature
3. Centrifuge at 3000 rpm for 15 minutes
4. Remove supernatant
5. Heat at 56°C for 30 minutes (water bath) to denature complement
6. Store at -20°C in 500 µL aliquots in Eppendorf tubes

## **PHOSPHATE BUFFERED SALINE (PBS)**

Dissolve 5 PBS powder sachets in 5 L distilled water

Check pH 7.4

## **PHOSPHATE BUFFERED SALINE-BOVINE SERUM ALBUMIN (PBS-BSA)**

Weigh out 100 mg bovine serum albumin (BSA) and dissolve in 100 mL PBS

0.1% (w/v) BSA

Store at 4°C

## **SODIUM CITRATE BUFFER**

For 0.01M sodium citrate (pH 6.0 at 25°C):

1. Weigh out 2.1 g citric acid monohydrate
2. Add 950 mL distilled water
3. Add 13 mL 2M NaOH. Make up to 1 L
4. Adjust pH 6.0.
5. Store at 4°C

**APPENDIX II:**  
**PUBLICATIONS AND CONFERENCE PROCEEDINGS**  
**FROM THIS THESIS**

**PUBLICATIONS**

1.       **OA Branford**, DA Lee, KJ Rolfe, AO Grobbelaar.  
  
Attachment of Intrinsic and Extrinsic Tendon Cells and Adhesion Cells  
to Collagen and Fibronectin.  
  
Submitted to **Plastic and Reconstructive Surgery** July 2011.
  
2.       **OA Branford**, DA Lee, DL Bader, AO Grobbelaar.  
  
Relating Structure to Hierarchical Mechanics of Immobilized and  
Mobilized Flexor Tendon Adhesions.  
  
Submitted to **Journal of Hand Surgery [Eur]** April 2011.
  
3.       **OA Branford**, RA Brown, DA McGrouther, AO Grobbelaar, V Mudera.  
  
Shear-Aggregated Fibronectin with Anti-Adhesive Properties.  
  
**Journal of Tissue Engineering and Regenerative Medicine** Jan 2011;  
5(1): 20-31.
  
4.       **OA Branford**, V Mudera, RA Brown, DA McGrouther, AO Grobbelaar.  
  
A Novel Biomimetic Material to Engineer Post-Surgical Adhesion Using  
the Injured Digital Flexor Tendon-Synovial Complex as an *In Vivo*  
Model.  
  
**Plastic and Reconstructive Surgery** March 2008; 121(3): 781-793.

## **PUBLISHED ABSTRACTS**

1. **OA Branford, D Lee, D Bader and AO Grobbelaar.**

The Quantitative Assessment of Flexor Tendon Scarring – Novel models to evaluate new therapies.

**Journal of Plastic, Reconstructive and Aesthetic Surgery** September 2006; 59(9): S4-S5.

2. **OA Branford, D Lee, D Bader and AO Grobbelaar.**

The Quantitative Assessment of Flexor Tendon Adhesion – A Novel use of Confocal Microscopy to Evaluate Local Strain, Orientation and Organisation.

**The Journal of Hand Surgery: Journal of the British Society for Surgery of the Hand** June 2006; 31(S1): 3.

3. **OA Branford, D Lee, AO Grobbelaar.**

The Attachment of the Cellular Components of the Digital Flexor Tendon Complex to Collagen and Fibronectin.

**Transactions of the 52<sup>nd</sup> Annual Meeting of the Orthopaedic Research Society** March 2006; 31: 1117.

4. **OA Branford, AO Grobbelaar, DL Bader, DA Lee.**

The Development of a New Real-Time 3D Strain Model to Quantify Cellular Displacement in Injured Flexor Tendon Adhesions.

**Transactions of the 52<sup>nd</sup> Annual Meeting of the Orthopaedic Research Society** March 2006; 31: 34.



5. **OA Branford, DA McGrouther, V Mudera, AO Grobbelaar.**  
A Novel Biomaterial in Digital Flexor Tendon Repair – An Adhesion Free Future?  
**European Journal of Plastic Surgery** July 2005; 27(8): 401 – 417.
6. **OA Branford, DA McGrouther, V Mudera, AO Grobbelaar.**  
The Double-Edged Sword of Digital Flexor Tendon Healing – A Tissue Engineering Approach to an Unsolved Problem – *In Vitro* and *In Vivo* Assessments of a Novel Biomaterial.  
**Journal of Hand Surgery (British and European Volume)** June 2005; 30B: S1: 22.

## **CONFERENCE PROCEEDINGS:**

### **INTERNATIONAL PRESENTATIONS**

1. **OA Branford, DA Lee, AO Grobbelaar.**  
The Quantitative Assessment of Flexor Tendon Adhesion – A Novel Use of Confocal Microscopy to Evaluate Local Strain, Orientation and Organisation.  
**Federation of the European Societies for Surgery of the Hand (FESSH)** XIth Congress, Glasgow, 28<sup>th</sup> June 2006.
2. **OA Branford, AO Grobbelaar, DL Bader, DA Lee.**  
The Development of a New Real-Time 3D Strain Model to Quantify Cellular Displacement in Injured Flexor Tendon Adhesions.

**Orthopaedic Research Society (ORS)** 52nd Annual Meeting, Chicago, Illinois, 19<sup>th</sup> March 2006.

3. **OA Branford, DA Lee, AO Grobbelaar.**

The Attachment of the Cellular Components of the Digital Flexor Tendon Complex to Collagen and Fibronectin.

**Orthopaedic Research Society (ORS)** 52nd Annual Meeting (Poster), Chicago, Illinois, 19<sup>th</sup> -22<sup>nd</sup> March 2006.

4. **OA Branford, DA McGrouther, V Mudera, AO Grobbelaar.**

No More Adhesions in No Man's Land? An *in Vitro* and *in Vivo* Assessment of a Novel Biomaterial.

**American Society for Surgery of the Hand (ASSH) and the American Society of Hand Therapists (ASHT)** Joint Annual Meeting (Poster), San Antonio, Texas, 22<sup>nd</sup> – 24<sup>th</sup> September 2005.

5. **OA Branford, DA Lee, DL Bader, AO Grobbelaar.**

The Quantitative Assessment of Flexor Tendon Scarring – Novel Models to Evaluate New Therapies.

**European Conference of Scientists and Plastic Surgeons (ECSAPS)**, 9th Annual Meeting, Leuven, Belgium, 16<sup>th</sup> September 2005.

6. **OA Branford**, DA McGrouther, V Mudera, AO Grobbelaar.  
The “Double-Edged Sword of Digital Flexor Tendon Healing” – A Tissue- Engineering Approach to an Unsolved Problem – *In vitro* and *in vivo* assessments of a novel biomaterial.  
**Federation of the European Societies for Surgery of the Hand (FESSH)** Xth Congress in Göteborg, Sweden, 17<sup>th</sup> June, 2005.
7. **OA Branford**, DA McGrouther, V Mudera, AO Grobbelaar.  
A Novel Biomaterial in Digital Flexor Tendon Repair – An Adhesion Free Future?  
**European Conference of Scientists and Plastic Surgeons (ECSAPS)**, 8th Annual Meeting, Munich, Germany, 15<sup>th</sup> October 2004.
8. V Mudera, **OA Branford**, AO Grobbelaar, DA McGrouther, R Brown.  
Development of a Novel Fibronectin Based Biomaterial: A Slick Solution to a Sticky Problem.  
**Tissue Engineering Society International (TESI) and European Tissue Engineering Society (ETES)** Joint Meeting (Poster), Lausanne, Switzerland, 10<sup>th</sup> – 13<sup>th</sup> October 2004.

## **CONFERENCE PROCEEDINGS:**

### **NATIONAL PRESENTATIONS**

- 1. OA Branford, DA Lee, DL Bader, AO Grobbelaar.**

A Novel Approach to Assessing Flexor Tendon Scarring – The Use of Confocal Microscopy as a Measure of Strain and Disorganisation within Adhesions.

**British Association of Plastic Surgeons (BAPS)** Winter Meeting, Royal College of Surgeons, London, 30<sup>th</sup> November 2005.

- 2. OA Branford, DA McGrouther, V Mudera, AO Grobbelaar.**

A Fibronectin-Based Biomaterial in Digital Flexor Tendon Repair.

**British Society for Surgery of the Hand (BSSH)**, London, 5<sup>th</sup> November 2004.